

Operational Modal Analysis of Flexible Robots and Contact Force Estimation for Robotic Grinding Applications

by

Quoc Cuong NGUYEN

MANUSCRIPT-BASED THESIS PRESENTED TO ÉCOLE DE
TECHNOLOGIE SUPÉRIEURE IN PARTIAL FULFILLMENT FOR THE
DEGREE OF DOCTOR OF PHILOSOPHY
Ph. D.

MONTREAL, NOVEMBER 03, 2022

ÉCOLE DE TECHNOLOGIE SUPÉRIEURE
UNIVERSITÉ DU QUÉBEC



Quoc Cuong Nguyen, 2022



This Creative Commons license allows readers to download this work and share it with others as long as the author is credited. The content of this work can't be modified in any way or used commercially.

BOARD OF EXAMINERS
THIS THESIS HAS BEEN EVALUATED
BY THE FOLLOWING BOARD OF EXAMINERS

Mr. Marc Thomas, Thesis Supervisor
Department of Mechanical Engineering, École de Technologie Supérieure

Mr. Viet-Hung Vu, Thesis Co-supervisor
Department of Mechanical Engineering, École de Technologie Supérieure

Mr. Ilian Bonev, President of the Board of Examiners
Department of System Engineering, École de Technologie Supérieure

Mr. Zhaoheng Liu, Member of the jury
Department of Mechanical Engineering, École de Technologie Supérieure

Mr. Philippe Micheau, External Evaluator
Department of Mechanical Engineering, Université de Sherbrooke

THIS THESIS WAS PRESENTED AND DEFENDED
IN THE PRESENCE OF A BOARD OF EXAMINERS AND PUBLIC
ON 19 OCTOBER 2022
AT ECOLE DE TECHNOLOGIE SUPERIEURE

ACKNOWLEDGMENT

First and foremost, I would like to express my deepest appreciation to my research director Prof. Marc Thomas for allowing me to enter the Ph.D. program in the Department of Mechanical Engineering at ETS. Without his support, it would not have been possible. I am deeply grateful to him for all his attentive, immense scientific knowledge, but also for the hard questions which cited me to widen my research from various perspectives. His guidance helped me in all the time of research and writing of this thesis. I could not have imagined having a better supervisor for my Ph.D. study.

I would also hugely appreciate my co-supervisor, Dr. Viet-Hung Vu, for giving me intellectual freedom in my research, and indispensable for his insightful comments, encouragement, and constant support. His scientific advice and friendly attitude helped me to overcome all the difficulties throughout the period of my Ph.D. study.

My sincere thanks also go to the SCOMPI team at DYNAMO laboratory for all the technical help and support during my entire experimental study. I also would like to thank the jury members who evaluated my thesis for their constructive suggestions and helpful advice.

I would like to gratefully thank the Vietnam International Education Development (VIED) - Ministry of Education and Training of Vietnam, from my home country Vietnam, and NSERC for their financial support via scholarship project 911 and Discovery Research grants. Without their sponsorship, I could not complete this work.

Finally, I warmly thank and appreciate my family, for always supporting me during the most difficult time and my entire study. This thesis is dedicated to them for all their love and constant support.

Analyses modale opérationnelle de robots flexibles et estimation de la force de contact pour des applications de meulage robotique

Quoc Cuong NGUYEN

RÉSUMÉ

De nos jours, la rectifieuse est l'un des processus de fabrication les plus importants, et la technologie de ce processus a été largement développée ces dernières années. Lors d'une opération de meulage robotique, la faible rigidité du manipulateur est un facteur clé affectant le comportement du robot et provoquant des phénomènes d'impact. Cette thèse s'inscrit dans un projet de recherche lancé par l'ETS et l'Institut de recherche d'Hydro-Québec sur la dynamique d'un robot manipulateur flexible nommé SCOMPI (Super COMPact robot Ireq) dans le but d'améliorer ses performances de meulage et d'éviter les vibrations lors du processus d'usinage. La qualité du fini de surface dépend du processus de meulage qui à son tour repose sur la stabilité du processus, car un meulage instable introduit des vibrations, ce qui compromet la précision géométrique, le fini de surface et réduit la durée de vie de l'outil. Il est donc crucial de comprendre les mécanismes des vibrations de meulage afin de mieux les contrôler. En effet, il a été observé que le processus de meulage par le robot sous étude est interrompu à chaque tour de meule plutôt que d'avoir une action de coupe continue. Ce comportement de coupe par sauts apparaît en raison de la faible rigidité du manipulateur flexible sous des forces de meulage élevées. Indépendamment du régime et des conditions de meulage, une prédiction précise de la force de contact est nécessaire pour le contrôle du processus ou la prédiction d'un broutage potentiel de la pièce. Par conséquent, l'estimation de la force de contact de l'effecteur terminal et l'analyse modale opérationnelle sont des aspects importants à prendre en compte dans le meulage robotisé.

Comme le montre le titre de cette thèse, le travail porte sur deux aspects de la recherche en robotique. Dans le premier, une attention particulière a été accordée à une meilleure compréhension de la force dynamique en ligne ainsi que de leurs paramètres de contact au point de contact de l'effecteur en cours d'opération. Une contribution remarquable de cette

VIII

recherche est le développement d'une méthodologie inverse pour estimer la force de contact inconnue en utilisant un modèle de sortie ARX uniquement sans l'exigence d'une connaissance précise de la dynamique du manipulateur flexible ou des paramètres physiques. Les effets de certains paramètres expérimentaux ont également été mis en examen. Dans un deuxième objectif, l'analyse modale opérationnelle est effectuée pour identifier la fréquence naturelle modale et le taux d'amortissement du manipulateur flexible lors de l'opération de meulage en utilisant uniquement les réponses vibratoires. Les paramètres modaux opérationnels ont été étudiés de manière approfondie à partir des tests réels via différentes méthodologies proposées, en mettant davantage l'accent sur la synthèse de l'amortissement, ce qui est extrêmement important pour prédire les niveaux de vibration. Cette thèse contribue également à un nouvel algorithme de sélection d'un ordre de modèle optimal basé sur une variance d'erreur minimale des fonctions de transfert identifiées, tout en considérant l'effet de l'erreur de modélisation et du bruit de mesure.

L'efficacité de toutes les méthodes proposées a été validée par des signaux de simulation, des données numériques et expérimentales sur un robot flexible en fonctionnement. Sur la base de l'amélioration de la précision des résultats estimés, la recherche fournit un outil utile aux utilisateurs non experts pour appliquer les techniques analyse modale opérationnelle et la prédiction de la force d'entrée. Les études de cette thèse contribuent également à la compréhension de la dynamique vibratoire qui régit le processus de broyage robotisé. Le développement ultérieur de la technologie robotisée pour le profilage de précision des pièces industrielles peut s'appuyer sur de telles bases de compréhension. Des recommandations pour de futures recherches sont également proposées à la fin.

Mots clés : robot SCOMPI, manipulateur flexible, processus de meulage, analyse modale opérationnelle, paramètres modaux, vibration, identification de force, paramètres de force de contact, modèle de sortie uniquement, sélection d'ordre optimal

Operational modal analysis of flexible robots and contact force estimation for robotic grinding application

Quoc Cuong NGUYEN

ABSTRACT

Nowadays grinding machine is one of the most important manufacturing processes, and the technology of this process has been widely developed in recent years. In flexible robotic grinding, low manipulator stiffness is a key factor affecting process behavior and causing impact phenomena. This thesis is part of a research project launched by ETS and Hydro-Québec's research institute on the dynamics of a flexible manipulator robot named SCOMPI (Super COMPact robot Ireq) in an effort of improving its grinding performance and avoid vibrations under the machining process. The surfaces quality depends on grinding process which in turn relies on process stability, since unstable grinding introduces vibration, which compromises geometrical accuracy, surface finishing, and reduces the tool life. Therefore, it is crucial to understand the mechanisms of grinding vibration in order to control them effectively. It is observed that the grinding process by this robot is interrupted at each revolution of the wheel rather than having a continuous cutting action. This impact cutting behavior appears due to the low stiffness of the flexible manipulator under high grinding forces. Regardless of grinding regime and conditions, an accurate contact force prediction is necessary for process control or predicting potential workpiece burn or chatter. Consequently, end-effector contact force estimation and operational modal analysis are important aspects must be considered in robotic grinding.

As can be seen from the title of this thesis, the work is concerned with two aspects of robotics research. In the first one, special attention has been given to gain a better understanding of the online dynamical force as well as their contact parameters at the end-effector contact point under operation. A remarkable contribution of this research is the development of an inverse methodology to estimate unknown contact forces by using an ARX output-only model without the requirement of knowledge of the flexible manipulator dynamics or physical parameters.

The effects of some experimental parameters have been also put into examinations. In a second objective, the Operational Modal Analysis is carried out to identify the modal natural frequency and damping ratio of the flexible manipulator under grinding operation using vibration responses only. Operational modal parameters have been drastically investigated from the real tests via different proposed methodologies, with greater emphasis on the synthesis of damping, which is extremely important in predicting vibration levels. This thesis is also contributing a new algorithm for selecting an optimal model order based on a minimum error variance of the identified transfer functions, which is correctly incorporated with the effect of modeling error and measurement noise.

The effectiveness of all the proposed methods has been validated through simulation signals, numerical and experimental data on a flexible robot in operation. Based on the improved accuracy of the estimated results, the research provides a useful tool for non-expert users to apply operational modal analysis techniques and input force prediction. The studies in this thesis also contribute to understand the vibratory dynamics that govern the robotic grinding process. Further development of the robotized technology for precision profiling of industrial parts can rely on such understanding bases. Recommendations for future research are also offered at the end.

Keywords: SCOMPI robot, flexible manipulator, grinding process, operational modal analysis, modal parameters, vibration, force identification, contact force parameters, output-only model, optimal order selection

TABLE OF CONTENTS

	Page
INTRODUCTION.....	1
CHAPTER 1 RESEARCH OUTLINES AND OBJECTIVES	5
1.1 The problem definition.....	5
1.2 Scope of study and objectives	9
1.3 Overview of the state of the art	11
1.3.1 Vibration in grinding.....	11
1.3.2 Operational modal analysis	13
1.3.3 Time series model	18
1.3.4 Kalman filter	24
1.3.5 Force estimation technique.....	27
1.3.6 Contact force parameters identification.....	30
1.4 Originalities and contributions	33
CHAPTER 2 A KALMAN FILTER BASED ARX TIME SERIES MODELING FOR FORCE IDENTIFICATION ON FLEXIBLE MANIPULATORS	37
2.1 Résumé.....	37
2.2 Abstract	38
2.3 Introduction	39
2.4 Force identification method.....	44
2.4.1 State space representation of ARX model.....	45
2.4.2 Recursive forces identification	50
2.5 Numerical and experimental simulation on a cantilever beam	52
2.5.1 Modal analysis of the cantilever beam.....	53
2.5.2 Simulation of the identification of excitation forces with different noise levels	56
2.6 Experimentation on the cantilever beam.....	61
2.7 Experimental tests on the COMPI robot	63
2.8 Conclusion.....	71
2.9 Acknowledgements	71
2.10 References	72
CHAPTER 3 OPTIMAL ARMAX MODEL ORDER IDENTIFICATION OF DYNAMIC SYSTEMS.....	79
3.1 Résumé.....	79
3.2 Abstract	80
3.3 Introduction	81
3.4 Time series modeling	84
3.5 A model order determination approach.....	88
3.6 Industrial application on a SCOMPI robot.....	93
3.6.1 Description of the test structure.....	93

XII		
	3.6.2	Experimental procedure 94
3.7		Identification procedure96
	3.7.1	Model orders estimation..... 96
	3.7.2	Frequency Response Function identification.....102
	3.7.3	Extraction of model parameters106
3.8		Conclusion..... 110
3.9		Acknowledgements 111
3.10		References 111
CHAPTER 4	A NONLINEAR IDENTIFICATION OF CONTACT PARAMETERS: APPLICATION TO A FLEXIBLE MANIPULATOR UNDER GRINDING OPERATION 117	
4.1		Résumé..... 117
4.2		Abstract 118
4.3		Introduction 119
4.4		Damping identification..... 122
	4.4.1	Covariance driven stochastic subspace identification123
	4.4.2	Damping estimation from ambient vibrations.....124
	4.4.3	Stabilization criteria and selection of poles.....125
4.5		Contact force model and identification technique..... 125
	4.5.1	Contact force model125
	4.5.2	Proposed method by using Unscented Kalman Filter.....130
4.6		Experiments on a SCOMPI robot..... 133
	4.6.1	Description of the test structure.....133
	4.6.2	Measurement test setup134
4.7		Identification results..... 136
	4.7.1	Output only modal analysis.....136
	4.7.2	Contact force parameters estimation139
4.8		Conclusion..... 141
4.9		Acknowledgements 142
4.10		References 142
	SYNTHESIS 147	
	CONCLUSION 149	
	RECOMMENDATIONS 151	
APPENDIX I	ARX MODEL FOR EXPERIMENTAL VIBRATION ANALYSIS OF FLEXIBLE MANIPULATOR DURING GRINDING 153	
	LIST OF BIBLIOGRAPHICAL REFERENCES..... 175	

LIST OF TABLES

	Page
Table 2.1	Properties of the cantilever beam53
Table 2.2	Natural frequencies and damping ratios of the cantilever beam55
Table 2.3	Identification errors with different measurement noise levels57
Table 2.4	Identified natural frequencies and damping ratios of SCOMPI robot manipulator.....66
Table 2.5	Comparison of the estimated and measured force RMS68
Table 3.1	Grinding conditions of the SCOMPI test95
Table 3.2	Comparison of estimated modal parameters between ARMAX and ARX models.....109
Table 4.1	Grinding condition of SCOMPI robot.....136
Table 4.2	Estimated damping ratio138
Table 4.3	Estimated contact damping and stiffness result141

LIST OF FIGURES

		Page
Figure 1.1	The SCOMPI robot in machining process	6
Figure 1.2	Kinematic drawing of SCOMPI.....	7
Figure 1.3	Waviness of ground surface	8
Figure 1.4	System scheme for classical Experimental Modal Analysis approach.....	13
Figure 1.5	System scheme for Operational Modal Analysis	15
Figure 1.6	System scheme of ARMAX model (a) and ARMA model (b).....	20
Figure 1.7	System scheme of ARX model (a) and AR model (b).....	21
Figure 1.8	Stabilization diagram of time series analysis by SSI-COV method.....	23
Figure 1.9	The block diagram of Kalman filter	25
Figure 1.10	An alternative flow chart of the Kalman Filter algorithm.....	26
Figure 1.11	Unequally constrained robot. Free motion (left), contact (right).....	30
Figure 2.1	Flow chart of the estimation method.....	45
Figure 2.2	Experimental test set-up on a cantilever aluminum beam	53
Figure 2.3	Stabilization diagram of ARX model.....	55
Figure 2.4	Force identification results without measurement noise	58
Figure 2.5	Force identification results with 5% noise	58
Figure 2.6	Force identification results with 10% noise	58
Figure 2.7	Force identification results with 15% noise	59
Figure 2.8	Force identification results with 20% noise	59
Figure 2.9	Force identification results with 30% noise	59
Figure 2.10	Force identification results with 50% noise	60
Figure 2.11	Force identification results with 100% noise	60

Figure 2.12	Time history of measured accelerations on the beam.....	61
Figure 2.13	Estimated force in time domain, RMS error = 3.5 (%).....	62
Figure 2.14	Amplitude spectrum of the estimated force	63
Figure 2.15	Overall grinding test configuration on SCOMPI robot.....	64
Figure 2.16	Recorded acceleration time histories and their corresponding Fourier amplitudes spectra.....	65
Figure 2.17	Frequency stabilization diagram of SCOMPI robot.....	65
Figure 2.18	NOF evolution and efficient order selection on measured accelerations ...	67
Figure 2.19	Estimated force in the X direction in the time domain, RMS error = 7.9 %.....	68
Figure 2.20	Estimated force in the Y direction in the time domain, RMS error = 5.8 %.....	69
Figure 2.21	Estimated force in the Z direction in the time domain, RMS error = 6.8 %.....	69
Figure 2.22	Estimated forces in frequency domain on each direction.....	70
Figure 3.1	Model structures of ARX (a) and ARMAX (b).....	87
Figure 3.2	Structure of SCOMPI robot (Hazel et al., 2012a, 2012b).....	94
Figure 3.3	Experimental setup for SCOMPI robot during grinding operation.....	95
Figure 3.4	Measured data on SCOMPI robot	96
Figure 3.5	Model order selection based on AIC and BIC criteria for different sets of data:.....	97
Figure 3.6	Model orders selection based on the proposed approach for different sets of data:.....	98
Figure 3.7	NOF evolution and efficient model orders selection for different sets of data:.....	99
Figure 3.8	Moving average order (a) and time delay order (b) selection	100
Figure 3.9	Residual errors histogram and normal probability plot of an estimated ARMAX (10,10,8,2) model.....	101

Figure 3.10	Autocorrelation function (ACF) and Partial Autocorrelation Function (PACF) of the residual ARMAX (10,10,8,2)	101
Figure 3.11	Estimated Frequency Response Function FRF_{xx}	102
Figure 3.12	Estimated Frequency Response Function FRF_{xy}	103
Figure 3.13	Estimated Frequency Response Function FRF_{xz}	103
Figure 3.14	Estimated Frequency Response Function FRF_{yx}	103
Figure 3.15	Estimated Frequency Response Function FRF_{yy}	104
Figure 3.16	Estimated Frequency Response Function FRF_{yz}	104
Figure 3.17	Estimated Frequency Response Function FRF_{zx}	104
Figure 3.18	Estimated Frequency Response Function FRF_{zy}	105
Figure 3.19	Estimated Frequency Response Function FRF_{zz}	105
Figure 3.20	Stabilization diagram by the ARX model	108
Figure 3.21	Stabilization diagram based on average estimated FRFs in X direction by the ARMAX model	108
Figure 3.22	Stabilization diagram based on average estimated FRFs in Y direction by the ARMAX model	108
Figure 3.23	Stabilization diagram based on average estimated FRFs in Z direction by the ARMAX model	109
Figure 4.1	Single point contact environment model of SCOMPI robot	126
Figure 4.2	The structure of SCOMPI robot	134
Figure 4.3	Experimental on SCOMPI under grinding task (left) and sensors configuration (right)	135
Figure 4.4	Stabilization diagram by SSI-COV algorithm	137
Figure 4.5	Damping ratio estimation by SSI-COV method	138
Figure 4.6	Comparison of estimated contact damping (left) and contact stiffness (right) at different grinding powers	140

LIST OF ABBREVIATIONS

e.g.	For example
i.e.	In other words
ACF	Autocorrelation Function
AIC	Akaike Information Criterion
AKF	Augmented Kalman Filter
ANN	Artificial Neural Network
AR	Auto Regressive
ARX	Auto Regressive eXogenous
ARMA	Auto Regressive Moving Average
ARMAX	Auto Regressive Moving Average eXogenous
BIC	Bayesian Information Criterion
BJ	Box-Jenkins
DGP	Data Generating Process
DOF	Degree of Freedom
EKF	Extended Kalman Filter
EMA	Experimental Modal Analysis
ETFE	Empirical Transfer Function Estimate
FD	Frequency domain
FEA	Finite Element Analysis
FEM	Finite Element Method
FFT	Fast Fourier Transform

FRF	Frequency Response Function
H-C	Hunt Crossley
ITD	Ibrahim Time Domain
IREQ	Hydro Quebec's Research Institute
IRF	Impulse Response Function
ISF	Inverse Structural Filter
K-B	Kelvin-Boltzman
KF	Kalman Filter
K-V	Kelvin-Voigt
LS	Least Squares
LSCE	Least Squares Complex Exponential
LTI	Linear Time Invariant
MA	Modal analysis
MAC	Modal Assurance Criterion
MDL	Minimum Description Length
MIMO	Multi Input - Multi Output
MISO	Multi Input - Single Output
MPE	Modal Parameters Estimation
MRR	Material Removal Rate
MSE	Means Square Error
MTM	Modal Transformation Method
NOF	Noise-ratio Order Factor

NSR	Noise to Signal Ratio
ODS	Operating Deflection Shape
OE	Output Error
OMA	Operational Modal Analysis
OMAX	Operational Modal Analysis with eXogenous inputs
OO	Output Only
PACF	Partial Autocorrelation Function
PSD	Power Spectrum Density
QQ	Quantile-Quantile
RMS	Root Mean Square
RNN	Recurrent Neural Network
RLS	Recursive Least Squares
RVM	Relevance Vector Machine
SCOMPI	Super COMPact Ireq
SD	Spatial domain
SLD	Stability Lobe Diagram
SI	System Identification
SISO	Single Input - Single Output
SIMO	Single Input - Multi Output
SSI	Stochastic Subspace Identification
SSI-COV	Covariance Driven Stochastic Subspace Identification
STFT	Short Time Fourier Transform
SVD	Singular Value Decomposition

SWAT	Sum of Weight Acceleration Technique
TF	Transfer Function
TD	Time domain
UKF	Unscented Kalman Filter
UF	Unscented Transformation
VCM	Virtual Contact Manipulator

LIST OF SYMBOLS

Symbol	Unit	Description
$u(t)$	N	Input Force Signals
$y(t)$	m/s ²	Measured Acceleration Signals
p	-	Model Order
p_{optimal}	-	Optimal Model Order
n_a	-	Model order of Auto Regressive part
n_b	-	Model order of Exogenous input part
n_c	-	Model order of Moving Average part
n_k	-	The pure time delay in the system
f_{nl}	Hz	Natural frequencies
f_r	Hz	Rotational frequencies
ζ_l	%	Damping ratio
ϕ_l	-	Mode shapes
M	kg	Mass matrix
C	Ns/m	Damping matrix
K	N/m	Stiffness matrix
E_p	%	Noise Level Percentage
$\mathcal{E}_{\%RMS}$	%	Root Means Square Error
ΔT	s	Sampling period
F	N	Interaction force
x	m	Displacement
\dot{x}	m/s	Velocity
h	N/m	Stiffness coefficient
b	Ns/m	Damping coefficient

P	W	Grinding power
ω	rpm	Rotational speed
θ	rad	Angle of grinding cup
L	m	Length of grinding cut
W	m	With of grinding cut
D	m	Depth of grinding cut
v_k	dB	Process Noise
η_k	dB	Measurement Noise
K_k	-	Kalman gain
γ	-	Forgetting factor
x	-	System state
\hat{x}_k	-	Estimated state
$x_{k k-1}$	-	Predicted state
y_k	-	Measurement
$y_{k k-1}$	-	Predicted measurement
P_k	-	Estimated state covariance
$P_{k k-1}$	-	Predicted state covariance
$P_{y_{k k-1}}$	-	Predicted measurement covariance

INTRODUCTION

During the past decades, robot manipulators have undergone significant changes and widely deployed in various industrial sectors, such as automotive and semiconductor manufacturing. This can greatly improve productivity, quality and reduce operational costs. However, more than 80 percent of the application of industrial robot is limited in the field of welding and material handling (Zengxi Pan, 2006). Conventional manipulators are considered to be stiff structures. However, with the innovation of technology in recent years regarding materials, fabrication technology, and numerical analysis, robotic manipulators are now constructed with reasonable flexibility of links and joints. Compared to rigid robot manipulators, the design of the flexible structure allows them for attaining higher load weight ratios and operating speeds. The flexible robots are not only lighter than conventional ones, but they are also offering some advantages such as lightweight, low inertia, and lower power consumption. However, one of the major hurdles preventing the adoption of flexible robots for the machining process is vibration. (Quintana & Ciurana, 2011) and (Siddhpura & Paurobally, 2012) recognized that the most powerful source of chatter and self-excitation were regenerative and mode coupling effects. Mode-coupling vibrations are associated with natural frequency modes of the structure, while self-excited vibration results from the interaction between the dynamics of the tool holder and the cutting process. In fact, vibration can happen in all machining processes to a certain extent. But if we are not properly controlled vibration, it can result in poor surface quality, abrasion or damage to machine tools, and limited production rates.

Recently, following advancements in the robotic machining domain, robotic grinding has attracted the attention of numerous researchers. It has turned out to be a valuable solution that involves finishing steps in the manufacture of faucets, turbine blades, camshafts, etc., and relieved humans from working in dirty and noisy environments. The robot can be programmed to machine complex geometries with the only exception of having problems with geometric accuracy due to the robot's low structural stiffness. At Hydro-Quebec's Research Institute, a robot named "SCOMPI", which stands for "Super COMPact Ireq robot" was developed for on-side maintenances and inspections. It is a track-based six-joint serial robot with a total

weight of about 33 kg and is designed to access difficult-to-reach locations such as turbine blades and unmovable parts like large hydropower equipment for maneuverability during material removals tasks such as grinding or polishing (Hazel, Côté, Laroche, & Mongenot, 2012a, 2012b). In general, grinding is used as a finishing procedure with low material removal rate. However, this work is performed by SCOMPI at high material removal rate, which causes significant vibratory responses of the compliant robotic tool holder. Severe chatter has been a problem reported ever since robots were first applied in the machining operation (Hazel *et al.*, 2012b). Due to the flexible structure, a small deflection of links or joints might result in significant vibration during the machining process. In order to improve the precision and quality of the grinding process and avoid the unwanted chatter vibration caused by the high flexibility of the robot, we need to understand the dynamical behavior of the robot at the end effector. Consequently, with the aim of gaining knowledge of the dynamic responses of the SCOMPI structure, Operational Modal Analysis (OMA) has been applied via different proposed approaches. From which the modal parameters of the machining system in terms of natural frequencies, damping rates, and modal deformation must be identified. These modal parameters can reflect the dynamic characteristics of the structure and can be used to control vibration.

In addition, since robots are being used to perform tasks that require contact between the robot and the workpiece, the interaction with the environment will constrain the robot's motion. Force interaction between the tool and workpiece can cause elastic deformations of the robot, the grinding wheel, and the workpiece. Grinding force-induced deflections can lead to misalignment of the grinding process and inaccuracy of surface finish. Implementing grinding with constant normal force is a well-known approach for improving surface quality. Moreover, there should be a relationship between the abovementioned chatter and the contact force at the end effector. However, most robot manipulators are poor at measuring and controlling force, especially force of contact. At a general level, estimating when contact occurs, and the forces involved, are elemental requirements in building cognitive information that enables robots to adapt to an unstructured environment. As a result, an accurate estimation of input forces as well as characterizing its contact parameters must be considered for structural analysis to

minimize the deformation and the chatter during the grinding process induced by the interaction force between the tool and the workpiece. A comprehensive study of the force and its parameters is necessary. It not only prevents excessive contact force which could damage the workpiece but also regulates the desired force intending to stabilize the structure under working conditions.

Organization of thesis

This research work is presented as a manuscript-based thesis in various stages of publication and divided into four chapters. Each one is devoted to the development of methods aiming at solving specific parts of the problem discussed before.

Chapter 1 gives information about the problems, providing the basis for this research, outlines the research, states the objectives, and defining the scope of the study. The literature review of related research and state of the art in this field are also covered in this chapter. Subsequently, the methodology is described, emphasizing the originalities and contributions of the research for each task.

Chapter 2 presents the first journal article published in the *Journal of Mechanical System and Signal Processing*. In this work, a new method for estimating the operational excitation forces in multiple directions has been introduced. The method is developed by using a Kalman filter based on a time series Auto-Regressive eXogenous (ARX) modeling to deal with the inverse problems, where the ARX model is modified by employing ambient vibration data only. The reliability and robustness of the proposed method against noise have been validated via different examples with numerical simulations and experiments on SCOMPI robot.

Chapter 3 presents the second journal article published in the *London Journal of Engineering Research*. A new algorithm was proposed for effectively determining the optimal order of model, which enables the model to extract uncorrelated residuals and better identify the dynamical behavior of the system by using both observation input and output data. The concept

is based on the minimum means square error of the estimated transfer functions, which can effectively cope with measurement noise and modeling error to identify the appropriate low-order transfer functions of the structure via an Auto Regressive Moving Average eXogenous (ARMAX) model. This model exhibits the lowest complexity and ease in computation with sufficient performance at low order despite the noise-contaminated experimentally on measurement data.

Chapter 4 presents the third journal article submitted in the *Journal of Dynamic System, Measurement, and Control*. This paper presents an experimental approach for estimating the unknown parameters of the constraint environment characterized by environmental stiffness and damping parameters based on the Unscented Kalman Filter (UKF) in conjunction with the nonlinear Hunt-Crossley contact model by using output measurement only. The method was verified by the common Recursive Least Square (RLS) algorithm and showed its robustness and efficiency in terms of estimating contact parameters. Knowing these contact force parameters is not only necessary for force-controlled applications but also for operating robots in an unstructured environment.

Finally, all the works have synthesized at the end, the accomplishments of this thesis are emphasized in conclusion, while suggestions for future work are also presented.

CHAPTER 1

RESEARCH OUTLINES AND OBJECTIVES

1.1 The problem definition

During the past decades, the use of industrial robots can be seen worldwide and has significantly increased with a faster growingly trend in many applications, especially in automation and manufacturing industries. Most of them are being used for material handling, welding, grinding, painting, assembling, etc. The benefits of automatic control for industrial manipulation are well documented in the literature (Box, Jenkins, & MacGregor, 1974; Dwivedy & Eberhard, 2006; Sciavicco & Siciliano, 2001; Tokhi, Azad, Morris, & Hossain, 1994). By exploiting the repetitive nature of the manufacturing and material handling process, automation has reduced labor costs and improved repeatability and efficiency. Many modern production lines typically implement a large number of industrial robots. However, the majority of existing robotic manipulators are conventionally designed with large stiffness, in an attempt to minimize system vibration at the end effector to achieve good positional accuracy. Consequently, such robots are usually heavy with respect to the operating payload. This, in turn, limits the speed of operation of the robot manipulation, increases the size of the actuator, boosts energy consumption, and increases the overall cost. Moreover, the payload to robot weight ratio under such situations is low. In order to solve these problems, robotic manipulators are now designed to be lightweight and provided some levels of flexibility by being constructed with more flexible links and joints. Conversely, flexible robot manipulators exhibit many advantages over their rigid counterparts. For example, they require less material, lighter in weight, have higher manipulation speed, lower energy consumption, require smaller actuators, are more maneuverable and transportable, have less overall cost, and higher payload to robot weight ratio (Book & Majette, 1983; Tokhi *et al.*, 1994). Due to their inherent advantages over the rigid body counterparts, flexible manipulators are widely used in various industrial applications, like space exploration and nuclear plants.

The robotic machining technology which is used in this study (Hazel, Côté, Laroche, & Mongenot, 2012a, 2012b) provides maneuverability to automate the in-situ maintenance works on hydroelectric equipment. The 6-DOF robot called SCOMPI shown in Figure 1.1 was developed at Hydro Quebec research institute (IREQ) for maintenance operations on hydropower equipment by profiling large parts and complex geometries with a high material removal rate. It uses a lightweight structure (≈ 30 kg) which is much lighter than the average robots used for machining (≈ 200 kg) to provide a portable solution at the cost of extreme flexibility, thus avoiding the cost of dismantling parts and minimizing shutdowns. The manipulator's unique kinematic design uses a track-based installation for its first prismatic joint rather than being installed on a rigid grounded shoulder like the robots used in factory lines. The track may be straight, circular on a series of circular sections so that such feature provides a track long extended working envelope to gain access for machining awkward locations. The manipulator can perform in situ maintenance of hydro turbines by grinding in the very confined areas between the blades for maintenance jobs, thanks to its fully extended arm with the help of its track-based kinematics. Such intervention works are infeasible to perform by manual workers. Over the past 20 years, it has been extensively employed for a variety of field applications on such equipment as turbines, headgates, and penstocks (Hazel *et al.*, 2012a).



Figure 1.1 The SCOMPI robot in machining process
Taken from Hazel *et al.* (2012b, p. 113)

The grinding task performed by SCOMI is a demanding job that involves heavy material removal aimed at modifying parts' dimensions rather than generating a glossy surface only. The SCOMPI can travel along straight or curved rails, work on geometrically complex surfaces, and access hard-to-reach areas to perform complex tasks. This electric multi-process robot allows an extensible and conformable working envelope, and its configuration was optimized for easy movement between turbine blades to address a variety of maintenance and repair situations typically encountered with hydroelectric turbines. Figure 1.2 (A) represents the robot working in envelop space and Figure 1.2 (B) is a kinematic drawing of the robot in which L1 to L6 denote the links and J1 to J6 denote the joints.

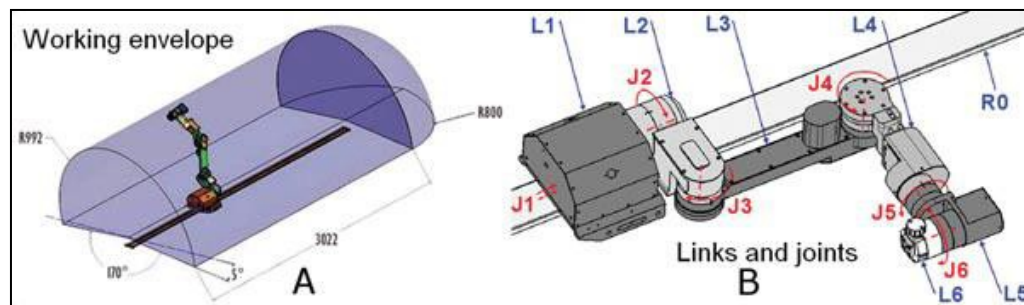


Figure 1.2 Kinematic drawing of SCOMPI
Taken from Hazel et al. (2012a, p. 71)

The robot, therefore, has five rotating joints and one sliding joint. A smaller version of SCOMPI, the “Mini-SCOMPI” is 30% smaller and was developed to perform welding jobs on smaller turbines (Hazel et al., 2012b). Thanks to their lightweight and compact design, the maneuverability that robots bring into the operations makes them become the only practical solution for machining in hard-to-reach areas.

Despite their attractive properties, controlling lightweight robot manipulators is a challenging task as their flexibility induces structure vibrations that deteriorate the trajectory tracking accuracy and may lead to instability issues. Because of the compact and flexible structure, concerns arise regarding its dynamic behavior due to self-regenerative chatter vibration during the grinding process. Regenerative chatter is a well-known machining problem that occurs in the grinding process of machine tools, and results in the unstable cutting process, poor surface

quality, limiting productivity, deteriorating tool wear, and shortening machine tool service life span (Rafieian, Hazel, & Liu, 2014). This undesired self-excited vibration problem is one of the main obstacles to utilizing the total capacity of a machine tool in production. This problem will affect the positional accuracy of the flexible manipulator, or even, in the case of large amplitude, it may cause a safety accident. An example of chatter vibration on the ground surface is given in Figure 1.3.

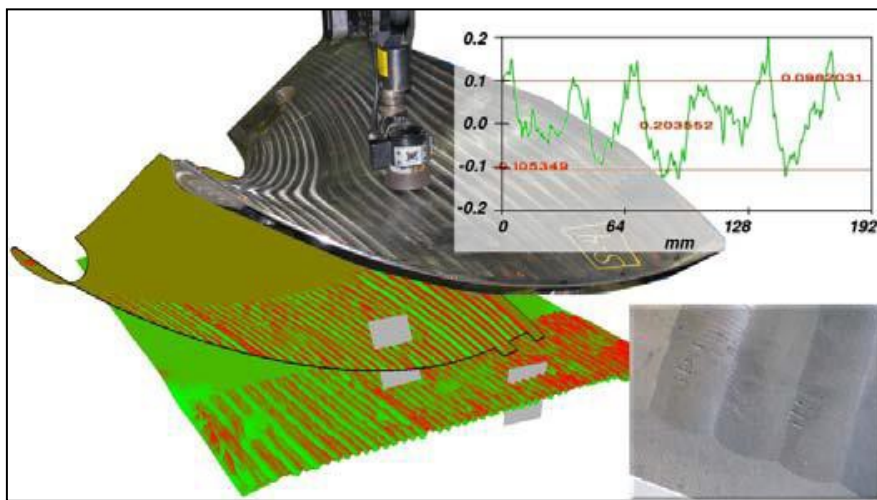


Figure 1.3 Waviness of ground surface
Taken from Sabourin et al. (2010, p. 5)

In robotic applications, vibrations are probably the most harmful and complex problem existing in working processes, that hurdle to achieving high accuracy in performing tasks. Flexible structures exhibit large vibrations in presence of external disturbances, which leads to a deterioration of positioning accuracy and efficiency. Therefore, it is crucial to understand the mechanisms of grinding vibration and its dynamical behavior in order to suppress vibration effectively. Furthermore, vibration modes shapes, and frequencies of flexible robots vary over the robot's workspace. Controllability of the structural vibration is also configuration-dependent to stabilize the grinding process. Some other specific conditions such as depth of cut, cutting force, and cutting power are also needed to put into consideration in order to improve its operational efficiency.

Operational contact forces (Viet Hung Vu, Liu, Thomas, Tahvilian, & Hazel, 2015) are believed another factors contributing to the instability of the grinding process. To make robotic manipulators function intelligently, accurate estimation of the end-effector force is very important. Specifically, for robot compliance control schemes, such as force control or impedance control, the acquisition of contact forces is a critical issue, and the performance of the system is directly related to the accuracy of contact forces. The control of force, as well as the position of the end-effector in a manipulator, has become a crucial requirement in many applications.

In addition, overlapping grinding passes at the contact zone can be a source of vibration amplifications, which leave a wavy surface on the workpiece. Therefore, an accurate characterization of contact force parameters during operation is important for structural analysis and minimizing the deformation during the grinding process induced by the interaction force between the tool and the workpiece.

1.2 Scope of study and objectives

In the light of the problems and motivations discussed in the previous section, the investigation will progress through a series of tasks and objectives designed to facilitate the effective delivery of the thesis. The goal of this work is to resolve the force estimation problem and the operational modal parameters identification with an emphasis on the damping ratio in order to provide a better understanding of the dynamical behavior of SCOMPI robot under grinding conditions. Therefore, the main objective is broken down into a series of specific objectives with intermediate validation and given in the following details tasks:

- As the robot body is flexible, its modal parameters are crucial to the dynamical behavior at the end effector. However, the dynamic parameters of a machine tool under the operating state are different from those under a static state. It is more representative to use the dynamic parameters in the operating state to simulate the machining process and predict the machining stability. Therefore, an Operational Modal Analysis

approach must be considered for the estimation of structural modal parameters as well as its operational Frequency Response Functions (FRF).

- Despite the modern modal identification techniques, with the assistance of vibration measurement equipment, can provide accurate estimates of natural frequencies and mode shapes, the estimation of the modal damping ratio from ambient vibration data is more challenging. The synthesis of damping in structural systems and machines is extremely important if a model is to be used in predicting vibration levels, transient response, transmissibility, decay times, or characteristics in design and analysis that are dominated by energy dissipation. Therefore, the synthesis of modal damping ratios is the further target of the thesis.
- In industrial applications, establishing an identified dynamic model of a system is very important since the model can be applied in a variety of applications such as control, navigation system, and optimal design of a structure. However, one of the most important factors that influence the success of the parameter identification process is the selection of the model order. Since the modeling of SCOMPI system results in high-order models, which makes it complex in dynamic analysis, numerical calculation, and control design. Hence, the model order must be determined properly to obtain a dominant reduced model in which the essential characteristics of the real system can be preserved.
- In physical robot interaction, accurate estimation of the end-effector force is very important. As a result, another goal of this thesis is to focus on developing a new technique for estimating the time-varying forces acting in a structural system based on its response measurements only.
- Equally important, since robots are in contact with an unknown or poorly structured environment, controlling the interaction forces with respect to contact parameters is crucial, which helps us avoid surface damage such as burn, or chatter. Consequently,

the estimation of contact parameters at contact interfaces between the grinding cup and workpiece needs to be addressed.

1.3 Overview of the state of the art

In the previous sections, we have discussed the importance of understanding the dynamical behavior of a flexible robot via its vibration analysis and estimation of excitation force at the contact zone. As a result, a special attention is given to the force and its contact parameters estimation, while Operational Modal Analysis is carried out as the motivation for this thesis. In this section, we conducted a literature survey of the research on vibration control of flexible manipulator robots via operational modal analysis and force estimation. Since they are the foundation and the state-of-the-art for the development of the different solutions to tackle the all the problems that we have discussed above.

1.3.1 Vibration in grinding

The grinding process is regarded as an essential part of machining in the metal manufacturing industry. It is used to remove surface defects and material and to reduce the surface roughness for a better quality of the next process, which may be polishing or grinding. In industrial applications, machine tools are often vibrating as a result of the forces generated during the machining process. Many efforts have been made on vibration origin and mechanism study in machine tools. Part quality and production rate can be affected by the vibrations produced during the grinding operation. Metal cutting processes can entail three different types of mechanical vibrations:

- Free vibrations occur when the mechanical system is displaced from its equilibrium and then is allowed to vibrate freely. In metal removal operations, free vibrations appear, for example, at the acceleration or deceleration of the machine tool at the entrance or exit of the tool in the workpiece (Feldman, 1994; Nardini & Brebbia, 1983).

- Forced vibrations appear due to external harmonic excitation associated, for example, with an unbalanced shaft or by the periodical hitting of the tools' teeth on the workpiece. The effects of workpiece-wheel contact stiffness on machine vibrations have also been studied (Ghayesh, Amabili, & Farokhi, 2013; Shaw, 1985; Waki, Mace, & Brennan, 2009).
- Self-excited vibrations are produced due to a dynamic instability generated by the cutting process itself. When the destabilization of the process occurs, the vibration level grows quickly until a limit cycle is reached. This type of vibration is called chatter, which brings the system instability and is the most harmful and the least controllable type of vibration. Chatter vibration in cutting can occur when the "cutting process stiffness" is higher than the machine's dynamic stiffness (Merritt, 1965). There are four main factors that determine the appearance of chatter: cutting conditions, workpiece material properties, tool geometry, and the dynamics of the machine tool system and workpiece. Chatter has several negative effects, interrelated among them such as poor surface quality, part rejection, increased tool replacement needs, excessive tool wear or tool breakage, excessive noise, machine tool components damage, reduced material removal rate, more frequent maintenance needs, waste of materials, waste of energy, environmental drawback, increased production time, increased costs (Merritt, 1965; Quintana & Ciurana, 2011).

In order to maintain process stability and precision, the vibration is introduced into the grinding process needs to be monitored and controlled to achieve an optimum disengagement between the tool and a workpiece (DeLio, Tlustý, & Smith, 1992; Faassen, Doppenberg, N, Oosterling, & Nijmeijer, 2006; Khachan & Ismail, 2009; Movahhedy & Mosaddegh, 2006; Wiercigroch, Wiercigroch, & Budak, 2001; Yao, Mei, & Chen, 2010). Much research has been done and focused on understanding the effects of chatter on the machine dynamics through experimentally derived stability criteria for vibration amplitude growth as a function of the machine stiffness, wheel-workpiece contact stiffness, wheel, and rotating speed, etc. (Beri

& Stepan, 2018; Peng, Wang, & Liao, 2015; Quintana, Ciurana, Ferrer, & Rodriguez, 2009; Vela- Martínez, Jáuregui-Correa, Rubio-Cerda, Herrera-Ruiz, & Lozano-Guzmán, 2008).

1.3.2 Operational modal analysis

Modal analysis has been significantly applied in many fields such as structural dynamics modification, analytical model updating, optimal dynamic design, vibration control, as well as vibration-based structural health monitoring in aerospace, mechanical and civil engineering. The traditional method called Experiment Modal Analysis (EMA) (Brown, Allemang, & Zimmerman, 1979) makes use of input (excitation) and output (response) measurement to estimate modal parameters such as natural frequencies, damping ratios, mode shapes, and modal participation factors. EMA has obtained substantial progress in the last few decades. Various modal identification algorithms, from Single-Input/Single-Output (SISO), Single-Input/Multi-Output (SIMO) to Multi-Input/Multi-Output (MIMO) techniques in Time-Domain (TD), Frequency Domain (FD), and Spatial Domain (SD) have been developed. However, there are some limitations of the EMA technique such as Frequency Response Function (FRF) or Impulse Response Function (IRF) would be very strenuous or even impracticable measure in large structures or in real operational conditions. In flexible structures, the dynamic parameters obtained by traditional EMA in the static state may not represent the real dynamic of the machine tool structure in operation. Especially excitations are impossible to measure during operation since they can have various sources all at the same time (Figure 1.4).

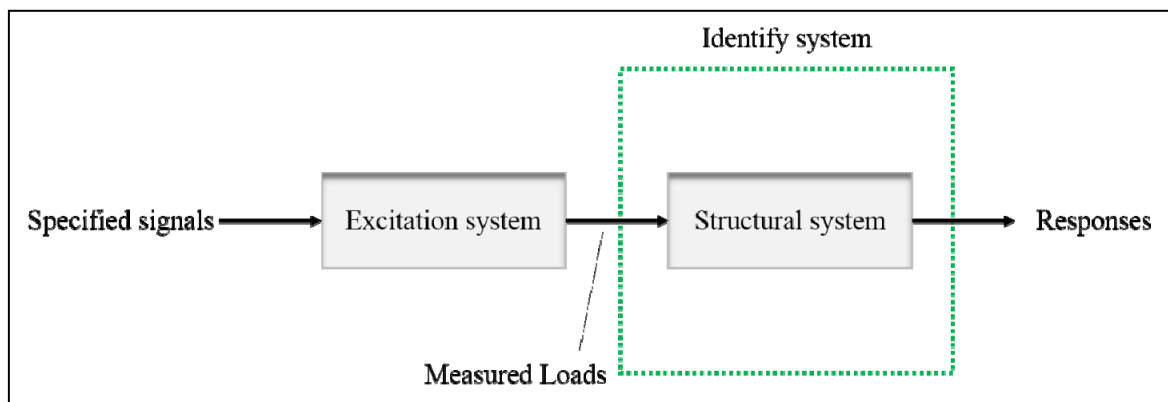


Figure 1.4 System scheme for classical Experimental Modal Analysis approach
Taken from Motte et al. (2015, p.10)

In recent years, there are numerous researchers switch to another technique namely Operational Modal Analysis (OMA) (Quintana et al., 2009). The field of Operational Modal Analysis has recently become an emerging research interest. OMA is a technique to identify modal parameters of a structure from output response only. It is an emerging field in structural dynamics and has replaced traditional EMA techniques in complex structures where the EMA method is difficult to apply. Furthermore, the implementation of OMA has resulted in the development of modal analysis applications. The principle uncommon between OMA and EMA is the source of the applied forces. In EMA, the system is tested under the known applied forces and the input force is measured while in OMA the system is tested in its real working situation under ambient forces, and consequently, the test is carried out with no measurement of the inputs. With OMA the modal parameters are extracted by processing only the system response data (Figure 1.5). This novel technique processes the identification of modal parameters such as natural frequencies, damping ratios, structural modes directly from only output responses of the system without having to know the excitation forces (Quintana et al., 2009; V. H. Vu, Thomas, Lakis, & Marcouiller, 2011). This technique becomes especially useful in situations where the measurement of input forces to the system is either infeasible or extremely complicated.

According to (Masjedian & Keshmiri, 2009), OMA has been the center of deliberation in civil, mechanic, and aerospace engineering since many years ago, because of its following main benefits:

- Compared with the EMA test, the ambient test is less expensive and does not need excitation and boundary conditions simulation.
- With OMA, the dynamic characteristics of the whole system are achieved, instead of just a part of it.
- Due to the use of real random forces applied to different points of structure, a linear model is obtained around the operating conditions rather than experimental conditions.

- OMA is an appropriate method for complex and complicated structures because in this method the analysis is essentially a Multi-Input Multi-Output (MIMO) analysis, repeated or close modes can be easily identified.
- Owing to its online application, OMA can be used for vibration control of the structures as well as damage detection and health monitoring.

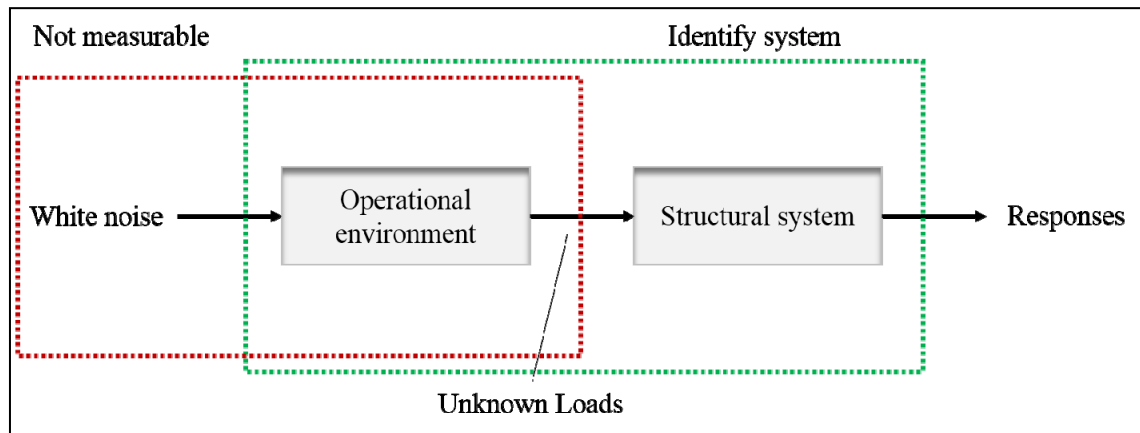


Figure 1.5 System scheme for Operational Modal Analysis
Taken from Motte et al. (2015, p.10)

In the past few decades, there have been numerous studies conducted on different methods and applications of OMA, and thousands of articles have been published in this field. Many researchers compared the different methods of OMA and figured out the advantages of these methods, based on industrial applications. Herman illustrated that none of OMA's existing methods are the ideals for all applications. This means that each application needs a specific method (Hermans & Van Der Auweraer, 1999). There are several algorithms for modal parameters estimation from output-only data have introduced in the literature. These algorithms can be divided into three classes based on the domain they work with, for example, the time domain, frequency domain, and spatial domain. However, the time domain is more suitable for operational modal analysis and can be classified into two groups. The first group lies in the fitting of the response correlation functions, including the Ibrahim Time Domain (ITD) method (Ibrahim & Mikulcik, 1977), the Least Square Complex Exponential (LSCE) method (Brown et al., 1979), the Covariance-driven Stochastic Subspace Identification (SSI-

COV) method (Peeters, 2000), and several modified versions of these methods for different applications, particularly under harmonic excitations (Gagnon, Tahan, Coutu, & Thomas, 2006; Mohanty & Rixen, 2004). Other methods, based on parametric models, require choosing a mathematical model to idealize the structural dynamic responses. Parametric model-based structural identification methods involve the use of mechanical models to represent structural system behavior in either time or frequency domain.

- **Time domain**

The equation of motion is traditionally given in the time domain. For a general multi-degree of freedom (MDOF) system the equation of motions is:

$$[\mathbf{M}][\ddot{\mathbf{y}}(t)] + [\mathbf{C}][\dot{\mathbf{y}}(t)] + [\mathbf{K}][\mathbf{y}(t)] = [\mathbf{f}(t)] \quad (1.1)$$

where $[\mathbf{M}]$, $[\mathbf{C}]$, and $[\mathbf{K}]$ symbolizes the constant mass, damping and stiffness matrix for the system respectively. $[\ddot{\mathbf{y}}(t)]$, $[\dot{\mathbf{y}}(t)]$ and $[\mathbf{y}(t)]$ symbolizes the acceleration, velocity, and displacement respectively, $[\mathbf{f}(t)]$ symbolizes the force vector. The solution for the dynamic parameters of the MDOF system is represented by different modes, which relates to the relative displacement of the system's degree of freedom. Each mode has a natural frequency (ω_n) and a damping ratio (ζ). One way to extract these dynamic parameters is to solve the differential equation (1.1). This difference equation is assumed to have a solution on the form (Box, Jenkins, Reinsel, & Ljung, 2015).

$$[\mathbf{y}(t)] = [q]e^{\lambda t} \quad (1.2)$$

Derivative of the displacement gives:

$$[\dot{\mathbf{y}}(t)] = \lambda [q]e^{\lambda t} \quad (1.3)$$

$$[\ddot{\mathbf{y}}(t)] = \lambda^2 [q]e^{\lambda t} \quad (1.4)$$

Putting equation (1.2), (1.3) and (1.4) into equation (1.1) and assuming the system is unloaded ($\mathbf{f}(t) = 0$) gives:

$$(\lambda^2 [\mathbf{M}] + \lambda [\mathbf{C}] + [\mathbf{K}])q = [0] \quad (1.5)$$

The solution of equation (1.5) depends on the damping of the system. For most civil structures and mechanical system, the damping of the system is underdamped which means that the solution for λ is a complex conjugate pair. One of the solutions are:

$$\lambda_k = -\zeta\omega_n \pm \sqrt{1-\zeta^2}\omega_n i \quad (1.6)$$

Which gives:

$$\omega_n = |\lambda_k| \quad (1.7)$$

$$\omega_d = \text{Im}(\lambda_k) \quad (1.8)$$

$$\zeta = -\frac{\text{Re}(\lambda_k)}{|\lambda_k|} \quad (1.9)$$

- **Frequency domain**

By applying the Fourier transform, to equation (1.1) it becomes a set of linear algebraic equations (Box et al., 2015).

$$(-\omega^2 [\mathbf{M}] + i\omega[\mathbf{C}] + [\mathbf{K}])[\mathbf{Y}(\omega)] = [\mathbf{F}(\omega)] \quad (1.10)$$

where $[\mathbf{Y}(\omega)]$ and $[\mathbf{F}(\omega)]$ are the Fourier transform of $[\mathbf{y}(t)]$ and $[\mathbf{f}(t)]$ respectively and i is the imaginary unit. By introducing the frequency response function (FRF) $\mathbf{H}(\omega)$:

$$[\mathbf{H}(\omega)]^{-1} = -\omega^2 [\mathbf{M}] + i\omega[\mathbf{C}] + [\mathbf{K}] \quad (1.11)$$

Substituting equation (1.11) into equation (1.10) gives:

Which means that the FRF represents the ratio between the Fourier transforms of the input and the output:

$$[\mathbf{H}(\omega)] = \frac{[\mathbf{Y}(\omega)]}{[\mathbf{F}(\omega)]} \quad (1.12)$$

Ambient vibration test with Operational Modal Analysis (OMA) method is very powerful to estimate dynamic characteristics of structure, which can provide very accurate estimates of natural frequencies and mode shapes. It is usually observed that the corresponding damping

estimates present a significant scatter (Magalhães, Cunha, Caetano, & Brincker, 2010). The amplitude of vibrations at resonance depends on these values inversely and have a strong influence on the structural dynamic behavior. Papageorgiou and Gantes were presented a work that was to come up with equivalent modal damping ratios and used them in analysis of irregularly damped structure (Papageorgiou & Gantes, 2010). By contrast, Huang et al. proposed a method to extracted modal damping ratios from a complex valued procedure and their validity in a real valued analysis procedure (Huang, Leung, Lam, & Cheung, 1996). As we can see all structure exhibits some forms of damping, but despite a large literature on the damping, it remains one of the least well-understood aspects of general vibration analysis. Therefore, more attention should be paid to synthesis this modal factor.

1.3.3 Time series model

A time-series represents a collection of data points captured over time. This type of data is actively studied in many fields of application, such as healthcare, mechanical, signal processing, finance, energy, and climate (Box & Pierce, 1970; Brockwell & Davis, 2002; Harvey, 1990; Leonard & Wolfe, 2005; Wei, 2006). The generalized interest in time series arises from the dynamic characteristics of many real-world phenomena, where events naturally occur and evolve over time. A time series can be continuous or discrete. The usual process for time series analysis and forecasting is:

- Preprocess data for analysis. The preprocessing stage may involve some initial analysis steps e.g., plotting data, determining time series characteristics such as trends, seasonality, etc.
- Determine a suitable model for the preprocessed time series.
- Apply/fit the model to time series data.
- Perform forecasting and prediction of future values of time series.

In essence, time series models are used for predicting or forecasting the future behavior of variables (Brockwell & Davis, 2002). According to (Leonard & Wolfe, 2005), other

applications of time series models include separation (or filtering) of noise from signals and predicting one series from observations of another. Models for time series data can have many forms and represent different stochastic processes. Since there are various types of time series data (i.e stationary vs. non-stationary, linear vs. nonlinear, seasonal vs. non-seasonal, etc.) (Brockwell & Davis, 2002; Wei, 2006), it is necessary to select an appropriate model, estimate its parameters, and validate the model's sufficiency and accuracy by generated uncorrelated residual (Box *et al.*, 2015).

There is a numerous number of research have been applied time series analysis methodology in various fields, especially to detect, locate and estimate the extent of the structure changes under working conditions (Fassois, 2001; Gul & Catbas, 2011; Liu, He, & Chen, 2012; Moore, Lai, & Shankar, 2007a, 2007b; Soderstrom, Fan, Carlsson, & Bigi, 1997). These methodologies usually make use of AR (Auto-Regressive), ARX (Auto-Regressive models with eXogenous outputs) and/or ARMA (Auto-Regressive Moving Average) models. The AR model is known as the simplest time series representation that linearly depends on the output data (the vibration responses). In the availability of both the input (the measurable and known excitation force) and output data, the ARX model is usable. It is possible to combine these models with the MA term and produced an ARMA representation for the output-only cases and the ARMAX model for the input-output conditions. The general parametric model is introduced by (Box *et al.*, 1974) where the input $\mathbf{u}(t)$, the output $\mathbf{y}(t)$, and the noise $\mathbf{e}(t)$ are modeled by parameters of the model via a regressor operator z . In vibrational applications, the input plays the role of excitation while the outputs are dynamic responses.

The general formulation of a time series model by incorporating the input, output, and error terms is expressed as follows:

$$\begin{aligned} y(t) + a_1y(t-1) + \dots + a_p y(t-p) = \\ = b_1u(t-1) + \dots + b_q u(t-q) + e(t) + c_1e(t-1) + \dots + c_r e(t-r) \end{aligned} \quad (1.13)$$

where $\mathbf{u}(t)$ and $\mathbf{y}(t)$ denote the input and output data at the time t , $\mathbf{e}(t)$ is the residual sequence, which corresponds to the difference between the measured time-series data and the predicted one gained by the model. This model is referred to as ARMAX (Autoregressive Moving

Average with eXogenous excitation) and is consider the model complete for vibration modeling (Figure 1.6a). In equation (1.13) $\mathbf{A} = [a_1 \dots a_p]$, $\mathbf{B} = [b_1 \dots b_q]$, $\mathbf{C} = [c_1 \dots c_r]$, represent the unknown parameters of the model. Moreover, the orders of output, input, and error terms are defined as p , q , and r , respectively. It is possible to rewrite equation (1.13) as more compact form as follows:

$$\mathbf{A}(z)\mathbf{y}(t) = \mathbf{B}(z)\mathbf{u}(t) + \mathbf{C}(z)\mathbf{e}(t) \quad (1.14)$$

where $\mathbf{A}(z)$, $\mathbf{B}(z)$ and $\mathbf{C}(z)$ are polynomials in the delay operator z^{-1} , which can be formulated as:

$$\mathbf{A}(z) = 1 + a_1 z^{-1} + a_2 z^{-2} + \dots + a_p z^{-p} \quad (1.15)$$

$$\mathbf{B}(z) = 1 + b_1 z^{-1} + b_2 z^{-2} + \dots + b_q z^{-q} \quad (1.16)$$

$$\mathbf{C}(z) = 1 + c_1 z^{-1} + c_2 z^{-2} + \dots + c_r z^{-r} \quad (1.17)$$

As a note, it would be interesting to know equation (1.14) refers to the formulation of ARMAX. Since excitation is not always measurable, it is necessary to have a model to perform an operational modal analysis without knowing the excitation forces. The model ARMA (Figure 1.6b) is now considered an ambient excitation in order (p, q) . For the identification of the modal parameters (frequency and rate of damping), these models are widely used in the form of a univariate model with a single channel of measure (Smail, Thomas, & Lakis, 1999).

$$\mathbf{A}(z)\mathbf{y}(t) = \mathbf{C}(z)\mathbf{e}(t) \quad (1.18)$$

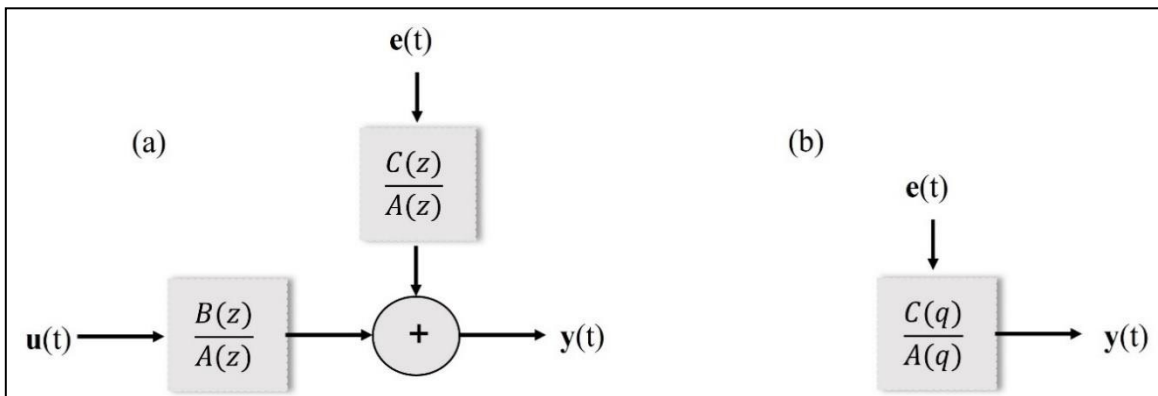


Figure 1.6 System scheme of ARMAX model (a) and ARMA model (b)

Taken from Box et al. (2015, p. 75)

In fact, the operational modal analysis concerns the identification of the modal parameters from the vibrational responses only, and the autoregressive part contains all modal parameters information. Since the ambient excitation is assumed to be of type white Gaussian, we can reduce the model to the output only and the ARMA model becomes the AR (Figure 1.7b). The noise becomes the error of the self-regulating model and denotes as $\mathbf{e}(t)$.

$$\mathbf{A}(z)\mathbf{y}(t) = \mathbf{C}(z)\mathbf{e}(t) \quad (1.19)$$

Also, the AR model can replace the ARMA model if its order is chosen sufficiently high (Box *et al.*, 1974).

In the case of $r = 0$, the error term or $\mathbf{C}(z)$ is removed from the equation (1.14), the model becomes ARX. The estimation of an ARX model is the most efficient of the polynomial estimation methods because it is results from solving linear regression equation in analytic form. When the noise is small, it can reach to high system accuracy. In contrary, when the noise is a little big, the order of the model can be raised appropriately to compensate the influence on the system identification accuracy from noise. The ARX model has the form as follows:

$$\mathbf{A}(z)\mathbf{y}(t) = \mathbf{B}(z)\mathbf{u}(t) + \mathbf{e}(t) \quad (1.20)$$

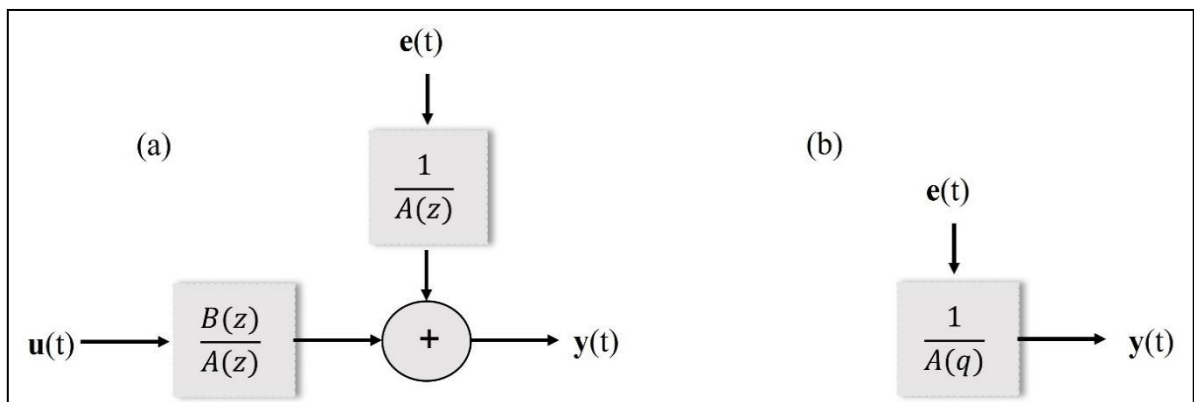


Figure 1.7 System scheme of ARX model (a) and AR model (b)
 Taken from Box *et al.* (2015, p. 75)

There are many applications of ARX model (Figure 1.7a) in the literature. For example, Lu and Gao used a modified ARX model for damage identification by choosing the acceleration

response at one location as the input to their ARX model to predict the outputs at the other locations of the structure. Then a similar model is used to predict the outputs of the damaged structure. For verifying their methodology, the researchers used two shear-type numerical spring-mass models to validate their results and showed that their approach was successful in the identification of the damage in those models for noise-free data (Lu & Gao, 2004). In another study, Mustafa Gull et al, presented two different approaches based on ARX models to estimate the extent of the damaged structure. For the first approach, the coefficients of the ARX models are directly used as the Damage Features (DFs) to detect the damage on 4 DOF numerical models. A second approach is presented based on using ARX model fits ratios as the DFs in case of considering the effect of noise and flexible model. The second approach is first applied to the same 4 DOF numerical model and then applied to the experimental data (Gul & Catbas, 2011). Or Liu Huaiyuan et al., applied the least square method based on the ARX model, and Akaike Information Criterion (AIC) was used in the identification of model order, compared with the original model to study the fitting accuracy. Compared to other program identification methods, it has a short time modeling time, and it is clear, reliable, intuitive visual, and has good scalability (H. Y. Liu *et al.*, 2012). Equally important, ARX is regarded as an effective empirical model for estimating the input forces (excitation forces) applied to the structure. This technique involves obtaining an empirical relationship between the output response and input force data using system identification (S.Rajkumar, Bhagat, C.Sujatha, & S.Narayanan, 2015). Consequently, in this research, an ARX model was proposed for force identification and modal analysis of robot structure (Nguyen, Vu, & Thomas, 2022).

Stochastic Subspace Identification (SSI) is another well-known operational modal analysis (OMA) algorithm that works directly in time domain (Peeters & De Roeck, 2001). Subspace identification technique emerged from the field of system identification in system and control theory in the late 1980s. Katayama gives a detailed mathematical framework of subspace methods (Katayama, 2005). Recently, the fields of civil and mechanical engineering have adopted SSI it into their special case of system identification (Brincker & Andersen, 2006).

The model is based on state-space representation of a discrete linear time invariant (LTI) system described as:

$$\begin{aligned}\mathbf{x}_{k+1} &= \mathbf{A}\mathbf{x}_k + \mathbf{w}_k \\ \mathbf{y}_k &= \mathbf{C}\mathbf{x}_k + \mathbf{v}_k\end{aligned}\quad (1.21)$$

where \mathbf{y} is the vector of measured responses, \mathbf{x} is the vector of state variables matrix, \mathbf{A} is the state transition matrix, \mathbf{C} is the output matrix and \mathbf{w}_k and \mathbf{v}_k are process and measurement noise vectors.

As is clear from equation (1.21), SSI algorithm operates on measured output data only. From the point of view of modal parameter estimation, it is the estimation of state transition matrix \mathbf{A} that is most important as eigenvalue decomposition of this matrix reveals modal parameters. There are two variants of this algorithm that are popular in practice: Data-Driven (SSI-DATA) and covariance-driven (SSI-COV). These variants differ in terms of the data on which they operate. SSI-Data operates directly on measured output response data without processing it (Li, Vu, Liu, Thomas, & Hazel, 2017; V.-H. Vu, Liu, Thomas, & Hazel, 2015). On the other hand, SSI-COV required that covariance functions are first estimated from raw output time histories, and it is these covariance functions that SSI-COV utilizes for the purpose of modal parameters estimation (Reynders, Maes, Lombaert, & De Roeck, 2016).

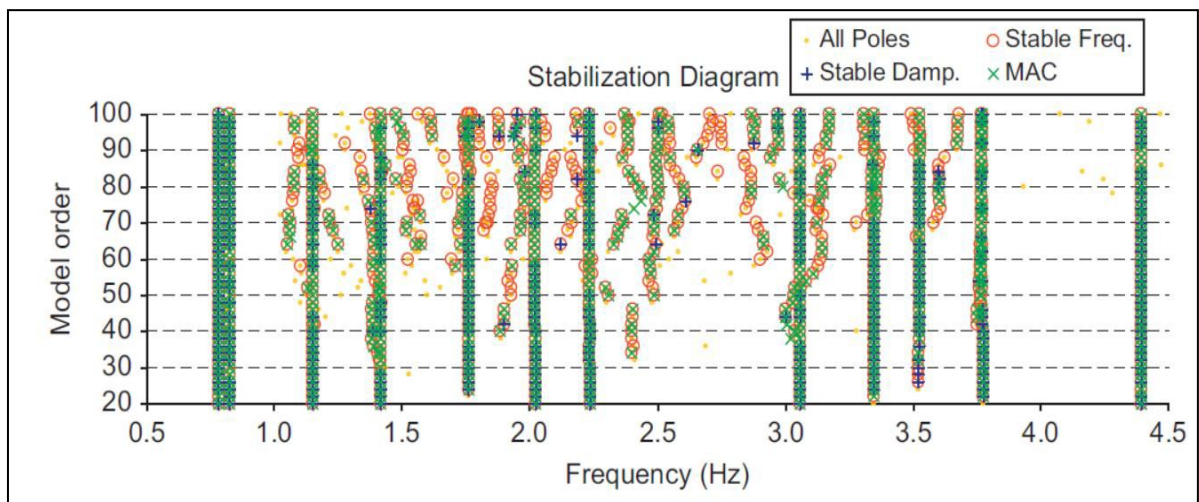


Figure 1.8 Stabilization diagram of time series analysis by SSI-COV method
Taken from Magalhães et al. (2009, p. 322)

When the model parameters are found, a stabilization diagram can be constructed (Figure 1.8). Hence the estimated natural frequencies are plotted for each order. Since the order of the system is overestimated, the plot will contain noise frequencies from the mathematical models. The aim of the stabilization diagram is to separate the physical poles from the computational poles. The computational poles tend to be more scattered and typically do not stabilize. Therefore, physical modes can be determined from an alignment of stable poles. To find these alignments you need to separate the stable poles from the unstable ones. This is based on the comparison of the poles associated to a given model order with those obtained from a one-order lower model (Box *et al.*, 2015).

The natural frequencies and damping ratio of poles from two orders are compared:

$$\frac{|\omega(n-1) - \omega(n)|}{\omega(n-1)} < x \quad (1.22)$$

$$\frac{|\zeta(n-1) - \zeta(n)|}{\zeta(n-1)} < y \quad (1.23)$$

Only the poles that fulfill a stabilization criterion defined by the user (x and y) are labeled as stable. The size of these depends on several factors, among them the structure complexity and measurements accuracy. For natural frequency the values should coincide well, and a low stability requirement should be used. However, for damping ratios the values can vary more and are difficult to estimate compared to natural frequencies of system. Especially for lightly damped modes where their percentage variation could be relatively large. The value should initially be chosen relatively small and then increased if needed.

1.3.4 Kalman filter

The Kalman filter is a recursive filter that estimates the states of the dynamics of a system by noisy measurement. It was published in 1960 by Rudolf E. Kalman and is now used in numerous applications of engineering, economics, and science (Kalman, 1960). This filter originally started as a solution to the state estimation problem in linear time-invariant state-

space model structures, in which a linear, stochastic dynamic system is represented by a set of differential equations. Its recursive algorithm that moves between a prediction step and an estimation. These steps generate states and associated errors of the system that are philosophically also referred to as a priori and posteriori. The Kalman filter estimates a state value through a process using a feedback control in the form of noisy measurements. The filter can also be referred to as a predictor-corrector algorithm. We highlight the flow of the algorithm in Figure 1.9.

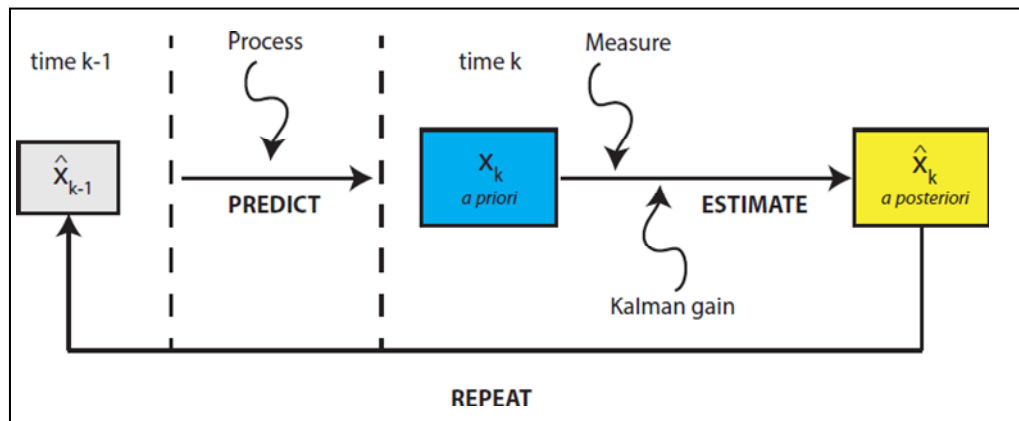


Figure 1.9 The block diagram of Kalman filter
Taken from Iqbal et al. (2019, p. 25)

Predicting the state

Consider the equation,

$$\mathbf{x}_k = \mathbf{G}\hat{\mathbf{x}}_{k-1} \quad (1.24)$$

This is the *Time update* equation or the *Prediction equation*. This equation predicts the current states from the previous estimates. Here, \mathbf{G} is the state transition matrix, \mathbf{x}_k is the prediction at the current time step and $\hat{\mathbf{x}}_{k-1}$ is the state estimate from the previous time step.

Similarly, the uncertainty associated with each state variable embedded in the error covariance matrix \mathbf{P} is also updated as given below.

$$\mathbf{P}_k = \widehat{\mathbf{G}}\mathbf{P}_{k-1}\mathbf{G}^T + \mathbf{Q} \quad (1.25)$$

where, \mathbf{P}_k is the predicted error covariance matrix at the current time step, $\widehat{\mathbf{P}}_{k-1}$ is the estimated state covariance matrix from the previous, and \mathbf{Q} is the process noise covariance matrix.

Correcting the prediction

The measurement update equations also referred to as the correction equations, act as a feedback channel to the filter's original prediction returned from the time update step. Following a set of equations perform the correction step for the filter for every application.

$$\mathbf{y}_k = \mathbf{z}_k - \mathbf{H}\mathbf{x}_k \quad (1.26)$$

$$\mathbf{K}_k = \mathbf{P}_k \mathbf{H}^T (\mathbf{H}\mathbf{P}_k \mathbf{H}^T + \mathbf{R})^{-1} \quad (1.27)$$

$$\hat{\mathbf{x}}_k = \mathbf{x}_k + \mathbf{K}_k \mathbf{y}_k \quad (1.28)$$

$$\mathbf{P}_k = (\mathbf{I} - \mathbf{K}_k \mathbf{H}) \mathbf{P}_k \quad (1.29)$$

An alternative flow chart of this entire process is exhibited in Figure 1.10.

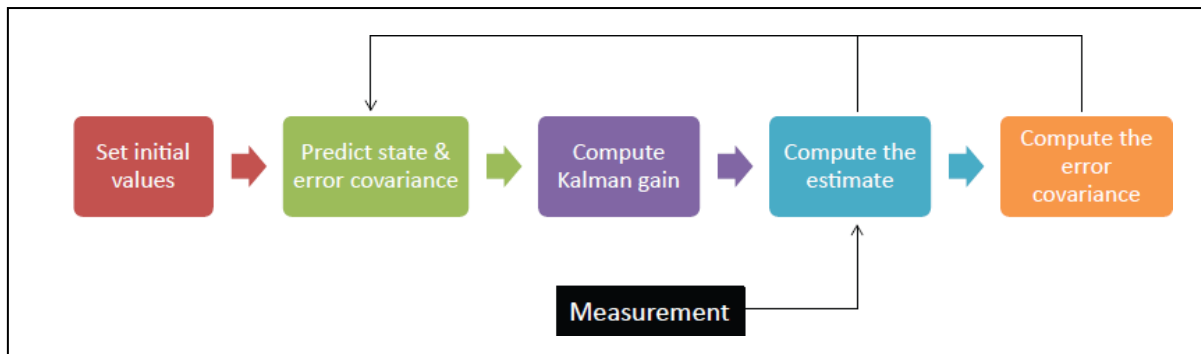


Figure 1.10 An alternative flow chart of the Kalman Filter algorithm
Taken from Iqbal et al. (2019, p. 27)

Since this filter is a linear and optimal estimator, and due to its widespread use in problem-solving, it became necessary to extend its use to nonlinear systems. Since its creation, the Kalman filter has been modified several times to provide a better response, solve some operational limitations, and tackle more complex problems. The Extended Kalman Filter was created in 1966 (Sorenson, 1966) to reduce the dimensionality of the state estimation without overlooking the effects of the additional state on the calculation of the covariance matrix and Kalman gain. In the engineering field, most of the problems to be solved have nonlinear characteristics. The mechanism employed by the EKF, therefore, leads to a series of approximation problems (Julier & Uhlmann, 1997; Wan & Merwe, 2000). An improvement in

this sense is achieved by using the Unscented Transform (UT), creating the Unscented Kalman Filter (UKF), which is based on the premise that it is easier to approximate a probability distribution than an arbitrary linear transformation. This modification consists of selecting a group of deterministic points in the state space, called sigma points to capture some of the inherent properties of the distributions to be estimated.

The Kalman filter and its variants have been used in a wide range of tasks including all forms of navigation, nuclear plant instrumentation, demographic models, and manufacture. Among others, robotics has been one of the fields that have benefited the most from this filter and its variant in different areas that range from parameters identification and robot control to the autonomous navigation of mobile robots. In (Minchul & Dongsoo, 2015), it is employed to estimate the angular velocity of a motor in the low-speed range and in the presence of random external disturbances. Several types of robots employ the KF or one of its subsequent modifications in tasks such as determining the position and orientation of a vehicle at any moment, denominated localization, which is crucial to achieving autonomous, reliable, and robust navigation (Khatib, Jaradat, Abdel-Hafez, & Roigari, 2015; Odry, Fuller, Rudas, & Odry, 2018). The Augmented Kalman filter (Lourens, Reynders, De Roeck, Degrande, & Lombaert, 2012) or a Dual Kalman filter (Eftekhar Azam, Chatzi, & Papadimitriou, 2015) are another modified version of Kalman for identifying the states of unknown input force of a linear state space model by using sparse noisy acceleration measurements. In this thesis, a Kalman filter is proposed to inversely estimated input force of SCOMPI robot under machining operation with the assistance of model identification technique. Further development is applied for contact force parameters identification by using Unscented Kalman Filter to deal with nonlinear contact force model.

1.3.5 Force estimation technique

Inverse problems such as input estimation from the responses (acceleration, velocity, or displacement) of structure play a crucial role in many applications where the input forces acting on structures cannot be measured directly due to the difficulty of installation and dynamic

characteristic altering problems. Meanwhile, the response data can be easily obtained by using transducers such as strain gauges, vibrometers, or accelerometers. Estimation of force excitation is highly essential in obtaining optimal structural design, noise suppression, vibration control as well as condition monitoring. For instant, the wind excitation load on a multi-story building or dynamic vehicle load acting on a bridge, etc. Therefore, force estimation using the inverse method has been developed widely to solve these problems. Identification of the input forces and their locations is helpful to identify areas that are more susceptible to damage, especially in flexible structures. The amplitude of force reflects the vibration condition of the structure so that any requirements for stiffening or structural modification can be identified to preserve better structural integrity. Stevens has presented an outline of force estimation for the discrete and continuous linear vibration system (Stevens, 1987). The force estimation method is used to predict the unknown force from the dynamic response, measured using accelerometers (Hollandsworth & Busby, 1989) or strain gauges (Ödeen & Lundberg, 1991). Hillary and Ewins conducted the study on the estimation of sinusoidal load excited on a cantilever beam and based on the least-squares identification technique by the use of strain gauges, they calculated the impact forces on aircraft engine turbine blades (Hillary, 1984). Many dynamic force estimation methods have been developed and a great number of them can be categorized into the direct method and the optimization method. The direct method identifies excitation force directly by multiplying the system's inverse Frequency Response Function (FRF) with the measured responses. It can be distinguished into two types, i.e., FRF-based direct inverse method and Modal Transformation Method (MTM). In general, the FRF-based direct inverse method has advantages over the MTM in terms of force estimation accuracy. Meanwhile, the optimization method finds the unknown input force by matching the estimated and measured responses. In practice, the optimization method requires higher computational and training time compared to the direct method (Khoo *et al.*, 2014).

There are many other regularization methods, for example, sum of weighted acceleration technique. It is one of the methods used in force estimation with the measured linear or nonlinear structural response, where the input forces are obtained by determining the weights

or weight factors, while the input forces are obtained by summing the product of acceleration values with suitable weight factors in the time domain. When acceleration data can be obtained by using accelerometers, this method can be adopted very easily (Rainieri & Fabbrocino, 2014; Wang & Kreitinger, 1994). In another approach, Pseudo Inverse Technique is regarded as an accurate and effective tool for determining the forces in the frequency domain from measured FRF, where the FRF is obtained by exciting the system with a known input force. S.Y.Khoo et al. applied an algorithm that is able to inverse a non-square matrix. This is applicable to different cases i.e., under-determined, even determined, and over-determined cases (Khoo *et al.*, 2014). Based on Kalman Filter and a recursive least-squares algorithm, Ma et al. used an online recursive inverse method to estimate the input forces of beam structures (C. K. Ma, Chang, & Lin, 2003). S.Rajkumar has also applied the Kalman filter technique for estimation of input force and computation of frequency response function (FRF) from measured response data. This technique involves modeling the system in the state space form, where displacement and velocity are considered to be the two states of the system; also, parameters like stiffness, and damping ratio should be known prior to estimate the input force acting on the system (Rajkumar, 2015). Similarly, Jui-Jung Liu was applied the Kalman Filter technique to determine the input force of a mechanical grey-box model from the measured systematic response by an inverse algorithm (C.-K. Ma, Tuan, Lin, & Liu, 1998). By comparison, the Kalman filter technique is more accurate than that estimated by other methods for various types of input excitation such as sweep input and random load.

From the literature review on the force identification topic, especially on the flexible manipulators, it is clearly seen that the research on this domain is still limited. Particularly, there is no research of SCOMPI robot has been working on estimating the dynamical contact force under machining conditions. Only (Rafieian, Hazel, & Liu, 2014) has constructed vibro-impact cutting model in consideration of material removal rate and depth of cut for analyzing vibratory dynamic of the robot. Therefore, more attention should be paid to the exploitation of this approach.

1.3.6 Contact force parameters identification

Controlling the physical interaction between a robotic manipulator and the environment is crucial for the successful execution of a plethora of practical tasks where the robot's end-effector must manipulate an object or perform some operation on an unknown object. Today's industrial robots are almost always programmed using a position control scheme. Typically, the end effector follows a designed trajectory in space that has been pre-defined or "taught" before run-time. However, for some applications, it is more important to precisely control the force applied by the end-effector rather than controlling the robot's position.

A robot that is required to interact with its environment can be modeled as a robot with an unequally constrained motion (Choi & Krishnamurthy, 1994; Grabbe, Carroll, Dawson, & Qu, 1992) because this interaction often involves both contact and free space motion. This means that when the distance x between the robot's end-effector and a contact surface is greater than zero the force F_c is equal to zero (see Figure 1.11), and when the distance x is zero then $F_c > 0$.

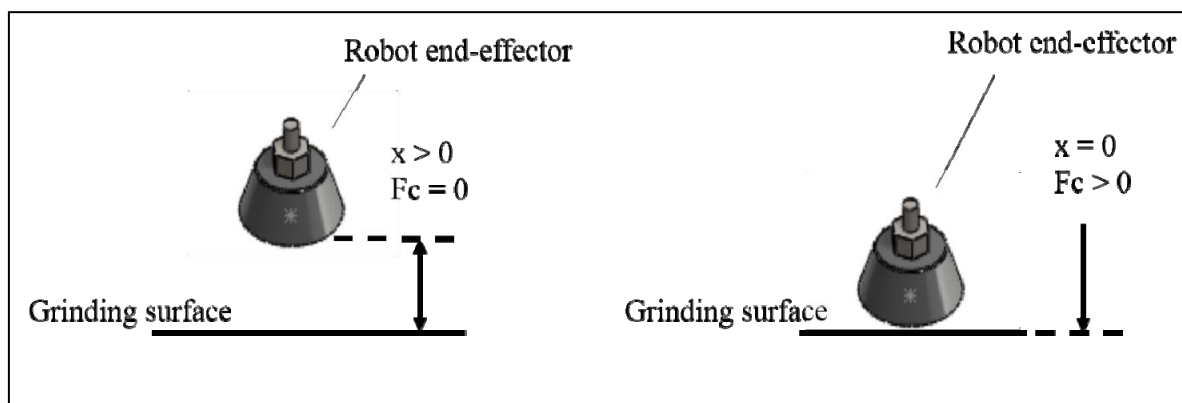


Figure 1.11 Unequally constrained robot. Free motion (left), contact (right)
Taken from Arevalo Reggeti et al. (2017, p. 15)

Before going any further, it is important to differentiate between contact and impacts, as these two phenomena usually have very different treatments in the literature. The impact is a complex phenomenon that occurs when two or more bodies undergo a collision (Flores &

Ambrósio, 2010; Sánchez, Le, Liu, Zemiti, & Poignet, 2012) and it is characterized by very short duration, rapid energy dissipation, large acceleration (positive and negative), and very high force levels. On the other hand, contact is a term used to describe a situation where two or more bodies come in touch with each other, and it implies a continuous process that takes place over a finite time. Note that contact may include an impact at the beginning of the process, but an impact is always described as a very short event.

In the related literature, there are basically two types of approaches to describe the impact. The first type is referred to as the impulse-momentum method, and the second is as force-based method (Flores & Ambrósio, 2010). The first class of methods cannot be easily applied to robot interaction tasks, although recent studies have successfully used this approach in simulation through the solution of complementarity problems. There has been research studied the vibro-impact behavior governing material removal performed by a compliant robot SCOMPI. The grinding force and power are formulated based on the impacting dynamics of material removal (Rafieian, Hazel, & Liu, 2014). However, this method has some limitations since it requires additional relations and constraints to be imposed such as zero velocity in the tangential direction, which does not hold in some cases, especially in high-velocity impacts where deformation is a common phenomenon. On the other hand, the force-based method was coming up as an alternative solution to generally describe the contact force.

$$\mathbf{F}_c = \mathbf{F}_v(\dot{\mathbf{x}}) + \mathbf{F}_d(\mathbf{x}) \quad (1.30)$$

where \mathbf{F}_c is a function of the local deformation, which is modeled as a displacement x . \mathbf{F}_v and \mathbf{F}_d are the reaction forces proportional to the indentation and velocity of indentation respectively

- Spring-dashpot model

$$\mathbf{F}_c = b\dot{\mathbf{x}} + k\mathbf{x} \quad (1.31)$$

In this model, the contact force is modeled as a linear spring and a linear damper connected in parallel, to ensure elastic behavior and energy dissipation (Skrinjar, Slavič, & Boltežar, 2018).

- Hertz's model

$$\mathbf{F}_c = \mathbf{F}_{c,\max} \left(\frac{\mathbf{x} - \mathbf{x}_p}{\mathbf{x}_{\max} - \mathbf{x}_p} \right) \quad (1.32)$$

where $\mathbf{F}_{c,\max}$, and \mathbf{x}_{\max} are the maximum normal force and indentation respectively, \mathbf{x} is the local indentation and \mathbf{x}_p is the permanent indentation. It is important to note that although it is referred to as Hertz's model, this model is an adaptation of Hertz's original model to include permanent deformation, which was not considered by Hertz (Muthukumar & DesRoches, 2006).

- Nonlinear damping model

$$\mathbf{F}_c = b\mathbf{x}^p\dot{\mathbf{x}}^q + k\mathbf{x}^n \quad (1.33)$$

This model is very similar to the spring-dashpot model, with the particularity that speed depends linearly on the speed and the position (Mu & Sharf, 2007; Vukobratović & Potkonjak, 1999).

Based on this foundation, multiple research projects have been done on environment parameters estimation. The method can be differentiated according to the contact models assumed, the estimated approach, and the interaction control system by using obtained data. Derived from the concept of Virtual Contact Manipulators (VCM) (Bruyninckx, Demey, Dutré, & De Schutter, 1995), geometric contact models were developed for the contact between generally curved surfaces. Dedicated geometric models for polyhedral contact, which were established as limit cases in (Bruyninckx et al., 1995) were developed in (Lefebvre, Bruyninckx, & Schutter, 2003). Early efforts in contact modeling and identification were partly based on work at the University of Victoria and focused on modeling contact dynamics for objects with simple geometries (Di Renzo & Di Maio, 2004; D. Erickson, Weber, & Sharf, 2003; J. S. Erickson, Sundaram, & Stebe, 2000; Mu & Sharf, 2007; Van Vliet, Sharf, & Ma, 2000), and complex, known geometries (D. Erickson et al., 2003; Weber, Patel, Ma, & Sharf, 2005). The initial focus was on the identification of stiffness, damping, and mass parameters, while modeling and identification of friction were also considered later (Weber *et al.*, 2005). Eventually, nonlinear contact models were also considered (Mu & Sharf, 2007). At the same time, other research revealed that geometric uncertainties can have a considerable effect on the identification of contact dynamics.

These observations led to the research focused on this thesis, which considers the identification of contact dynamics parameters. Better contact models and identification methods can improve the quality of the information that a robot receives from the environment. From texture differentiation to obstacle avoidance, especially in environments where visual feedback is not possible. It also can improve the feedback given to an operator. Moreover, high-quality tactile feedback is a must when a robot is contact with an unstructured environment. To make a robot safely interact with its environment, the robot's mechanical behavior should be selected according to the environment with which it will be in contact.

1.4 Originalities and contributions

The work performed in this thesis has produced the following contributions to the State of the Art:

- The first contribution of this thesis is the introduction of a new method for estimating unknown input force excitation on SCOMPI robot, which is developed through the combination of the Kalman Filter with the assistance of a system identification technique by using output measurement data only. This work is inspired by the original method in (C. K. Ma *et al.*, 2003). The original method was applied to a simple structure such as a beam, where all the structural properties are already known in advances such as mass, damping, and stiffness. Unfortunately, in complex structures such as flexible manipulators like SCOMPI robot, there is no knowledge of the system's detailed characteristics. Therefore, a novel technique is introduced in this thesis by integrating the model identification technique to obtain the model properties of the structure via a state-space model before applying the Kalman filter. The innovation point of the research is despite the ARX model is an input-output scheme, but we have modified the algorithm where only acceleration data were taken into account for the force identification. Different numerical simulations are employed to evaluate the performance of the proposed approach and prove its robustness in handling noisy

measurements. The method is proven to work well even in the case of 30% noise contaminated.

- In general, the time-domain technique will identify force in real-time history, but our force estimation methodology was going to a further step, to validate on both time and frequency domains and provided a good result. The estimated force in the frequency domain has proved its advantage over the force's measurement since the frequency diagrams clearly revealed some frequency components which cannot be captured by the dynamometer. The mathematical background and the details of the proposed method, and the simulation studies are explained in Chapter 2.
- In this thesis, the time series model is used to develop a new technique for operational modal analysis. According to the literature review, choosing a sufficient and correct model order has a significant impact on the performance of time series modeling. Consequently, a new algorithm for choosing an optimal model order is presented as another contribution to this thesis. This algorithm is not only helping the model successfully represent the underlying phenomenon of the structure with the lowest complexity but also useful for the validation of the inference procedures. This work comes up with a feasible and useful means square errors of estimated transfer frequency function approach that provides adequate and practical models at minimum order.
- Instead of working on the simple Auto-Regressive model as usual, this research presented a method to estimate the model order and it is added it to the framework of the ARMAX model. In this contribution, explicit expressions of the estimated transfer function are used for selecting an optimal order. It is derived to fit noisy measurement data, by marginalization over the error model or so-called under modeling errors, which do not capture by some original methods such as AIC or BIC. Technically, the optimal representative ARMAX model achieves demonstrably by white residuals. Therefore, the test by Autocorrelation and Partial Autocorrelation Function are implemented after choosing the optimal order set. Importantly, the computational burden on modal

parameters identification is significantly reduced. The robotic grinding system is also characterized by the real grinding operation to determine the modal properties of the system through the estimated low-order FRFs. The details of the algorithm are presented in Chapter 3.

- Finally, the work presented in this thesis contributions to the state of the art on dynamic contact modeling and identification. Instead of using a simple linear contact model, we formulated a nonlinear contact model for the stiff single point contact and demonstrates the feasibility of identifying contact parameters by using output measurement data only. The validity of the identification results is corroborated by a separated set of experiments under difference power levels. According to the literature review on existing on-line estimation algorithm, the Recursive Least Squares (RLS) method is perhaps the most commonly use online parameter estimation algorithms and is applied in many adaptive control designs. Unfortunately, the conventional RLS algorithm is limited in some cases where measuring inputs is difficult or impractical. Eventually, the estimated results of this method are heavily depending on choosing the forgetting factor, since it is very sensitive to measurement noise. To overcome shortcomings of the classical RLS, this thesis presented a Kalman Filter approach for contact force parameters identification.
- Importantly demonstrated via this thesis, the Kalman Filter exhibits in a different way by using Unscented Transform to deal with nature nonlinear characteristics of contact force model. Additionally, unlike the classical RLS methods, Unscented Kalman Filter (UKF) approach demonstrates robust estimation without using excitation signals, this makes the UKF approach very well suited for real time estimation applications and effectively in estimation of contact parameters. The developed contact force model can explain how contact parameters, including the contact stiffness, and damping affect the normal contact force. The results validation on SCOMPI robot have proved the feasibility of the proposed method in parameters estimation, leading to dramatically improve accuracy as compared to traditional RLS method.

These contributions have given place to the publications arising from this research in indexed scientific journals and conference paper listed below:

1. Nguyen, Quoc Cuong., Vu, Viet Hung., & Thomas, Marc. (2022). A Kalman filter based ARX time series modeling for force identification on flexible manipulators. **Mechanical Systems and Signal Processing**, 169, 108743. doi: <https://doi.org/10.1016/j.ymsp.2021.108743>
2. Nguyen, Quoc Cuong., Vu, Viet Hung., & Thomas, Marc. (2022). Optimal ARMAX Model Order Identification of Dynamic Systems, **London Journal of Engineering Research**, Volume 22, Issue 01, Compilation 1.0.
3. Nguyen, Quoc Cuong., Vu, Viet Hung., & Thomas, Marc. (2022). A nonlinear online identification of contact parameters: application to a flexible manipulator under grinding operation, **Journal of Dynamic System, Measurement, and Control**, Submitted.
4. Nguyen, Quoc Cuong., Vu, Viet Hung., & Thomas, Marc. (2019). ARX model for experimental vibration analysis of the grinding process by flexible manipulator, **Surveillance, Vishno and AVE conferences**, Lyon, France, p. 392-406, 2019, <https://survishno.sciencesconf.org/243272/document>.

CHAPTER 2

A KALMAN FILTER BASED ARX TIME SERIES MODELING FOR FORCE IDENTIFICATION ON FLEXIBLE MANIPULATORS

Quoc Cuong Nguyen^a, Viet Hung Vu^b and Marc Thomas^c,

^{a,b,c} Department of Mechanical Engineering, École de Technologie Supérieure,
1100 Notre-Dame West, Montreal, Quebec, H3C 1K3

Paper published in *Journal of Mechanical System and Signal Processing*, December 2021

Highlights

- Identification of operating forces
- Using measurement of acceleration responses only
- ARX time series model in conjunction with Kalman filter is applied
- The robustness against noise is investigated by numerical simulations
- The modal parameters are identified

2.1 Résumé

Les manipulateurs flexibles multiaxiaux sont des structures généralement utilisées dans la maintenance de grands équipements hydroélectriques tels que les roues de turbine. Ce type de robot multiprocessus a été spécifiquement conçu pour les travaux de réparation liés à l'enlèvement de matière par meulage ou polissage. En général, l'estimation des forces de contact entre la meule et la pièce est cruciale pour améliorer les performances du robot et minimiser les vibrations indésirables au niveau de l'effecteur final. Cependant, en raison du travail dans un environnement difficile, les mesures de force directes ne peuvent pas être mises en œuvre. Cet article présente une nouvelle méthode utilisant un filtre de Kalman basé sur une modélisation de série temporelle Auto Régressive avec eXogenous excitation (ARX) pour traiter le problème inverse, où le modèle ARX est modifié en utilisant uniquement des données

de vibration ambiante. L'algorithme récursif des moindres carrés est adopté pour réduire l'effet des bruits aléatoires élevés, permettant ainsi d'identifier les forces d'excitation dans plusieurs directions lors des opérations de meulage. La méthode proposée a été illustrée par différents exemples avec des simulations numériques et des expérimentations sur une poutre en porte-à-faux et sur un manipulateur flexible. Les simulations numériques permettent d'étudier la robustesse de la méthode contre le bruit, tandis que sa capacité à identifier les forces et les propriétés modales des structures est également présentée.

Mots clés : Analyse modale, Modèle ARX, Filtre de Kalman, Modèle d'espace d'état, Identification des forces.

2.2 Abstract

Multi-axial flexible manipulators are structures typically employed in the maintenance of large hydropower equipment such as turbine runners. This kind of multi-process robot was specifically designed for repair jobs related to material removal via grinding or polishing. In general, the estimation of the contact forces between the grinding cup and the workpiece is crucial for improving the robot's performance and minimizing unwanted vibration at the end effector. However, due to working in a harsh environment, direct force measurements cannot be implemented. This paper introduces a new method using a Kalman filter based on a time series Auto Regressive with eXogenous excitation (ARX) modeling to deal with the inverse problem, where the ARX model is modified by employing ambient vibration data only. The recursive least squares algorithm is adopted to reduce the effect of high random noises, thus allowing to identify the excitation forces in multiple directions under grinding operations. The proposed method was illustrated via different examples with numerical simulations and experiments on a cantilever beam and on a flexible manipulator. The numerical simulations allow for investigating the robustness of the method against noise, while its ability to identify the forces and the modal properties of structures is also presented.

Keywords: Modal analysis, ARX model, Kalman filter, State-space model, Forces identification.

2.3 Introduction

The need for high performance in the machining industry has led to the development of lightweight and flexible manipulators. Thanks to their compact design and high flexibility in performing complex tasks, these light robots have come to represent a potential and promising alternative to standard machine tools. However, their lack of rigidity is still a great limitation for precision tasks and productivities. The SCOMPI (Super COMPact Ireq) robot manipulator developed by Hydro-Québec's research institute is a typical example. It was specifically designed to work in a confined space with hydraulic turbines for grinding or polishing jobs (Hazel, Côté, Laroche, & Mongenot, 2012a, 2012b). The repair of mechanical components in situ is a key when it comes to handling maintenance problems in the power generation industry. Thanks to its unique portable track-based kinematics design, this robot provides a good work envelop in a turbine runner for maintenance without requiring the entire disassembly of equipment for off-site repairs. However, due to its lightweight and flexible structure, undesired vibrations appear during the grinding process, significantly limiting its productivity. Operational contact forces at the tool-piece contact zone could be one of the main factors contributing to this problem. An accurate characterization of input forces during operation is vital for structural analysis. Identifying these external forces is not only improving the structural dynamical behavior by minimizing the vibration but also avoiding damage during machining operations.

The external forces can be measured directly during operation or obtained by some indirect methods. However, in practical applications, measuring the excitation forces under operational conditions is often troublesome due to several technical reasons. The identification of unknown forces from measured responses has overcome these difficulties and represented as an alternative tool for the reconstruction and evaluation of operational excitations. Recent years have seen tremendous advances in dynamic system monitoring, which have boosted the scope

of research investigating force identification. Many algorithms have been proposed and successfully developed to detect, quantify and localize input forces with different levels of efficiency (Inoue, Harrigan, J., & Reid, 2001; Sanchez & Benaroya, 2014). These techniques can broadly be divided into three key categories: stochastic, deterministic, and techniques based on artificial intelligence. A pure stochastic technique is based on finding statistical relations between the input forces and the system responses. This class notably includes the Inverse Structural Filter (ISF) algorithm presented by Steltzner and Krammer (D. Kammer & Steltzner, 2001), in which the external forces applied to a structural system were successfully identified, when the forces and the response sensors are non-collocated. Allen et al. (Allen & Carne, 2008) also extended the ISF by using data multiple time steps simultaneously to improve the accuracy of the proposed method. Recently, the Artificial Neural Network (ANN) has emerged as a trendy technique for predicting the amplitude of impact forces (Al-Abdullah, Abdi, Lim, & Yassin, 2018; X. Liu, Zhao, Ge, Wu, & Mei, 2019). The application of machine learning to estimate the forces applied during the operational process can avoid the need for analytical models (Colomé, Pardo, Alenyà, & Torras, 2013). The main advantage of the neural network technique is that it can work well even when the relationship between the input forces and the responses presents some nonlinearities. For instance, Zhou *et al.* (Zhou, Dong, Guan, & Yan, 2019) introduced a method for force identification by using a deep Recurrent Neural Network (RNN). The performance of the approach proposed in the present work is analyzed via different nonlinear cases, including nonlinear three-degree-of-freedom, damped oscillators, and nonlinear composite plates. However, this technique requires a considerable number of data sets for training.

The category-based on deterministic techniques is regarded as the largest group of algorithms that solve the inverse problems predominantly either in the time domain or frequency domain. In the frequency domain, the straightforward force estimation technique is evaluating the Frequencies Response Function (FRF) of the measured responses and their inverse. This method has been applied in estimating the in-flight loading forces of a helicopter model during flight (Mendrok, Kurowski, & Uhl, 2008), or the applied forces on railway vehicle wheelsets from measured responses based on a Finite Element Model (FEM) (Mehrpooya & Ahmadian,

2009). However, this technique requires the inverse of the transfer function, which causes inherent instability due to possible ill-posed inverse problems, particularly when the measured responses are contaminated with noise. These difficulties can be tackled using several different methods; for example, the Pseudo-inverse method via Singular Value Decomposition (SVD) (Yu & Chan, 2003), the Tikhonov regularization (Y. Liu & Shepard, 2005) or the Singular Value Decomposition (SVD) method based on an enhanced Least Squares (LQ) algorithm (Jiang & Hu, 2009). Another frequency domain approach is based on a Modal Filter (Mendrok & Uhl, 2009) to extract the modal coordinates of each individual mode from the system output by mapping the response vector from the physical space to the modal space. Khoo *et al.* applied the Pseudo-inverse method for impact force identification based on Operating Deflection Shape (ODS) analysis and Frequency Response Function (FRF) measurements (Khoo *et al.*, 2014). Their approach was validated for different under-determined, even determined, and over-determined cases, and the results revealed that sensor locations and the number of measured responses have a significant impact on the accuracy of identified forces. On the other hand, the time domain approach provides a potentially effective solution for rapid monitoring applications and direct reconstruction of external loads. The estimated time history of input forces has attracted significant attention among researchers and many methods have been introduced to address inverse problems in the time domain. For instance, a regularization technique with Markov parameters is proposed by Kammer for the reconstruction of input excitations (D. C. Kammer, 1998), while Wang *et al.* presented two different sensors placement methods, in combination with the Tikhonov regularization for the enhancement of the precision of identified input forces (J. Wang, Law, & Yang, 2013). In the early sixties, the Kalman filter was proposed and has since won wide acclaim among engineers, scientists, and researchers (Kalman, 1960). Several works have pointed out the great advantage of using accelerations or displacement responses data in obtaining improved real-time estimates by employing an appropriate Kalman filter. Ma *et al.* successfully applied the Kalman filter (C. K. Ma, Chang, & Lin, 2003) and extended the Kalman filter (C.-K. Ma & Ho, 2004) in conjunction with an online recursive inverse method for estimating input forces acting on linear and nonlinear structures. In their work, the Kalman filter was used to effectively handle noisy measurements and to generate residual innovation sequences, a priori state estimates, and innovation

covariances, which were used for input force identification via the least-squares algorithm. The Augmented Kalman Filter (AKF) is another modified version of the Kalman filter developed by Lourens for unknown force identification under noisy environment and modeling errors (Lourens, Reynders, De Roeck, Degrande, & Lombaert, 2012), while Hwang *et al.* proposed a new procedure based on Kalman filtering for modal wind load identification by using limited measured responses (Hwang, Kareem, & Kim, 2011). Additionally, Naets *et al.* improved the force identification accuracy based on the Kalman filter and provided a good result in the case of an unbiased load (Naets, Cuadrado, & Desmet, 2015). A dual Kalman filter was proposed by Azam *et al.* for identifying the states and unknown input of a linear state-space model by using sparse noisy acceleration measurements (Eftekhar Azam, Chatzi, & Papadimitriou, 2015). Alternatively, instead of traditional regularization methods, some other techniques based on the selection of sensor locations have been introduced with the aim of improving the accuracy of identified forces. Currently, some novel methods were proposed in the literature for force localization and reconstruction such as Group Relevance Vector Machine (Feng, Li, Lu, Li, & Wang, 2021) or a sparse Kalman filter (Feng, Li, & Lu, 2020), the spatial distribution of forces at each time step is estimated by Relevance Vector Machine (RVM) and sparse Kalman filter was applied to monitor forces with a limited number of sensors. Thite *et al.* also presented an approach to reduce the errors of identified forces by choosing locations for measuring responses (Thite & Thompson, 2006). The Sum of Weighted Accelerations Technique (SWAT) has been applied to a variety of different real-world applications and has shown great potential in the identification of the time history of excitation forces (M. L. Wang & Kreitinger, 1994). Their technique allows the reconstruction of applied forces by summing the acceleration responses with the appropriate weights. The average acceleration discrete algorithm formulated in the state space form is proposed in (Ding *et al.*, 2013) to appropriately estimate external excitations. E. Zhang *et al.* presented a Bayesian force estimation methodology based on the inversion of an uncertain structural model that can deal with measurement noises, model uncertainty, and unexpected environmental disturbances (Zhang, Antoni, & Feissel, 2012). Additionally, a novel sequential Bayesian was recently proposed in (Sedehi, Papadimitriou, Teymouri, & Katafygiotis, 2019) for state and input estimation by using output-only measurement. Rajdip *et al.* introduced the Gaussian process latent force

model to tackle the problem of input force estimation in a stochastic setting (Nayek, Chakraborty, & Narasimhan, 2019). An enhanced sparse regularization method was developed in (Qiao, Liu, Liu, Yang, & Chen, 2019) and has proven its advantage over the classical regularization method for solving the ill-posed nature of the inverse problem of impact force identification, which is more robust to the choice of turning parameters and noisy measurement. The group sparse regulation method is a further development of this approach, where the mixed $l_{2,1}$ -norm regularization model is constructed for the inverse problem (Qiao, Mao, Liu, Zhao, & Chen, 2019; Wambacq, Maes, Rezayat, Guillaume, & Lombaert, 2019). Thanks to its group sparsity-inducing, the proposed method provides a robust solution for highly noisy measurements with higher accuracy of impact force identification compared to the classical Tikhonov regularization.

In this paper, a new technique aimed at identifying the time-varying input forces acting in the multi directions of SCOMPI robot under an operational process by using ambient vibration data only is presented. The framework of this paper is inspired by the work of Ma *et al.* (C. K. Ma *et al.*, 2003), where both the Kalman filter and the recursive least squares estimator were taken into consideration but we have developed and applied it in a different way. The original method can apply to a simple structure where all the structural properties are already known in advance. Unfortunately, in a complex structure such as a flexible manipulator like COMPI robot, there is no knowledge of the system's details characteristics are given beforehand. Therefore, our methodology is innovative by using the model identification technique to obtain the initial input data where only acceleration responses were used for forces identification. First, a technique based on an Auto-Regressive with eXogenous excitation (ARX) model time series was introduced for experimentally analyzing the modal parameters of a flexible robot under working conditions. With some simplifications, an ARX is expressed such that only response signals are involved in an initial step to obtain the modal properties of the structure based on modal analysis and discretized state equations. However, the discretization of continuous state space equations may cause computational instability and subsequently affect inverse analysis estimation results. Therefore, a Kalman filter is adopted in this paper to suppress noise while a least-squares algorithm is applied in order to minimize the effects of

the high random noise levels and improve the accuracy of the identified solution. Furthermore, the technique is also extended to the case of high noise levels in order to investigate the robustness of the proposed approach. Consequently, this paper adds the following original contributions to the existing literature from a different perspective. The ARX model is proposed to experimentally analyze the vibrations of a system under operational conditions and establish a reference state-space model by using only the measured accelerations. Subsequently, the forces are estimated by using the Kalman filter and least-squares algorithms. The adaptability of the proposed method is evaluated via both numerical simulations and laboratory experiments on a cantilever beam and on a flexible manipulator.

The paper is organized as follows. In section 2, the force reconstruction algorithm based on the ARX time series model combined with the Kalman filter is presented. A numerical simulation on a cantilever beam is discussed in section 3, while the effectiveness of the method is validated by experiments on an aluminum clamp-free beam in section 4. The final assessment is experimentally performed on the SCOMPI robot in section 5 in order to verify the proposed approach in an industrial environment. To end the work, section 6 summarizes some concluding remarks and presents prospective improvements for future research.

2.4 Force identification method

In the algorithm scheme, the ARX model combined with the Kalman filter is examined for its susceptibility to perform impact force identification under a noisy environment. The state-space formulation represented by the ARX model is established first, thus allowing the noise terms to be introduced directly into a state-space form that enables evaluating their effects on the model performance. The demonstration of the model in a state-space form simplifies the implementation of the Kalman filter, which comprises two stages, namely, prediction and correction. Finally, the magnitudes of excitation forces are identified by means of a recursive least squares algorithm. The entire force identification procedure is summarized in Fig. 2.1.

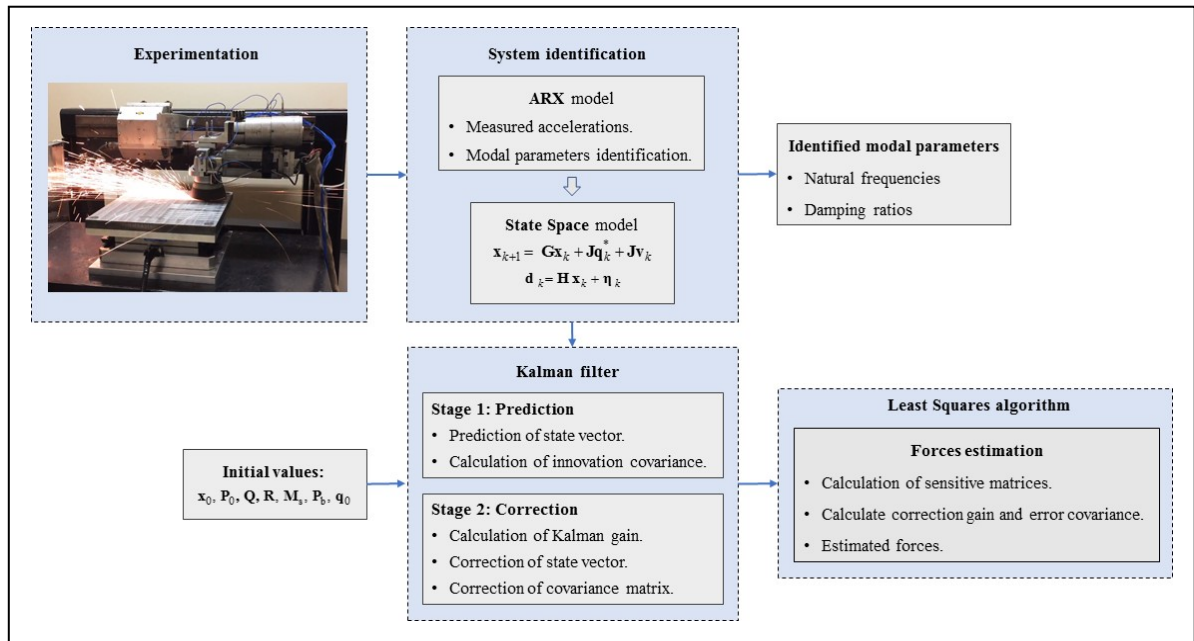


Figure 2.1 Flow chart of the estimation method

2.4.1 State space representation of ARX model

The time series modeling approach is built from the observed input and output sequences with no knowledge of the system's detailed characteristics. In the time series family, many models are available to be chosen, including the Box-Jenkins (BJ), Auto-Regressive (AR), Auto-Regressive eXogenous (ARX), Auto-Regressive Moving Average eXogenous (ARMAX), and Auto-Regressive Moving Average (ARMA) models. In comparison with other models, the ARX model is outstripped due to its simplicity and avoids a heavy computational burden. It also provides an elegant and powerful solution from an online computational effort and data storage perspective. Their coefficients have a direct correlation with a state-space model, which relates closely to the dynamic properties of the system, thus enabling the reconstruction of impact forces.

Since the output response of a mechanical system is measured at m predefined locations with constant sampling time Δk , a time series analysis Auto-Regressive model of a p^{th} orders is mathematically expressed as follows (Vu, Thomas, Lakis, & Marcouiller, 2011):

$$\mathbf{d}(k) = \sum_{i=1}^p [\mathbf{A}_i] \mathbf{d}[k-i.\Delta k] + \mathbf{w}(k) \quad (2.1)$$

where $\mathbf{d}(k)$ of size $m \times 1$ is the time signal to be predicted, while $\mathbf{d}(k-i.\Delta k)$ of size $m \times 1$ is the measured response vector at time $k-i.\Delta k$, $[\mathbf{A}_i] = [a_1, a_2, \dots, a_p]^T$ of size $p \times 1$ represents the vector of autoregressive parameters, p^{th} is the orders of the model with the sampling time Δk , $i = 1, \dots, p$ refers to the normalized discrete time, and $\mathbf{w}(k)$ of size $m \times 1$ is the backward prediction error assumed to be a white noise with zero mean, and is defined as follows:

$$E[\mathbf{w}(k)] = 0 \text{ and } E[\mathbf{w}(k-i)\mathbf{w}^T(k-j)] = \delta_{ij} \mathbf{W} \quad (2.2)$$

where E indicates the mean value operation, while δ_{ij} is the Kronecker symbol, and \mathbf{W} denotes the covariance matrix of $\mathbf{w}(k)$.

In this paper, another form of the AR with eXogenous input (ARX) model is proposed for impact force reconstruction. An ARX (n_a, n_b) model can be described by the following linear differential equation (Nguyen, Vu, & Thomas, 2019):

$$\mathbf{d}(k) = \sum_{i=1}^{n_a} [\mathbf{A}_i] \mathbf{d}[k-i.\Delta k] + \sum_{j=0}^{n_b} [\mathbf{B}_j] \mathbf{q}[k-j.\Delta k] + \mathbf{w}(k) \quad (2.3)$$

where $\mathbf{q}(k)$ is the exogenous input, while $\mathbf{d}(k)$ is the output which is influenced by the noise term $\mathbf{w}(k)$. The additive noise $\mathbf{w}(k)$ is introduced as direct noise in the differential equation (2.3). $[\mathbf{A}_i] \in \mathbb{R}^{m \times 1}$ and $[\mathbf{B}_j] \in \mathbb{R}^{m \times 1}$ are the coefficient matrices of AR, which refers to the Auto-Regressive part, and is related to the output data and X refers to the eXogenous part, which is related to the input data, respectively.

Under the assumption of a linear structure, equations (2.1) and (2.3) should share the same AR parameters because the eigenvalues of the structure do not depend on the types of input used. The parameters n_a and n_b are the model orders of $[\mathbf{A}_i]$ and $[\mathbf{B}_j]$, and the variables n_a and n_b used in equation (2.3) are assumed to be equal to or less than the parameter p used in equation (2.1) and normally synchronized with the same order $n_a = n_b$.

Unfortunately, the measurement of excitation is not always available, especially for a system working under ambient vibration, as in an industrial environment. Therefore, the process

can be established with the output response data only. Any output response may be considered as an exogenous variable, while the remaining responses are output in the framework of the ARX model (Roy, Bhattacharya, & Ray-Chaudhuri, 2015). Since there is no input excitation data of a structure under operating conditions available, we assume that input excitation can be modeled by Gaussian white noise. Following the formulation given by Lu and Gao (Gao & Lu, 2006; Lu & Gao, 2005), we consider the system as a Single Input – Multi Output system, and the ARX output only model for the structure can be expressed in the following form:

$$\bar{\mathbf{d}}(k) = \sum_{i=1}^{n_a} [\bar{\mathbf{A}}_i] \bar{\mathbf{d}}[k - i.\Delta k] + \sum_{j=0}^{n_b} [\bar{\mathbf{B}}_j] \mathbf{d}^*[k - j.\Delta k] + \mathbf{w}(k) \quad (2.4)$$

where $\bar{\mathbf{d}}(k) = [\mathbf{d}_2(k) \ \mathbf{d}_3(k) \ \dots \ \mathbf{d}_{n_a}(k)]^T$ are acceleration responses, while the input is replaced by a response at one sensor location.

It should be emphasized that equation (2.4) is analogous with equation (2.3), but the input $\mathbf{q}(k)$ is replaced by the output $\mathbf{d}^*(k)$ and the coefficient matrices is different. Actually, we can consider any DOF as a reference point, however in this paper, the measured response of the first DOF is chosen as the input $\mathbf{d}^*(k) = \mathbf{d}_1(k)$. We can rewrite equation (2.4) in a concise notation by defining the parameter vector $\boldsymbol{\theta}$ and the information vector $\boldsymbol{\varphi}(k)$:

$$\bar{\mathbf{d}}(k) = \boldsymbol{\theta}^T \boldsymbol{\varphi}(k) + \mathbf{w}(k) \quad (2.5)$$

where:

$$\boldsymbol{\theta} = [\bar{a}_1, \bar{a}_2, \dots, \bar{a}_{n_a}, \bar{b}_0, \bar{b}_1, \dots, \bar{b}_{n_b}]^T \in \square^{(n_a+n_b+1) \times 1} \quad (2.6)$$

$$\boldsymbol{\varphi}(k) = [-\bar{d}(k-1), -\bar{d}(k-2), \dots, -\bar{d}(k-n_a), d_1(k), d_1(k-1), \dots, d_1(k-n_b)]^T \in \square^{(n_a+n_b+1) \times 1} \quad (2.7)$$

If we consider N consecutive values of the responses from $\mathbf{d}(k)$ to $\mathbf{d}(k+N-1)$ by minimizing the norm of $\mathbf{w}(k)$, the identification of the model can be determined by a standard Least Squares (LS) technique (Soderstrom, Fan, Carlsson, & Bigi, 1997), while the model structure selection referring to the determination of the AR and X orders is achieved by fitting increasingly high-order models to the data until no further improvement is observed.

$$\Phi = \arg \min \left(\frac{1}{N} \sum_{k=t}^{t+N-1} \|\mathbf{w}(k)\|^2 \right) = \arg \min \left(\frac{1}{N} \sum_{k=t}^{t+N-1} \|\bar{\mathbf{d}}(k) - \boldsymbol{\theta}^T \boldsymbol{\varphi}(k)\|^2 \right) \quad (2.8)$$

where $\|\cdot\|$ denotes the Euclidean.

The modal frequencies and damping rates of the system can be identified from eigen decomposition of the state matrix in the form of autoregressive parameters.

$$\text{Eigenvalues:} \quad [S, \lambda] = \text{eig}(\mathbf{\Pi}) \quad (2.9)$$

$$\text{where:} \quad [\mathbf{\Pi}]_{n_a \times n_b} = \begin{bmatrix} -\bar{a}_1 & -\bar{a}_2 & \cdots & -\bar{a}_{n_a-1} & -\bar{a}_{n_a} \\ \mathbf{I} & \mathbf{0} & \cdots & \mathbf{0} & \mathbf{0} \\ \mathbf{0} & \mathbf{I} & \cdots & \mathbf{0} & \mathbf{0} \\ \cdots & \cdots & \cdots & \cdots & \cdots \\ \mathbf{0} & \mathbf{0} & \cdots & \mathbf{I} & \mathbf{0} \end{bmatrix} \quad (2.10)$$

The frequencies and damping rates of the system can be computed as follows:

$$\text{Frequencies:} \quad \omega_j = \sqrt{\text{Re}^2(\lambda_j) + \text{Im}^2(\lambda_j)} \quad (2.11)$$

$$\text{Damping rates:} \quad \xi_j = -\frac{\text{Re}(\lambda_j)}{\omega_j} \quad (2.12)$$

In order to apply the Kalman filter to the ARX model and estimate unknown forces applied to the system, it is advantageous to express the system in state space formulation, which expresses the equation of motion as a first order differential equation. It is well known that ARX model estimation with varying parameters can be transformed into a general state space model through a standard procedure (Isaksson, 1993; Jansson, 2003; Olesen, Huusom, & Jørgensen, 2013). By introducing a variable vector \mathbf{x}_k , the ARX model of Eq. (2.4) can be expressed in a state-space form as follows:

$$\mathbf{x}_{k+1} = \mathbf{G}\mathbf{x}_k + \mathbf{J}\mathbf{q}_k \quad (2.13)$$

$$\mathbf{d}_k = \mathbf{H}\mathbf{x}_k + \boldsymbol{\eta}_k \quad (2.14)$$

where the state parameters G, J, H are realized in observer canonical form and related to the ARX model parameters as follows (Gao & Lu, 2006).

$$\mathbf{G} = \begin{bmatrix} -\bar{a}_1 & 1 & 0 & 0 & 0 \\ -\bar{a}_2 & 0 & 1 & 0 & 0 \\ \vdots & \vdots & \vdots & \ddots & \vdots \\ -\bar{a}_{\rho-1} & 0 & 0 & \cdots & 1 \\ -\bar{a}_\rho & 0 & 0 & \cdots & 0 \end{bmatrix}; \quad \mathbf{J} = \begin{bmatrix} \bar{b}_1 \\ \bar{b}_2 \\ \vdots \\ \bar{b}_{\rho-1} \\ \bar{b}_\rho \end{bmatrix}; \quad (2.15)$$

$$\mathbf{H} = [1 \quad 0 \quad 0 \quad \cdots \quad 0];$$

where the size of the state vector is $\rho = \max(n_a, n_b)$.

And $\boldsymbol{\eta}_k$ is noise content in the measured output accelerations, which is normally distributed white noise processes with covariances \mathbf{R} and defined as follow.

$$E(\boldsymbol{\eta}_k \boldsymbol{\eta}_j^T) = \mathbf{R} \delta_{kj} = \text{diag}[\boldsymbol{\sigma}_R^2] \quad (2.16)$$

In equation (2.13) and (2.14) \mathbf{d}_k is refers to the measured output, while \mathbf{q}_k is supposed to be the true input signal. However, as \mathbf{q}_k in the present model is actually an acceleration response at a particular DOF of the structure. In this situation, there are two scenarios can be considered. In the first scenario, the inputs are simply neglected, and the system can be treated as Stochastic Subspace (SSI) output only (Wu et al., 2009). However, this approach will affect the variance properties and bias in the model might be occur. One the second one, (Linder & Enqvist, 2017) has shown that it is possible to mitigate these effects by utilizing other available signals to create an approximation of the unknown input. Since the input data is typically unknown, the achieved estimate of the input signals is in fact an optimal estimate of the *virtual* input. We define \mathbf{q}_{vir} as a virtual input of the system and assumed to be measured with noise.

$$\mathbf{q}_{vir} = \mathbf{q}_k^* + \mathbf{v}_k \quad (2.17)$$

where \mathbf{q}_k^* is the force to be estimated and \mathbf{v}_k is a vector of white Gaussian noise and defined as follow:

$$E(\mathbf{v}_k \mathbf{v}_j^T) = \mathbf{Q} \delta_{kj} = \text{diag}[\boldsymbol{\sigma}_Q^2] \quad (2.18)$$

where \mathbf{Q} is the covariance matrix, δ_{kj} denotes the Kronecker delta and σ is the standard deviation. Consequently, the system should be re-written as below by substituting (2.17) into (2.13).

$$\mathbf{x}_{k+1} = \mathbf{G}\mathbf{x}_k + \mathbf{J}\mathbf{q}_{vir} = \mathbf{G}\mathbf{x}_k + \mathbf{J}\mathbf{q}_k^* + \mathbf{J}\mathbf{v}_k \quad (2.19)$$

$$\mathbf{d}_k = \mathbf{H}\mathbf{x}_k + \boldsymbol{\eta}_k \quad (2.20)$$

where the state parameters \mathbf{G} , \mathbf{J} and \mathbf{H} are those of Eq. (2.15).

This model is referred as *indirect* modelling for treating a problem of unknown input systematically (Linder & Enqvist, 2017; Van Den Hof & Schrama, 1993). The resulting indirect model could be used together with the measured outputs data to estimate the desired information. Actually, the virtual input \mathbf{q}_{vir} does not have any physical explanation, the additive term $\mathbf{J}\mathbf{q}_k^* + \mathbf{J}\mathbf{v}_k$ is added to the system to obtain the true state derivative $\hat{\mathbf{x}}_{k|k-1}$ and thus the true dynamic state $\hat{\mathbf{x}}_{k|k}$ associated to the system will be determined by following Kalman filter algorithm.

2.4.2 Recursive forces identification

The Kalman filter is an excellent solution for identifying the state of a time-varying system from noisy measurements. This filter can be highly accurate, even in the presence of noise, by minimizing the estimated error covariance. Due to its robustness and suitability for real-time applications, the Kalman filter has been widely employed to acquire estimates of state variables or input forces. In this paper, the Kalman filter is employed to establish a regression model between the residual innovation and the input excitation forces, in conjunction with the proposed ARX model, by filtering the measured noisy signals for subsequent force identification purposes. The filter is equipped two stages: “*Time update*” and “*Measurement update*”. In the first stage, the state will be determined based on the dynamical model, after which a priori estimates for the current step are obtained in accordance with the previous state and error covariance. In the next stage, the error covariance of the estimator is minimized by executing the recursive algorithm for the correction of the estimated state based on measured data.

Time update equations:

State estimation time update

$$\hat{\mathbf{x}}_{k|k-1} = \mathbf{G} \mathbf{x}_{k-1|k-1} \quad (2.21)$$

Error covariance time update

$$\mathbf{P}_{k|k-1} = \mathbf{G} \mathbf{P}_{k-1|k-1} \mathbf{G}^T + \mathbf{J} \mathbf{Q} \mathbf{J}^T \quad (2.22)$$

Innovation Covariance time calculation

$$\mathbf{S}_k = \mathbf{H} \mathbf{P}_{k|k-1} \mathbf{H}^T + \mathbf{R} \quad (2.23)$$

Measurement update equations:

Kalman gain calculation

$$\mathbf{K}_{a_k} = \mathbf{P}_{k|k-1} \mathbf{H}^T \mathbf{S}_k^{-1} \quad (2.24)$$

Error covariance measurements update

$$\mathbf{P}_{k|k} = (\mathbf{I} - \mathbf{K}_{a_k} \mathbf{H}) \mathbf{P}_{k|k-1} \quad (2.25)$$

Calculation innovation

$$\hat{\mathbf{d}}_k = \mathbf{d}_k - \mathbf{H} \hat{\mathbf{x}}_{k|k-1} \quad (2.26)$$

State estimation measurement update

$$\hat{\mathbf{x}}_{k|k} = \hat{\mathbf{x}}_{k|k-1} - \mathbf{K}_{a_k} \hat{\mathbf{d}}_k \quad (2.27)$$

Equations (2.21) - (2.27) update the Kalman algorithm from time $k-1$ to k . As soon as the new observation value \mathbf{d}_k is known, the estimate of \mathbf{x}_k at time k can be calculated via equation (2.27), where $\hat{\mathbf{x}}_{k|k}$ is considered an estimate of \mathbf{x}_k , while \mathbf{K}_{a_k} is the Kalman gain. In these equations, \mathbf{P}_k denotes the filter's error covariance matrix, \mathbf{S}_k represents the innovation covariance and $\hat{\mathbf{d}}_k$ is the innovation.

A recursive relationship between a residual innovation originating from the Kalman filter and the input excitation force is established, considering discrete time input excitation forces in a specific time interval \mathbf{q}_k^* with $k = 1, 2, \dots$. The force will be determined by introducing two sensitivity matrices, \mathbf{B}_{s_k} and \mathbf{M}_{s_k} :

$$\mathbf{B}_{s_k} = \mathbf{H} (\mathbf{G} \mathbf{M}_{s_{k-1}} + \mathbf{I}) \mathbf{J} \quad (2.28)$$

$$\mathbf{M}_{s_k} = (\mathbf{I} - \mathbf{K}_{a_k} \mathbf{H})(\mathbf{G} \mathbf{M}_{s_{k-1}} + \mathbf{I}) \quad (2.29)$$

Finally, the input force vector is determined by the equation (2.30)

$$\hat{\mathbf{q}}_k^* = \hat{\mathbf{q}}_{k-1}^* + \mathbf{K}_{b_k} (\hat{\mathbf{d}}_k - \mathbf{B}_{s_k} \hat{\mathbf{q}}_{k-1}^*) \quad (2.30)$$

where

$$\mathbf{K}_{b_k} = \gamma^{-1} \mathbf{P}_{b_{k-1}} \mathbf{B}_{s_k}^T (\mathbf{B}_{s_k} \gamma^{-1} \mathbf{P}_{b_{k-1}} \mathbf{B}_{s_k}^T + \mathbf{S}_k)^{-1} \quad (2.31)$$

is the correction gain for the updating input force vector $\hat{\mathbf{q}}_k^*$.

The error covariance of the estimated input forces vector $\hat{\mathbf{q}}_k^*$ is defined as \mathbf{P}_{b_k}

$$\mathbf{P}_{b_k} = (\mathbf{I} - \mathbf{K}_{b_k} \mathbf{B}_{s_k}) \gamma^{-1} \mathbf{P}_{b_{k-1}} \quad (2.32)$$

In this scheme, the scalar forgetting factor γ ($0 < \gamma \leq 1$) is selected as a compromise between a fast-adaptive capacity and a loss of estimation accuracy. The superscripts -1 and T respectively denote an inverse and a transpose of a matrix or vector. In order to run this procedure, we must determine some initial conditions. Choosing initial state errors \mathbf{P}_k and \mathbf{P}_{b_k} is done based on the size of the errors, which are unknown, but actually, the estimators can be initialized as huge numbers at the diagonal of these matrices. These selections have an effect on the processing of the initial errors. The initial state \mathbf{x}_0 at time step $k = 0$ is considered a random variable and does not have to be known precisely in most deterministic settings. The choice of the diagonal elements of the covariance matrices \mathbf{Q} and \mathbf{R} is determined in accordance with the order of magnitude of the state vector and the accuracy of the sensors, respectively.

2.5 Numerical and experimental simulation on a cantilever beam

To validate the presented method, numerical and experimental studies on a cantilever beam structure as shown in Fig 2.2 are developed to examine the force identification algorithms outlined above. The numerical simulation is designed to examine the stability of the regularization solution as well as the robustness of the proposed approach with different

relatively high measurement noise levels. Detailed properties of the beam with a rectangular cross-section are given in Table 2.1.

Table 2.1 Properties of the cantilever beam

Material	Length (m)	Height (m)	With (m)	Density (kg/m ³)	Young's modulus (N/m ²)	Poisson coefficient
Aluminum alloy	0.8	0.02	0.01	2700	$6.9 \cdot 10^{10}$	0.35

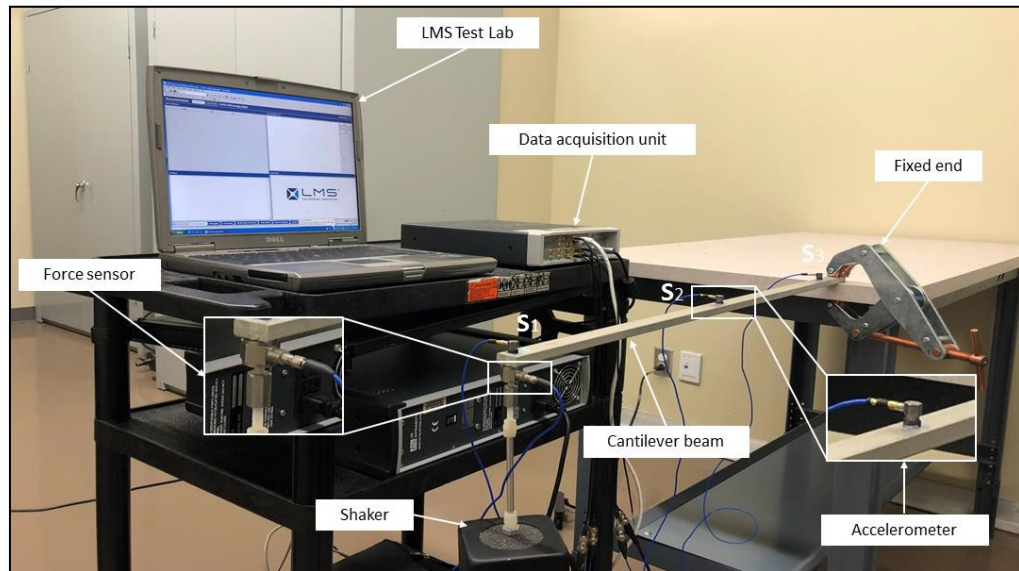


Figure 2.2 Experimental test set-up on a cantilever aluminum beam

2.5.1 Modal analysis of the cantilever beam

In this section, we will identify the modal properties of the cantilever beam under a harmonic excitation. The equation of motion for forced vibration with viscous damping can be written as:

$$[\mathbf{M}]\ddot{\mathbf{x}}(t) + [\mathbf{C}]\dot{\mathbf{x}}(t) + [\mathbf{K}]\mathbf{x}(t) = \mathbf{f}(t) \quad (2.33)$$

where $[\mathbf{M}]$, $[\mathbf{C}]$, $[\mathbf{K}]$ are the mass, damping and stiffness matrices, while $\ddot{\mathbf{x}}(t)$, $\dot{\mathbf{x}}(t)$, $\mathbf{x}(t)$ and $\mathbf{f}(t)$ are time-varying acceleration, velocity, displacement and force vectors, respectively.

A numerical simulation of the cantilever beam was developed using the Finite Element Method (FEM) to validate the accuracy of the proposed approach. A simple six-degrees-of-freedom model was adopted for validation and for simulating the acceleration responses. Subsequently, a force identification approach is implemented in order to reconstruct the impulsive load. After applying the frontier conditions, the global matrices \mathbf{M} and \mathbf{K} of the beam in flexion are obtained as below.

$$\mathbf{M} = \begin{bmatrix} 0.1070 & 0 & 0.0185 & -0.0012 & 0 & 0 \\ 0 & 0.0002 & 0.0012 & -0.0001 & 0 & 0 \\ 0.0185 & 0.0012 & 0.1070 & 0 & 0.0185 & -0.0012 \\ -0.0012 & -0.0001 & 0 & 0.0002 & 0.0012 & -0.0001 \\ 0 & 0 & 0.0185 & 0.0012 & 0.0535 & -0.0020 \\ 0 & 0 & -0.0012 & -0.0001 & -0.0020 & 0.0001 \end{bmatrix} \quad (2.34)$$

$$\mathbf{K} = 10^5 \begin{bmatrix} 1.4584 & 0 & -0.7292 & 0.0972 & 0 & 0 \\ 0 & 0.0346 & -0.0972 & 0.0086 & 0 & 0 \\ -0.7292 & -0.0972 & 1.4584 & 0 & -0.7292 & 0.0972 \\ 0.0972 & 0.0086 & 0 & 0.0346 & -0.0972 & 0.0086 \\ 0 & 0 & -0.7292 & -0.0972 & 0.7292 & -0.0972 \\ 0 & 0 & 0.0972 & 0.0086 & -0.0972 & 0.0173 \end{bmatrix} \quad (2.35)$$

Next, the ARX model is applied to perform a modal analysis of the beam structure through a standard least squares method (Soderstrom et al., 1997). Figure 2.3 shows the frequency stabilization diagram of the beam system up to a model order of 100, where all the natural frequencies of the beam are clearly shown.

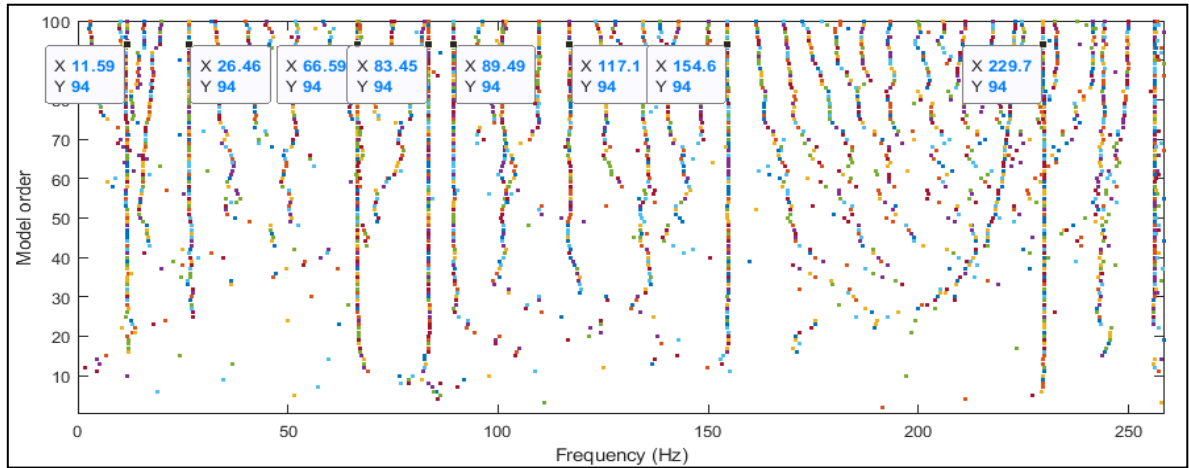


Figure 2.3 Stabilization diagram of ARX model

The results obtained from the ARX model were compared with those obtained by the finite element model in flexion. A comparison of the natural beam frequencies identified between the two approaches is given in Table 2.2. The ARX model can identify all frequencies, and furthermore, provide their damping ratios, which can be used to compute the damping matrix.

Table 2.2 Natural frequencies and damping ratios of the cantilever beam

Mode No.	Natural frequencies f (Hz)		Damping ratios ζ (%)	Mode types
	FEM method	ARX model		
1	12.77	11.59	0.3	Flexural mode
2	-	26.46	0.22	Torsional mode
3	-	66.59	2.09	Torsional mode
4	80.3	83.45	0.61	Flexural mode
5	-	89.49	0.64	Torsional mode
6	-	117.1	1.3	Torsional mode
7	-	154.6	0.23	Torsional mode
8	226.92	229.7	0.86	Flexural mode

The Rayleigh damping matrix \mathbf{C} is assumed to be a linear combination of the mass and stiffness matrices, which can be expressed by the following relation:

$$\mathbf{C} = \alpha \mathbf{M} + \beta \mathbf{K} \quad (2.36)$$

where α and β are scalar damping coefficients and can be determined from damping measurements by selecting the first two pairs of natural frequencies and damping ratios.

$$\beta = \frac{2(\zeta_i \omega_i - \zeta_j \omega_j)}{\omega_i^2 - \omega_j^2}; \alpha = 2\zeta_i \omega_i - \omega_i^2 \beta \quad (2.37)$$

In this regard, the first two natural frequencies in flexion, along with their damping ratios, are considered: 12.77 Hz (80.26 rad/s) with a 0.3% damping rate and 80.3 Hz (504.58 rad/s) with a 0.61% damping rate. The damping matrix is computed and given in equation (2.38). Information related to mass, stiffness and damping matrices will be used to obtain the acceleration responses in order to inversely identify the original excitation force acting on the beam structure in the following section.

$$\mathbf{C} = \begin{bmatrix} 337.0432 & 0 & -166.1149 & 22.1914 & 0 & 0 \\ 0 & 7.9109 & -22.1914 & 1.9737 & 0 & 0 \\ -166.1149 & -22.1914 & 337.0432 & 0 & -166.1149 & 22.1914 \\ 22.1914 & 1.9737 & 0 & 7.9109 & -22.1914 & 1.9737 \\ 0 & 0 & -166.1149 & -22.1914 & 168.5216 & -22.2984 \\ 0 & 0 & 22.1914 & 1.9737 & -22.2984 & 3.9555 \end{bmatrix} \quad (2.38)$$

2.5.2 Simulation of the identification of excitation forces with different noise levels

In this section, the proposed identification technique is applied to reconstruct the excitation forces. A multiple sine wave excitation, as described in equation (2.39) is applied on the beam in order to obtain vibratory temporal responses data.

$$\mathbf{f}(t) = 20 \sin(20\pi t + 0.2\pi) + 15 \sin(80\pi t + 0.5\pi) + 10 \sin(160\pi t + 0.3\pi) \quad (\text{N}) \quad (2.39)$$

In practical engineering measurements, a certain level of noise contamination is unavoidable, and it can adversely affect the accuracy of any identification method. Therefore, various noise levels are artificially added to the measured responses in order to evaluate the robustness of the method against noise. The simulated responses of the cantilever beam will be applied in estimation algorithms (2.21) - (2.32) in order to identify the corresponding force. The total sampling simulation duration is 1 s, and the sampling rate is 512 Hz. The polluted responses are described by adding a normal random component to the unpolluted structural responses.

$$\ddot{\mathbf{x}}_{noise} = \ddot{\mathbf{x}}_{original} + E_p N_r \sigma(\ddot{\mathbf{x}}_{original}) \quad (2.40)$$

where $\ddot{\mathbf{x}}_{noise}$ denotes the noise added to the original measured signals, while E_p is the noise level percentage, N_r is a standard normal distribution vector with zero mean and unit standard deviation, and $\sigma(\ddot{\mathbf{x}}_{original})$ is the standard deviation of the original measured responses.

For validation purposes, normalized error measurements are used to evaluate the accuracy of the force identification results. The Root Mean Square (RMS) error in the estimated force is defined as follows:

$$\mathcal{E}_{\%RMS} = \frac{\sqrt{(\hat{\mathbf{f}}(i)_{est} - \mathbf{f}(i)_{real})^2}}{\sqrt{\mathbf{f}(i)_{real}^2}} \times 100\% \quad (i = 0, 1, 2, \dots, N) \quad (2.41)$$

where $\hat{\mathbf{f}}_{est}$ is the RMS of the estimated time histories of force and \mathbf{f}_{real} denotes the RMS of the real input force.

Various noise levels 5%, 10%, 15%, 20%, 30%, 50% and 100% are selected. The force identification results are presented in Figures 2.4-2.11 in both the time and frequency domains, while Table 2.3 lists the RMS errors between the identified forces and the simulated ones under different measurement noise levels.

Table 2.3 Identification errors with different measurement noise levels

RMS Error (%)	Measurement noise levels (%)							
	0%	5%	10%	15%	20%	30%	50%	100%
	0.5	7	16	22	24	35	63	487

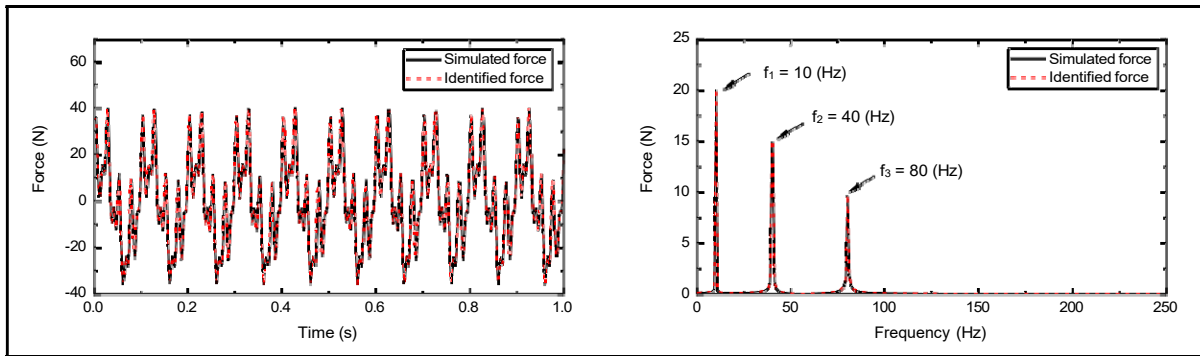


Figure 2.4 Force identification results without measurement noise

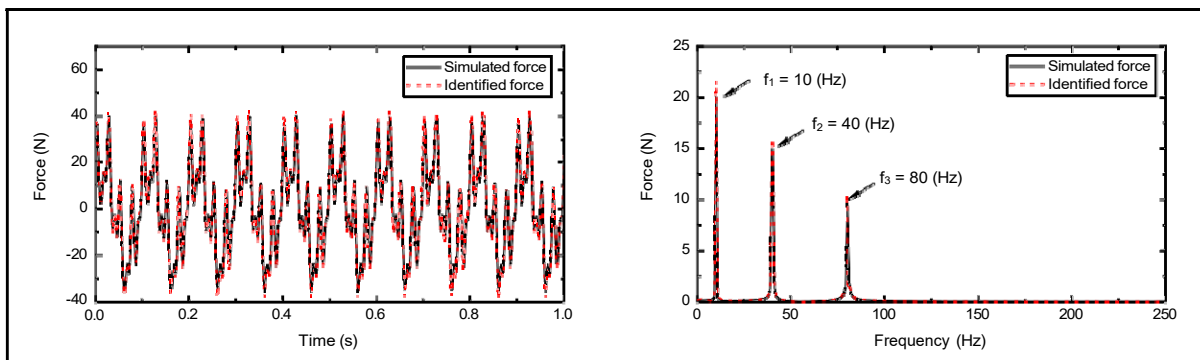


Figure 2.5 Force identification results with 5% noise

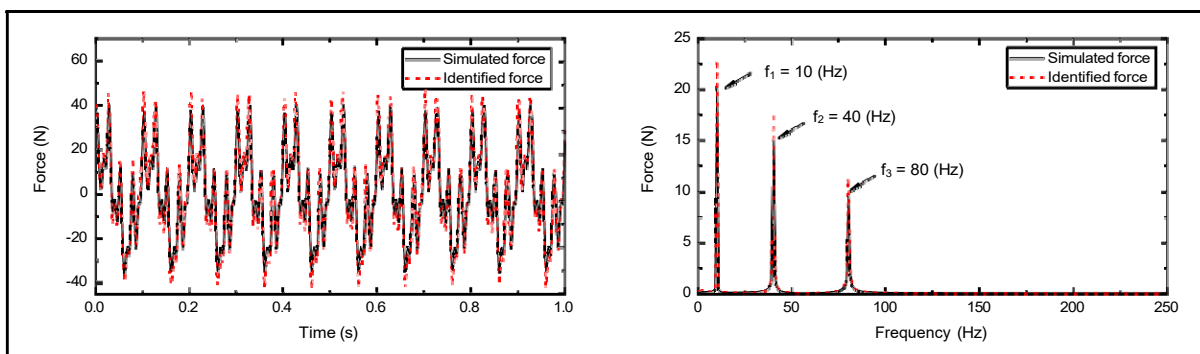


Figure 2.6 Force identification results with 10% noise

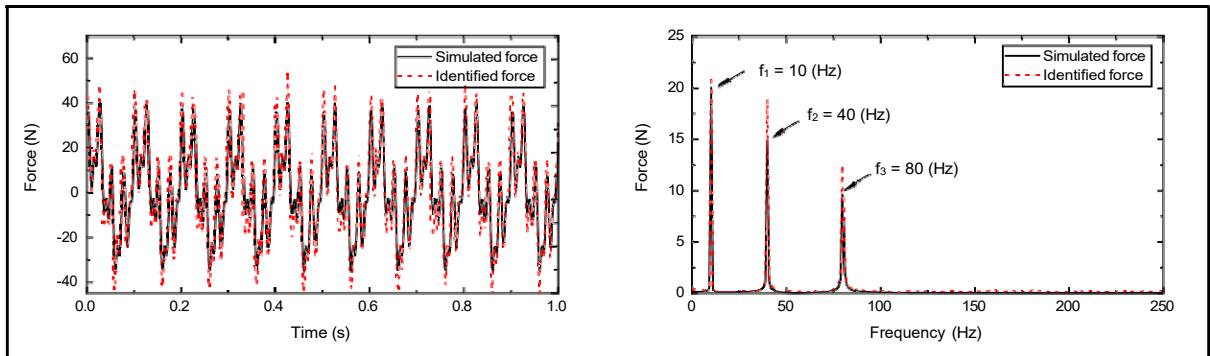


Figure 2.7 Force identification results with 15% noise

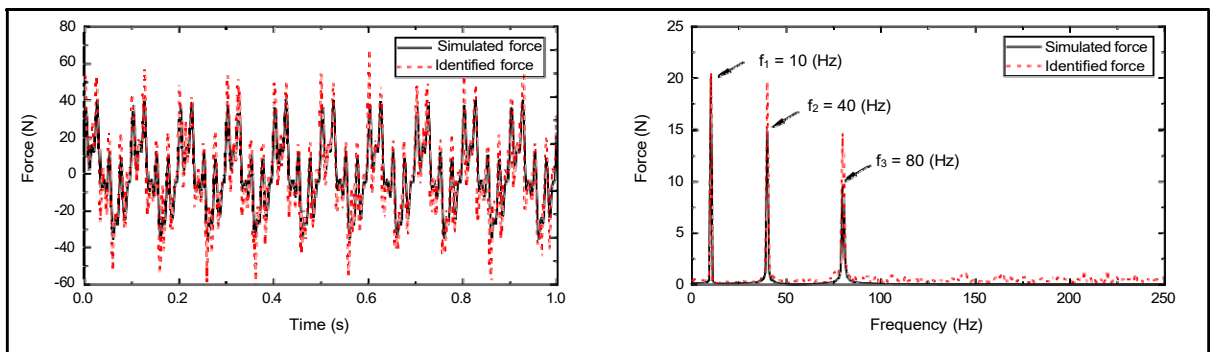


Figure 2.8 Force identification results with 20% noise

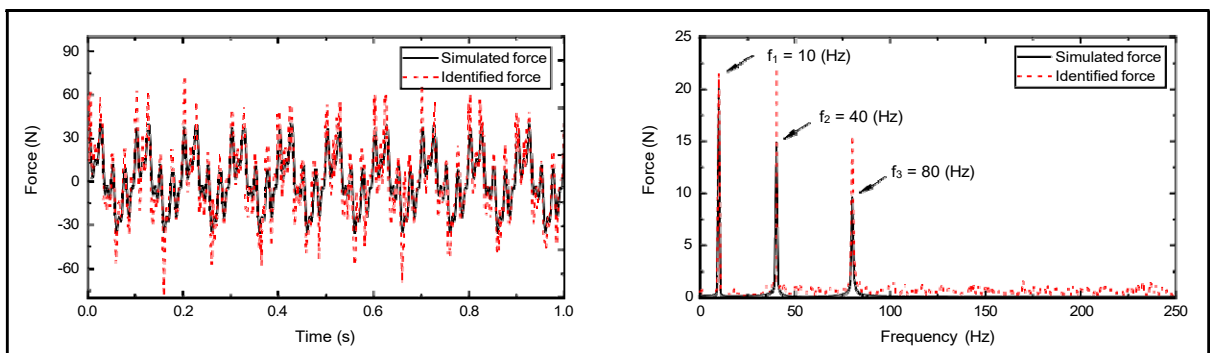


Figure 2.9 Force identification results with 30% noise

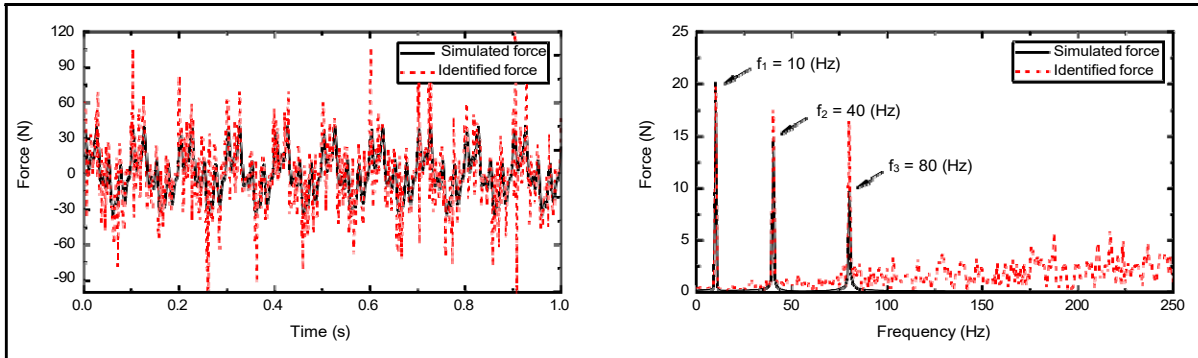


Figure 2.10 Force identification results with 50% noise

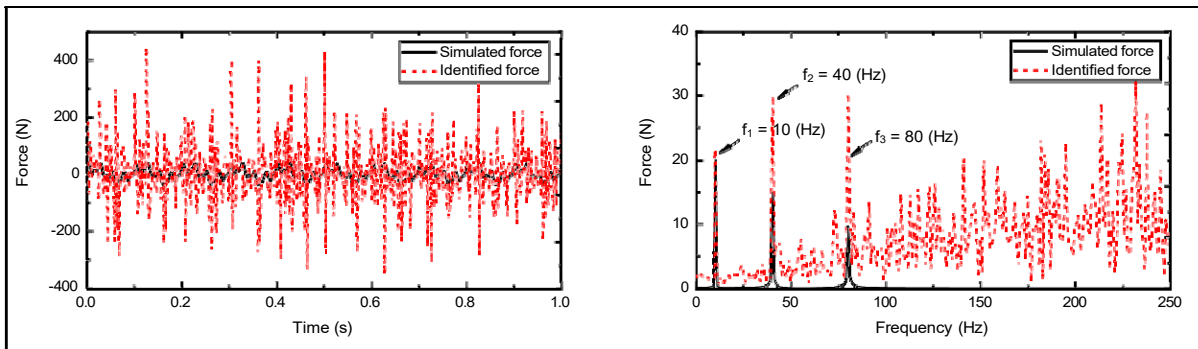


Figure 2.11 Force identification results with 100% noise

The simulation results of the estimated forces acting on the beam structure show a good accuracy in recapturing the original excitation under the noise-free environment (Figure 2.4). The identification results in this case are excellent in both the time and frequency domains. With the presence of noise, the force frequency identification may be considered acceptable with a noise level up to 30%, but computational frequencies appear when the noise level increases further. Adding 50% and 100% noise results in a significant change in the amplitude of the identified force, as indicated in Figures 2.10-2.11, with a very high percentage of errors. By comparing the RMS errors in the different noise level cases, it can be concluded that the measurement noise causes fluctuations and can lead to great amplitude variations.

2.6 Experimentation on the cantilever beam

In this section, the effectiveness of the proposed force identification algorithm based on the ARX combined with the Kalman filter is experimentally assessed on the cantilever beam. In practical applications, to improve the force identification accuracy, the number of sensors should be larger than the number of unknown forces if many possible locations are available. However, this can involve excessive calculation. Therefore, in this experiment, three piezoelectric accelerometers S_1 , S_2 , S_3 (PCB 352C34, sensitivity ± 100 mV/g) are placed along the span of the beam to simultaneously record the responses at locations measured by an LMS Test Lab system for the sake of identify the excitation force at S_1 location (Figure 2.2). Due to the long structure, the way of locating sensors along the beam is believed not only provides the modal data required by structural dynamics, but also produces an enhanced modal identification. The beam is randomly excited with an RMS amplitude of 0.9973 (N) by a shaker at the free end of the beam. The dynamic responses are recorded with 4096 data points and sampled at a sampling frequency of 512 Hz. In order to measure the force applied by the shaker, a force transducer was placed between the beam and the stinger for later validation. All sensors were connected to the LMS Test Lab system, which in turn was controlled by a portable computer. The time history of the measured responses at the three locations is shown in Figure 2.12.

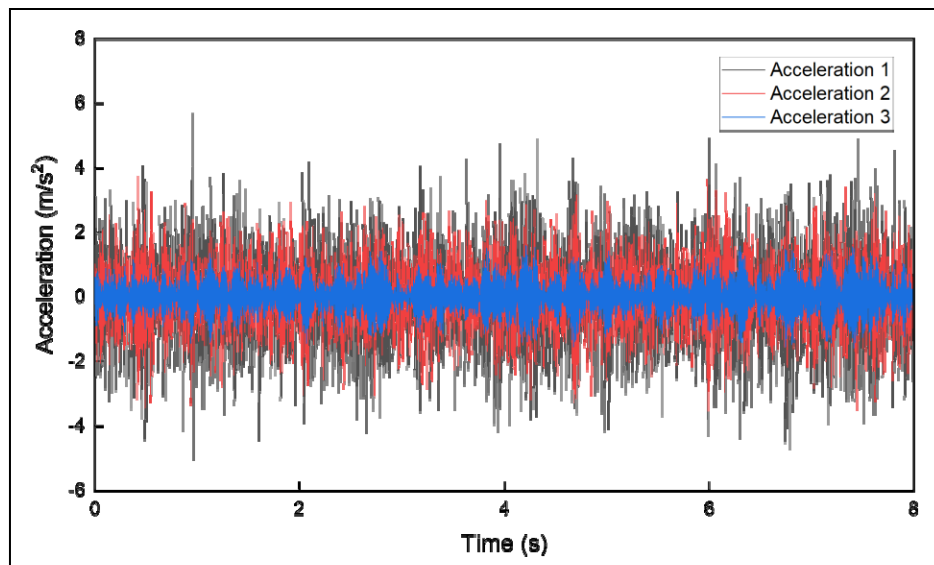


Figure 2.12 Time history of measured accelerations on the beam

The Kalman filter algorithm is used to obtain the covariance and Kalman gain, while the recursive least squares algorithm is employed to estimate the time history of the excitation force applied on the beam. The initial conditions for the Kalman filter are given by $\mathbf{x}_{k-1|k-1} = [0\ 0]^T$, whereas $\mathbf{M}s_{k-1}$ and \mathbf{q}_{k-1} are set to zeros for the least squares algorithm. Since \mathbf{P}_{k-1} and $\mathbf{P}_{b_{k-1}}$ are normally unknown, the estimator is initialized with an extremely large number, such as $\text{diag}[10^9]$. These selections speed up the converging rate of the estimation error. Comparison results in the time domain between the measured and identified forces are presented in Figure 2.13. The zoomed views demonstrate that the proposed method can properly estimate the force amplitude based on measured dynamic responses, with an RMS error of only 3.5%. It can be seen that the predicted values are slightly greater than the real ones.

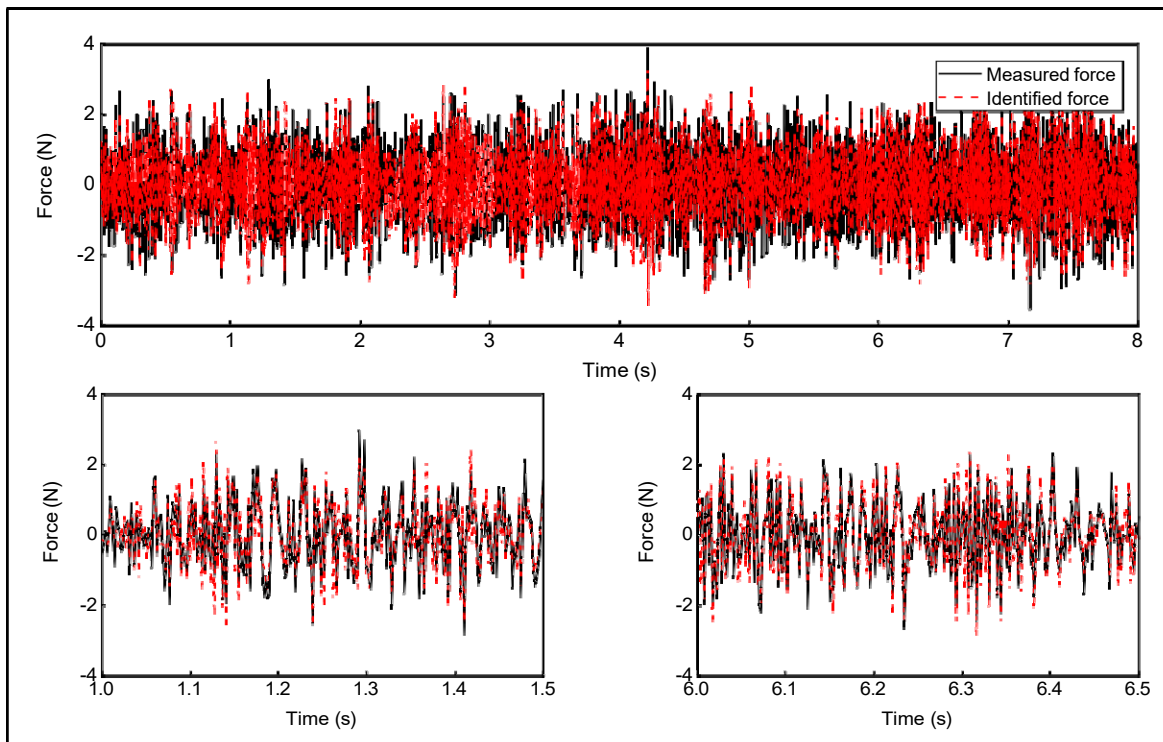


Figure 2.13 Estimated force in time domain, RMS error = 3.5 (%)

The Fast Fourier Transform is applied to the time signals in order to check the validity of the estimated results in the frequency domain (Figure 2.14).

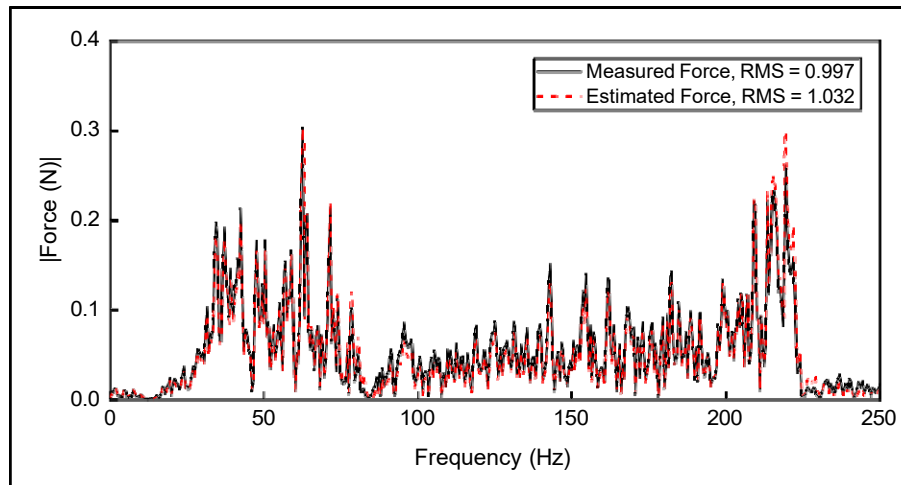


Figure 2.14 Amplitude spectrum of the estimated force

The results in both the time and frequency domains show that the proposed method can track the forces with an acceptable precision. The error in the estimated results is relatively low and the present approach shows a good tracking capability when it comes to identifying the excitation loads under random ambient vibrations. For further examination, the validation will be implemented on a flexible robot manipulator.

2.7 Experimental tests on the COMPI robot

The proposed approach is now implemented to the portable robot, SCOMPI. Figure 2.15 presents the structure of SCOMPI, which is used for repair tasks at Hydro-Québec power plants, particularly for grinding job.

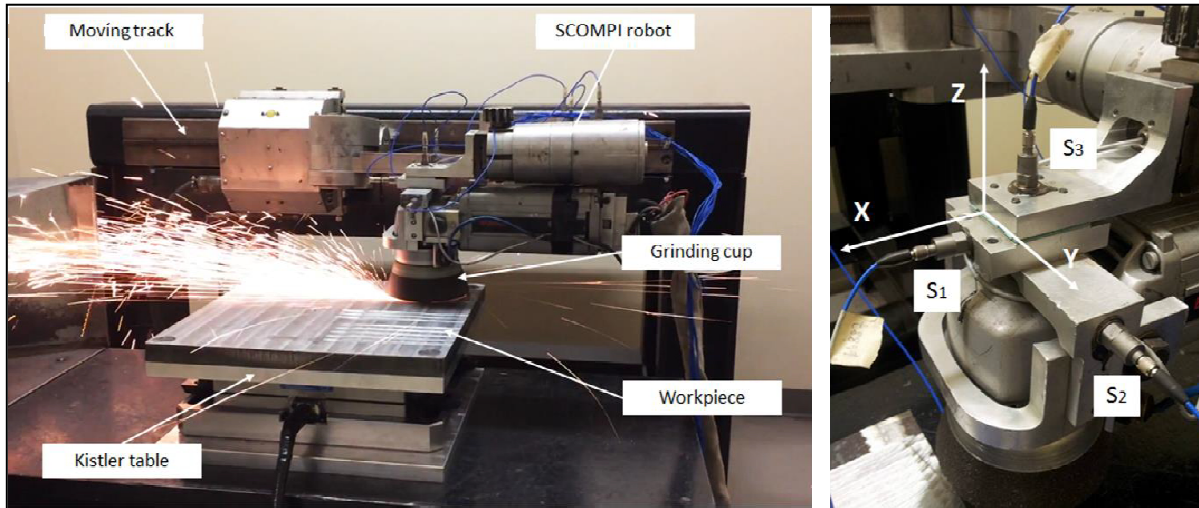


Figure 2.15 Overall grinding test configuration on SCOMPI robot

The SCOMPI robot was tested under a grinding operation in the laboratory. It is seen that the precision of the grinding is highly affected by the vibration at the end effector where the tool is installed, therefore our attention is typically pay to the dynamical behavior of the robot at the end of manipulator. Consequently, the robot is set for testing in the most compact configuration of joints and links “*Home position*”, while three accelerometers were mounted at the end effector in the X, Y and Z triaxial directions, where the contact forces are directly acted on the structure via grinding cup. These locations were selected in order to obtain information of acceleration responses during grinding performance, all these channels are synchronized and acquired at the same time without repetition. Throughout the entire process, only a prismatic joint was moving to perform the grinding tasks, while other revolute joints were set up to retain low internal friction and minimum configuration changes. The load sensors were installed under the workpiece in three directions to record the grinding force via a multi-component Kistler table dynamometer CH8408. The power was set to 1500 W and the grinding motor rotated at a constant speed of 3225 (rpm) in performing each single grinding pass for 8 seconds. Data were acquired at a sampling rate of 512 Hz. The time history and FFT from the measured responses in multiple directions are shown in Figure 2.16.

First, the measured acceleration responses at the end effector of SCOMPI were used for modal analysis of the SCOMPI structure based on the ARX model. Then, the estimation of external

forces was carried out with the assistance of the Kalman filter. An order of 100 was applied to construct the stabilization diagram (Figure 2.17). It may be noticed that all the frequencies previously presented can be observed. Spurious frequencies were eliminated after examining the stability of identified frequencies.

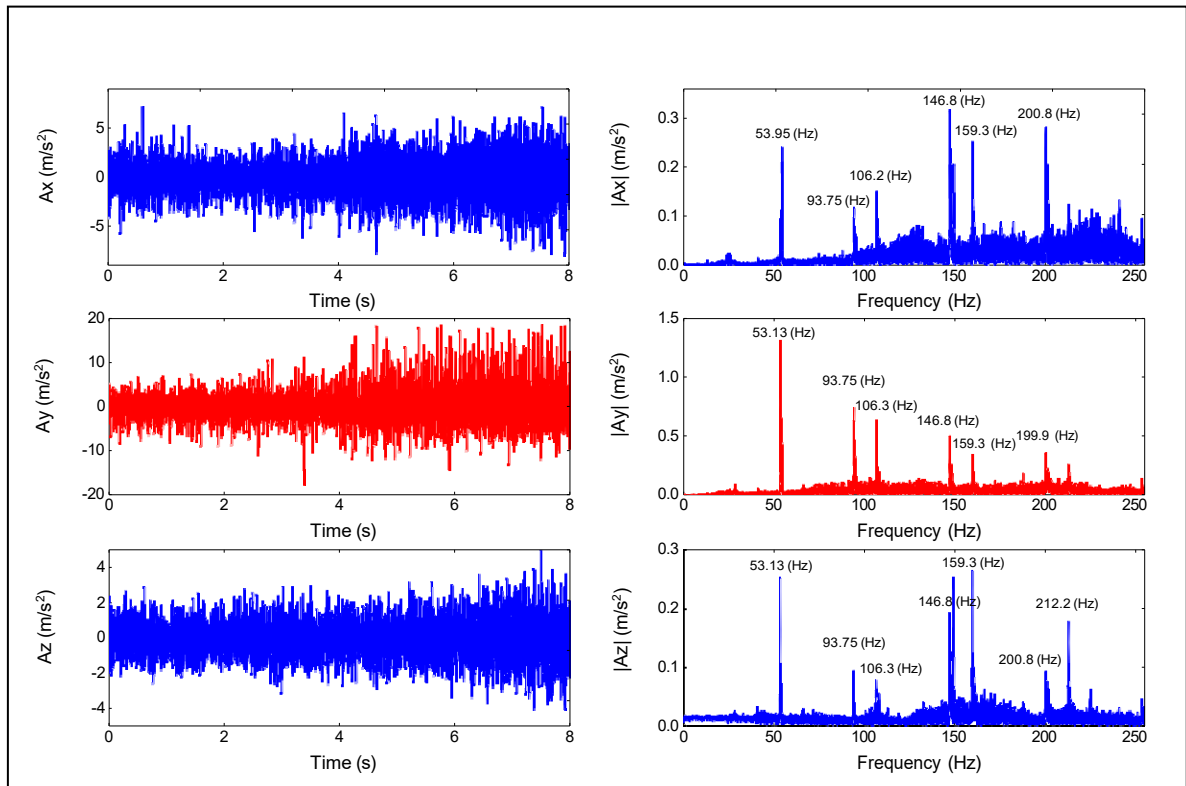


Figure 2.16 Recorded acceleration time histories and their corresponding Fourier amplitudes spectra

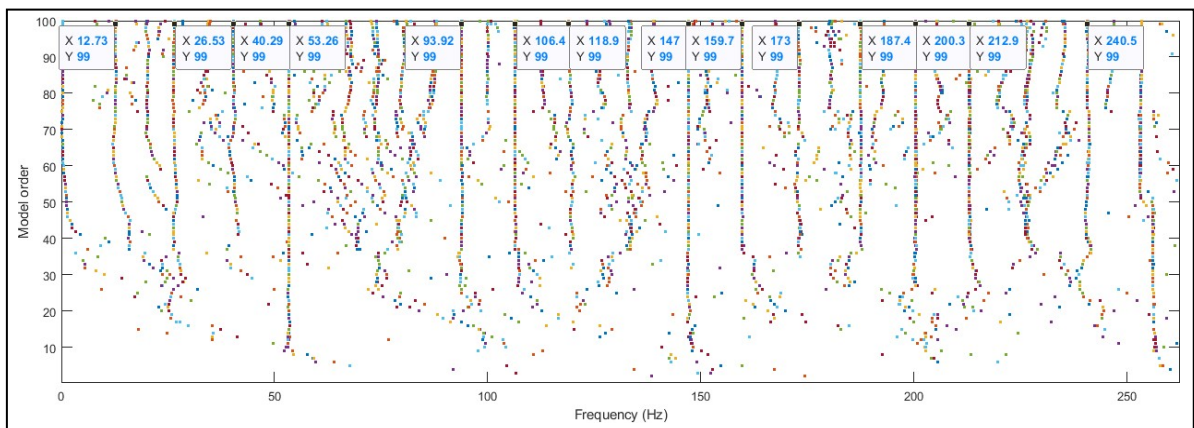


Figure 2.17 Frequency stabilization diagram of SCOMPI robot

Figure 2.17 illustrates the stabilization diagram of the SCOMPI robot, where we can observe all the frequencies of the structure, along with their harmonics. Table 2.4 lists all the identified natural frequencies and their damping ratios in the 0-256 Hz frequency range. By applying Fast Fourier Transform (FFT) on the measured accelerations in Figure 2.16, we can identify the most significant frequencies, such as 53.26 Hz, 93.92 Hz, 106.4 Hz, 147 Hz, 159.7 Hz, 200.3 Hz and 212.9 Hz. Especially, the rotating frequency of a grinding cup at 53.75 Hz and its harmonic frequencies are clearly revealed in both the FFT plot and in the stabilization diagram.

Table 2.4 Identified natural frequencies and damping ratios of SCOMPI robot manipulator

Mode	Mode 1	Mode 2	Mode 3	1 st harmonic	Mode 4	2 nd harmonic	Mode 5
f (Hz)	12.73	26.53	40.29	53.26	93.92	106.4	118.9
ξ (%)	7.17	2.55	2.31	0	0.14	0	1.39
Mode	Mode 6	3 rd harmonic	Mode 7	Mode 8	Mode 9	4 th harmonic	Mode 10
f (Hz)	147.0	159.7	173	187.4	200.3	212.9	240.5
ξ (%)	0.07	0	0.85	0.59	0.22	0	0.28

In the following steps, the measured accelerations at the end effector are used to reconstruct the forces in the triaxial directions, assisted by the Kalman filter. According to Vu *et al.* [50], it is necessary to determine an efficient model order rather than setting an arbitrarily large number. In fact, if an excessive model order is selected, we can encounter an over-parameterization trend, as well as unfavorable prediction ability, while the model complexity will increase significantly. Furthermore, extra spurious modes may have a great impact on the prediction accuracy. It is recommended not to use a model order higher than necessary, and thus, an optimum model order should be determined. The estimated Noise-to-Signal Ratio (NSR) presented by Vu *et al.* is employed as an asymptotic criterion for choosing an efficient model order (Vu, Thomas, Lafleur, & Marcouiller, 2013; Vu *et al.*, 2011). The method is based

on the evolution of error covariance with respect to the model order. The estimate \hat{NSR} is given in the equation (2.42) based on the trace norm part of error covariance matrices $\hat{\mathbf{E}}$ and the estimated deterministic $\hat{\mathbf{D}}$.

$$\hat{NSR} = \frac{\text{Trace}(\hat{\mathbf{E}})}{\text{Trace}(\hat{\mathbf{D}})}(\%) \quad \text{or} \quad \hat{NSR} = 10 \log_{10} \frac{\text{Trace}(\hat{\mathbf{E}})}{\text{Trace}(\hat{\mathbf{D}})}(\text{dB}) \quad (2.42)$$

A Noise-ratio Order Factor (NOF) is calculated as being a variation of the NSR between two successive orders:

$$\text{NOF}^{(p)} = \text{NSR}^{(p)} - \text{NSR}^{(p+1)} \quad (2.43)$$

The NOF is a representative factor for the convergence of the NSR, which changes dramatically at low orders and converges at high orders. Since this criterion is positive and close to zero, the convergent to zero property can be used as an efficient model order.

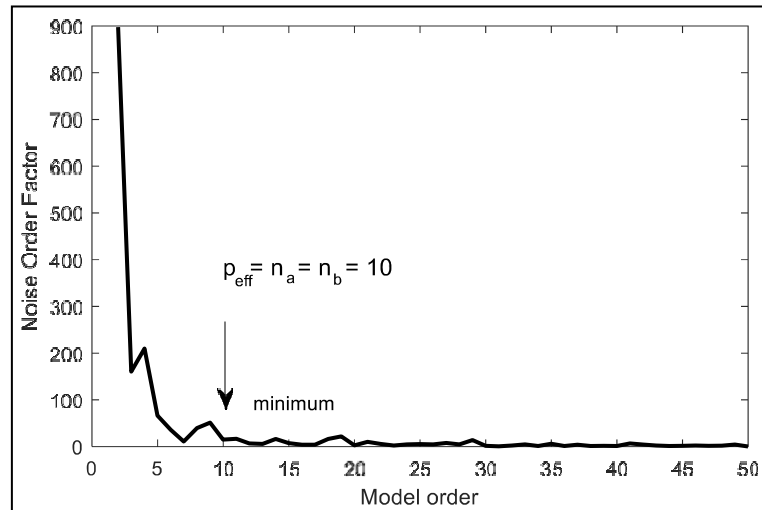


Figure 2.18 NOF evolution and efficient order selection on measured accelerations

According to the model order selection in Figure 2.18, the noise order factor can be seen stable from model order 10. Therefore, the ARX model (10, 10, 0) was chosen for our force identification algorithms, leading to auto-regressive, exogenous and delay orders of 10, 10 and 0, respectively. Subsequently, the state matrix and the measurement matrix were determined through the implementation of stochastic subspace identification. The dynamic excitation

forces in each direction were identified from a set of observed output data by using the Kalman filter with a recursive least squares estimator. Figures 2.19-2.21 display the time history of forces identified in each direction for the full test series, as compared to the measured ones. Table 2.5 shows a comparison of RMS values in each direction between the real and predicted forces.

Table 2.5 Comparison of the estimated and measured force RMS

	X direction	Y direction	Z direction
RMS of real force (N)	479	294	365
RMS of identified force (N)	517	311	390
RMS error (%)	7.9	5.8	6.8

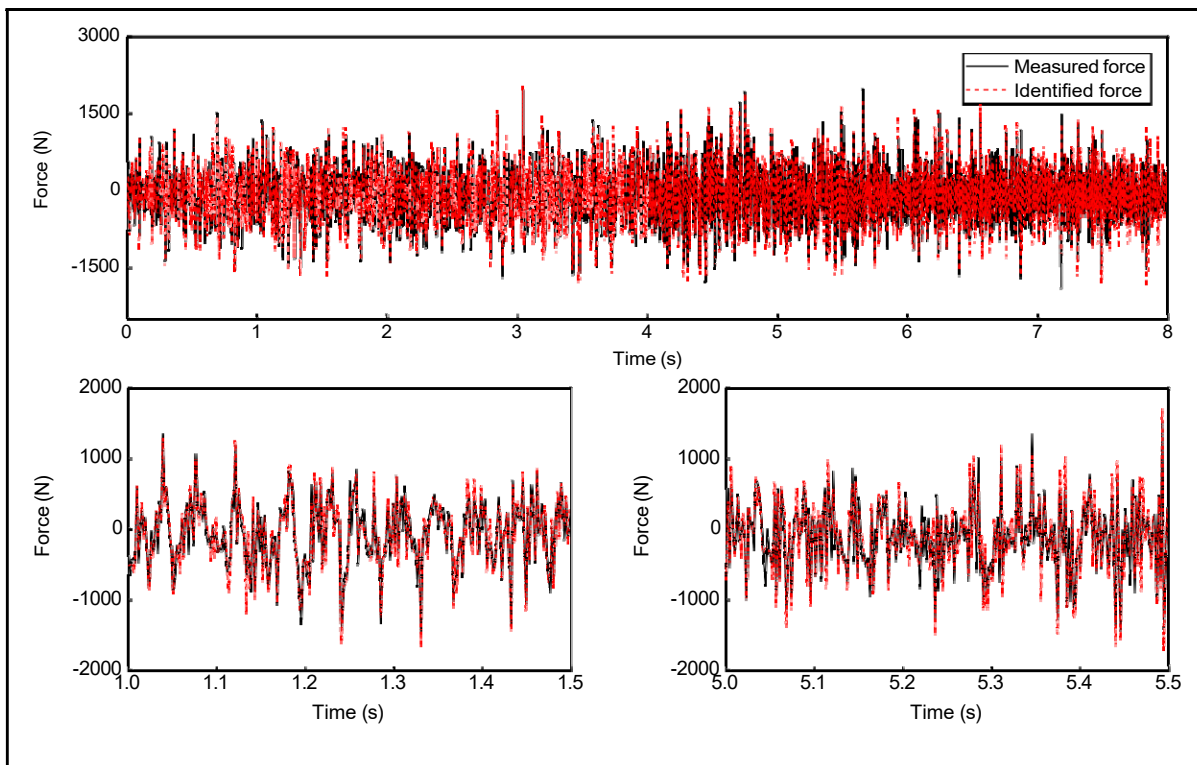


Figure 2.19 Estimated force in the X direction in the time domain, RMS error = 7.9 %

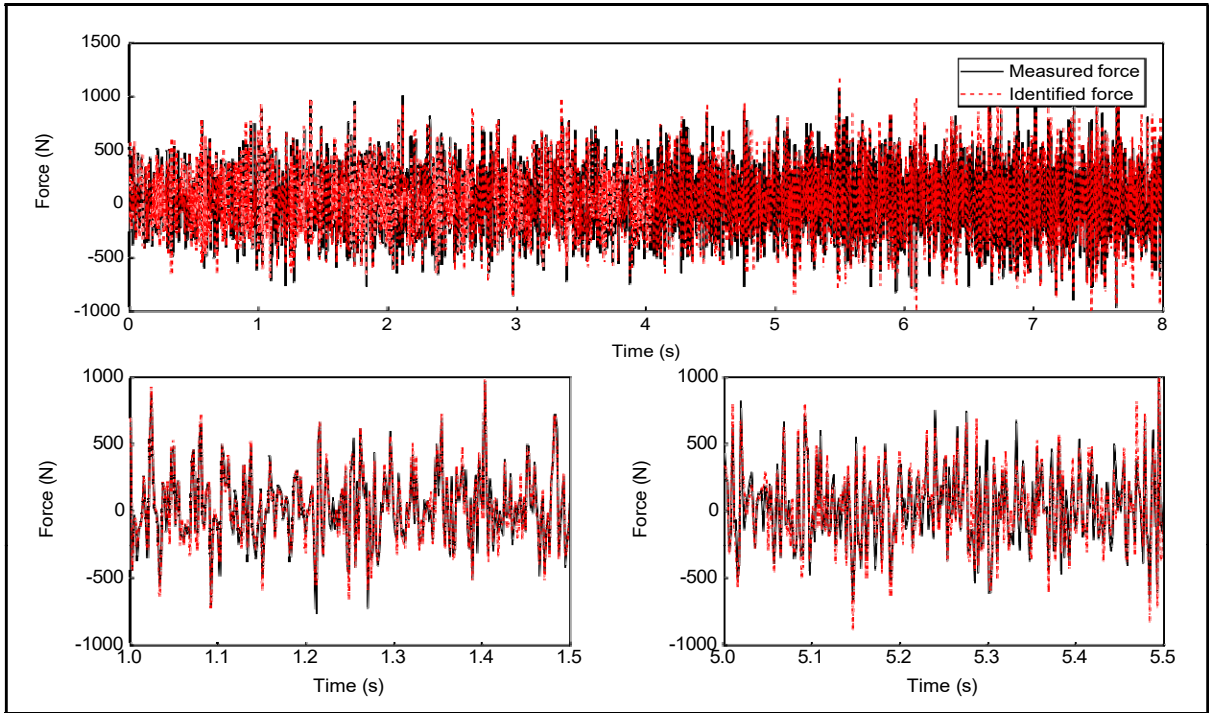


Figure 2.20 Estimated force in the Y direction in the time domain, RMS error = 5.8 %

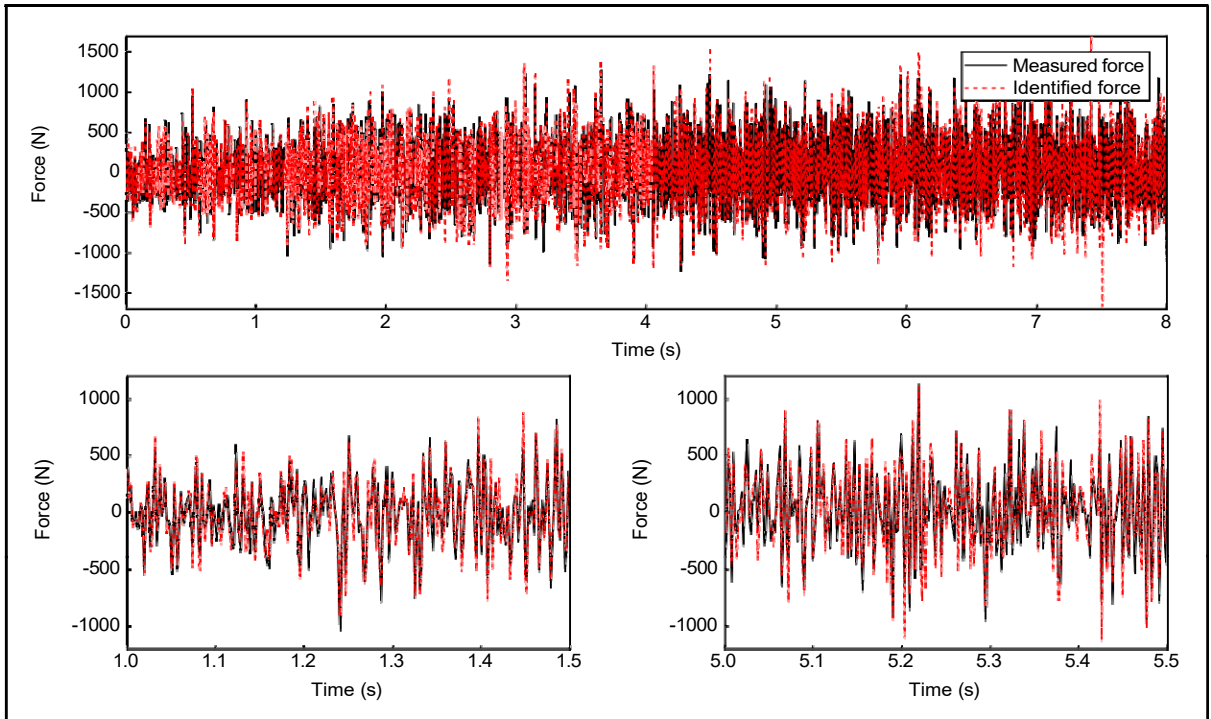


Figure 2.21 Estimated force in the Z direction in the time domain, RMS error = 6.8 %

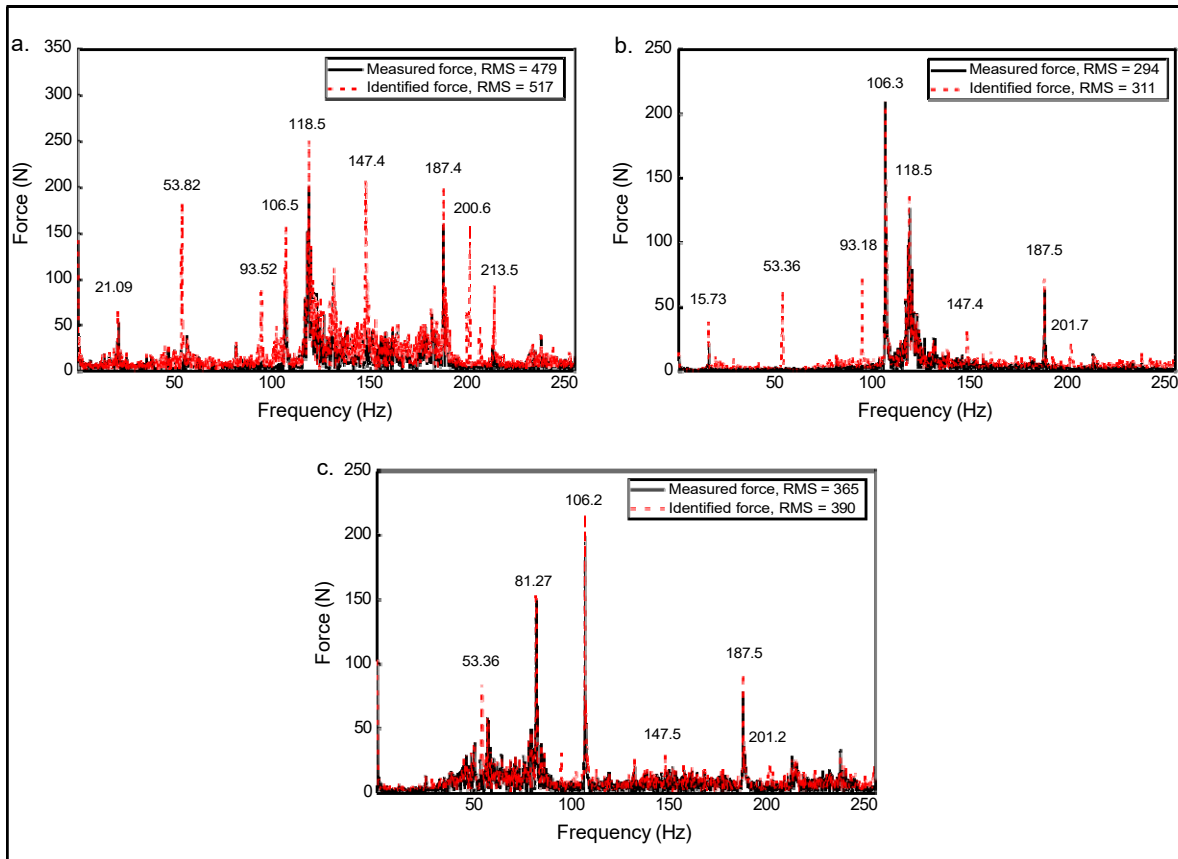


Figure 2.22 Estimated forces in frequency domain on each direction

a. X direction, b. Y direction, c. Z direction

As can be seen from the identification results in Figure 2.19-2.21, the identified forces appear similar to the measured ones, with RMS errors lower than 8% at the selected ARX (10,10,0) model. The good matching can be observed more clearly in the zoom graphs. It may be noticed that the predicted values are greater than the real ones in all three directions. In the frequency domain, the estimated and measured force are also computed in Figure 2.22. The identification results are revealed the amplitudes of other frequencies components which cannot be captured by the dynamometer but clearly identified in the previous stabilization diagram (Figure 2.17) such as 53 (Hz), 93 (Hz), 147 (Hz) and 200 (Hz). This is attributable to the energies come from the natural modes which are captured by accelerometers but not by the force sensors. It is an advantage of the proposed method on the frequency identification over the force's measurement. The estimation results indicate that the present identification technique is

capable of working on complex structures such as the robot manipulator under noisy conditions by applying the Kalman filter and ARX model, which stabilizes the computation and avoids ill-conditioned data. Additionally, using a time series model helps implement algorithm schemes conveniently without knowing the properties of the structure in advance.

2.8 Conclusion

This paper demonstrates an inverse method for computing the time-varying excitation forces acting on a structural system based on its response measurements, with the assistance of a system identification technique, in conjunction with the Kalman filter. The proposed method was investigated via both numerical simulations and experimental tests. The results show that the proposed technique is not only capable of handling noisy measurement data in satisfactorily identifying the modal parameters of the structure, but it also can estimate real unknown forces in the time domain. A comparison between the measured and estimated results confirms that the proposed approach can estimate the excitation forces with a good accuracy. It is our belief that the proposed method provides a useful tool for quantifying discrete input forces experienced during structural operations, which can be used in many subsequent analyses, such as structural analysis and health monitoring. One of the interesting points that make this approach feasible is its implementation by means of the Kalman filter, which can handle noisy measurements lower than 30% with an acceptable accuracy. The outcome of this study is an important step for further analysis and for the robot's control design. Since the contact forces are well estimated, ongoing research is being conducted on identifying added contact stiffness and damping in the interest of monitor chatter vibration phenomenon, which might happen during grinding operation.

2.9 Acknowledgements

This research was supported by NSERC (Natural Sciences and Engineering Research Council of Canada) through the Discovery Research RGPIN-2016-05859 grants and the Vietnam International Education Development (VIED) – Ministry of Education and Training of

Vietnam. The authors would like to thank Hydro-Québec's Research Institute for their technical support. This support is gratefully acknowledged.

2.10 References

- Al-Abdullah, K. I. A.-I., Abdi, H., Lim, C. P., & Yassin, W. A. (2018). Force and temperature modelling of bone milling using artificial neural networks. *Measurement*, *116*, 25-37. doi:<https://doi.org/10.1016/j.measurement.2017.10.051>
- Allen, M. S., & Carne, T. G. (2008). Delayed, Multi-Step Inverse Structural Filter for Robust Force Identification. *Mechanical Systems and Signal Processing*, *22*, 1036-1054.
- Colomé, A., Pardo, D., Alenyà, G., & Torras, C. (2013, 6-10 May 2013). *External force estimation during compliant robot manipulation*. Paper presented at the 2013 IEEE International Conference on Robotics and Automation.
- Ding, Y., Law, S. S., Wu, B., Xu, G. S., Lin, Q., Jiang, H. B., & Miao, Q. S. (2013). Average acceleration discrete algorithm for force identification in state space. *Engineering Structures*, *56*, 1880-1892. doi:<https://doi.org/10.1016/j.engstruct.2013.08.004>
- Eftekhar Azam, S., Chatzi, E., & Papadimitriou, C. (2015). A dual Kalman filter approach for state estimation via output-only acceleration measurements. *Mechanical Systems and Signal Processing*, *60-61*, 866-886. doi:<https://doi.org/10.1016/j.ymssp.2015.02.001>
- Feng, W., Li, Q., & Lu, Q. (2020). Force localization and reconstruction based on a novel sparse Kalman filter. *Mechanical Systems and Signal Processing*, *144*, 106890. doi:<https://doi.org/10.1016/j.ymssp.2020.106890>
- Feng, W., Li, Q., Lu, Q., Li, C., & Wang, B. (2021). Group Relevance Vector Machine for sparse force localization and reconstruction. *Mechanical Systems and Signal Processing*, *161*, 107900. doi:<https://doi.org/10.1016/j.ymssp.2021.107900>
- Gao, F., & Lu, Y. (2006). A Kalman-filter based time-domain analysis for structural damage diagnosis with noisy signals. *Journal of Sound and Vibration*, *297*(3), 916-930. doi:<https://doi.org/10.1016/j.jsv.2006.05.007>

- Hazel, B., Côté, J., Laroche, Y., & Mongenot, P. (2012a). Field repair and construction of large hydropower equipment with a portable robot. *Journal of Field Robotics*, 29(1), 102-122. doi:<https://doi.org/10.1002/rob.20427>
- Hazel, B., Côté, J., Laroche, Y., & Mongenot, P. (2012b). A portable, multiprocess, track-based robot for in situ work on hydropower equipment. *Journal of Field Robotics*, 29(1), 69-101. doi:<https://doi.org/10.1002/rob.20425>
- Hwang, J.-S., Kareem, A., & Kim, H. (2011). Wind load identification using wind tunnel test data by inverse analysis. *Journal of Wind Engineering and Industrial Aerodynamics*, 99(1), 18-26. doi:<https://doi.org/10.1016/j.jweia.2010.10.004>
- Inoue, H., Harrigan, J., J., & Reid, S. R. (2001). Review of inverse analysis for indirect measurement of impact force. *Applied Mechanics Reviews*, 54(6), 503-524. doi:10.1115/1.1420194
- Isaksson, A. J. (1993). Identification of ARX-models subject to missing data. *IEEE Transactions on Automatic Control*, 38(5), 813-819. doi:10.1109/9.277253
- Jansson, M. (2003). Subspace Identification and ARX Modeling. *IFAC Proceedings Volumes*, 36(16), 1585-1590. doi:[https://doi.org/10.1016/S1474-6670\(17\)34986-8](https://doi.org/10.1016/S1474-6670(17)34986-8)
- Jiang, X. Q., & Hu, H. Y. (2009). Reconstruction of distributed dynamic loads on a thin plate via mode-selection and consistent spatial expression. *Journal of Sound and Vibration*, 323(3), 626-644. doi:<https://doi.org/10.1016/j.jsv.2009.01.008>
- Kalman, R. E. (1960). A New Approach to Linear Filtering and Prediction Problems. *Journal of Basic Engineering*, 82(1), 35-45. doi:10.1115/1.3662552
- Kammer, D., & Steltzner, A. (2001). Input Force Estimation Using an Inverse Structural Filter. *Journal of Vibration and Acoustics*, 123, 524-532.
- Kammer, D. C. (1998). Input Force Reconstruction Using a Time Domain Technique. *Journal of Vibration and Acoustics*, 120(4), 868-874. doi:10.1115/1.2893913
- Khoo, S. Y., Ismail, Z., Kong, K. K., Ong, Z. C., Noroozi, S., Chong, W. T., & Rahman, A. G. A. (2014). Impact force identification with pseudo-inverse method on a lightweight structure for under-determined, even-determined and over-determined cases. *International Journal of Impact Engineering*, 63, 52-62. doi:<https://doi.org/10.1016/j.ijimpeng.2013.08.005>

- Linder, J., & Enqvist, M. (2017). Identification of systems with unknown inputs using indirect input measurements. *International Journal of Control*, 90(4), 729-745. doi:10.1080/00207179.2016.1222557
- Liu, X., Zhao, F., Ge, S. S., Wu, Y., & Mei, X. (2019). End-Effector Force Estimation for Flexible-Joint Robots With Global Friction Approximation Using Neural Networks. *IEEE Transactions on Industrial Informatics*, 15(3), 1730-1741. doi:10.1109/TII.2018.2876724
- Liu, Y., & Shepard, W. S. (2005). Dynamic force identification based on enhanced least squares and total least-squares schemes in the frequency domain. *Journal of Sound and Vibration*, 282(1), 37-60. doi:<https://doi.org/10.1016/j.jsv.2004.02.041>
- Ljung, L. (1985). On the estimation of transfer functions. *Automatica*, 21(6), 677-696. doi:[https://doi.org/10.1016/0005-1098\(85\)90042-1](https://doi.org/10.1016/0005-1098(85)90042-1)
- Lourens, E., Reynders, E., De Roeck, G., Degrande, G., & Lombaert, G. (2012). An augmented Kalman filter for force identification in structural dynamics. *Mechanical Systems and Signal Processing*, 27, 446-460. doi:<https://doi.org/10.1016/j.ymsp.2011.09.025>
- Lu, Y., & Gao, F. (2005). A novel time-domain auto-regressive model for structural damage diagnosis. *Journal of Sound and Vibration*, 283(3), 1031-1049. doi:<https://doi.org/10.1016/j.jsv.2004.06.030>
- Ma, C.-K., & Ho, C.-C. (2004). An inverse method for the estimation of input forces acting on non-linear structural systems. *Journal of Sound and Vibration*, 275(3), 953-971. doi:[https://doi.org/10.1016/S0022-460X\(03\)00797-1](https://doi.org/10.1016/S0022-460X(03)00797-1)
- Ma, C. K., Chang, J. M., & Lin, D. C. (2003). INPUT FORCES ESTIMATION OF BEAM STRUCTURES BY AN INVERSE METHOD. *Journal of Sound and Vibration*, 259(2), 387-407. doi:<https://doi.org/10.1006/jsvi.2002.5334>
- Mehrpouya, M., & Ahmadian, H. (2009). Estimation of applied forces on railway vehicle wheelsets from measured vehicle responses. *Int. J. Vehicle Structures & Systems*, 1(4), 104-110.
- Mendrok, K., Kurowski, P., & Uhl, T. (2008). *Operational Forces Identification From Helicopter Model In-Flight Data With Use of Inverted Regressive Parametric Models*. <https://doi.org/10.1115/DETC2008-49790>

- Mendrok, K., & Uhl, T. (2009). Load Identification Using a Modified Modal Filter Technique. *Journal of Vibration and Control*, 16(1), 89-105. doi:10.1177/1077546309103274
- Naets, F., Cuadrado, J., & Desmet, W. (2015). Stable force identification in structural dynamics using Kalman filtering and dummy-measurements. *Mechanical Systems and Signal Processing*, 50-51, 235-248. doi:<https://doi.org/10.1016/j.ymssp.2014.05.042>
- Nayek, R., Chakraborty, S., & Narasimhan, S. (2019). A Gaussian process latent force model for joint input-state estimation in linear structural systems. *Mechanical Systems and Signal Processing*, 128, 497-530. doi:<https://doi.org/10.1016/j.ymssp.2019.03.048>
- Nguyen, Q., Vu, V. H., & Thomas, M. (2019). *ARX model for experimental vibration analysis of grinding process by flexible manipulator*.
- Olesen, D. H., Huusom, J. K., & Jørgensen, J. B. (2013, 17-19 June 2013). *A tuning procedure for ARX-based MPC of multivariate processes*. Paper presented at the 2013 American Control Conference.
- Qiao, B., Liu, J., Liu, J., Yang, Z., & Chen, X. (2019). An enhanced sparse regularization method for impact force identification. *Mechanical Systems and Signal Processing*, 126, 341-367. doi:<https://doi.org/10.1016/j.ymssp.2019.02.039>
- Qiao, B., Mao, Z., Liu, J., Zhao, Z., & Chen, X. (2019). Group sparse regularization for impact force identification in time domain. *Journal of Sound and Vibration*, 445, 44-63. doi:<https://doi.org/10.1016/j.jsv.2019.01.004>
- Roy, K., Bhattacharya, B., & Ray-Chaudhuri, S. (2015). ARX model-based damage sensitive features for structural damage localization using output-only measurements. *Journal of Sound and Vibration*, 349, 99-122. doi:<https://doi.org/10.1016/j.jsv.2015.03.038>
- Sanchez, J., & Benaroya, H. (2014). Review of force reconstruction techniques. *Journal of Sound and Vibration*, 333, 2999-3018. doi:10.1016/j.jsv.2014.02.025
- Sedehi, O., Papadimitriou, C., Teymouri, D., & Katafygiotis, L. S. (2019). Sequential Bayesian estimation of state and input in dynamical systems using output-only measurements. *Mechanical Systems and Signal Processing*, 131, 659-688. doi:<https://doi.org/10.1016/j.ymssp.2019.06.007>

- Soderstrom, T., Fan, H., Carlsson, B., & Bigi, S. (1997). Least squares parameter estimation of continuous-time ARX models from discrete-time data. *IEEE Transactions on Automatic Control*, 42(5), 659-673. doi:10.1109/9.580871
- Thite, A. N., & Thompson, D. J. (2006). Selection of response measurement locations to improve inverse force determination. *Applied Acoustics*, 67(8), 797-818. doi:<https://doi.org/10.1016/j.apacoust.2006.01.001>
- Van Den Hof, P. M. J., & Schrama, R. J. P. (1993). An indirect method for transfer function estimation from closed loop data. *Automatica*, 29(6), 1523-1527. doi:[https://doi.org/10.1016/0005-1098\(93\)90015-L](https://doi.org/10.1016/0005-1098(93)90015-L)
- Vu, V. H., Thomas, M., Lafleur, F., & Marcouiller, L. (2013). Towards an automatic spectral and modal identification from operational modal analysis. *Journal of Sound and Vibration*, 332(1), 213-227. doi:<https://doi.org/10.1016/j.jsv.2012.08.019>
- Vu, V. H., Thomas, M., Lakis, A. A., & Marcouiller, L. (2011). Operational modal analysis by updating autoregressive model. *Mechanical Systems and Signal Processing*, 25(3), 1028-1044. doi:<https://doi.org/10.1016/j.ymsp.2010.08.014>
- Wambacq, J., Maes, K., Rezayat, A., Guillaume, P., & Lombaert, G. (2019). Localization of dynamic forces on structures with an interior point method using group sparsity. *Mechanical Systems and Signal Processing*, 115, 593-606. doi:<https://doi.org/10.1016/j.ymsp.2018.06.006>
- Wang, J., Law, S. S., & Yang, Q. S. (2013). Sensor placement methods for an improved force identification in state space. *Mechanical Systems and Signal Processing*, 41(1), 254-267. doi:<https://doi.org/10.1016/j.ymsp.2013.07.004>
- Wang, M. L., & Kreitinger, T. J. (1994). Identification of force from response data of a nonlinear system. *Soil Dynamics and Earthquake Engineering*, 13(4), 267-280. doi:[https://doi.org/10.1016/0267-7261\(94\)90031-0](https://doi.org/10.1016/0267-7261(94)90031-0)
- Wu, A.-L., Loh, C.-H., Yang, J. N., Weng, J.-H., Chen, C.-H., & Ueng, T.-S. (2009). Input force identification: Application to soil-pile interaction. *Structural Control and Health Monitoring*, 16(2), 223-240. doi:<https://doi.org/10.1002/stc.308>

- Yu, L., & Chan, T. H. T. (2003). Moving force identification based on the frequency–time domain method. *Journal of Sound and Vibration*, 261(2), 329-349. doi:[https://doi.org/10.1016/S0022-460X\(02\)00991-4](https://doi.org/10.1016/S0022-460X(02)00991-4)
- Zhang, E., Antoni, J., & Feissel, P. (2012). Bayesian force reconstruction with an uncertain model. *Journal of Sound and Vibration*, 331(4), 798-814. doi:<https://doi.org/10.1016/j.jsv.2011.10.021>
- Zhou, J. M., Dong, L., Guan, W., & Yan, J. (2019). Impact load identification of nonlinear structures using deep Recurrent Neural Network. *Mechanical Systems and Signal Processing*, 133, 106292. doi:<https://doi.org/10.1016/j.ymssp.2019.106292>

CHAPTER 3

OPTIMAL ARMAX MODEL ORDER IDENTIFICATION OF DYNAMIC SYSTEMS

Quoc Cuong Nguyen^a, Viet Hung Vu^b and Marc Thomas^c,

^{a,b,c} Department of Mechanical Engineering, École de Technologie Supérieure,
1100 Notre-Dame West, Montreal, Quebec, H3C 1K3

Paper published in *London Journals of Engineering Research*, May 2022

Highlights

- New method for optimizing model order selection.
- Minimum means square error of the estimated transfer functions is applied.
- ARMAX time series model is implemented.
- Using transfer functions for modal analysis.
- The algorithm is verified by using experimental data obtained from a grinding test of SCOMPI robot.

3.1 Résumé

Cet article décrit une approche efficace pour la détermination de l'ordre du modèle, qui permet d'identifier le comportement dynamique du système mécanique en utilisant des données observées d'entrée-sortie. Le concept est basé sur l'erreur quadratique moyenne minimale des fonctions de transfert estimées, qui peut considérer le bruit de mesure et les erreurs de modélisation pour identifier les fonctions de transfert d'ordre inférieur appropriées des structures via un modèle ARMAX (Auto-Régressive Moving Average eXogenous). L'efficacité de la méthode proposée est validée exclusivement à l'aide de données expérimentales issues d'un test de meulage d'un robot manipulateur industriel SCOMPI. Certains autres critères, tels que le critère d'information d'Akaike (AIC), le critère d'information bayésien (BIC) et le facteur d'ordre du bruit (NOF), sont étudiés pour vérifier les

performances de la méthodologie proposée. Les résultats ont démontré que la présente technique est rentable en termes de détermination optimale de l'ordre du modèle, et le modèle ARMAX s'avère être la représentation la plus appropriée pour l'extraction de caractéristiques à l'ordre inférieur. Grâce à sa flexibilité dans la gestion des perturbations du modèle, la stratégie d'optimisation proposée peut capturer tous les modes d'oscillation dominants de la structure aux ordres bas, et les propriétés modales du système sont déterminées efficacement et automatiquement. En revanche, les performances du modèle ARX s'avèrent moins efficaces lorsque les commandes sont faibles.

Mots-clés : modèle ARMAX, modèle ARX, fonctions de réponse en fréquence, ordres optimaux, identification modale.

3.2 Abstract

This paper describes an efficient approach for model order determination, which allows identifying the dynamical behavior of the mechanical system by using observation input-output data. The concept is based on the minimum means square error of the estimated transfer functions, which can effectively tackle measurement noise and modeling errors to identify appropriate low-order transfer functions of the structures via an Auto-Regressive Moving Average eXogenous (ARMAX) model. The effectiveness of the proposed method is validated exclusively using experimental data obtained from a grinding test of an industrial manipulator SCOMPI robot. Some other criteria, such as the Akaike Information Criterion (AIC), the Bayesian Information Criterion (BIC), and the Noise Order Factor (NOF), are investigated to verify the performance of the proposed methodology. The results demonstrated that the present technique is cost-effective in terms of optimal model order determination, and the ARMAX model turns out to be the most appropriate representation for feature extraction at the low order. Thanks to its flexibility in handling model disturbance, the proposed optimization strategy can capture all the dominant oscillation modes of the structure at the low orders, and system modal properties are efficiently and automatically determined. In contrast, the performance of the ARX model is shown to be less efficient when working at low orders.

Keywords: ARMAX model, ARX model, Frequency Response Functions, Optimal orders, Modal identification.

3.3 Introduction

Operational Transfer Functions (TFs) or Frequency Response Functions (FRFs) of mechanical structures play a vital role in understanding the dynamic characteristics of the systems and in solving general vibration problems during the operational process. They constitute an effective tool aiding the extraction of modal parameters. Estimating the transfer functions of a mechanical system has thus become an important task in many engineering applications. Different representations of transfer functions are crucial in the description and analysis of system properties. In industrial applications, a measurement of the transfer functions defining the structure properties in the frequency domain can be implemented using vibration instrumentations. Different methodologies are proposed in the literature with the aim of estimating operational transfer functions, with the most common applying the Fourier analysis. The Empirical Transfer Function Estimate (ETFTE) is a natural nonparametric method that identifies transfer functions by taking the ratios of the Fourier transform of the outputs to those of the inputs (Ljung, 1985). However, this method requires more data points and raw ETFTE estimates are generally not accurate enough. With these estimates, the variance does not decrease as the number of data points increases because they contain no information compression feature. Researchers have conducted various experimental studies on structural dynamics under operational conditions. In (Saupe & Knoblach, 2015), the FRFs of a flexible joint industrial manipulator with a serial kinematic were identified based on a non-parametric closed loop. However, due to the nonlinearities of the robot, the method faced a challenge in eliminating disturbances in the estimated FRFs. Operational Modal Analysis (OMA) is another approach for identifying the modal properties of the structure using vibration data obtained under operating conditions. Yili Peng *et al.* identified in-process FRFs based on the OMA and Experimental Modal Analysis (EMA), which uses the natural frequencies and damping ratios to build FRFs under operating conditions (Peng *et al.*, 2018). A simulation of a three-degree-

of-freedom mass-spring-damper system and experiments on a machine tool are adopted to verify the proposed method. Similarly, Zaghbani et al. used OMA in the identification of the dynamics of a milling machine under a cutting process work (Zaghbani & Songmene, 2009). At the same time, another method was presented in (Smith & Randall, 2016) to generate FRFs from identified poles and zeros in the low-frequency domain. Recently, Coppotelli *et al.* proposed an approach for estimating FRFs from operational data by changing different mass and stiffness distributions (Coppotelli, 2009). This method also allows evaluating the modal parameters of the structure via operational modal testing. Conversely, Özşahin et al. introduced a new technique to calculate the variation in tool point FRFs under different working conditions by using an inverse analysis of self-excited chatter vibration (Özşahin, Budak, & Özgüven, 2015). In their method, chatter frequencies were experimentally determined and applied to estimate tool point FRFs on a 5-axis milling machine via the relation between the measured force inputs and acceleration outputs. However, the tool point FRFs are not well estimated at high spindle speeds due to the presence at those speeds of a low signal-to-noise ratio and the bandwidth limitation of the dynamometer. Another in-process FRF identification approach of the spindle structure was presented in (Postel, Özşahin, & Altintas, 2018). In that case, the tooltip FRFs were identified under operational conditions based on an inverse solution of critical stability limits. The method is helpful for predicting the stability of the tool holders when the direct measurement of the tool point FRFs is uncompromised. Parametric estimation methods constitute another system identification class. In these methods, it is suggested to use time series modeling for the mathematical description of the transfer functions. It combines the advantage and information obtained from both measurements and theoretical modeling. Depending on the availability of the measurement signals, the Auto Regressive model (AR) (V.-H. Vu, Liu, Thomas, Li, & Hazel, 2016; V. H. Vu, Thomas, Lakis, & Marcouiller, 2011) or the Auto Regressive Moving Average model (ARMA) can be used if only the output is available (Chen, Lee, & Tsuei, 1993). In (M. Smail, M. Thomas, & A. Lakis, 1999a; M. Smail, M. Thomas, & A. A. Lakis, 1999b), a modal analysis was conducted in different industrial structures based on three Auto-Regressive Moving Average methods, namely, the recursive least-square, output error, and corrected covariance matrix methods to determine the optimal model order. Conversely, in the case of measurable or identifiable excitation forces, the Auto-

Regressive eXogenous (ARX) model can exploit, by assuming that the model's errors and disturbances are white noise (Viet Hung Vu, Zhaoheng, Thomas, Tahvilian, & Hazel, 2016). However, because of the unavoidable noise contaminated in the measured signals, the quality of estimated FRFs can be adversely affected by noise originating from the test environment. When the system operates in an industrial condition with a lot of disturbance, identifying the transfer functions of a complex structure may become difficult.

In this paper, we present an original method designed for automatically extracting the modal parameters from identified transfer functions based on the concept of the optimal ARMAX model. Particular attention is paid to selecting optimal model orders, which can closely reflect the dynamic system. The work contributes to the determination of a model order based on the estimated transfer functions, by using the framework of the ARMAX model. The proposed method is experimentally applied to a robot during its grinding operation, and the results are compared to those of the original ARX model. The measured grinding forces may be considered the exogenous inputs excitation, and the disturbances of the system are taken into account by adding the Moving Average part into the model. The estimated orders are verified based on the most common selection criteria, such as the Akaike Information Criteria (AIC) (H. Akaike, 1974), the Bayesian Information Criteria (BIC) (Gideon, 1978), and the Noise Order Factor (NOF) (V. H. Vu, Thomas, Lafleur, & Marcouiller, 2013). In this study, the ARMAX model is expressed in a convenient way for computation at the low orders, which gives a more parsimonious representation and helps improve the modeling performance, with less computational complexity. We have organised the rest of this paper in the following way. The motivation for the research is established in Section 2 through a detailed description of the time series modeling, with a focus on the ARX and ARMAX models. Section 3 proposes an original method to determine an optimal model order of the mechanical system. Experiments are then conducted on the flexible manipulator, SCOMPI, under grinding operation to validate the proposed methods in Section 4, followed by the identification procedure and the results. We end by drawing several conclusions from this research.

3.4 Time series modeling

System identification is the art of modeling a dynamical system from raw time series data. We consider the problem of estimating a dynamic system model based on the measurement of an N points input-output data, which will be pre-classified into input $\mathbf{u}(t) \in \mathbb{R}^m$, $t = 1, \dots, T$ and output $\mathbf{y}(t) \in \mathbb{R}^n$, $t = 1, \dots, T$:

$$\mathbf{Z}^N = (\mathbf{u}(t), \mathbf{y}(t))_{t=1}^N \quad (3.1)$$

Various representations of linear time series such as Auto-Regressive (AR), Auto-Regressive Moving Average (ARMA), Auto-Regressive eXogenous (ARX), and Auto-Regressive Moving Average eXogenous (ARMAX) can be employed to extract dynamic parameters (Lennart, 1999). Since there are various time series data types, we should choose an appropriate model. In general, such models are based on an Auto-Regressive (AR) part or output, an eXogenous (X) part or input, or a Moving Average (MA) part or error term, depending on the situation. The AR model is the simplest time series representation, which linearly depends on output data (the vibration responses). In the availability of both input (the measurable and known excitation force) and output data, the ARX model is usable. It is possible to combine these models with the MA term and produce the ARMA representation for the output-only cases and the ARMAX model for the input-output conditions. Once the most appropriate modal structure is selected, we can apply a model to the measurement by minimizing certain criteria:

$$\hat{\boldsymbol{\theta}}_N = \operatorname{argmin}_{\boldsymbol{\theta}} \mathbf{V}_N(\boldsymbol{\theta}, \mathbf{Z}^N) \quad (3.2)$$

where $\boldsymbol{\theta}$ is the unknown parameter vector of the parametric model structure.

In automatic control applications, given the current state and input signal, the model can be applied to predict the output of the system by choosing a cost function in the form.

$$\mathbf{V}_N(\boldsymbol{\theta}, \mathbf{Z}^N) = \frac{1}{N} \sum_{t=1}^N l(\mathbf{L}(q)\boldsymbol{\varepsilon}(t, \boldsymbol{\theta})) \quad (3.3)$$

where $\mathbf{L}(q)$ represents a filter that removes unwanted properties in the measurement data, and $l(\cdot)$ is a convex function.

The following quantity is the prediction error. $\hat{y}(t|t-1, \theta)$ is the one-step-ahead predictor representing the model of the system:

$$\varepsilon(t, \theta) = \mathbf{y}(t) - \hat{\mathbf{y}}(t|t-1, \theta) \quad (3.4)$$

A common representation of the Linear Time-Invariant (LTI) system can be expressed in the form of the linear transfer function model:

$$\mathbf{y}(t) = \mathbf{G}(q, \theta) \mathbf{u}(t) + \mathbf{H}(q, \theta) \mathbf{w}(t) \quad (3.5)$$

where q is the forward shift operator, that is, $q^{-k} \mathbf{y}(t) = \mathbf{y}(t-k)$. Here, $\mathbf{y}(t)$ is a n_y dimensional vector of output, $\mathbf{u}(t)$ is a n_u dimensional vector of input, and $\mathbf{w}(t)$ is the disturbance sequence with an appropriate dimension and assumed to be an independent and identically distributed stochastic process, respectively. Furthermore, the transfer functions $\mathbf{G}(q, \theta)$ and $\mathbf{H}(q, \theta)$ are rational functions in the backward shift operator q , and the coefficients are given by the elements of the parameter vector θ .

The predictor associated with the output is given by (Lennart, 1999):

$$\hat{\mathbf{y}}(t|t-1, \theta) = \mathbf{H}^{-1}(q, \theta) \mathbf{G}(q, \theta) \mathbf{u}(t) + (1 - \mathbf{H}^{-1}(q, \theta)) \mathbf{y}(t) \quad (3.6)$$

where:

$$\mathbf{H}^{-1}(q, \theta) = 1 / \mathbf{H}(q, \theta) \mathbf{u}(t) \quad (3.7)$$

This model structure is quite general, but we can develop some special cases. A simple case is the ARX model structure, which is:

$$\mathbf{A}(q) \mathbf{y}(t) = \mathbf{B}(q) \mathbf{u}(t) + \mathbf{w}(t) \quad (3.8)$$

that can be rewritten in a more general polynomial form as:

$$\{\mathbf{y}(t)\} + \sum_{k=1}^{n_a} [\mathbf{A}_k] \{\mathbf{y}[t-k]\} = \sum_{k=1}^{n_b} [\mathbf{B}_k] \{\mathbf{u}[t-n_k-k+1]\} + \{\mathbf{w}(t)\} \quad (3.9)$$

where:

$$\mathbf{A}(q) = I + a_1 q^{-1} + a_2 q^{-2} \dots + a_{n_a} q^{-n_a} \quad (3.10)$$

$$\mathbf{B}(q) = b_0 + b_1 q^{-1} + b_2 q^{-2} \dots + b_{n_b} q^{-n_b-n_b+1} \quad (3.11)$$

are autoregressive and exogenous matrix parameters, with I denote the identity matrix. n_a , n_b , and n_k are the orders of the ARX model, n_a is equal to the number of poles and n_b is the

number of zeros, while n_k is the pure time delay in the system. Since $\mathbf{G}(q, \theta) = \mathbf{B}(q) / \mathbf{A}(q)$ and $\mathbf{H}(q, \theta) = 1 / \mathbf{A}(q)$, the predictor of the output can be written as:

$$\hat{\mathbf{y}}(t|t-1, \theta) = \mathbf{B}(q)\mathbf{u}(t) + (1 - \mathbf{A}(q)\mathbf{y}(t)) = \boldsymbol{\varphi}(t)^T \boldsymbol{\theta} \quad (3.12)$$

where

$$\boldsymbol{\varphi}(t) = (-y(t-1) \cdots -y(t-n_a) \ u(t-1) \cdots u(t-n_b))^T \quad (3.13)$$

$$\boldsymbol{\theta} = (a_1 \cdots a_{n_a} \ b_1 \cdots b_{n_b})^T \quad (3.14)$$

When the noise is assumed to be a white Gaussian process with zero means, which is uncorrelated with the regressors, the model parameters $\boldsymbol{\theta}$ are estimated via the Least-Square (LS) estimator (Soderstrom, Fan, Carlsson, & Bigi, 1997):

$$\hat{\boldsymbol{\theta}}_N^{LS} = \operatorname{argmin} \frac{1}{N} \sum_{t=1}^N (\mathbf{y}(t) - \boldsymbol{\varphi}(t)^T \boldsymbol{\theta})^2 \quad (3.15)$$

The variance $\mathbf{y}(t) - \boldsymbol{\varphi}(t)^T \boldsymbol{\theta}$ represents the remaining un-modelled behavior of the data.

The corresponding transfer function is $\mathbf{G}(q, \theta) = \mathbf{B}(q) / \mathbf{A}(q)$ (3.15a)

However, in this case, only the deterministic part of equation (3.1) is estimated by considering no noise $\mathbf{H}(q, \theta)$. If a noise model is sought, additional steps are needed, assuming that the noise is described by a Moving Average process $\mathbf{C}(q)$, which results in an ARMAX structure:

$$\mathbf{A}(q)\mathbf{y}(t) = \mathbf{B}(q)\mathbf{u}(t) + \mathbf{C}(q)\mathbf{w}(t) \quad (3.16)$$

and its polynomial form

$$\{\mathbf{y}(t)\} + \sum_{k=1}^{n_a} [\mathbf{A}_k] \{\mathbf{y}[t-k]\} = \sum_{k=1}^{n_b} [\mathbf{B}_k] \{\mathbf{u}[t-n_k-k+1]\} + \sum_{k=1}^{n_c} [\mathbf{C}_k] \{\mathbf{e}[t-k]\} + \{\mathbf{w}(t)\} \quad (3.17)$$

where:

$$\mathbf{C}(q) = 1 + c_1 q^{-1} + c_2 q^{-2} \cdots + a_{n_c} q^{-n_c} \quad (3.18)$$

is the polynomial of order n_c which represents for Moving Average term.

In contrast with the simpler ARX model, this presentation form offers a noisy transfer function $\mathbf{H}(q, \theta) = \mathbf{C}(q) / \mathbf{A}(q)$, which allows representing different types of noise characteristics through a proper choice of the MA polynomial term. In engineering applications, it is

unavoidable when environmental noise contaminated in measured data. Therefore, a parametric system identification algorithm should be adopted to identify the modal parameters from the noisy data. Under this condition, the ARMAX model with real-time identification proves to be efficient. Figure 3.1 presents the structures of both ARX and ARMAX models.

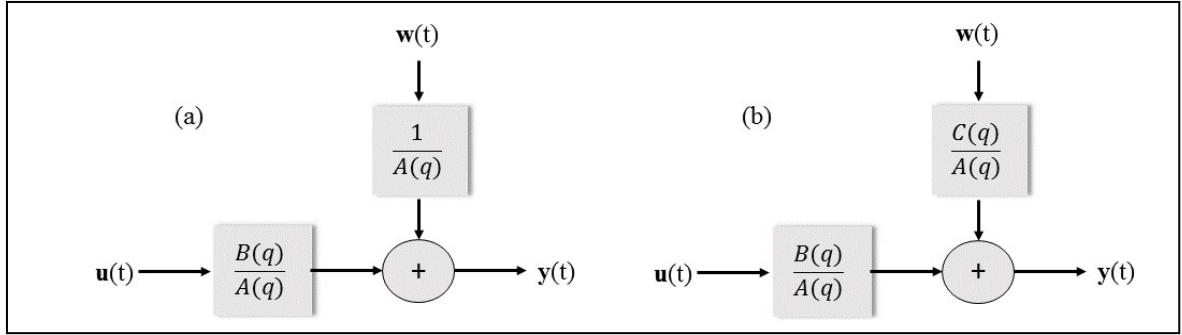


Figure 3.1 Model structures of ARX (a) and ARMAX (b)
Taken from Lennart et al. (1999)

If only the ARX model is use, the noise model is described as $\mathbf{H}(q) = 1/\mathbf{A}(q)$, where $\mathbf{A}(q)$ is also used as the denominator of $\mathbf{G}(q)$, describing the dynamic model. This model implies that the polynomial form must be an average estimate of the poles of $\mathbf{G}(q)$ and $\mathbf{H}(q)$. However, the noise model can be better estimated using the ARMAX model, as described by the numerator polynomial term $\mathbf{C}(q)$. When parametric methods use for model estimation, the transfer functions to be estimated are defined as a function of a parameter vector $\boldsymbol{\theta}_N \square (a_1 \cdots a_{n_a} \ b_1 \cdots b_{n_b} \ c_1 \cdots c_{n_c})^T$. For the identification of the value $\hat{\boldsymbol{\theta}}_N$, $\hat{\mathbf{G}}(q, \hat{\boldsymbol{\theta}}_N)$ and $\hat{\mathbf{H}}(q, \hat{\boldsymbol{\theta}}_N)$ are closest to $\mathbf{G}(q, \boldsymbol{\theta}_N)$, and $\mathbf{H}(q, \boldsymbol{\theta}_N)$. In (Ljung & Söderström, 1983), the authors showed that under reasonable conditions,

$$\hat{\boldsymbol{\theta}}_N \rightarrow \boldsymbol{\theta}_N^* \quad (3.19)$$

where:

$$\boldsymbol{\theta}_N^* = \arg \min \frac{1}{N} \sum_{k=1}^N \varepsilon \{ \varepsilon_k^2(\boldsymbol{\theta}) \} \quad (3.20)$$

and $\varepsilon(t, \theta)$ is prediction error and defined in equation (3.4). According to (Goodwin, Gevers, & Ninness, 1992; Schoukens & Pintelon, 1994), with this definition of θ_N^* , it is possible to split the total estimation error between the true frequency response function $\mathbf{G}(q)$ and the estimated one $\mathbf{G}(q, \hat{\theta}_N)$ into two parts as follows:

$$\mathbf{G}(q) - \mathbf{G}(q, \hat{\theta}_N) = \left[\mathbf{G}(q) - \mathbf{G}(q, \theta_N^*) \right] + \left[\mathbf{G}(q, \theta_N^*) - \mathbf{G}(q, \hat{\theta}_N) \right] \quad (3.21)$$

As we can see in equation (3.21), the errors in the estimated FRF have two components. The first contribution $\left[\mathbf{G}(q) - \mathbf{G}(q, \theta_N^*) \right]$ is the bias contribution, a deterministic quantity due to the modeling error. If the selected model has a lower or a higher complexity than the true system, this bias error will be present at some frequencies. Choosing the model order should be flexible enough to allow a good fit to the measurement data but adequately constrained so that noise does not invoke unsuitable models. Consequently, selecting an optimal model order respecting this compromise is an important issue in system identification. This concern is analyzed in the following section to select the optimal model orders of an ARMAX model. The second contribution $\left[\mathbf{G}(q, \theta_N^*) - \mathbf{G}(q, \hat{\theta}_N) \right]$ represents the noise or variance errors, which are due to noise in the measured input and output data. It is a random variable that will disappear if there is no noise or if the number of data tends to infinity.

3.5 A model order determination approach

When time series modeling ARX or ARMAX models employed, the performances may be affected by selecting the model order. Choosing a sufficient and correct model order has always been a challenging issue. Once the model orders are properly selected, the models successfully represent the underlying phenomenon with the lowest complexity. This method aims not only to find a model capable of describing a specific set of data but is also helpful for the validation of the inference procedures. Consequently, there is a need to develop a reliable method to identify the orders of AR, MA, and eXogenous polynomials. In general, most of the mechanical structures are operated in the low-frequency range with limited bandwidth. Having

a model with orders that are too high may lead to an overfitting problem as it includes too much irrelevant oscillation information and generates high computational costs, and a model with orders that are too low will not be solid enough to capture the underlying physical system dynamics. For its part, a model with an appropriate order can precisely describe the dynamic characteristics of the system. Because of its important role in system identification, model order determination has attracted much attention in the literature, with researchers proposing different criteria for order determination (Stoica & Selen, 2004). The final prediction error (FPE) criterion was originally proposed by Akaike (Hirotugu Akaike, 1969) for determining the AR order and was extended to the ARMA model by (Beveridge & Oickle, 1994). After adding the inflating effects of estimated coefficients, the optimal order was chosen by minimizing the one-step-ahead mean square forecast error. A method based on the eigenvalues of a modified covariance matrix, which is robust to noise levels, was proposed in (Smail et al., 1999a; Smail *et al.*, 1999b) for determining the model order. Some other concept as information theory like Akaike's Information Criterion (AIC) (H. Akaike, 1974), Bayesian Information Criterion (BIC) (Gideon, 1978) or Minimum Description Length (MDL) (Barron, Rissanen, & Bin, 1998) were developed to produce an estimate model order. Among these techniques, the AIC is a heuristic approach, which has attracted much attention in the literature. His technique penalizes the likelihood of the number of parameters in the model by attempting to choose the most suitable model order.

Considering an N-dimensional time-series data, the AIC is given by equation (22):

$$\mathbf{AIC}(z) = N \ln(\det |\hat{\Sigma}|) + 2(z) \quad (3.22)$$

where N denotes the number of data points, (z) is a dimension associated with the vector of unknown parameters to be estimated and

$$\hat{\Sigma} = \frac{1}{N} \sum_{t=1}^N \hat{\mathbf{w}}[t] \cdot \hat{\mathbf{w}}^T[t] \quad (3.23)$$

$\hat{\Sigma}$ is the covariance matrix of the innovation sequence associated with the estimated coefficients, the $\mathbf{w}[t]$ is innovation square, or the model error.

When the AIC value is at a minimum, we obtained the most suitable order. A minimum AIC is theoretically situated at a sufficient value of (z) that best represents the dimension of the unknown parameters. For an ARMAX $(n_a, n_b, n_c, n_k)(p)$ model, (z) would typically be equal to $(n_a+n_b+n_c+n_k)$, with n_a, n_b, n_c and n_k orders for its AR, MA, eXogenous components and time delay, respectively, while p represents the number of orthonormal functions by which each of these components is multiplied. Here, it should be noted that although there would be many possible combinations of n_a, n_b, n_c and n_k that can produce the same adequate value of (z) , only the right combination would yield the smallest AIC value. The z value may be defined as:

$$z = (n_a + n_b + n_c + n_k)(p) \quad (3.24)$$

The AIC corresponding to an ARMAX $(n_a, n_b, n_c, n_k)(p)$ model is written here as:

$$\mathbf{AIC}(n_a, n_b, n_c, n_k)(p) = N \ln(\det |\hat{\Sigma}|) + 2(n_a + n_b + n_c + n_k)(p) \quad (3.25)$$

where z is the number of scalar parameters in the ARMAX model.

However, in many cases, AIC does not give an optimal order. (Bozdogan, 1987) showed empirical evidence that AIC tends to pick models which are over-parameterized. The BIC overcomes this shortcoming by including an additional term that penalizes the model complexity and enhances the procedure, which are based on the same concepts governing the AIC but are better suited for large data sequences. The BIC criterion has the following general form:

$$\mathbf{BIC}(z) = \ln(\det |\hat{\Sigma}|) + (z) \frac{\ln(N)}{N} \quad (3.26)$$

In this paper, it is written as:

$$\mathbf{BIC}(n_a, n_b, n_c, n_k)(p) = \ln(\det |\hat{\Sigma}|) + (n_a + n_b + n_c + n_k)(p) \frac{\ln(N)}{N} \quad (3.27)$$

These criteria rely on the evolution of the error covariance, which monotonically diminishes concerning the model order. It asymptotically chooses the correct order model if the underlying multiple time series has high dimensions but tends to overestimate the model order as the data length increases. Thus, selected model orders can be greater than the optimal model orders. However, attention has recently shifted to the equally important problem of bias resulting from under-modeling. Wahlberg and Ljung (Wahlberg & Ljung, 1986) have conducted excessive research on the distribution of bias and variance in the estimated transfer function.

In this paper, we present an improved approach to determining time series model orders based on means square errors of the estimated transfer function. This approach is different from traditional criteria such as AIC and BIC. We transformed an averaged frequency means square error on the estimated transfer function into a mean square output prediction error criterion. The proposed method allows extracting the modal residuals with a sufficient order that guarantees the extraction of uncorrelated residual samples and the avoidance of an overfitting problem. The selection of the optimal order is based on a minimal variance of the total mean square error $\mathcal{E}\left\{\left|\mathbf{G}(q) - \mathbf{G}(q, \hat{\theta}_N)\right|^2\right\}$ between the true and estimated transfer functions based on N observation data. As we mentioned in the previous section, the means square error between $\mathbf{G}(q)$ and $\mathbf{G}(q, \hat{\theta}_N)$ is shown to be the sum of two terms, which both depend on the order of the estimated model, namely, a bias term that decreases with the model order and a variance term which increases with this order. We defined $\mathbf{P}_{\text{optimal}}$ as the optimal order of the structure while assuming that both input and output data are available. The criteria can be formulated as follows:

$$\mathbf{P} \square \frac{1}{2\pi} \int_{-\pi}^{\pi} \hat{\mathbf{E}}_{p_o}(\omega) \mathbf{D}_u(\omega) d\omega \quad (3.28)$$

where $\hat{\mathbf{E}}_{p_o}(\omega)$ is the estimated Means Square Error (MSE) between the true and estimated transfer functions, $\mathcal{E}\left\{\left|\mathbf{G}(q) - \mathbf{G}(q, \hat{\theta}_N)\right|^2\right\}$. The input $\mathbf{u}(t)$ is assumed to be a quasi-stationary sequence with zero time average and $\mathbf{D}_u(\omega)$ denotes the Power Spectrum Density (PSD) of the input.

The optimal order obtained when:

$$\mathbf{P}_{\text{optimal}} = \arg \min_{p_o=1,2,\dots} \left(\frac{1}{2\pi} \int_{-\pi}^{\pi} \hat{\mathbf{E}}_{p_o}(\omega) \mathbf{D}_u(\omega) d\omega \right) \quad (3.29)$$

The aim of this technique is converting the bias error into a random variable by ascribing a prior distribution to it. Consequently, we obtain an estimate for the average characteristics of

the total errors. We assume that the transfer function represented by $\mathbf{G}_T(q)$ is a stochastic process indexed by the variable ω , and given some value of θ_0 , it can be decomposed as the sum of a parameterized $\mathbf{G}_T(q, \theta_0)$ plus the residual $\mathbf{G}_\Delta(q)$:

$$\mathbf{G}_T(q) = \mathbf{G}_T(q, \theta_0) + \mathbf{G}_\Delta(q) \quad (3.30)$$

where $\mathbf{G}_\Delta(q)$ is a zero-mean stochastic process:

$$\varepsilon\{\mathbf{G}_\Delta(q)\} = 0 \quad (3.31)$$

Each system will provide one realization and analogous to the embedding of the single noise realization in a stochastic process. In the framework of an ARMAX model, for ease of implementation, we restrict our consideration to the linear model structures of the Single Input Single Output (SISO) case. The question of computing asymptotic variance expressions in the presence of under-modeling for transfer function prediction errors in frequency domain identification is addressed in this paper. The discrete linear transfer function of the ARMAX model can be expressed in the following form:

$$\mathbf{G}(q, \hat{\theta}_N) = \frac{\mathbf{B}(q, \theta)}{\mathbf{A}(q, \theta)} = \frac{b_0 + b_1 q^{-1} + b_2 q^{-2} \dots + b_{n_b} q^{-n_k - n_b + 1}}{I + a_1 q^{-1} + a_2 q^{-2} \dots + a_{n_a} q^{-n_a}} \quad (3.32)$$

The true transfer function can be expressed by the relationship between the measured input and output of the system:

$$\mathbf{G}_T(q) = \frac{\mathbf{y}(t)}{\mathbf{u}(t)} \quad (3.33)$$

The $\hat{\mathbf{E}}_{p_o}(\omega)$ means square error between the true and estimated transfer function in (28) is calculated by the following equations:

$$\hat{\mathbf{E}}_{p_o}(\omega) = \varepsilon\left\{\left|\mathbf{G}(q, \hat{\theta}_N) - \mathbf{G}_T(q)\right|^2\right\} = \text{Trace}\{\mathbf{Q}_{\tilde{g}}\} \quad (3.34)$$

where:

$$\mathbf{Q}_{\tilde{g}} \square \varepsilon\left\{\tilde{g}(q) \tilde{g}(q)^T\right\} \quad (3.35)$$

$$\tilde{g}(q) \square \begin{bmatrix} \text{Re}\{\mathbf{G}_T(q) - \mathbf{G}(q, \hat{\theta}_N)\} \\ \text{Im}\{\mathbf{G}_T(q) - \mathbf{G}(q, \hat{\theta}_N)\} \end{bmatrix} \quad (3.36)$$

This index is an effective criterion since it includes the stochastic participation in the denominator by adding an input power spectral density $\mathbf{D}_u(\omega)$. We converted an average frequency means square error criterion on the estimated transfer functions into a mean square output prediction error criterion. Due to the presence of measurement errors, the proposed method is adopted to determine the optimal model orders and proved its robustness to parameter uncertainties. This modification bridged the connection between classical variable selection criteria such as AIC and BIC and the non-concave penalized likelihood methodology that allows greater flexibility in choosing the desired models. The goodness of its performance will be assessed in the next section through a comparison with traditional validation methods. The optimal model will be tested by the quality of the residuals, the histogram, and autocorrelation functions.

3.6 Industrial application on a SCOMPI robot

3.6.1 Description of the test structure

Flexible manipulators are employed in the maintenance of large hydro electronic equipment as they represent an effective solution for repair jobs (Zhu *et al.*, 2020). Despite their attractive properties, controlling lightweight robot manipulators is still a challenging task. Their flexibility induces structure vibration that deteriorates the trajectory tracking accuracy and may lead to instability issues. In this part, the present method is adopted to identify the dynamic behavior of a light, portable, track-based multi-process manipulator named SCOMPI (Super-COMPact Ireq) (Hazel, Côté, Laroche, & Mongenot, 2012a, 2012b). The dynamical transfer functions and modal parameters must be monitored during the grinding process to control vibrations. Figure 3.2 presents the working envelop and the construction of the robot, with its links and joints.

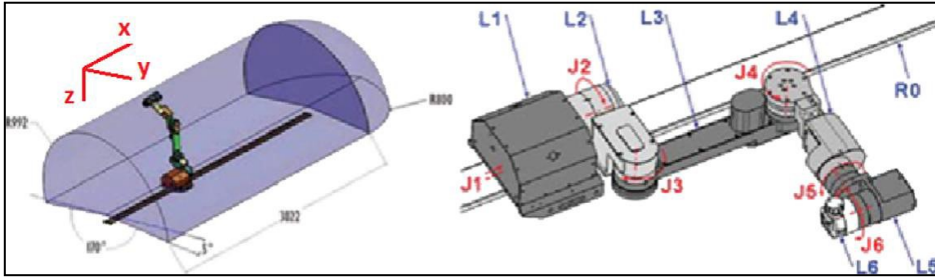


Figure 3.2 Structure of SCOMPI robot (Hazel et al., 2012a, 2012b)

3.6.2 Experimental procedure

The tool contact point Frequency Response Functions (FRFs) and their modal parameters represent the key for solving the dynamics analysis. In this paper, the actual grinding forces are used as the input excitations in estimating the FRFs. The grinding test is performed at the 3225-rpm rotating speed with an average 0.08 mm axial depth of grinding cut. The grinding work is realized on a hard steel EN31-64HNC workpiece with the dimensions of $150 \times 7 \times 48$ mm. During the cutting operation, cutting forces are measured with a type CH8408 3-axis Kistler dynamometer, which is directly attached under the workpiece to record the normal force direction (F_x), the tangential force direction (F_y) and the axial force direction (F_z). At the same time, three PCB-352C34 piezoelectric sensors with a sensitivity of 5.29 mV/G are used to measure accelerations at the robot's end-effector ($S_1 - S_3$) to capture the vibration in three directions. The measurement is conducted through the LMS data acquisition system for 10 s at a 512 Hz sampling frequency. Figure 3.3 shows the actual experimental setup of the SCOMPI robot under a real grinding operation. An LMS test lab system was used for acquiring the data in real-time during experiments, as well as for calculating averaged FRFs, which were used to validate the estimated results of the proposed approach.

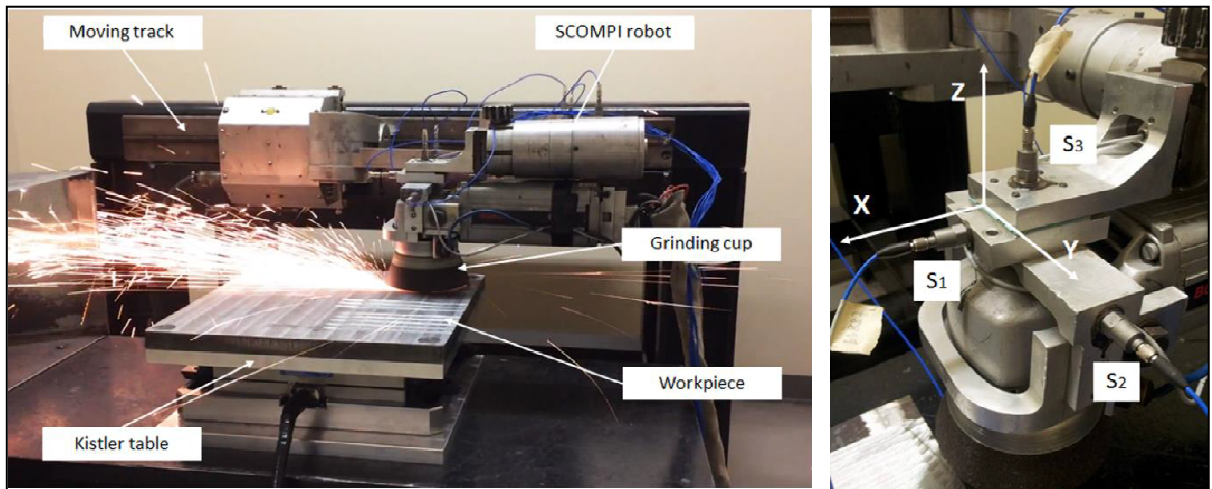


Figure 3.3 Experimental setup for SCOMPI robot during grinding operation

The structure is excited through a grinding operation, during which all the effects related to the rotating tool, or the grinding process are considered. FRFs are obtained during the cutting operation through the relations of the cutting forces and the vibration responses. The measured cutting forces are taken as the excitation sources of the system. In this paper, the operational FRFs are determined from the relation between the cutting forces and responses through the time series ARMAX modeling. The detailed experimental description is provided in Table 3.1.

Table 3.1 Grinding conditions of the SCOMPI test

No.	Experimental description	Information	Units
1	Grinding cup (Norton BuleFire) diameter	12.7	cm
2	Workpiece material	AISI 1081	-
3	Density of AISI 1081	7.87	g/cm^3
4	Workpiece dimensions	20.32 x 25.4 x 2.54	cm
5	Grinding direction	Normal direction	-
6	Power	500 – 3400	W
7	Length of cut	16.2 – 18.5	cm
8	Width of cut	1 – 1.55	cm
9	Depth of cut	0.0158 – 0.00165	cm
10	Rotation speed	3225	rpm
11	Angle of grinding cup	5-10	degree

The measured grinding forces and the acceleration responses in each direction are shown in Figure 3.4.

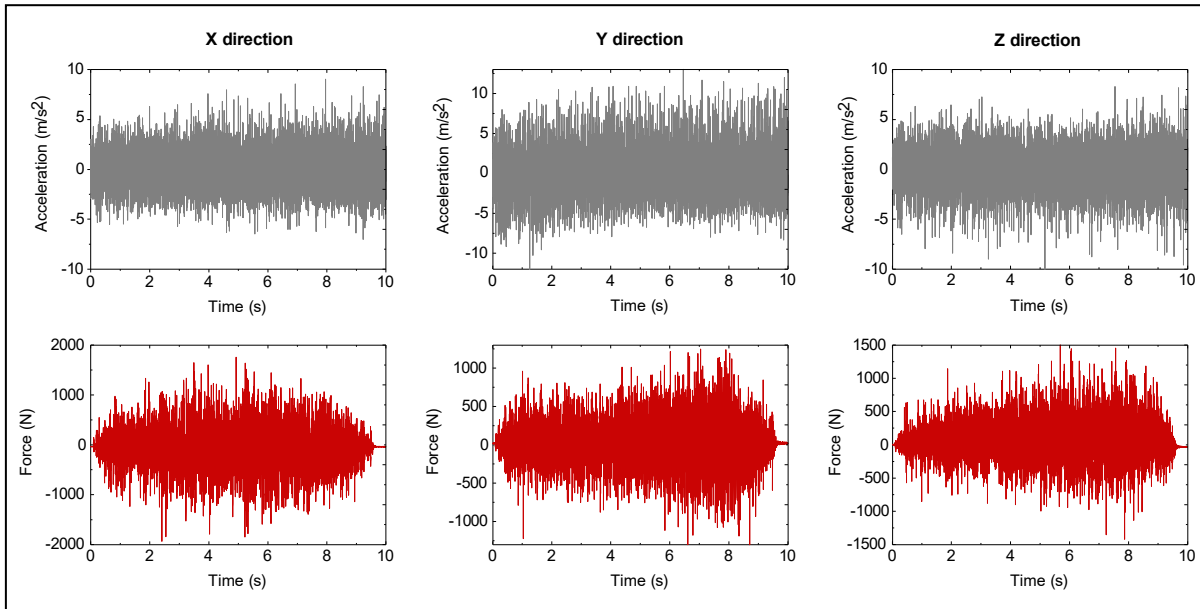


Figure 3.4 Measured data on SCOMPI robot

3.7 Identification procedure

3.7.1 Model orders estimation

The parametric identification of the structural dynamics is based on force and response signals with a 10s sample length. The modeling strategy consists of the successive fitting of the ARMAX (n_a, n_b, n_c, n_k) model. First, the model orders are selected based on the Akaike Information Criterion (AIC) and the Bayesian Information Criterion (BIC). Figure 3.5 plots result from the AIC and BIC techniques respectively obtained by directly fitting the ARMAX model of increasing orders $p = 1-60$ to the different sets of experimental data.

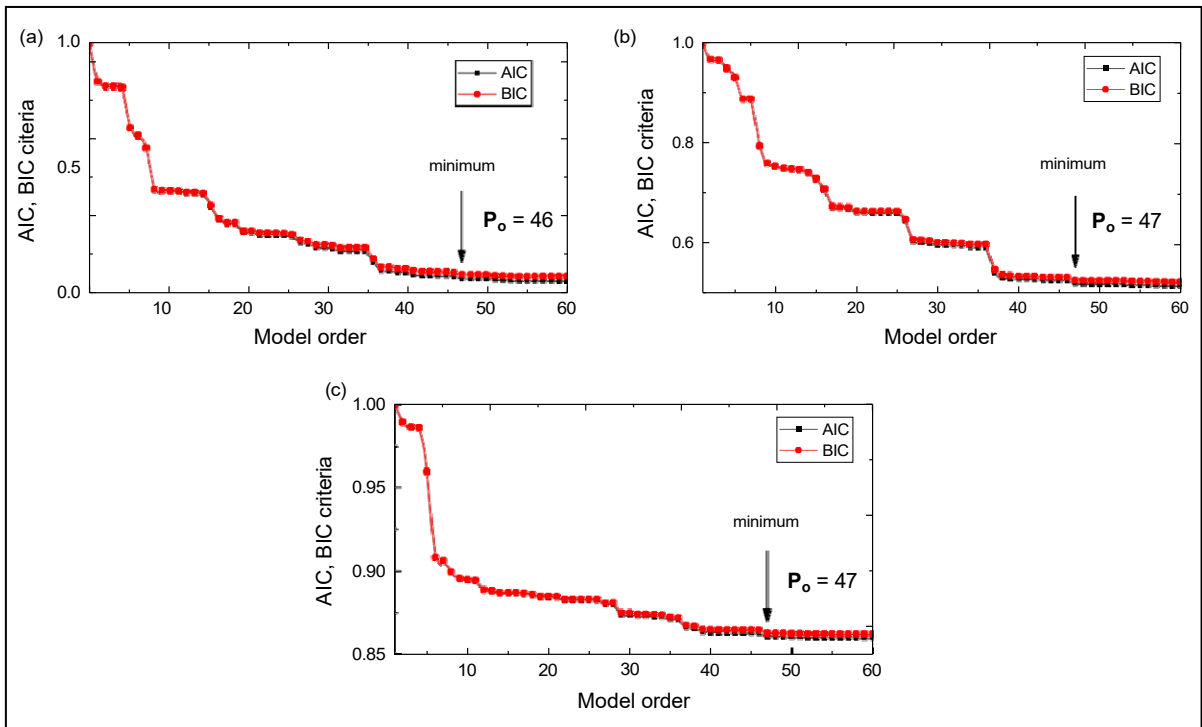


Figure 3.5 Model order selection based on AIC and BIC criteria for different sets of data:

(a) X data, (b) Y data, (c) Z data

By dividing the experiment into different test directions based on the operation of the robot, we can decompose and characterize the dynamical behavior of the system for each direction. From Figure 3.5, both the AIC and BIC methods decrease with the model order, and a minimum may be assumed close to 47. However, the main limitation of using such techniques is that they may suggest different model orders and not determine the optimal orders. Thus, these values must be judged carefully.

By applying the proposed method in selecting an optimal model order, the orders for which all curves lead to a stable value are identified. Figure 3.6 illustrates an optimal order, defined as the smallest order value. The point of convergence starts at around order of 10 in all three directions.

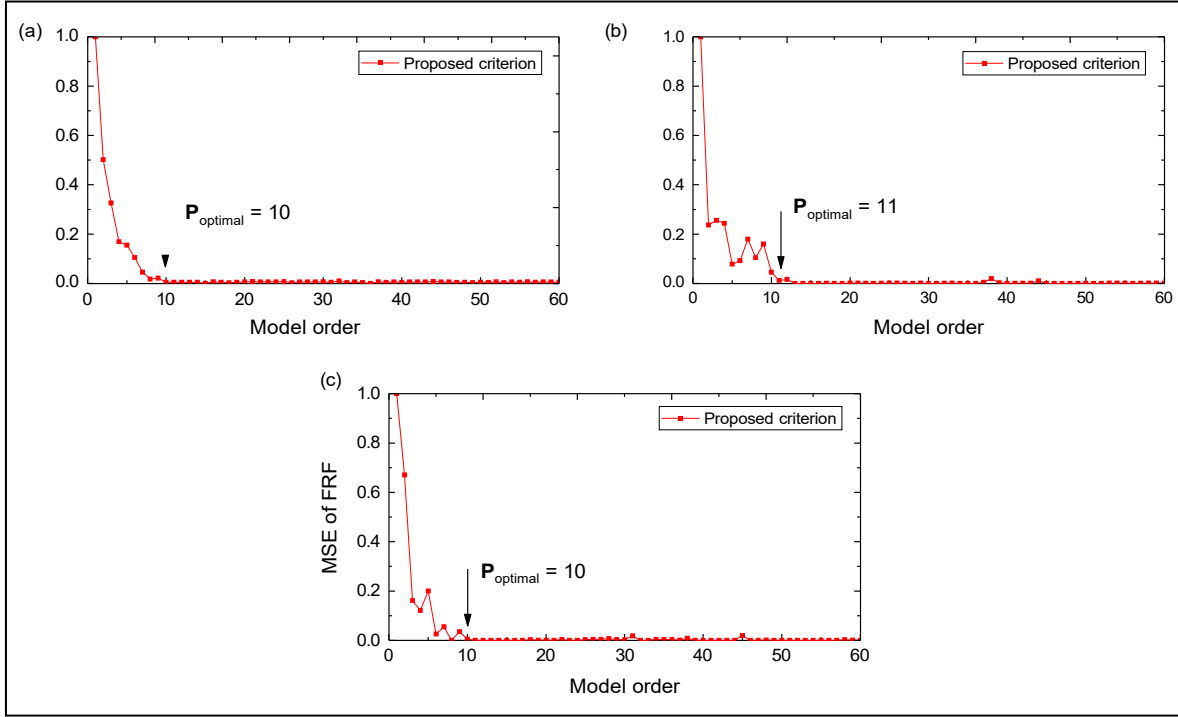


Figure 3.6 Model orders selection based on the proposed approach for different sets of data:
 (a) X data, (b) Y data, (c) Z data

To compare the efficiency of the present method, Vu et al. proposed a technique for determining an efficient model order p_{eff} based on the analysis of the Noise-to-Signal Ratio (NSR) (V. H. Vu et al., 2013). The estimated $\hat{\text{NSR}}$ is given in equation (3.37) based on the trace norm part of the error covariance matrices $\hat{\mathbf{M}}$ and the estimated deterministic $\hat{\mathbf{K}}$.

$$\hat{\text{NSR}} = \frac{\text{Trace}(\hat{\mathbf{M}})}{\text{Trace}(\hat{\mathbf{K}})} (\%) \text{ or } \hat{\text{NSR}} = 10 \log_{10} \frac{\text{Trace}(\hat{\mathbf{M}})}{\text{Trace}(\hat{\mathbf{K}})} (\text{dB}) \quad (3.37)$$

A Noise-ratio Order Factor (NOF) is calculated as a variation of the NSR between two successive orders:

$$\text{NOF}^{(p)} = \text{NSR}^{(p)} - \text{NSR}^{(p+1)} \quad (3.38)$$

The NOF is a representative factor for the convergence of the NSR, which changes dramatically at low orders and converges at high orders. Since this criterion is positive and close to zero, the convergence may be assumed close to 10, considered as an efficient model order (Figure 3.7).

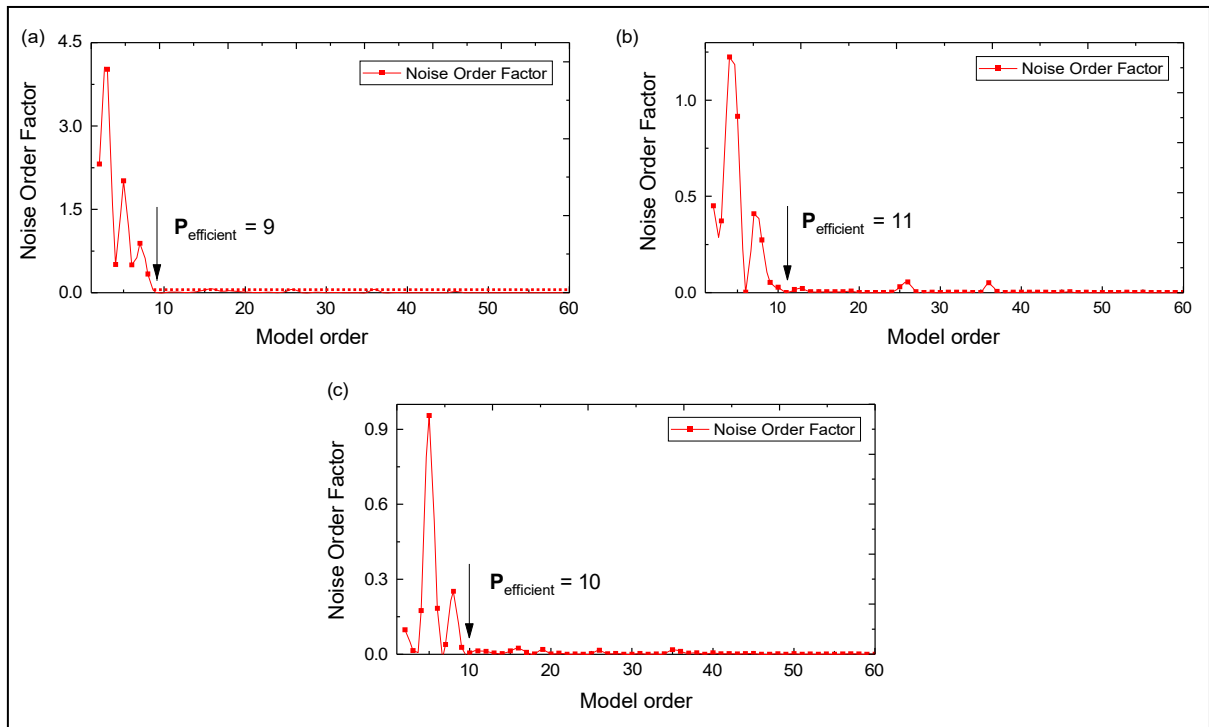


Figure 3.7 NOF evolution and efficient model orders selection for different sets of data:

(a) X data, (b) Y data, (c) Z data

Theoretically, the modeling of a complex structure like the SCOMPI robot should result in a high-order model. Based on the AIC and BIC criteria, a 47-order model should be selected as a suitable choice. However, a lower order could be chosen with all essential characteristics of the real system preserved. By comparison, the Noise-to-Signal Ratio and the proposed method are selected with a model order of around 10. However, in the case of the complex ARMAX model, it is characterized by three different orders, the model order estimation is not straightforward. In experimental modal analysis, the orders n_a , n_b , and n_c depend on the model parameterization. According to (Fassois, 2001; Florakis, Fassois, & Hemez, 2001), the choice of n_b is a function of the type of response measurements used and the inter-sample behavior of the data. Moore et al. suggest an ARMAX (p,p,p) model in which $p = n_a = n_b = n_c$, for the case of a vibration acceleration measurement, or ARMAX $(p, p - 1, p)$, for the case of a vibration displacement or velocity measurement with an appropriate time delay (Moore, Lai, & Shankar, 2007a). As can be noted, since structural vibrations are usually measured in terms of

acceleration rather than displacement and velocity in actual experiments, we would choose $p_{optimal} = n_a = n_b = 10$.

The Moving Average order is initially set equal to the Auto Regressive part since the resulting noise model has the flexibility of representing several stochastic processes, including white noise. There is some experimental evidence in the structural systems (Moore *et al.*, 2007a; Moore, Lai, & Shankar, 2007b), which indicates that for low noise levels, the required MA order is often smaller or equal to the AR one. The order n_c of the MA matrix and time delay order n_k are dependent on the noise present in the system, and generally, no information on the nature of this disturbance is available. Therefore, the extracted required value of the MA order, as well as an appropriate time delay order, will be carefully examined in this study. This can be done by initially setting $n_a = n_b = 10$, and then selecting the best model by using a proposed criterion to test the effectiveness of changing n_c and n_k from the set of (Peng *et al.*, 2018), resulting in the estimated results presented in Figure 3.8.

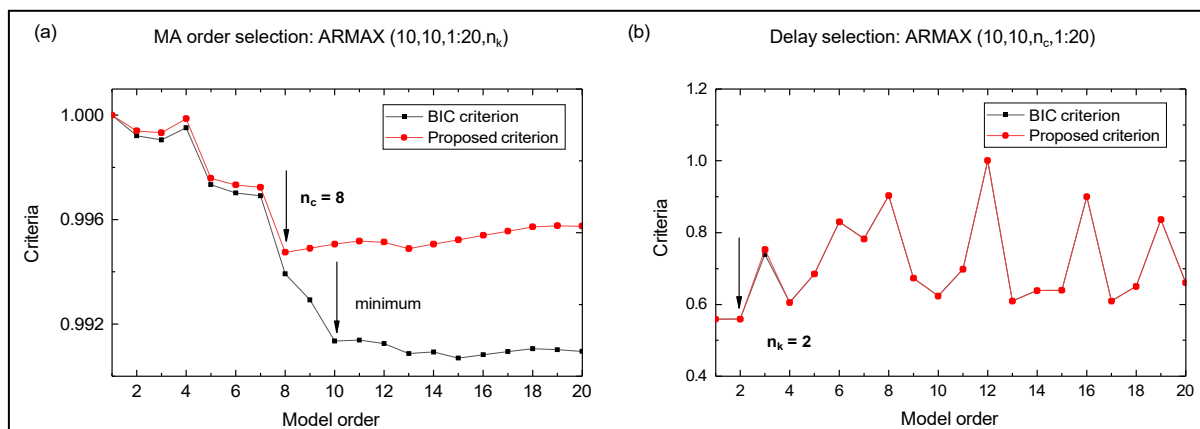


Figure 3.8 Moving average order (a) and time delay order (b) selection

Based on these results, the set of orders (10,10,8,2) is chosen as consisting of the smallest order values, which can be applied to fit the data with a negligible discrepancy and can be effectively utilized for modal analysis. However, a further step needs to be validated to assess the adequacy of the estimated model. Several diagnostic checks can be used to decide whether the ARMAX model is adequate based on the residuals, which characterized by an uncorrelated

sequence. Figures 3.9 and 3.10 display the histogram, Quantile-Quantile (QQ) plot, Autocorrelation Function (ACF), and Partial Autocorrelation Function (PACF) of the residuals of the ARMAX model. The histogram is unit-modal and symmetric around zero. From the QQ-plot, the residual approximately fit a straight line, and this can be assumed normal. The values of both ACF and PACF are located roughly between the upper and lower bounds of a confidence interval. Therefore, the residual can be assumed independent, and the selected orders can be used.

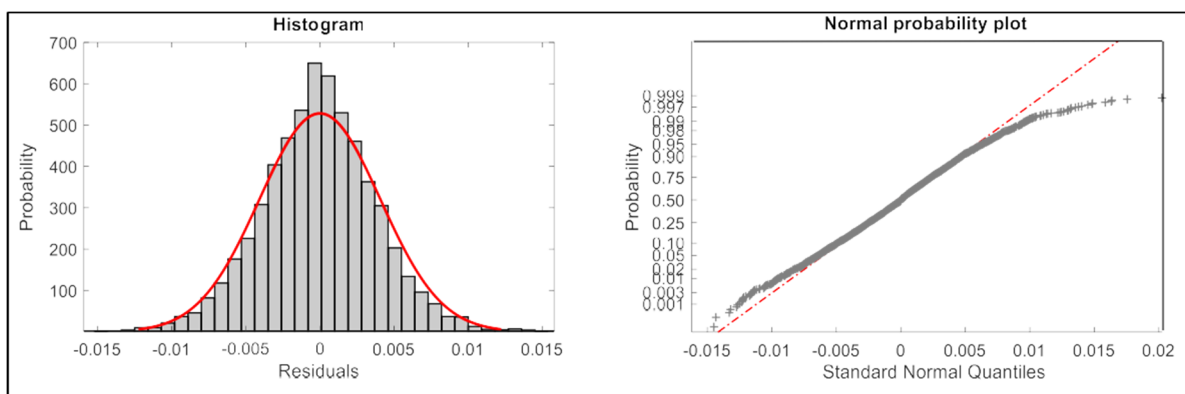


Figure 3.9 Residual errors histogram and normal probability plot of an estimated ARMAX (10,10,8,2) model

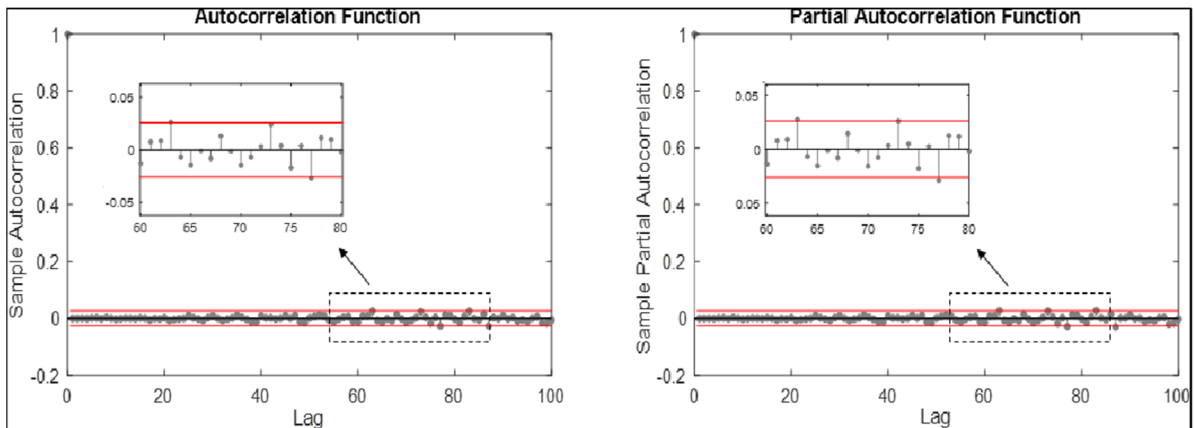


Figure 3.10 Autocorrelation function (ACF) and Partial Autocorrelation Function (PACF) of the residual ARMAX (10,10,8,2)

The above identification procedure leads to an optimal ARMAX (10,10,8,2) model, which is selected as an adequate model for structural analysis, and for the extraction of modal

parameters. The next section evaluates the performance and effectiveness of this dominant reduced model, in which all the essential characteristics of the real system can be retained.

3.7.2 Frequency Response Function identification

Based on the discussion above, once the excitation and vibration measurement data have been selected with the appropriate orders, an ARMAX model needs to be estimated within the model structure. In this section, the two parametric transfer function estimators for assessing the dynamic flexible manipulator are analyzed. The FRFs estimation is performed using two parametric models, ARX (n_a, n_b, n_k) and ARMAX (n_a, n_b, n_c, n_k), based on data records from the structure. A scalar Single Input – Single Output (SISO), ARX and ARMAX models are used at a time. The input signals to each model are the force signals, and the output signals are measured accelerations, respectively. The assessments of an ARX model, and an ARMAX model, are undertaken based on an experimental SCOMPI structure during the grinding operation. Figures 3.11-3.19 demonstrate the estimated Frequency Response Functions obtained by the ARX and ARMAX models, which are compared to those measured by the LMS system.

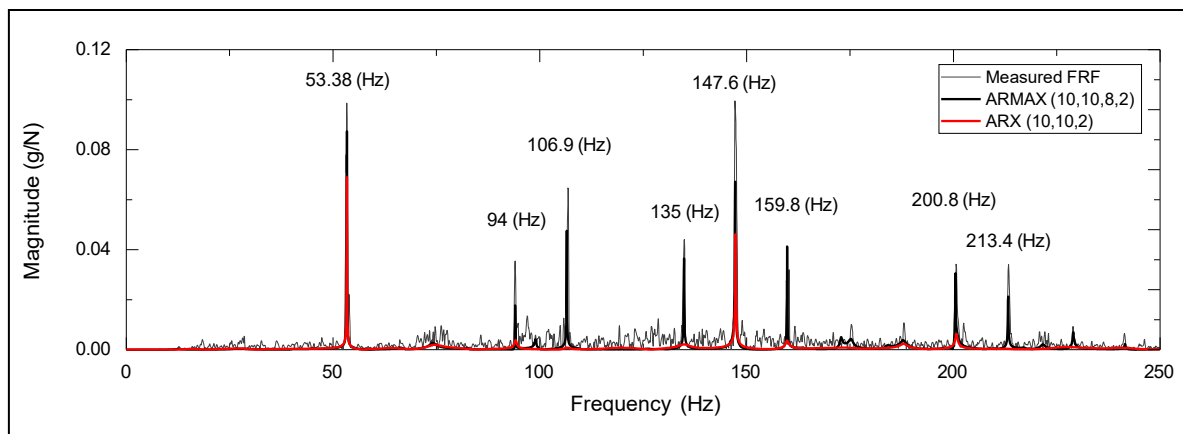


Figure 3.11 Estimated Frequency Response Function FRF_{xx}

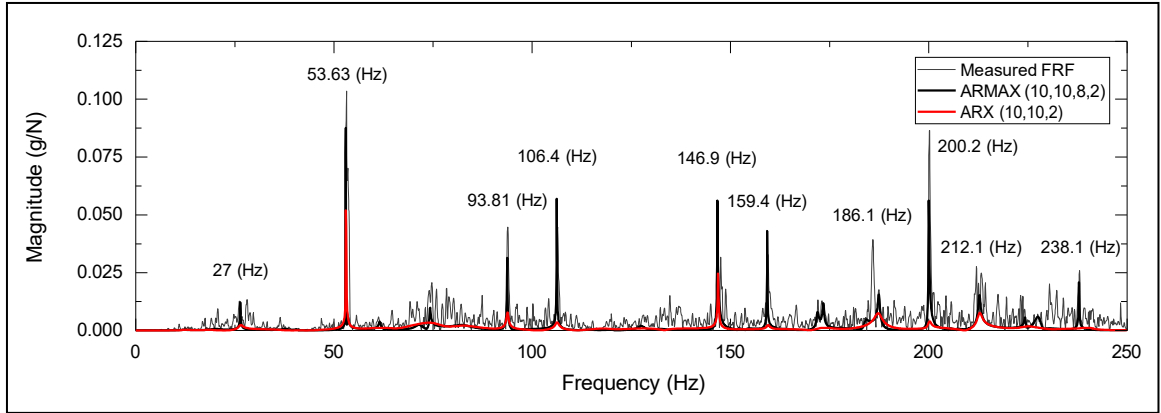


Figure 3.12 Estimated Frequency Response Function FRF_{xy}

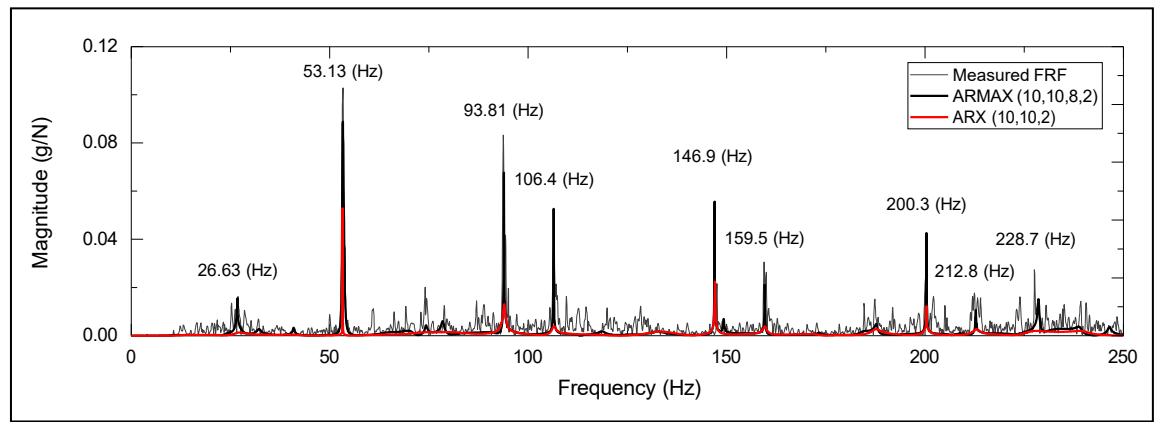


Figure 3.13 Estimated Frequency Response Function FRF_{xz}

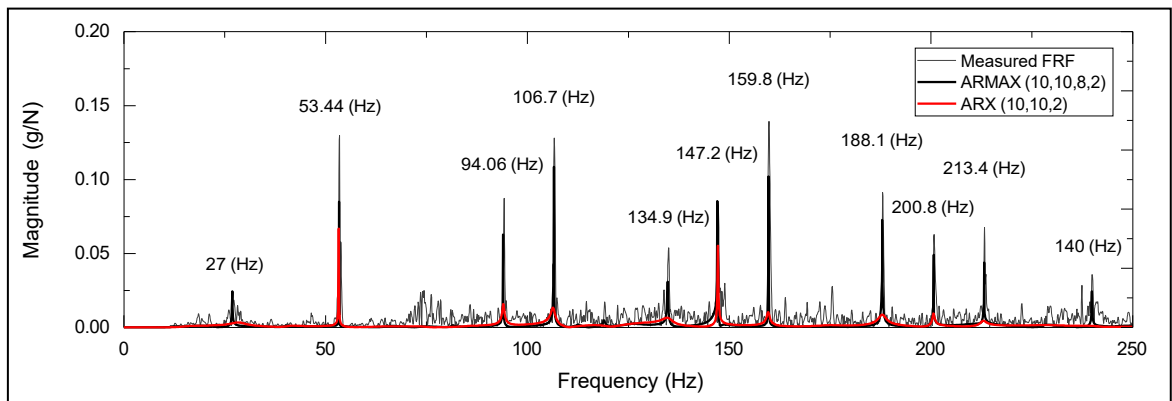


Figure 3.14 Estimated Frequency Response Function FRF_{yx}

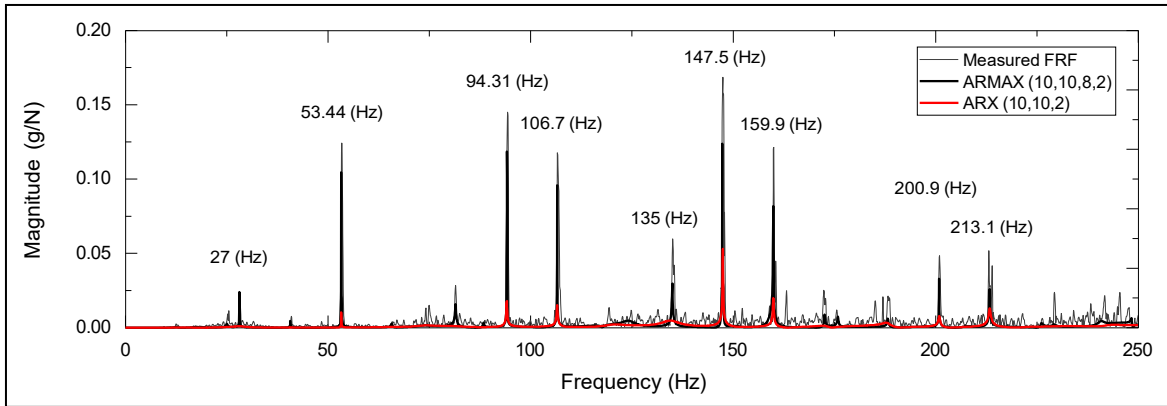


Figure 3.15 Estimated Frequency Response Function FRF_{yy}

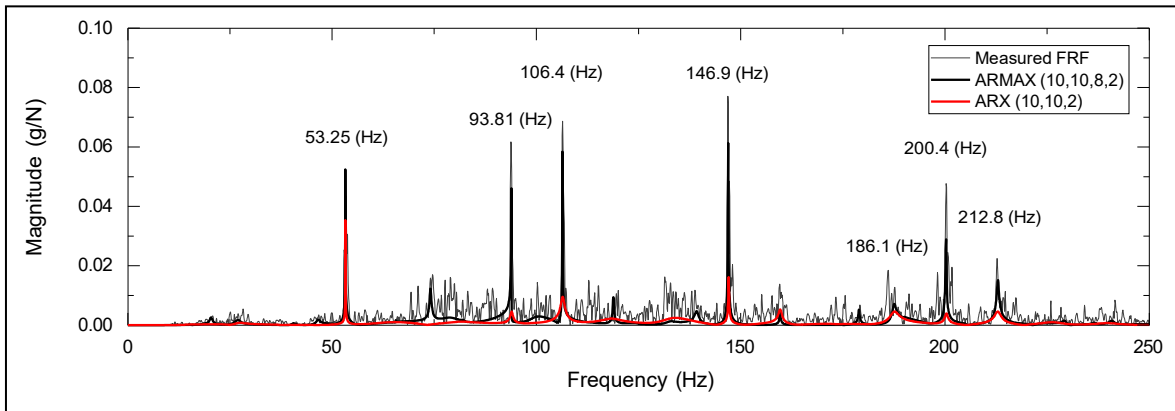


Figure 3.16 Estimated Frequency Response Function FRF_{yz}

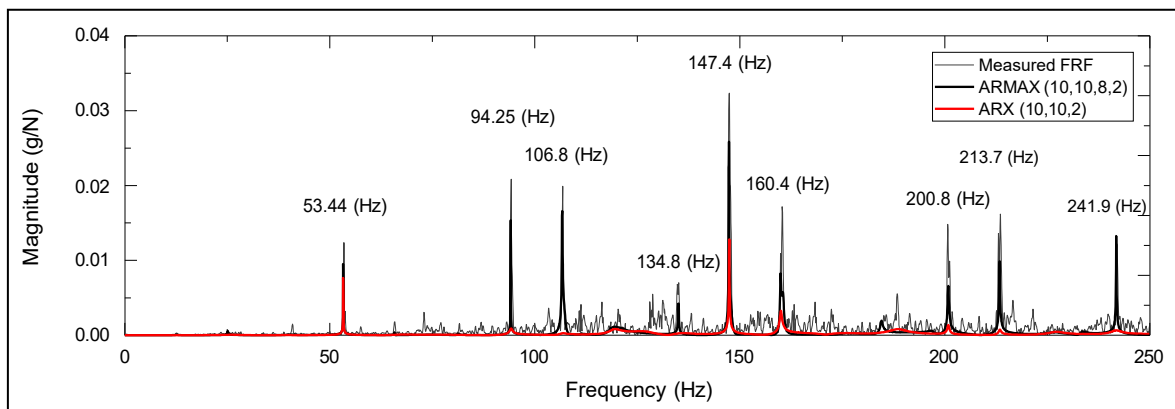


Figure 3.17 Estimated Frequency Response Function FRF_{zx}

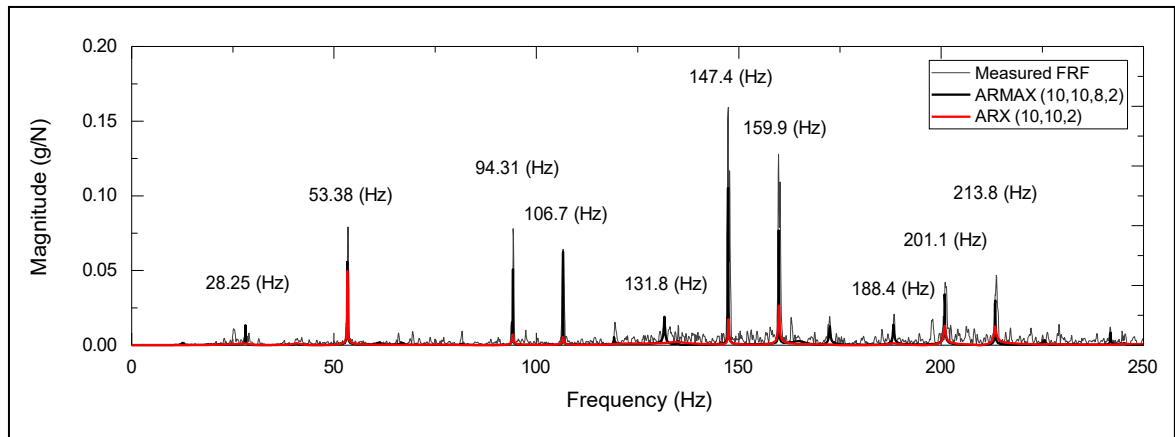


Figure 3.18 Estimated Frequency Response Function FRF_{zy}

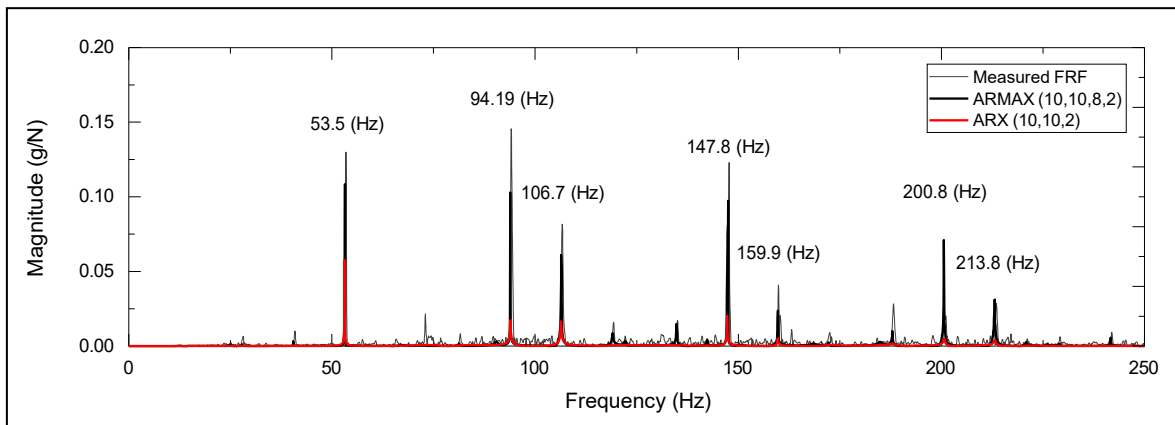


Figure 3.19 Estimated Frequency Response Function FRF_{zz}

In comparing the ARX and ARMAX models' performance with different measurement data, it can be observed that the ARMAX model achieves much better fit than the ARX counterpart at low orders, where all frequencies of the system are clearly revealed. Conversely, at the same model orders, the ARX model proves inadequate in providing accurate estimated FRFs compared to the measured one. The ARMAX method was both economic and effective in accurately identifying the frequency response functions of the structure based on input-output experimental data corrupted by noise. This model also gives a more parsimonious representation and precision. These results matching those of (Moore *et al.*, 2007b). The model orders of the ARMAX model are related to the number of structural modes in a given frequency range. Meanwhile, in the ARX model, the number of degrees of freedom devoted to the

description of the system dynamics is limited due to the fact that the system dynamics and the noise are partially described by the same polynomial $\mathbf{A}(q)$. For this reason, larger complexities are needed to achieve good adherence to the true system. Consequently, the orders of the ARX model tend to be chosen greater than those of the ARMAX model when considering the noise present in the measurements.

3.7.3 Extraction of model parameters

The estimated Frequency Response Functions (FRFs) representing the structural dynamic $\left[\mathbf{B}(q, \hat{\theta}) / \mathbf{A}(q, \hat{\theta}) \right]$ will be applied to distinguish the actual structural modes from the extraneous modes, based on the construction of the stabilization diagram, and will be used for the extraction of the modal parameters. Each transfer function representing a scalar excitation and response pair is evaluated directly from the estimated discrete ARMAX model. Complete model information such as natural frequencies, damping factors, and mode shapes can be obtained. Their global parameters can be extracted as follows:

$$f_{nl} = \frac{1}{T2\pi} \sqrt{\left(\frac{\ln(\lambda_l \cdot \lambda_l^*)}{2} \right)^2 + \left(\cos^{-1} \left(\frac{\lambda_l + \lambda_l^*}{2\sqrt{\lambda_l \cdot \lambda_l^*}} \right) \right)^2} \quad (3.39)$$

$$\zeta_l = \frac{1}{T} \sqrt{\frac{[\ln(\lambda_l \cdot \lambda_l^*)]^2}{[\ln(\lambda_l \cdot \lambda_l^*)]^2 + 4 \cdot \left(\cos^{-1} \left(\frac{\lambda_l + \lambda_l^*}{2\sqrt{\lambda_l \cdot \lambda_l^*}} \right) \right)^2}} \quad (3.40)$$

In the above expression, f_{nl} denotes the l th natural frequency in (hz) unit, ζ_l represents the corresponding damping ratio, (λ_l, λ_l^*) is the l^{th} discrete complex conjugate eigenvalue pair, and T is the sampling period. To determine the extraction mode, a particular discrete-to-continuous transformation must be performed for determining continuous-time residues. The l^{th} mode shape ϕ_l is then obtained as:

$$\phi_l = \left[1 \frac{\mathbf{R}_{i2l}}{\mathbf{R}_{i1l}} \dots \frac{\mathbf{R}_{iml}}{\mathbf{R}_{i1l}} \right]^T \quad (l=1,2,\dots,m) \quad (3.41)$$

where m represents the estimated number of structural degrees of freedom and \mathbf{R}_{ijl} is the ij^{th} element of the l^{th} ($l=1, 2, \dots, m$) residue matrix \mathbf{R}_l of the continuous time receptance transfer matrix.

In modal analysis, knowledge of the model order is necessary but insufficient. It is important to understand that with noisy data, the optimal model order is typically smaller than the existing order. When evaluating the parameters with the minimum order model, it is hard to obtain all the modes if the measurements are corrupted by experimental noise. Previous studies (Smail et al., 1999a; Smail et al., 1999b; V. H. Vu et al., 2013) have shown that it is more difficult to identify the damping rates than the natural frequency from ambient vibration data due to a higher sensitivity to measurement noise. Therefore, to obtain all the modes and construct a stabilization diagram, a value higher than the minimum required order to establish the convergence must be set. However, the advantage of the ARMAX modeling is that it includes the Moving Average part, which is already accounted for the noise present in the system. Consequently, there is no need to go up to a very high order, as in the case of AR or ARX models. To prevent the contamination of more numerical modes and avoid the overfitting problem, a computational model order should not be too much higher than the optimal one. In this paper, order 50 was selected for visually establishing stabilization diagrams and distinguishing between the structural and the spurious modes, and the identified low-order FRFs in the previous section were applied to extract the modal properties. The results computed by both the ARX and ARMAX models are illustrated in Figures 3.20-3.23.

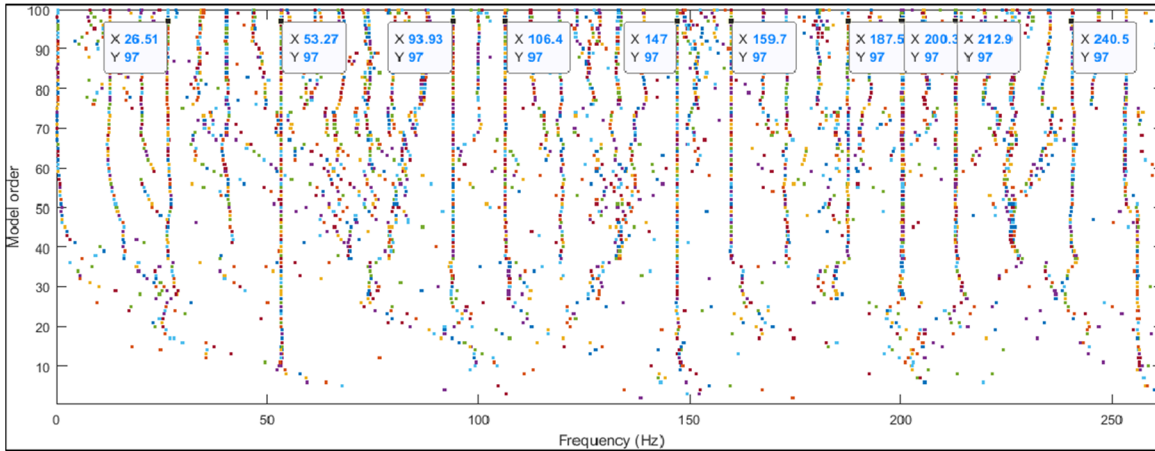


Figure 3.20 Stabilization diagram by the ARX model

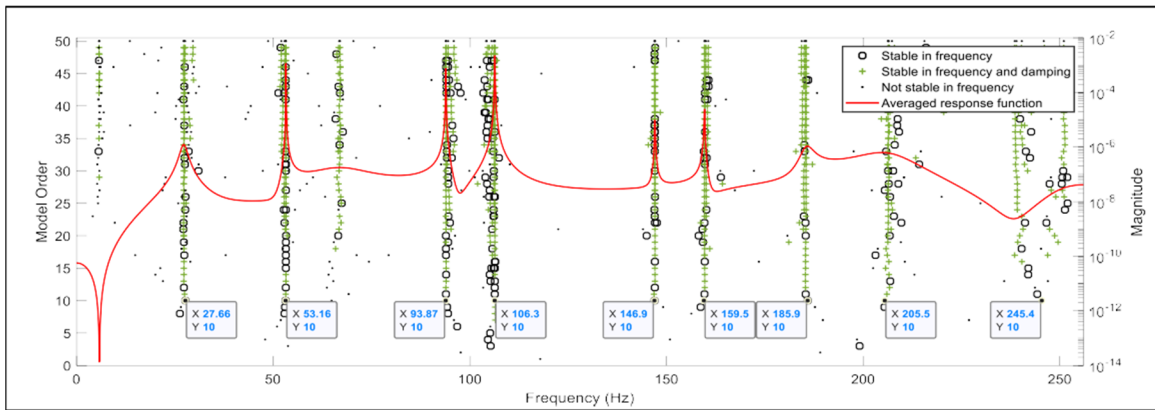


Figure 3.21 Stabilization diagram based on average estimated FRFs in X direction by the ARMAX model

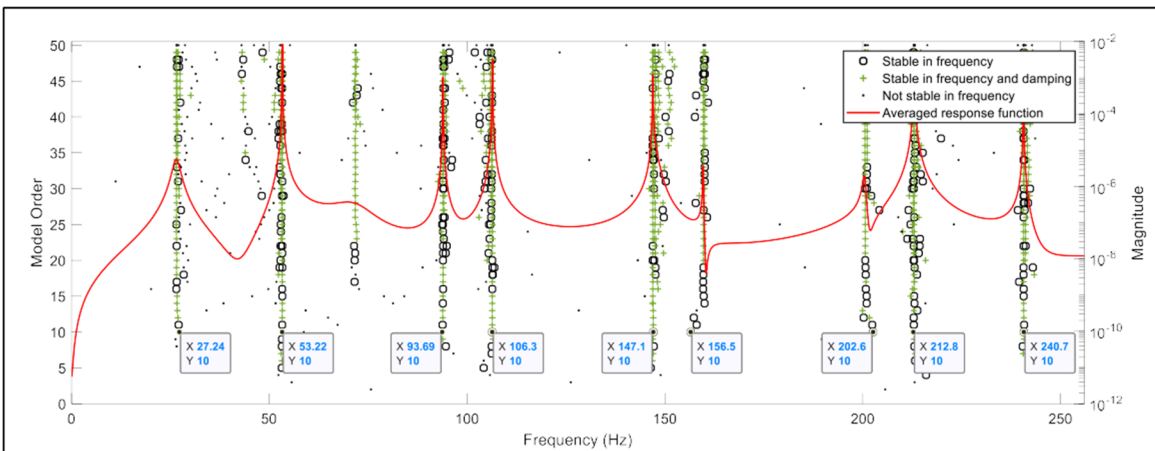


Figure 3.22 Stabilization diagram based on average estimated FRFs in Y direction by the ARMAX model

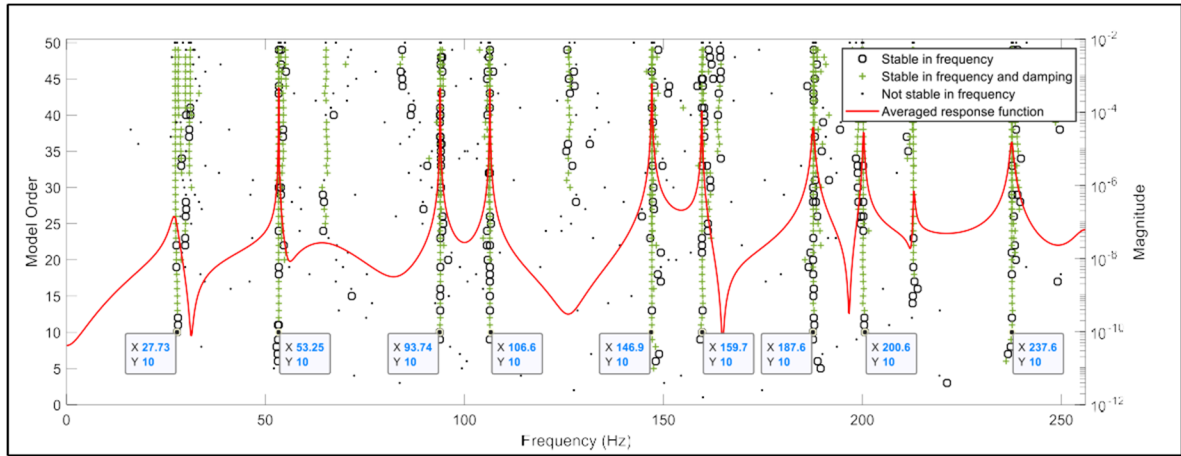


Figure 3.23 Stabilization diagram based on average estimated FRFs in Z direction by the ARMAX model

As can be seen from Table 3.2, all modal parameters obtained by two different methods are identified.

Table 3.2 Comparison of estimated modal parameters between ARMAX and ARX models

Modes	ARMAX model		ARX model (Least Squares)	
	Frequency (Hz)	Damping ratio (%)	Frequency (Hz)	Damping ratio (%)
1	27.54	1.28	26.51	2.55
2	53.21	0	53.27	0
3	93.76	0.15	93.93	0.14
4	106.40	0	106.4	0
5	146.96	0.13	147.0	0.07
6	158.56	0	159.7	0
7	186.75	0.27	187.5	0.59
8	202.90	0.31	200.3	0.22
9	212.80	0	212.9	0
10	239.13	0.23	240.5	0.28

The stabilization diagrams help to distinguish between spurious modes and vibration ones. Since the frequency response function is considered converging to the optimal order $p_{\text{optimal}} = 10$, all the natural frequencies in the measured range start to show up on the stabilization

diagrams, meaning that the optimal order p_{optimal} is the minimum value from which all available physical modal properties are revealed. The assessments of both the ARX model and of the ARMAX model are undertaken based on an experimental SCOMPI structure. As the results indicate in Table 3.2, both models are effective for modal identification, but using different approaches. In the case of the ARMAX model, the harmonic frequencies, the natural frequencies, and damping ratios are extracted directly from the estimated low-order frequency response functions. In contrast, the ARX model is based on the minimum Least Square method (Soderstrom *et al.*, 1997) at the higher orders. The ARMAX model exhibits the lowest complexity, while the ARX method requires many model parameters to extract the modal properties. As can be seen in Figure 3.20, due to an applied higher order up to 100 in the case of the ARX model, the stabilization diagram exhibits a lot of irrelevant oscillation information, which results in an overfitting problem and heavy computation. Meanwhile, the stabilization diagrams of an ARMAX model with different measurement data sets revealed all the frequencies, without overfitting problems and with less computational time. In general, the ARMAX model is better at capturing the significance of the mismatches introduced and provides satisfactory results in terms of frequencies and damping coefficients estimation. The model offers easy computation, with sufficient low-order performance despite the noise contamination in the experimentally measured data. However, in the case of the ARX model, there is a need for higher orders. Under such conditions, the time delay problem can also be neglected, which results in a time-consuming and higher computational burden.

3.8 Conclusion

To summarize, this paper presents an effective identification technique for computing optimal ARMAX model orders based on experimental measurement data. The present method allows selecting of a minimum order of the mechanical system in a given frequency range, which correctly incorporates the effect of modeling error and measurement noise under the expression of a minimum error variance of the identified transfer functions. The estimated results were validated with other common criteria, such as AIC, BIC, and NOF, to ensure that the selected model extracted uncorrelated residuals and simultaneously prevented overfitting. The search

for the best time delays is also addressed in this paper. The proposed optimization strategy was successfully applied on an industrial application, namely, the flexible SCOMPI manipulator robot under grinding operation. The relationship between the actual structural and disturbance dynamic is formulated in the discrete form of an ARMAX representation, which helps to improve the modeling performance and to gain flexibility in handling the residual error caused by environmental noises. Further validation was carried out by comparing model predictions with actual measurements of transfer functions from the LMS Test Lab system and the original ARX technique. Comparative results show that the identified ARMAX model is economic and appropriate for structural identification and achieves better results. The low-order transfer functions estimated by the present technique were scientifically closer to the measured values and are proposed for use in automatic modal extraction. Results show that the approach is successful and superior to a state-of-the-art order determination technique in obtaining a sufficient order and can accurately capture all the dominant oscillation modes with fewer discrepancies. The proposed method is expected to be a useful tool for capturing the transfer functions of difficult-to-measure structures such as rotating grinding systems. The determined low-order FRFs may eventually be used in the feedback controller design of the manipulator or in constructing a Stability Lobe Diagram (SLD) for determining operating and natural frequencies.

3.9 Acknowledgements

The support of NSERC (Natural Sciences and Engineering Research Council of Canada) through Discovery Research RGPIN-2016-05859 grants and of the Vietnam International Education Development (VIED) – Ministry of Education and Training of Vietnam is gratefully acknowledged. The authors would like to thank Hydro-Quebec's Research Institute for its substantial collaboration.

3.10 References

Akaike, H. (1969). Fitting autoregressive models for prediction. *Annals of the Institute of Statistical Mathematics*, 21(1), 243-247. doi:10.1007/BF02532251

- Akaike, H. (1974). A new look at the statistical model identification. *IEEE Transactions on Automatic Control*, 19(6), 716-723. doi:10.1109/TAC.1974.1100705
- Barron, A., Rissanen, J., & Bin, Y. (1998). The minimum description length principle in coding and modeling. *IEEE Transactions on Information Theory*, 44(6), 2743-2760. doi:10.1109/18.720554
- Beveridge, S., & Oickle, C. (1994). A Comparison of Box—Jenkins and objective methods for determining the order of a non-seasonal ARMA Model. *Journal of Forecasting*, 13(5), 419-434. doi:<https://doi.org/10.1002/for.3980130502>
- Bozdogan, H. (1987). Model Selection and Akaike's Information Criterion (AIC): The General Theory and Its Analytical Extensions. *Psychometrika*, 52, 345-370. doi:10.1007/BF02294361
- Chen, H. C., Lee, E. K., & Tsuei, Y. G. (1993). *Method for Determining System Eigenvalues From FRF for Noise Contaminated Subsystems*. <https://doi.org/10.1115/DETC1993-0275>
- Coppotelli, G. (2009). On the estimate of the FRFs from operational data. *Mechanical Systems and Signal Processing*, 23(2), 288-299. doi:<https://doi.org/10.1016/j.ymssp.2008.05.004>
- Fassois, S. D. (2001). MIMO LMS-ARMAX IDENTIFICATION OF VIBRATING STRUCTURES—PART I: THE METHOD. *Mechanical Systems and Signal Processing*, 15(4), 723-735. doi:<https://doi.org/10.1006/mssp.2000.1382>
- Florakis, A., Fassois, S. D., & Hemez, F. M. (2001). MIMO LMS-ARMAX IDENTIFICATION OF VIBRATING STRUCTURES—PART II: A CRITICAL ASSESSMENT. *Mechanical Systems and Signal Processing*, 15(4), 737-758. doi:<https://doi.org/10.1006/mssp.2000.1385>
- Gideon, S. (1978). Estimating the Dimension of a Model. *The Annals of Statistics*, 6(2), 461-464. doi:10.1214/aos/1176344136
- Goodwin, G. C., Gevers, M., & Ninness, B. (1992). Quantifying the error in estimated transfer functions with application to model order selection. *IEEE Transactions on Automatic Control*, 37(7), 913-928. doi:10.1109/9.148344
- Hazel, B., Côté, J., Laroche, Y., & Mongenot, P. (2012a). Field repair and construction of large hydropower equipment with a portable robot. *Journal of Field Robotics*, 29(1), 102-122. doi:<https://doi.org/10.1002/rob.20427>

- Hazel, B., Côté, J., Laroche, Y., & Mongenot, P. (2012b). A portable, multiprocess, track-based robot for in situ work on hydropower equipment. *Journal of Field Robotics*, 29(1), 69-101. doi:<https://doi.org/10.1002/rob.20425>
- Lennart, L. (1999). System identification: theory for the user. PTR Prentice Hall, Upper Saddle River, NJ, 28.
- Ljung, L. (1985). On the estimation of transfer functions. *Automatica*, 21(6), 677-696. doi:[https://doi.org/10.1016/0005-1098\(85\)90042-1](https://doi.org/10.1016/0005-1098(85)90042-1)
- Ljung, L., & Söderström, T. (1983). *Theory and Practice of Recursive Identification*. Cambridge: MIT Press.
- Moore, S. M., Lai, J. C. S., & Shankar, K. (2007a). ARMAX modal parameter identification in the presence of unmeasured excitation—I: Theoretical background. *Mechanical Systems and Signal Processing*, 21(4), 1601-1615. doi:<https://doi.org/10.1016/j.ymsp.2006.07.003>
- Moore, S. M., Lai, J. C. S., & Shankar, K. (2007b). ARMAX modal parameter identification in the presence of unmeasured excitation—II: Numerical and experimental verification. *Mechanical Systems and Signal Processing*, 21(4), 1616-1641. doi:<https://doi.org/10.1016/j.ymsp.2006.07.004>
- Özsahin, O., Budak, E., & Özgüven, H. N. (2015). In-process tool point FRF identification under operational conditions using inverse stability solution. *International Journal of Machine Tools and Manufacture*, 89, 64-73. doi:<https://doi.org/10.1016/j.ijmachtools.2014.09.014>
- Peng, Y., Li, B., Mao, X., Liu, H., Qin, C., & He, H. (2018). A method to obtain the in-process FRF of a machine tool based on operational modal analysis and experiment modal analysis. *The International Journal of Advanced Manufacturing Technology*, 95(9), 3599-3607. doi:10.1007/s00170-017-1405-8
- Postel, M., Özsahin, O., & Altintas, Y. (2018). High speed tooltip FRF predictions of arbitrary tool-holder combinations based on operational spindle identification. *International Journal of Machine Tools and Manufacture*, 129, 48-60. doi:<https://doi.org/10.1016/j.ijmachtools.2018.03.004>

- Saupe, F., & Knoblach, A. (2015). Experimental determination of frequency response function estimates for flexible joint industrial manipulators with serial kinematics. *Mechanical Systems and Signal Processing*, 52-53, 60-72. doi:<https://doi.org/10.1016/j.ymsp.2014.08.011>
- Schoukens, J., & Pintelon, R. (1994). Quantifying model errors of identified transfer functions. *IEEE Transactions on Automatic Control*, 39(8), 1733-1737. doi:10.1109/9.310063
- Smail, M., Thomas, M., & Lakis, A. (1999a). ARMA model for modal analysis: effect of model orders and sampling frequency. *Mechanical Systems and Signal Processing*, 13(6), 925-941. doi:<https://doi.org/10.1006/mssp.1999.1235>
- Smail, M., Thomas, M., & Lakis, A. A. (1999b). Assessment of optimal ARMA model orders for modal analysis. *Mechanical Systems and Signal Processing*, 13(5), 803-819. doi:<https://doi.org/10.1006/mssp.1999.1224>
- Smith, W. A., & Randall, R. B. (2016). Cepstrum-based operational modal analysis revisited: A discussion on pole-zero models and the regeneration of frequency response functions. *Mechanical Systems and Signal Processing*, 79, 30-46. doi:<https://doi.org/10.1016/j.ymsp.2016.02.030>
- Soderstrom, T., Fan, H., Carlsson, B., & Bigi, S. (1997). Least squares parameter estimation of continuous-time ARX models from discrete-time data. *IEEE Transactions on Automatic Control*, 42(5), 659-673. doi:10.1109/9.580871
- Stoica, P., & Selen, Y. (2004). Model-order selection: a review of information criterion rules. *IEEE Signal Processing Magazine*, 21(4), 36-47. doi:10.1109/MSP.2004.1311138
- Vu, V.-H., Liu, Z., Thomas, M., Li, W., & Hazel, B. (2016). Output-only identification of modal shape coupling in a flexible robot by vector autoregressive modeling. *Mechanism and Machine Theory*, 97, 141-154. doi:<https://doi.org/10.1016/j.mechmachtheory.2015.11.005>
- Vu, V. H., Thomas, M., Lafleur, F., & Marcouiller, L. (2013). Towards an automatic spectral and modal identification from operational modal analysis. *Journal of Sound and Vibration*, 332(1), 213-227. doi:<https://doi.org/10.1016/j.jsv.2012.08.019>

- Vu, V. H., Thomas, M., Lakis, A. A., & Marcouiller, L. (2011). Operational modal analysis by updating autoregressive model. *Mechanical Systems and Signal Processing*, 25(3), 1028-1044. doi:<https://doi.org/10.1016/j.ymssp.2010.08.014>
- Vu, V. H., Zhaoheng, L., Thomas, M., Tahvilian, A. M., & Hazel, B. (2016). *Identification of frequency response functions of a flexible robot as tool-holder for robotic grinding process.*
- Wahlberg, B., & Ljung, L. (1986). Design variables for bias distribution in transfer function estimation. *IEEE Transactions on Automatic Control*, 31(2), 134-144. doi:10.1109/TAC.1986.1104221
- Zaghbani, I., & Songmene, V. (2009). Estimation of machine-tool dynamic parameters during machining operation through operational modal analysis. *International Journal of Machine Tools and Manufacture*, 49(12), 947-957. doi:<https://doi.org/10.1016/j.ijmachtools.2009.06.010>
- Zhu, D., Feng, X., Xu, X., Yang, Z., Li, W., Yan, S., & Ding, H. (2020). Robotic grinding of complex components: A step towards efficient and intelligent machining – challenges, solutions, and applications. *Robotics and Computer-Integrated Manufacturing*, 65, 101908. doi:<https://doi.org/10.1016/j.rcim.2019.101908>

CHAPTER 4

A NONLINEAR IDENTIFICATION OF CONTACT PARAMETERS: APPLICATION TO A FLEXIBLE MANIPULATOR UNDER GRINDING OPERATION

Quoc Cuong Nguyen^a, Viet Hung Vu^b and Marc Thomas^c,

^{a,b,c} Department of Mechanical Engineering, École de Technologie Supérieure,
1100 Notre-Dame West, Montreal, Quebec, H3C 1K3

Paper submitted for publication in *Journal of Dynamic System, Measurement, and Control*,
March 2022

Highlights

- An approach for estimating unknown environmental contact parameters.
- Unscented Kalman Filter (UKF) in conjunction with Hunt Crossley contact model is applied without using input force.
- Modal analysis output only is performed by using Covariance Driven Stochastic Subspace algorithm (SSI-COV).
- An industrial SCOMPI robot under grinding operation has been used for validation.

4.1 Résumé

Cet article présente une méthode non linéaire utilisant le filtre de Unscented Kalman (UKF) en conjonction avec le modèle Hunt-Crossley pour la caractérisation de la force de contact, qui comprend l'amortissement et la rigidité de contact. Étant donné que l'entrée reste inconnue, l'algorithme d'identification du système est développé pour traiter uniquement les mesures de sortie. Le but de cet article est de développer une méthodologie expérimentale simple pour caractériser la rigidité et l'amortissement équivalents du manipulateur en boucle fermée pour réguler la dynamique d'interaction. Un robot industriel SCOMPI avec une meuleuse

pneumatique a été utilisé comme plate-forme de test pour illustrer la viabilité de la technique d'identification. L'analyse dynamique des manipulateurs flexibles a été réalisée en deux parties pour fournir une enquête à grande échelle. Dans la première étape, l'analyse modale, en particulier l'estimation de l'amortissement, est effectuée avec l'identification de Covariance Driven Stochastic Subspace Identification (SSI-COV) en utilisant les réponses aux vibrations ambiantes. Dans la deuxième étape, le filtre de Unscented Kalman est adopté pour traiter la modélisation de contact non linéaire. La méthode a été vérifiée par l'algorithme commun des moindres carrés récursifs (RLS) et montre sa robustesse et son efficacité en termes d'estimation des paramètres de contact.

Mots clés : Paramètres de contact, Analyse modale, Manipulateur flexible, Environnement inconnu, Filtre de Kalman.

4.2 Abstract

This paper presents a nonlinear method by using Unscented Kalman Filter (UKF) in conjunction with the Hunt-Crossley model for contact force characterization, which included contact damping and contact stiffness. Since ambient input remains unknown, the system identification algorithm is developed to deal with output measurements only. The goal of this paper is to develop a simple experimental methodology for characterizing the equivalent stiffness and damping of the closed-loop manipulator to regulate the interaction dynamic. An industrial SCOMPI robot with a pneumatic grinder has been used as a test platform to illustrate the viability of the identification technique. The dynamical analysis of flexible manipulators has been carried out into two parts to provide a full-scale investigation. In the first stage, modal analysis especially damping estimation is performed with Covariance Driven Stochastic Subspace Identification (SSI-COV) by using ambient vibration responses. In the second stage, Unscented Kalman Filter is adopted to deal with nonlinear contact modeling. The method was verified by the common Recursive Least Squares (RLS) algorithm and shows its robustness and efficiency in terms of estimating contact parameters.

Keywords: Contact parameters, Modal analysis, Flexible manipulator, Unknown environment, Kalman filter.

4.3 Introduction

Robotic machining is emerging as a viable alternative for some conventional machining tasks thanks to its advantages of high flexibility, low cost, and productivity. However, the rapid expansion in recent years in robotic systems has given rise to a new and challenging problem. These systems are expected to perform tasks that require a high degree of dexterity and adaptability to various and uncertain task conditions, but the relatively low stiffness of the robot can seriously affect its positioning accuracy, which may lead to poor machining quality and inferior production efficiency. Therefore, controlling the interaction forces with respect to contact parameters becomes an important issue. By identifying the dynamic behavior of the contact environment, the autonomy of the robot system can be considerably improved. Depending on the interaction between a robot manipulator and its workpiece, robotic tasks can be classified into two categories: unconstrained and constrained motion (Choi & Krishnamurthy, 1994; Grabbe, Carroll, Dawson, & Qu, 1992). Unconstrained motion occurs when the manipulator is instantaneously free to move in any direction without contacting the environment such as spray painting or visual inspection. By contrast, constrained motion occurs when the manipulator interacts with its environment through a point or multiple points of contact. Example of such tasks include grinding, cutting, or assembly. When a compliant robot manipulator interacts with the environment, forces are generated at the contact points, which are a function of environmental parameters such as stiffness, damping, and friction. The resulting contact forces has a great influence on the instability of the manipulator, that might cause chatter vibration. This problem assumes great importance when the environment is unknown or poorly structured. It is thus necessary to develop a mechanism that estimates the relevant environment parameters in real time allowing to perform the corresponding adaptation to the control and to provide realistic feedback to the operator. The stability and the performance of the interaction controllers, such as the impedance controller (Hogan, 1984) or intrinsically passive controllers (Stramigioli, 2001), are directly affected by the mechanical

properties of the interactive environment. The exploitation of knowledge of contact environment properties greatly improves the performance of the robotic system, and furthermore, corrective manipulations are carried out to achieve better orientation and positioning. Notwithstanding that various aspects of robotic systems have thus far been intensively investigated with the aid of increasingly powerful computer hardware and advanced software, the modeling and control of constrained robotic operations remain challenging (Skrinjar, Slavič, & Boltežar, 2018; Tian, Flores, & Lankarani, 2018; Zhang & Wei, 2017). Interfacial parameters, including contact stiffness and contact damping, are very important for contact dynamics and interface modeling. In many applications, characterizing and understanding the interfacial behavior of the contact force are critical (Gilardi & Sharf, 2002; Machado, Moreira, Flores, & Lankarani, 2012; Skrinjar *et al.*, 2018). Many authors have carried out research into environment parameters estimation. Related methods can be differentiated according to the contact models assumed, the approach, and the interaction control system, by using obtained data. The simplest such model is the Kelvin-Voigt model (Lewandowski & Chorażyczewski, 2010), which describes the relationship between the relative penetration of contact bodies and the contact force by presenting a linear spring and a viscous damper in parallel. This model was further developed in (McClamroch, 1989) and (Mills & Nguyen, 1992) by accounting for the dynamics of the contact surface. A Maxwell (MW) model was constructed by a serial spring and damper (Sakamoto, Higashimori, Tsuji, & Kaneko, 2007), while the Kelvin-Boltzmann (KB) model adds a spring in serial form to the Kelvin-Voigt (Sánchez, Le, Liu, Zemitte, & Pognet, 2012). However, these models are linear and involve unnatural forces, which will deteriorate the estimation solution at the beginning and end of the contact and fail to represent the nonlinear behavior of tool interaction (Diolaiti, Melchiorri, & Stramigioli, 2005). To accurately identify the environment and contact dynamics, attention has also turned toward the estimation of parameters of nonlinear contact dynamic models. The first well-known nonlinear force model for the contact between two spheres of isotropic materials was developed by Hertz (Muthukumar & DesRoches, 2006), but the model could not describe the whole contact process since it did not account for energy dissipation. Consequently, many nonlinear force models taking the damping term into account have been proposed to overcome the drawbacks of the Hertz model. For instance, Hunt-

Crossley (H-C) (Hunt & Crossley, 1975; Marhefka & Orin, 1999) and Lankarani-Nikravesh (Lankarani & Nikravesh, 1990) characterize the dynamics of both stiff and compliant materials. The H-C model showed great potential to secure a good dynamical behavior of the system with the physical damping coefficients, which characterize energy loss during impacts. Based on these models, different nonlinear estimation algorithms were proposed for tracking force and characterization of contact force parameters. One of the most common parameters estimation approaches is the Recursive Least Squares (RLS) method, which can be applied to either linear (Haddadi & Hashtrudi-Zaad, 2008b) or nonlinear contact models (Haddadi & Hashtrudi-Zaad, 2008a). Depending on the approach being considered, a set of assumptions, such as unbiased data or persistent excitation in the identification scheme, may be required. Recently, many researchers have focused on designing force tracking impedance controllers, which command the robot to exert a specified contact force on the environment. Seraji et al. demonstrated a force tracking impedance controller by estimating the environment stiffness and location (Seraji & Colbaugh, 1993). This was achieved using either direct or indirect adaptive control. Love and Book presented a method in which the Recursive Least Squares (RLS) technique is applied in a discrete form of contact dynamic equations. Then, estimated environment parameters were utilized in designing an impedance controller that was stable both during and at the onset of contact (Love & Book, 1995). The System Identification (SI) method using a Kalman filter or Extended Kalman Filter developed many years ago is another effective approach (Hun, Ong, Lim, & Koo, 2016). While the Kalman Filter works only in the linear model (Chua & Katupitiya, 1998), the extended Kalman Filter (EKF) is considered an improvement of the former, which typically deals with the nonlinear contact model (Zhu, Gao, Zhong, Gu, & Choi, 2021). This method has found widespread use in nonlinear state and parameters estimation thanks to its simplicity and ease of implementation and can achieve higher estimation accuracy than RLS. However, dynamic linearization incurs modeling errors, which may lead to biased filtering solutions. The Unscented Kalman Filter (UKF) was recently proposed by Julier and Uhlman (Julier & Uhlmann, 2004), and eliminated the derivation of Jacobian matrices, making it much easier to implement than the EKF by using a set of sigma points via unscented transformation. As a result, the UKF can estimate the posterior mean and covariances accurately to a higher order.

In this paper, a nonlinear method for online estimation of unknown constraints environment parameters is presented by combining the nonlinear Hunt Crossley contact model with the Unscented Kalman Filter algorithm (UKF). An experimental application is performed on a flexible robot under grinding operation. A UKF algorithm is developed based on instantaneous linearization to online quantify contact force parameters in real-time. The previous works by the authors (Nguyen, Vu, & Thomas, 2022) performed a contact force identification. Thus, in the present paper, we focus on two major research areas. The first deals with the identification of modal damping ratios by using the measured vibration output only via a Covariance Driven Stochastic Subspace Identification (SSI-COV) algorithm, which shows its efficiency and robustness when working in a noisy measurement. The second topic deals with contact modeling and unknown contact parameters identification. To characterize the interaction of robots with unstructured environments, the contact force model was established first under the concept of the Hunt Crossley model. Then, a nonlinear UKF algorithm was used to estimate the contact damping and contact stiffness. This method is verified by a traditional Recursive Least Squares algorithm and has proven beneficial and robust in parameters identification. The work performed in this paper thus provides the following contributions to the state of the art. First, a new experimental procedure based on the modal analysis concept is used to identify the dynamic parameters of industrial manipulator arms using only ambient vibration outputs, especially modal damping ratios, which are usually very difficult to predict at the design state but have a strong influence on the dynamic structural behavior. Second, a computationally efficient and easily implementable online parameters estimation algorithm is used to extract the contact properties from velocity and displacement data, themselves extracted from the measured acceleration of a robot under working conditions, without using the unknown input force excitation.

4.4 Damping identification

Output-only strategies in modern dynamical system monitoring, which only use response sensors to track the modal parameters of the system, have attracted a lot of attention over the

years (Peeters & De Roeck, 2001; Vu, Liu, Thomas, Li, & Hazel, 2016). Ambient vibration tests have the strong advantage of being very practical and economical, as they use freely available ambient excitation. Additionally, vibration data are obtained directly from normal working conditions of the structure, which makes the identified modal parameters associated with realistic vibration levels. Although these modern output-only modal identification techniques can provide very accurate estimates of natural frequencies and mode shapes, the accurate estimation of damping ratios needs improvement. In this section, a methodology based on the Covariance Driven Stochastic Subspace Identification (SSI-COV) algorithm is proposed. The damping estimation is obtained from a stabilization diagram computed at each identified natural frequency, by using the output-only measurements.

4.4.1 Covariance driven stochastic subspace identification

Firstly, the SSI-COV method is described, and the use of stabilization diagrams is briefly explained. The SSI-COV method performs the identification of the modal parameters using a stochastic state-space model that, which in its discrete form and assuming the excitation as white noise, is represented by the following equations (Peeters & De Roeck, 1999).

$$\begin{aligned} \mathbf{x}_{k+1} &= \mathbf{A} \cdot \mathbf{x}_k + \mathbf{w}_k \\ \mathbf{y}_k &= \mathbf{C} \cdot \mathbf{x}_k + \mathbf{v}_k \end{aligned} \quad (4.1)$$

where $\mathbf{x}_k \in \mathbb{R}^{n \times 1}$ is the discrete-time state vector at time instant k , $\mathbf{y}_k \in \mathbb{R}^{m \times 1}$ is a vector with the sampled outputs, with m is the number of measured accelerometers. $\mathbf{A} \in \mathbb{R}^{n \times n}$ is the discrete state matrix, $\mathbf{C} \in \mathbb{R}^{m \times n}$ is the discrete output matrix and $\mathbf{w}_k \in \mathbb{R}^n$ and $\mathbf{v}_k \in \mathbb{R}^m$ are vectors that represent the noise due to disturbances and modeling inaccuracies and the measurement noise due to sensor inaccuracy.

The first step of SSI-COV algorithm is the computation of output correlation, which is based on the covariance matrices of the measured structural response time series, and given by the following formula:

$$\mathbf{R}_i = \frac{1}{N-i} \sum_{k=0}^{N-i-1} \mathbf{y}_{k+1} \mathbf{y}_k^T \quad (4.2)$$

where N is the number of points of the time series and superscript T means transpose. These are then organized in a Toeplitz matrix:

$$T_{1|i} = \begin{bmatrix} \mathbf{R}_i & \mathbf{R}_{i-1} & \cdots & \mathbf{R}_1 \\ \mathbf{R}_{i+1} & \mathbf{R}_i & \cdots & \mathbf{R}_2 \\ \cdots & \cdots & \cdots & \cdots \\ \mathbf{R}_{2i-1} & \mathbf{R}_{2i-2} & \cdots & \mathbf{R}_i \end{bmatrix} \quad (4.3)$$

The algorithm of the method is based on the properties of a stochastic system and involves a singular value decomposition and the resolution of a least-squares equation. Subsequently, the modal parameters are straightforwardly extracted from the Toeplitz matrix (Magalhães, Cunha, & Caetano, 2009).

4.4.2 Damping estimation from ambient vibrations

In the time domain method, COV-SSI has been implemented following their original formulation explained above. The objective of this technique is to estimate a discrete-time system matrix \mathbf{A} . The eigenvalue decomposition of the system matrix is interpreted as a set of discrete complex system poles. The continuous-time poles are then determined as:

$$[\boldsymbol{\Psi}]^{-1} [\mathbf{A}] [\boldsymbol{\Psi}] = [\mathbf{Z}] \quad (4.4)$$

$$\lambda = \frac{\ln(Z_r)}{\Delta k} \quad (4.5)$$

where Z_r is the r^{th} component of the matrix \mathbf{Z} , and Δk is the time step.

The continuous poles can be related to the natural frequency, damping and mode shapes of the system.

$$\omega_r = \frac{\sqrt{(\lambda_r^R)^2 + (\lambda_r^I)^2}}{2\pi} \quad (4.6)$$

$$\zeta_r = \frac{|\lambda_r^R|}{\sqrt{(\lambda_r^R)^2 + (\lambda_r^I)^2}} \quad (4.7)$$

$$[\phi] = [C] \times [\Psi] \quad (4.8)$$

where λ_r^R and λ_r^I are respectively, the real and imaginary components of λ_r , ζ_r is damping factor for r^{th} mode, and $[\phi]$ is matrix of mode shapes.

4.4.3 Stabilization criteria and selection of poles

The pole estimate from the SSI algorithm undergoes scrutiny from stabilization criteria to assist in distinguishing between physical and spurious modes. For the order p^* , the resulting poles q^* are compared to all the poles from the preceding order $p = p^* - \sigma$, where $\sigma = 1, 2, \dots, s$ and s is an integer defining the required stability level. The pole q is obtained from the order p that maximizes the value of the Modal Assurance Criterion (MAC) number. The MAC number between complex-valued poles q and q^* is defined as follows (Deistler, 1994).

$$\text{MAC}_{q,q^*} = \frac{\left| \left\{ \phi_{q^*} \right\}^T \overline{\left\{ \phi_q \right\}} \right|^2}{\left\{ \phi_{q^*} \right\}^T \left\{ \phi_q \right\} \cdot \left\{ \phi_{q^*} \right\}^T \overline{\left\{ \phi_q \right\}}} \quad (4.9)$$

where $\overline{\left\{ \phi_q \right\}}$ corresponds to the complex conjugate of $\left\{ \phi_q \right\}$. The value of MAC_{q,q^*} lies between 0 and 1, where 1 indicates a maximum similarity.

4.5 Contact force model and identification technique

4.5.1 Contact force model

Controlling the force at the contact point and identifying the contact parameters have become an essential requirement in robotic applications. It is evident that these parameters, which include contact stiffness and damping coefficients, affect the force that is generated during the contact between a robot and its environment. Since the stiffness and damping coefficients are

generally unknown, contact parameters estimation refers to the process of using the robot to identify these physical quantities during an operational task. The modeling of unknown environments has been researched for many years (Di Renzo & Di Maio, 2004). Based on the complexity of the models' environment and features, many researchers have classified them under different categories, such as single-stage or second-stage impedance, by using the physics of mass, spring, and damper. Among these models, the second-stage impedance ones are seldom used because the effect of the environment mass is rarely important (Vukobratović & Potkonjak, 1999). In the context of robotic tasks, energy dissipation during the contact process must be taken into consideration to accurately describe the nonlinear nature of the process. Consequently, some nonlinear force models that consider the damping term have been proposed in the literature. In 1975, Hunt and Crossley (Hunt & Crossley, 1975) showed that a position-dependent environment damping model is more consistent with physical intuition, representing energy lost during impacts. In this paper, since the specific task of a SCOMPI robot is grinding in contact with a stiff workpiece, the contact events thus consider only one contact point, and the manipulator end-effector motion under grinding operation is in the normal direction to the workpiece.

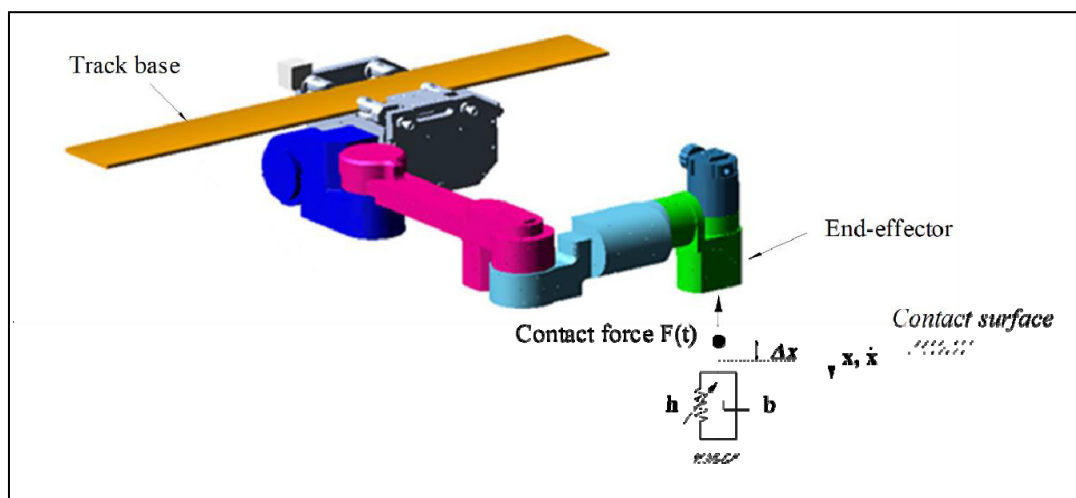


Figure 4.1 Single point contact environment model of SCOMPI robot

For online estimation, the nonlinear Hunt-Crossley model is proposed instead of the classical Kelvin-Voigt model. Consequently, a single-stage nonlinear contact model is presented in

Figure 1. The nonlinear model is shown to have a good agreement with physical environments. The normal force $\mathbf{F}_{(t)}$ acting on a body is a function of deformation, \mathbf{x} , of the body at the contact point. In this model, the spring represents the elastic behavior of the contact bodies while the damper describes the energy dissipation at its contact point. When the manipulator contacts the environment, a reaction force results. With the spring and damper model of the environment, this reaction force can be modeled by:

$$\mathbf{F}_{(t)} = \begin{cases} h\mathbf{x}^n(t) + b\mathbf{x}^n(t)\dot{\mathbf{x}}(t) & \mathbf{x}(t) \geq 0 \\ 0 & \mathbf{x}(t) < 0 \end{cases} \quad (4.10)$$

where $\mathbf{F}_{(t)}$ is the contact force, $\mathbf{x}(t)$ represents penetration in the environment and $\dot{\mathbf{x}}(t)$ is the rate of deformation, h and b present the environment stiffness and damping parameters, $h\mathbf{x}^n(t)$ denotes the nonlinear elastic force and $b\mathbf{x}^n(t)\dot{\mathbf{x}}(t)$ denotes the nonlinear viscous force. The parameter n is a positive scalar, typically between 1 and 2, depending on the material and the geometric properties of the contact.

By adding a system noise $\boldsymbol{\varepsilon}(t)$, the model becomes:

$$\mathbf{F}_{(t)} = h\mathbf{x}^n(t) + b\mathbf{x}^n(t)\dot{\mathbf{x}}(t) + \boldsymbol{\varepsilon}(t) \quad (4.11)$$

To linearize and decouple the above equation with respect to the parameter h , b and n , the natural logarithm of both sides is taken:

$$\ln(\mathbf{F}_{(t)}) = \ln h\mathbf{x}^n(t) \left(1 + \frac{b\dot{\mathbf{x}}(t)}{h} + \frac{\boldsymbol{\varepsilon}(t)}{h\mathbf{x}^n(t)} \right) \quad (4.12)$$

Applying the property of the natural logarithm: $\ln(1+\alpha) \cong \alpha$ for $|\alpha| \ll 1$, we have:

$$\left| \frac{b\dot{\mathbf{x}}(t)}{h} + \frac{\boldsymbol{\varepsilon}(t)}{h\mathbf{x}^n(t)} \right| \leq \left| \frac{b\dot{\mathbf{x}}(t)}{h} \right| + \left| \frac{\boldsymbol{\varepsilon}(t)}{h\mathbf{x}^n(t)} \right| \leq 1 \quad (4.13)$$

The equation (4.12) is linearized with respect to its dynamic parameters to

$$\ln(\mathbf{F}_{(t)}) \cong \ln(h) + \frac{b}{h}\dot{\mathbf{x}}(t) + n \ln(\mathbf{x}(t)) + \frac{\boldsymbol{\varepsilon}(t)}{h\mathbf{x}^n(t)} \quad (4.14)$$

Equation (4.14) can be further written into the following matrix form:

is a covariance matrix and $\hat{\mathbf{x}}$ is the estimated system state and $0 < \beta \leq 1$ is a

$$\ln(\mathbf{F}_k) = \begin{bmatrix} 1 & \dot{\mathbf{x}}(t) & \ln(\mathbf{x}(t)) \end{bmatrix} \begin{bmatrix} \ln(h) \\ \frac{b}{h} \\ n \end{bmatrix} + \bar{\boldsymbol{\varepsilon}}_k \quad (4.15)$$

where $\bar{\boldsymbol{\varepsilon}}_k = \frac{\boldsymbol{\varepsilon}_k}{h\mathbf{x}_k^n}$ represents the modeling error and force measurement noise at the sample time $t=k.T$.

Consequently, the equation (4.14) can be rewrite in the discrete compact form

$$\mathbf{y}_k = \boldsymbol{\Phi}_k^T \boldsymbol{\Theta}_k + \bar{\boldsymbol{\varepsilon}}_k \quad (4.16)$$

where k denotes the k th time points, $\mathbf{y}_k = \ln(\mathbf{F}_k)$ denotes the observation of the system,

$\boldsymbol{\Theta}_k = \begin{bmatrix} \ln(h) & \frac{b}{h} & n \end{bmatrix}^T$ denotes the system state which is made up of the unknown contact

force parameters, and $\boldsymbol{\Phi}_k = \begin{bmatrix} 1 & \dot{\mathbf{x}}(t) & \ln(\mathbf{x}(t)) \end{bmatrix}$ is the system function. It is obvious that the

system function $\boldsymbol{\Phi}_k$ depends on the output displacement and velocity, while independent of the system state $\boldsymbol{\Theta}_k$, indicating that the logarithmic linearization is a static process in terms of the system state.

Based on the system equation (4.16), the Recursive Least Square (RLS) procedure can be applied, which estimates system state parameters by minimizing the sum of squares of the errors between theoretical and measurement values. RLS minimizes the mean square value of the model error at every time step, then the parameter vector is calculated as follows:

$$\hat{\boldsymbol{\Theta}}_k = \hat{\boldsymbol{\Theta}}_{k-1} + \mathbf{L}_k \left[\mathbf{F}_k - \boldsymbol{\Phi}_k^T \hat{\boldsymbol{\Theta}}_{k-1} \right] \quad (4.17)$$

where:

$$\mathbf{L}_k = \mathbf{P}_{k-1} \boldsymbol{\Phi}_k \left(\beta + \boldsymbol{\Phi}_k^T \mathbf{P}_{k-1} \boldsymbol{\Phi}_k \right)^{-1} \quad (4.18)$$

$$\mathbf{P}_k = \beta^{-1} \left[\mathbf{I} - \mathbf{L}_k \boldsymbol{\Phi}_k^T \right] \mathbf{P}_{k-1} \quad (4.19)$$

where \mathbf{P}_k is a covariance matrix and $\hat{\boldsymbol{\Theta}}_k$ is the estimated system state and $0 < \beta \leq 1$ is a forgetting factor, whose value depends on the particular environment under examination.

However, conventional RLS requires the measurement of the input forces, which limits its application in cases where measuring inputs is difficult or impractical. Another drawback of this approach is that it depends on choosing the forgetting factor, which is very sensitive to measurement noise. Meanwhile, in practice, acceleration responses are usually measured, whereas velocity and displacement responses can be obtained through a single and double numerical integration, respectively. To address the limitation of the original RLS method, we proposed a simple technique by using the measured acceleration based on the Unscented Kalman Filter (UKF) to predict system states, which are a function of stiffness and damping parameters. As already mentioned above, the algorithms are inherently based on a one-point contact model between the pneumatic grinder and its environment. Further, they require the measurement of velocity and displacement at the contact point, which is typically not directly available, because accelerations are most commonly obtained (Flores & Ambrósio, 2010). Therefore, the accelerations are integrated using either the Runge-Kutta or predictor-corrector numerical integration routine to yield the velocities and displacements.

By assuming zero initial conditions, we can use the inherent relations between the displacement, velocity, and acceleration to obtain the velocity and displacement directly from the measured acceleration:

$$\dot{\mathbf{x}}(t) = \int_0^t \ddot{\mathbf{x}}(\tau) d\tau \quad (4.20)$$

$$\mathbf{x}(t) = \int_0^t \dot{\mathbf{x}}(\tau) d\tau \quad (4.21)$$

where $\ddot{\mathbf{x}}(t)$ is the acceleration time series that either recorded or synthesized, $\dot{\mathbf{x}}(t)$ and $\mathbf{x}(t)$ are the velocity and displacement time series, respectively.

Equations (4.20) and (4.21) can be convenient expressed in the discrete time form as

$$\dot{\mathbf{x}}(t) = \sum_{i=1}^N \frac{1}{2} (\ddot{\mathbf{x}}(i-1) + \ddot{\mathbf{x}}(i)) \Delta \tau \quad (4.22)$$

$$\mathbf{x}(t) = \sum_{i=1}^N \frac{1}{2} (\dot{\mathbf{x}}(i-1) + \dot{\mathbf{x}}(i)) \Delta \tau \quad (4.23)$$

where N is the number of sampling points in the acceleration time series, $\Delta\tau$ is the integral time step and is required to be sufficiently short to satisfy the condition of convergence.

4.5.2 Proposed method by using Unscented Kalman Filter

In this section, we propose a method using the Unscented Kalman Filter (UKF) for estimating contact force parameters, which utilizes the well-known features of the Kalman filter. However, the method employs the Unscented Transform (UT) to compute the prior probability distribution before the measurement update step is performed. These parameters need to components of the state to be identified. Unlike the Extended Kalman Filter (EKF), the UKF does not employ a linearization-based approximation of the nonlinear system. This model is achieved by carefully choosing a set of Sigma points, which capture the true mean and covariance of a given distribution, and then passing the means and covariance of estimated states through a nonlinear transformation. As a result, the UKF can estimate the posterior mean and covariances accurately to a high order.

Unscented Transformation (UT)

Based on the proposed contact force model given in the previous section, the following discrete-time nonlinear system can be described in the form of state and measurement equations:

$$\mathbf{x}_{k-1} = G(\mathbf{x}_k, \mathbf{w}_k) \quad (4.24)$$

$$\mathbf{z}_k = H(\mathbf{x}_k, \mathbf{v}_k) \quad (4.25)$$

where the subscript k represents the integration number, \mathbf{x}_k represents the unobserved state of the system, \mathbf{w}_k and \mathbf{v}_k are the additive process noise that drives the dynamical system and measurement sequence which are zero mean white with covariance matrices \mathbf{Q} and \mathbf{R} respectively, \mathbf{z}_k is the observed signal. The system dynamical model $G(*)$ and $H(*)$ can be nonlinear function and are assumed to be known.

In the unscented transform, these nonlinear functions are represented by discrete points called sigma points, which are carefully chosen so that their mean and covariance are $\bar{\mathbf{x}}$ and \mathbf{P}_x . Then the sigma points are passed through the nonlinear function to yield a set of transformed points, of which the mean and covariance can form a statistic estimate of the nonlinearly transformed variable \mathbf{x} .

The L dimension random variable x with mean $\bar{\mathbf{x}}$ and covariance \mathbf{P}_x is represented by a matrix χ of $2L+1$ sigma vector and their corresponding weight W_i as follows.

$$\chi_0 = \bar{\mathbf{x}} \quad (4.26)$$

$$\chi_i = \bar{\mathbf{x}} + \left(\sqrt{L + \lambda \mathbf{P}_x}\right)_i \quad i = 1, \dots, L \quad (4.27)$$

$$\chi_i = \bar{\mathbf{x}} - \left(\sqrt{L + \lambda \mathbf{P}_x}\right)_{i-L} \quad i = L + 1, \dots, 2L \quad (4.28)$$

$$W_0^{(m)} = \lambda / (L + \lambda) \quad (4.29)$$

$$W_0^{(c)} = \lambda / (L + \lambda) + (1 - \alpha^2 + \beta) \quad (4.30)$$

$$W_i^{(m)} = W_i^{(c)} = 1/2(L + \lambda) \quad i = 1, \dots, 2L \quad (4.31)$$

where $\left(\sqrt{L + \lambda \mathbf{P}_x}\right)_i$ is the i^{th} row or column of the matrix square root of $L + \lambda \mathbf{P}_x$, which can be obtained through the Cholesky decomposition $\lambda = \alpha^2(L + \zeta) - L$ is a scaling parameter, α determines the spread of the sigma points around $\bar{\mathbf{x}}$ and is usually set to a small positive value such as 0.003, ζ is a secondary scaling parameter which is usually set to zero, and β is used to incorporate prior knowledge of the distribution of \mathbf{x} (for Gaussian distribution, $\beta = 2$ is optimal (Julier & Uhlmann, 2004)). $W_i^{(m)}$ and $W_i^{(c)}$ are the weight corresponding to the i^{th} means and covariance, respectively.

Transforming each sigma vector through the nonlinear function leads to,

$$\mathbf{y}_i = g(\chi_i) \quad i = 0, 1, 2, \dots, 2L \quad (4.32)$$

The observation means and covariance for \mathbf{y} can be describe as follows, respectively.

$$\bar{\mathbf{y}} \approx \sum_{i=0}^{2L} W_i^{(m)} \mathbf{y}_i \quad (4.33)$$

$$\mathbf{P}_y \approx \sum_{i=0}^{2L} W_i^{(m)} (\mathbf{y}_i - \bar{\mathbf{y}})(\mathbf{y}_i - \bar{\mathbf{y}})^T \quad (4.34)$$

Implementation of the UKF

In this case the state random variable is augmented by the noise variables, that is, redefined as the concatenation of the original state, process noise and observation noise:

$$\mathbf{x}_k^\alpha = \begin{bmatrix} \mathbf{x}_k^T & \mathbf{w}_k^T & \mathbf{v}_k^T \end{bmatrix}^T \quad (4.35)$$

Following are the implementation algorithms for the UKF:

Initialization

$$\hat{\mathbf{x}}_0 = E[\mathbf{x}_0] \quad (4.36)$$

$$\mathbf{P}_0 = E\left[(\mathbf{x}_0 - \hat{\mathbf{x}}_0)(\mathbf{x}_0 - \hat{\mathbf{x}}_0)^T\right] \quad (4.37)$$

$$\hat{\mathbf{x}}_0^a = E[\mathbf{x}_0^a] = \begin{bmatrix} \hat{\mathbf{x}}_0^T & 0 & 0 \end{bmatrix} \quad (4.38)$$

$$\mathbf{P}_0^a = E\left[(\mathbf{x}_0^a - \hat{\mathbf{x}}_0^a)(\mathbf{x}_0^a - \hat{\mathbf{x}}_0^a)^T\right] = \begin{bmatrix} \mathbf{P}_0 & 0 & 0 \\ 0 & \mathbf{Q} & 0 \\ 0 & 0 & \mathbf{R} \end{bmatrix} \quad (4.39)$$

For $k = 1, \dots, \infty$, calculating the sigma points:

$$\boldsymbol{\chi}_{k|k-1}^a = \begin{bmatrix} \hat{\mathbf{x}}_{k-1}^a & \hat{\mathbf{x}}_{k-1}^a \pm \sqrt{(L + \lambda) \mathbf{P}_{k-1}^a} \end{bmatrix} \quad (4.40)$$

Time update equation:

$$\boldsymbol{\chi}_{k|k-1}^x = f\left(\boldsymbol{\chi}_{k|k-1}^x, \boldsymbol{\chi}_{k|k-1}^w\right) \quad (4.41)$$

$$\hat{\mathbf{x}}_k^- = \sum_{i=0}^{2L} W_i^{(m)} \boldsymbol{\chi}_{i,k|k-1}^x \quad (4.42)$$

$$\mathbf{P}_k^- = \sum_{i=0}^{2L} W_i^{(c)} \left[\boldsymbol{\chi}_{i,k|k-1}^x - \hat{\mathbf{x}}_k^- \right] \left[\boldsymbol{\chi}_{i,k|k-1}^x - \hat{\mathbf{x}}_k^- \right]^T \quad (4.43)$$

$$\mathbf{Z}_{k|k-1} = h\left(\boldsymbol{\chi}_{k|k-1}^x, \boldsymbol{\chi}_{k|k-1}^v\right) \quad (4.44)$$

$$\hat{\mathbf{z}}_k^- = \sum_{i=0}^{2L} W_i^{(m)} \mathbf{Z}_{i,k|k-1} \quad (4.45)$$

Measurement update equations:

$$\mathbf{P}_{\bar{z}_k \bar{z}_k} = \sum_{i=0}^{2L} W_i^{(c)} \left[\mathbf{Z}_{i,k|k-1} - \bar{\mathbf{z}}_k^- \right] \left[\mathbf{Z}_{i,k|k-1} - \bar{\mathbf{z}}_k^- \right]^T \quad (4.46)$$

$$\mathbf{P}_{x_k \bar{z}_k} = \sum_{i=0}^{2L} W_i^{(c)} \left[\boldsymbol{\chi}_{i,k|k-1}^x - \bar{\mathbf{x}}_k^- \right] \left[\mathbf{Z}_{i,k|k-1} - \bar{\mathbf{z}}_k^- \right]^T \quad (4.47)$$

$$\mathbf{K} = \mathbf{P}_{x_k \bar{z}_k} \mathbf{P}_{\bar{z}_k \bar{z}_k}^{-1} \quad (4.48)$$

$$\bar{\mathbf{x}}_k = \bar{\mathbf{x}}_k^- + \mathbf{K} \left(\mathbf{z}_k - \bar{\mathbf{z}}_k^- \right) \quad (4.49)$$

$$\mathbf{P}_k = \mathbf{P}_k^- + \mathbf{K} \mathbf{P}_{\bar{z}_k \bar{z}_k} \mathbf{K}^T \quad (4.50)$$

where $\boldsymbol{\chi}^a = \begin{bmatrix} (\boldsymbol{\chi}^x)^T & (\boldsymbol{\chi}^w)^T & (\boldsymbol{\chi}^v)^T \end{bmatrix}^T$, L is the dimension of the augmented variable, \mathbf{Q} is the process noise covariance, \mathbf{R} is the measurement noise covariance.

4.6 Experiments on a SCOMPI robot

4.6.1 Description of the test structure

A SCOMPI (Super COMPact Ireq) robot with a prismatic joint and five other rotating joints is considered as the research object. This special-purpose robot manipulator was developed to automate on-site repairs such as grinding, welding, and hammer peening (Hazel, Côté, Laroche, & Mongenot, 2012a, 2012b). The interaction between the dynamics of the tool holder and the cutting process is one of the major considerations in robotic grinding and has a strong correlation with material removal as well as a huge impact on surface quality. Therefore, contact force modeling is not only essential to control the material removal rate but also needs to maintain tasks precision. Both the structure of SCOMPI and its grinding performance in the hydraulic turbines are given in Figure 4.2.

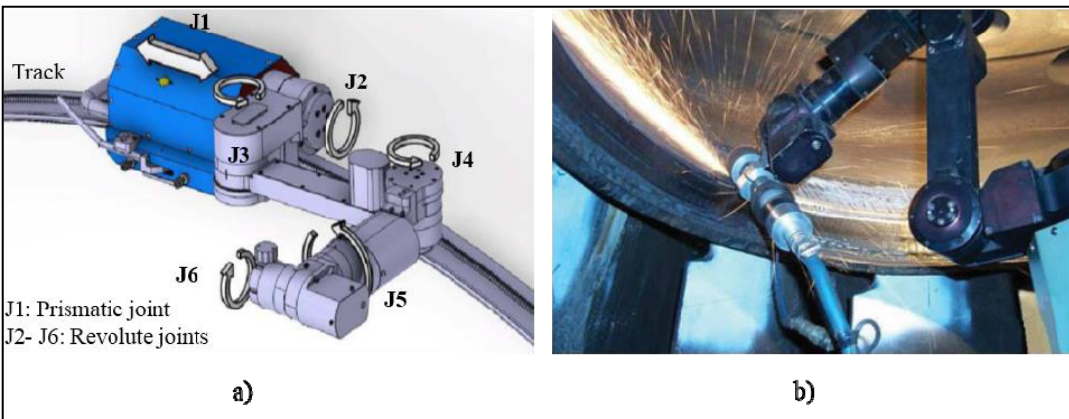


Figure 4.2 The structure of SCOMPI robot

a) 6-degree of freedom with track-mounted kinematic architecture; b) robotic performing grinding tasks

When performing the grinding task at a high Material Removal Rate (MRR), the robot faces a major hurdle such as significant vibratory responses at the end effector. The present research is going to dig deeper into this aspect by modeling of robot and its contact environment to identify the unknown contact properties at the contact point under grinding operation.

4.6.2 Measurement test setup

To illustrate the proposed contact identification concept, an experimental test was performed with the SCOMPI robot. Figure 3 shows the robot equipped with a high-frequency Norton Blue-Fire pneumatic grinder, under grinding operation. To avoid measuring the system disturbance, an ultra-rigid table was built using a concrete-and-steel structure whose first natural frequency was over 1.2 kHz. Both a dynamometer and workpiece were mounted on the table. Three PCB-352C34 piezoelectric sensors were mounted at the robot's end effector to capture the vibration in three directions X, Y, and Z, while a 3-axis Kistler dynamometer type CH8408 was placed under the workpiece for measuring the grinding contact force. The measurement was conducted through the LMS data acquisition system for a total duration of 20s at a sampling frequency of 512 Hz. A series of tests were conducted with SCOMPI, keeping the robots in their most stable configuration to minimize undesired dynamic and

vibration behaviors. During all the grinding experiments, the movement along the predefined path was maintained by the motion control. The measured acceleration data were obtained at different grinding paths to fully investigate the dynamics of the process. The feed speed was tested at a constant 8 cm/s. The wheel rotational speed was 3225 rpm, with an average 0.008 cm axial depth of grinding cut. Tests were run at five grinding power levels in the typical range for grinding tasks at 500W, 1500W, 2000W, 2500W, and 3000 W. Single-groove tests were performed over a length of 17.3 cm. The tests were repeated three times to ensure consistent measurements. A workpiece with dimensions of $20.32 \times 25.4 \times 2.54$ cm was used. The piece was made of hard steel AISI 1081, with a 71 HRC hardness.

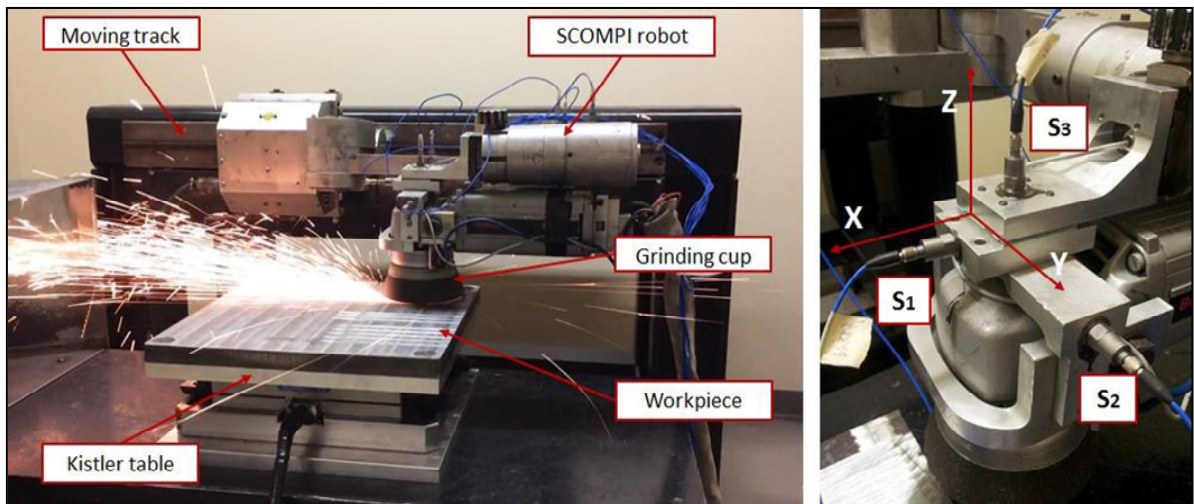


Figure 4.3 Experimental on SCOMPI under grinding task (left) and sensors configuration (right)

When the end effector contacted the workpiece, impact forces were created at the contact point, pushing the end effector off the contact. Afterward, a long-term contact was made until the robot was instructed to disconnect at $t = 20$ s. In this experiment, the identification algorithms were performed only when the end effector was in contact. Since accelerations at the end effector are obtained, the velocity $\dot{x}(t)$ and displacement $x(t)$ can be integrated from acceleration $\ddot{x}(t)$ numerically. The grinding conditions are shown in Table 4.1.

Table 4.1 Grinding condition of SCOMPI robot

No.	Experimental descriptions	Parameters	Unit
1	Grinder	Norton BlueFire 4NZ16-QB-X406	-
2	Maximum Operating Speed	7260	rpm
3	Grinding cup diameter	12,7	cm
4	Workpiece material	AISI 1081	-
5	Workpiece dimensions	20.32 x 25.4 x 2.54	cm
6	Power	500, 1500, 2000, 2500, 3000	W
7	Feed of speed	8	cm/s
8	Length of cut	16.2 – 18.5	cm
9	Large of cut	1 – 1.55	cm
10	Depth of cut	0.0158 – 0.00165	cm
11	Grinding direction	Normal direction	-
12	Rotation speed	3225	rpm
13	Angle of grinding cup	10	degree
14	Grinding condition	Dry grinding, single pass	-

4.7 Identification results

4.7.1 Output only modal analysis

One important step of the modal analysis identification algorithm is the separation of physical and spurious modes, which is obtained from a stabilization diagram. The stabilization diagram provides an effective means to discriminate the good frequencies from the spurious ones, by investigating the variation in frequency with the model order increments. Figures 4.4 presents the stabilization diagram associated with the analysis of the measurement data obtained by Covariance-Driven Stochastic Subspace Identification (SSI-COV).

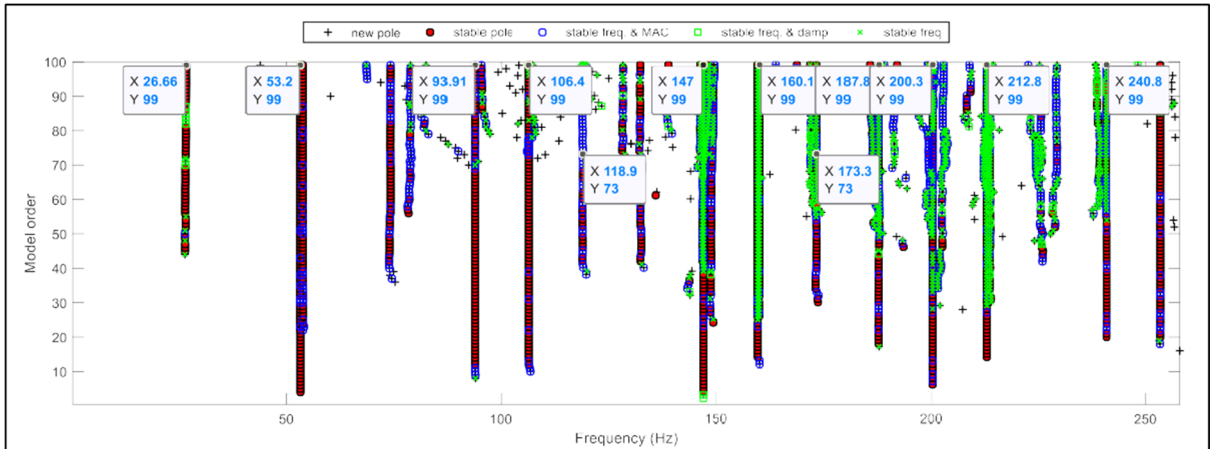


Figure 4.4 Stabilization diagram by SSI-COV algorithm

It can be seen that the SSI-COV demonstrated the identified natural frequencies of the system without the appearance of too many spurious modes. This is thanks to the implementation of the Toeplitz, which has a strong influence on the quality of the subsequent stabilization diagram. The damping ratios were extracted from this diagram at each mode and are presented in Figure 4.5 and in Table 4.2. One of the advantages of the SSI-COV method is that with it, the stabilization diagram can be constructed effectively without exhibiting too many spurious modes. It was noted that at some harmonic frequencies (e.g., 53.2 Hz, 106.4 Hz, and 212.8 Hz), the damping ratios were very low.

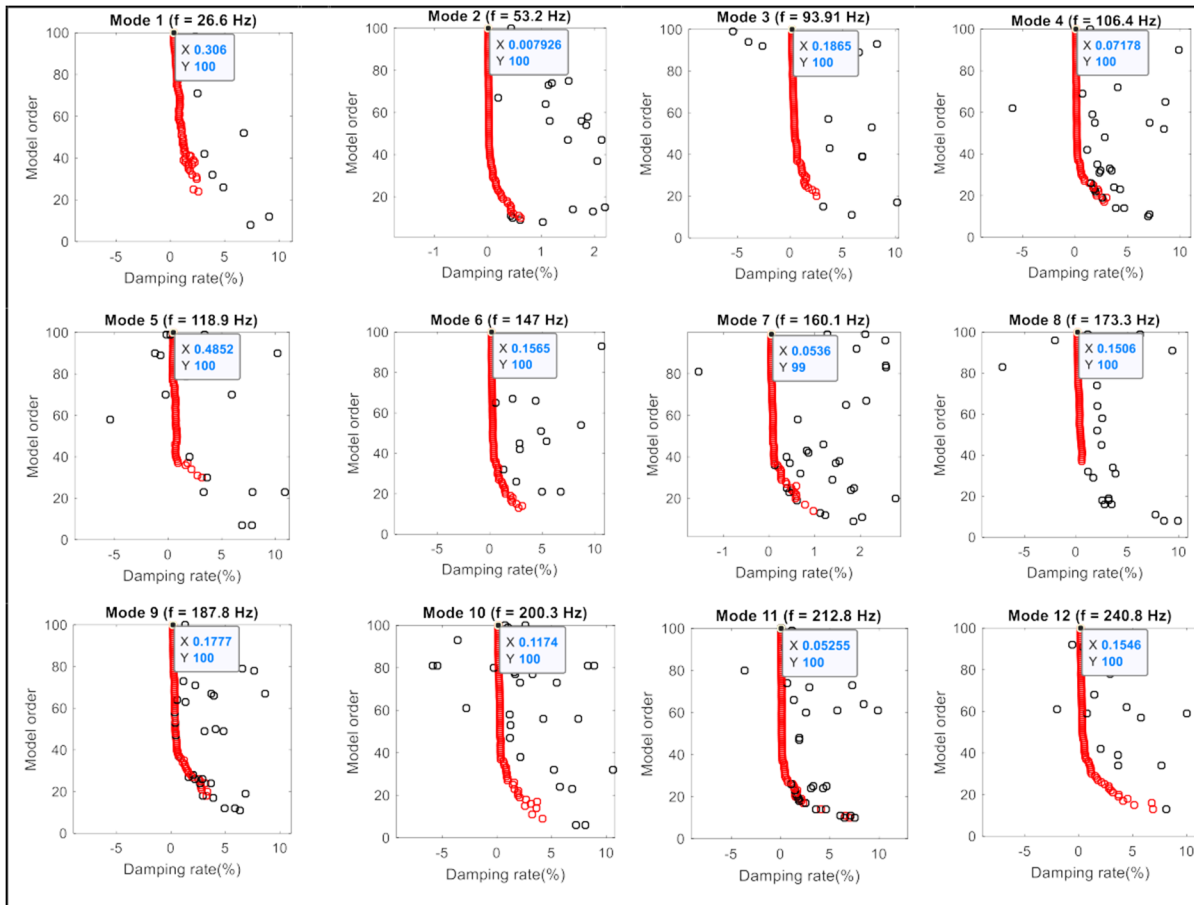


Figure 4.5 Damping ratio estimation by SSI-COV method

Table 4.2 Estimated damping ratio

Modes	Frequency (Hz)	Damping ratio (%)	Modes	Frequency (Hz)	Damping ratio (%)
1	26.66	0.3060	7	160.1	0.0536
2	53.20	0.0079	8	173.3	0.1506
3	93.91	0.1865	9	187.8	0.1777
4	106.4	0.0717	10	200.3	0.1174
5	118.9	0.4852	11	212.8	0.0525
6	147.0	0.1565	12	240.8	0.1546

4.7.2 Contact force parameters estimation

The measured vibration data obtained from the experiments were analyzed at each power to identify the contact force parameters with the goal of demonstrating the feasibility of the proposed method in a real grinding operation scenario. Comparison results between two methods, namely, Recursive Least Squares (RLS) and Unscented Kalman Filter (UKF), under various grinding contact environments are shown in Figure 4.6.

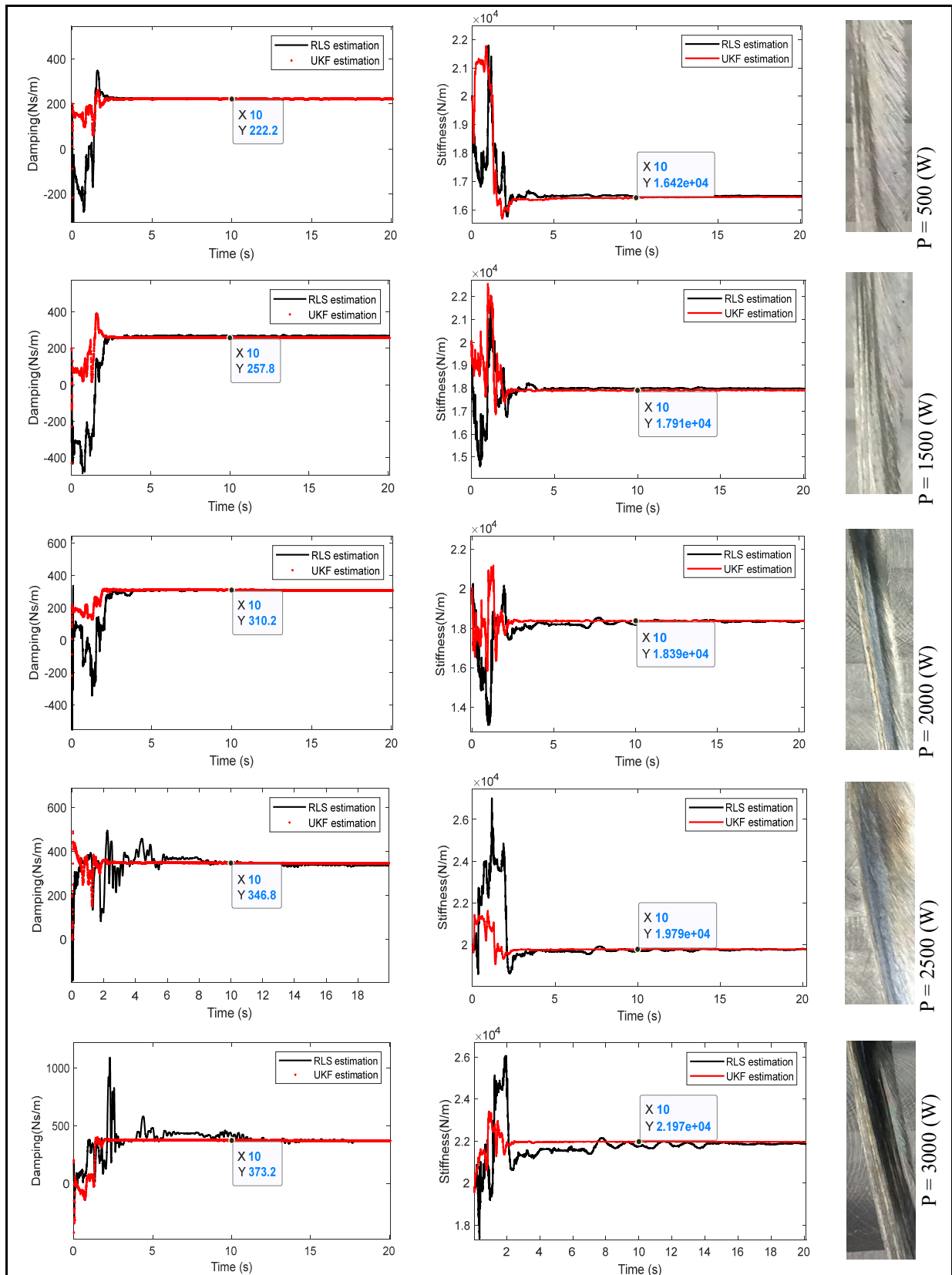


Figure 4.6 Comparison of estimated contact damping (left) and contact stiffness (right) at different grinding powers

Table 4.3 presents the estimated contact damping and contact stiffness directly obtained from the SCOMPI grinding experiment under different grinding powers 500 (W), 1500 (W), 2000 (W), 2500 (W) and 3000 (W).

Table 4.3 Estimated contact damping and stiffness result

Power (W)	Estimated damping (N.s/m)		Estimated Stiffness (N/m)	
	RLS	UKF	RLS	UKF
500	224.3	222.2	1.65×10^4	1.64×10^4
1500	268.5	257.8	1.79×10^4	1.79×10^4
2000	311.3	310.2	1.80×10^4	1.83×10^4
2500	353.5	346.8	1.99×10^4	1.97×10^4
3000	445.2	373.2	2.16×10^4	2.19×10^4

It was observed that the damping and stiffness estimates increased with the power levels. The vibration and instability phenomena were much more obvious for the RLS method, which proved the robustness and stability advantage provided by the UKF under a wider range of initial conditions. It would have been expected to have a lower estimation error than the RLS method. We noticed that the settling time for damping estimation was a little longer than for the stiffness estimation. It was shown that the higher the power generated, the higher the contact force was found, which may cause damage, such as burning to the surface. It is recommended that the grinding power for robot operation be chosen in the range of under 2000 (W). Furthermore, each grinding path had a line shape that makes the single contact point assumption reasonable. The contact force is composed of wheel contact stiffness and damping, which affect the grinding performance indicators such as workpiece quality and grinding accuracy.

4.8 Conclusion

In this paper, we examined the application of a modified and improved version of the Kalman filter to identify the contact damping and stiffness parameters at the contact point when the robot interacts with its environment. The work was carried out in two parts. A modal analysis

identification was first applied by using an automated SSI-COV procedure. The SSI-COV was found to be effective in modal identification by producing stable modes. Damping ratios were accurately estimated. In the second, we presented the results of an identification procedure developed for the estimation of the contact stiffness and damping for robots interacting with a stiff environment. The application of the Unscented Kalman filter (UKF) based on the Hunt Crossley nonlinear single point contact model was introduced to characterize contact parameters between the grinding wheel and its environment. Experimental results, as well as a comparison analysis, demonstrated the ability of the proposed methodology to effectively identify contact force parameters, leading to dramatically improved accuracy as compared to traditional Recursive Least Squares estimation. Online stiffness and damping estimation can be used to improve force tracking in explicit force control schemes. Future efforts in this area will address the estimation of all contact parameters, including the friction of complex contact geometries.

4.9 Acknowledgements

The support of NSERC (Natural Sciences and Engineering Research Council of Canada) through Discovery Research RGPIN-2016-05859, RGPIN-2014-05853 grants, and the Vietnam International Education Development (VIED) – Ministry of Education and Training of Vietnam is gratefully acknowledged. The authors would like to thank Hydro-Québec's Research Institute for its substantial collaboration.

4.10 References

- Choi, B. O., & Krishnamurthy, K. (1994). Unconstrained and constrained motion control of a planar two-link structurally flexible robotic manipulator. *Journal of Robotic Systems*, *11*(6), 557-571. doi:<https://doi.org/10.1002/rob.4620110609>
- Chua, A., & Katupitiya, J. (1998, 18-18 Dec. 1998). *Kalman filters for the identification of uncertainties in robotic contact*. Paper presented at the Proceedings of the 37th IEEE Conference on Decision and Control (Cat. No.98CH36171).

- Deistler, M. (1994). System Identification. Söderström and P. Stoica Prentice Hall International, 1989. *Econometric Theory*, 10(3-4), 813-815. doi:10.1017/S026646660000880X
- Di Renzo, A., & Di Maio, F. P. (2004). Comparison of contact-force models for the simulation of collisions in DEM-based granular flow codes. *Chemical Engineering Science*, 59(3), 525-541. doi:<https://doi.org/10.1016/j.ces.2003.09.037>
- Diolaiti, N., Melchiorri, C., & Stramigioli, S. (2005). Contact impedance estimation for robotic systems. *IEEE Transactions on Robotics*, 21(5), 925-935. doi:10.1109/TRO.2005.852261
- Flores, P., & Ambrósio, J. (2010). On the contact detection for contact-impact analysis in multibody systems. *Multibody System Dynamics*, 24(1), 103-122. doi:10.1007/s11044-010-9209-8
- Gilardi, G., & Sharf, I. (2002). Literature survey of contact dynamics modelling. *Mechanism and Machine Theory*, 37(10), 1213-1239. doi:[https://doi.org/10.1016/S0094-114X\(02\)00045-9](https://doi.org/10.1016/S0094-114X(02)00045-9)
- Grabbe, M. T., Carroll, J. J., Dawson, D. M., & Qu, Z. (1992, 12-14 May 1992). *Robust control of robot manipulators during constrained and unconstrained motion*. Paper presented at the Proceedings 1992 IEEE International Conference on Robotics and Automation.
- Haddadi, A., & Hashttrudi-Zaad, K. (2008a, 22-26 Sept. 2008). *A New Method for Online Parameter Estimation of Hunt-Crossley Environment Dynamic Models*. Paper presented at the 2008 IEEE/RSJ International Conference on Intelligent Robots and Systems.
- Haddadi, A., & Hashttrudi-Zaad, K. (2008b, 22-26 Sept. 2008). *Online Contact Impedance Identification for Robotic Systems*. Paper presented at the 2008 IEEE/RSJ International Conference on Intelligent Robots and Systems.
- Hazel, B., Côté, J., Laroche, Y., & Mongenot, P. (2012a). Field repair and construction of large hydropower equipment with a portable robot. *Journal of Field Robotics*, 29(1), 102-122. doi:<https://doi.org/10.1002/rob.20427>

- Hazel, B., Côté, J., Laroche, Y., & Mongenot, P. (2012b). A portable, multiprocess, track-based robot for in situ work on hydropower equipment. *Journal of Field Robotics*, 29(1), 69-101. doi:<https://doi.org/10.1002/rob.20425>
- Hogan, N. (1984, 6-8 June 1984). *Impedance Control: An Approach to Manipulation*. Paper presented at the 1984 American Control Conference.
- Hun, L., Ong, L., Lim, T. S., & Koo, V. (2016). Kalman Filtering and Its Real-Time Applications. In.
- Hunt, K. H., & Crossley, F. R. E. (1975). Coefficient of Restitution Interpreted as Damping in Vibroimpact. *Journal of Applied Mechanics*, 42(2), 440-445. doi:10.1115/1.3423596
- Julier, S. J., & Uhlmann, J. K. (2004). Unscented filtering and nonlinear estimation. *Proceedings of the IEEE*, 92(3), 401-422. doi:10.1109/JPROC.2003.823141
- Lankarani, H., & Nikravesh, P. (1990). A Contact Force Model With Hysteresis Damping for Impact Analysis of Multibody Systems. *J. of Mechanical Design*, 112, 369-376. doi:10.1115/1.2912617
- Lewandowski, R., & Chorążyczewski, B. (2010). Identification of the parameters of the Kelvin–Voigt and the Maxwell fractional models, used to modeling of viscoelastic dampers. *Computers & Structures*, 88(1), 1-17. doi:<https://doi.org/10.1016/j.compstruc.2009.09.001>
- Love, L. J., & Book, W. J. (1995, 21-27 May 1995). *Environment estimation for enhanced impedance control*. Paper presented at the Proceedings of 1995 IEEE International Conference on Robotics and Automation.
- Machado, M., Moreira, P., Flores, P., & Lankarani, H. M. (2012). Compliant contact force models in multibody dynamics: Evolution of the Hertz contact theory. *Mechanism and Machine Theory*, 53, 99-121. doi:<https://doi.org/10.1016/j.mechmachtheory.2012.02.010>
- Magalhães, F., Cunha, Á., & Caetano, E. (2009). Online automatic identification of the modal parameters of a long span arch bridge. *Mechanical Systems and Signal Processing*, 23(2), 316-329. doi:<https://doi.org/10.1016/j.ymsp.2008.05.003>
- Marhefka, D. W., & Orin, D. E. (1999). A compliant contact model with nonlinear damping for simulation of robotic systems. *IEEE Transactions on Systems, Man, and Cybernetics - Part A: Systems and Humans*, 29(6), 566-572. doi:10.1109/3468.798060

- McClamroch, N. H. (1989, 13-15 Dec. 1989). *A singular perturbation approach to modeling and control of manipulators constrained by a stiff environment*. Paper presented at the Proceedings of the 28th IEEE Conference on Decision and Control.
- Mills, J. K., & Nguyen, C. V. (1992). Robotic Manipulator Collisions: Modeling and Simulation. *Journal of Dynamic Systems, Measurement, and Control*, 114(4), 650-659. doi:10.1115/1.2897737
- Muthukumar, S., & DesRoches, R. (2006). A Hertz contact model with non-linear damping for pounding simulation. *Earthquake Engineering & Structural Dynamics*, 35(7), 811-828. doi:<https://doi.org/10.1002/eqe.557>
- Nguyen, Q.-C., Vu, V.-H., & Thomas, M. (2022). A Kalman filter based ARX time series modeling for force identification on flexible manipulators. *Mechanical Systems and Signal Processing*, 169, 108743. doi:<https://doi.org/10.1016/j.ymssp.2021.108743>
- Peeters, B., & De Roeck, G. (1999). Referenc-based Stochastic Subspace Identification for Output-only Modal Analysis. *Mechanical Systems and Signal Processing*, 13(6), 855-878. doi:<https://doi.org/10.1006/mssp.1999.1249>
- Peeters, B., & De Roeck, G. (2001). Stochastic System Identification for Operational Modal Analysis: A Review. *Journal of Dynamic Systems, Measurement, and Control*, 123(4), 659-667. doi:10.1115/1.1410370
- Sakamoto, N., Higashimori, M., Tsuji, T., & Kaneko, M. (2007, 10-14 April 2007). *An Optimum Design of Robotic Hand for Handling a Visco-elastic Object Based on Maxwell Model*. Paper presented at the Proceedings 2007 IEEE International Conference on Robotics and Automation.
- Sánchez, L. A., Le, M. Q., Liu, C., Zemiti, N., & Poignet, P. (2012, 14-18 May 2012). *The impact of interaction model on stability and transparency in bilateral teleoperation for medical applications*. Paper presented at the 2012 IEEE International Conference on Robotics and Automation.
- Seraji, H., & Colbaugh, R. (1993, 2-6 May 1993). *Force tracking in impedance control*. Paper presented at the [1993] Proceedings IEEE International Conference on Robotics and Automation.

- Skrinjar, L., Slavič, J., & Boltežar, M. (2018). A review of continuous contact-force models in multibody dynamics. *International Journal of Mechanical Sciences*, 145, 171-187. doi:<https://doi.org/10.1016/j.ijmecsci.2018.07.010>
- Stramigioli, S. (2001). *Modeling and IPC Control of Interactive Mechanical Systems - A Coordinate-Free Approach*.
- Tian, Q., Flores, P., & Lankarani, H. M. (2018). A comprehensive survey of the analytical, numerical and experimental methodologies for dynamics of multibody mechanical systems with clearance or imperfect joints. *Mechanism and Machine Theory*, 122, 1-57. doi:<https://doi.org/10.1016/j.mechmachtheory.2017.12.002>
- Vu, V.-H., Liu, Z., Thomas, M., Li, W., & Hazel, B. (2016). Output-only identification of modal shape coupling in a flexible robot by vector autoregressive modeling. *Mechanism and Machine Theory*, 97, 141-154. doi:<https://doi.org/10.1016/j.mechmachtheory.2015.11.005>
- Vukobratović, M. K., & Potkonjak, V. (1999). Dynamics of contact tasks in robotics. Part I: general model of robot interacting with environment. *Mechanism and Machine Theory*, 34(6), 923-942. doi:[https://doi.org/10.1016/S0094-114X\(97\)00091-8](https://doi.org/10.1016/S0094-114X(97)00091-8)
- Zhang, D., & Wei, B. (2017). A review on model reference adaptive control of robotic manipulators. *Annual Reviews in Control*, 43, 188-198. doi:<https://doi.org/10.1016/j.arcontrol.2017.02.002>
- Zhu, X., Gao, B., Zhong, Y., Gu, C., & Choi, K.-S. (2021). Extended Kalman filter for online soft tissue characterization based on Hunt-Crossley contact model. *Journal of the Mechanical Behavior of Biomedical Materials*, 123, 104667. doi:<https://doi.org/10.1016/j.jmbbm.2021.104667>

SYNTHESIS

Successful use of robots for machining in industrial applications requires careful design and analysis of the robotic system with attention given to the static and dynamic compliance of the robot in the presence of time-varying machining process induced forces. Forces generated during the grinding can cause elastic deformations of the robot, the grinding wheel and to workpiece. Any irregularities in the process can cause variations in the grinding forces that can dynamically excite the structure. Another limitation in robotic machining is structural vibration, which can result in poor surface quality of the part, reduction in wheel life, and limited production rates. Tool deflection during robotic grinding operation cause geometrical errors in the workpiece cross-section. Also, it makes difficult to control the grinding cutting depth.

The major objective of this thesis is to resolve the force estimation problem and identified operational modal parameters with an emphasis on damping estimation. Different chapters of this thesis have studied each task and provides solutions to them. Combining the achievements and results of all chapters in this thesis will profound our perception of vibratory dynamics that govern the robotic grinding process. This thesis is not only aim at adding a new method for contact force and its parameters identification, but also providing a deeper understanding of the dynamics of flexible structures working in industrial ambient vibration.

Chapter 2 presents an inversed method for computing the operational excitation force in multiple directions. The method is developed by using a Kalman filter based on a time series Auto Regressive eXogenous (ARX) modeling to deal with inverse problem, where ARX model is modified by employing ambient vibration data only. The validation on numerical simulation as well as experiments have proved the proposed method is successfully estimated unknown contact force and modal parameters of structure under noisy environment by virtue of Kalman Filter.

Force interaction between the tool and workpiece is significant for grinding operation. Estimating contact force parameters is helpful for controlling end point position and improving

surface quality. Consequently, an experimental approach for estimating the unknown parameters of the constraint environment characterized by environmental stiffness and damping parameters by means of Unscented Kalman Filter (UKF) in conjunction with the nonlinear Hunt-Crossley contact model by using output measurement only is presented in Chapter 4. Experimental results as well as comparison analysis demonstrate that the proposed methodology can effectively characterize contact force parameters, leading to dramatically improved accuracy comparing to traditional Recursive Least Square estimation. Online stiffness and damping estimation can be used to improve force tracking in explicit force control schemes.

In order to apply Operational Modal Analysis effectively and avoid over fitting problem. A new algorithm was proposed in chapter 3 for determining optimal order of model, which enables the model to extract uncorrelated residuals and better identify the dynamical behavior of the system by using both observation input and output data. The concept is based on minimum means square error of the estimated transfer functions, which can effectively cope with measurement noise and modeling error to identify the appropriate low-order transfer functions of the structure via an Auto Regressive Moving Average eXogenous (ARMAX) model. The comparison results show that the approach is successful and superior to a state-of-the-art order determination technique in obtaining a sufficient order and can accurately capture all the dominant oscillation modes with fewer discrepancies. The research provides a useful tool for capturing the transfer functions of difficult-to-measure structures such as rotating grinding systems.

In summary, different chapters of this thesis addressed some key problems of SCOMPI robot under machining operation. Both main objectives of this thesis which included contact force estimation and operational modal parameters identification have been achieved through various proposed approaches with intermediate validation in both experimental data and numerical simulation.

CONCLUSION

This thesis presents a study on the dynamic and vibration control of a flexible manipulator robot. It was combined experimental and numerical investigation to improve fundamental knowledge, which is useful in modeling flexible robotic grinding. The operational modal analysis based on time series models was proposed by using comprehensive measurement data, providing a better understanding of the dynamical behavior of robotics in operation and the consequences of the process involved. Furthermore, contact force and its parameters are successfully estimated with great accuracy, which can be used to improve process efficiency or perform a sensitivity analysis of the process. The main characteristic of the contact force simulations, and the resulting impact cutting regime were addressed. The results of this thesis together with the practical improvements are significant for minimizing vibration and enhancing its grinding performance. The major findings and contributions of this research pertain to the robotic grinding process performed by a light, flexible robot is summarized below.

Accurate force prediction is important for automatic robotic grinding operations since it can help to perform the operation with a constant force and prevent geometrical errors. In this thesis, we present a novel technique by using Kalman Filter based on a time series Auto Regressive with eXogenous excitation (ARX) modeling for input force estimation, where the ARX model was modified by employing ambient vibration data only. Both numerical simulation and experimental tests on SCOMPI were applied for validation. This method is not only enabled handling noisy measurement data in satisfactory identifying the modal parameters, but it also can estimate unknown input forces accurately.

A new algorithm for modal order determination was proposed for identifying the dynamical behavior of the flexible robot by using input-output data. The concept is based on the minimum means squares error of the estimated transfer functions, which can effectively tackle measurement noise and modeling errors to identify appropriate low-order transfer functions of the structures via an Auto-Regressive Moving Average eXogenous (ARMAX) model. The

effectiveness of the proposed method is validated exclusively using experimental data obtained from a grinding test of an industrial manipulator SCOMPI robot through different criteria such as the Akaike Information Criterion (AIC), the Bayesian Information Criterion (BIC), and the Noise Order Factor (NOF). Thanks to its flexibility in handling model disturbance, the proposed optimization strategy can capture all the dominant oscillation modes of the structure at the low orders, and system modal properties are efficiently and automatically determined. The low-order transfer functions estimated by the present technique were scientifically closer to the measured values.

Finally, a nonlinear method was introduced for contact force characterization, which included contact damping and stiffness by using the Unscented Kalman Filter based on the nonlinear Hunt-Crossley contact model. Experimental results, as well as comparison analysis, demonstrate that the proposed methodology can effectively identify contact force parameters, leading to dramatically improved accuracy compared to traditional Recursive Least Square estimation. Additionally, modal parameters of the robot under grinding operation are accurately estimated, especially damping ratios by using the automated SSI-COV algorithm.

RECOMMENDATIONS

The research work presented in this thesis might be continued through the recommendations listed in the following.

Although the Kalman filter based ARX model method is very promising in unknown force prediction, this model was assumed to work on a linear system only. Instead of keeping the robot configuration unchanged in order to minimize the nonlinearities of the system, the method can be further extended to a nonlinear case where the robot can freely move and change its configuration to perform grinding tasks. Since it is nonlinear, some variants of the Kalman filter such as Extended Kalman Filter or Unscented Kalman Filter can be applied to capture the whole picture of the dynamical behavior of SCOMPI robots under different perspectives. A comprehensive experimental investigation may be needed to completely understand its dynamical behavior under changing configurations, any effort deployed to better understand dynamical behavior will be beneficial.

The stability and the performances of the interaction controllers, such as the impedance controller or intrinsically passive controllers are directly affected by the mechanical properties of the interactive environment. By identifying the parameters of contact models online, robots are able to improve the accuracy and robustness of the low-level control, as well as the task execution. Since the contact forces and their parameters are successfully estimated, we can go a further step in designing the controller of the robot with respect to these parameters. Based on models of the interaction of robots with their environment, the control strategy and parameters of interaction tasks can be validated. In addition, the contact force model can be extended to the case of complex contact geometries in order to address the estimation of all contact parameters including the friction at the contact points.

Another attractive approach to stability analysis in grinding is constructing the stability lobe diagram (SLD) which is the function of tool point frequency response function (FRFs) to predict the chatter-free machining parameters. This diagram shows the boundary between chatter-free machining operations and unstable processes, in terms of the axial depth of cut as

a function of the rotating speed of the grinder. These diagrams are used to select chatter-free combinations of machining parameters. Since the results of the second journal has already give the identification of the operational transfer functions of the robot at the optimized model order, the SLD diagram can be built and used to predict chatter stability by choosing appropriate chatter-free machining boundary.

Finally, environmental effects such as temperature should be taken into account since this factor can greatly contribute to changes in the dynamic response of structures, and thus “true” contact parameters can be mistaken. Studies on temperature effect elimination are also recommended for future work.

APPENDIX I

ARX MODEL FOR EXPERIMENTAL VIBRATION ANALYSIS OF FLEXIBLE MANIPULATOR DURING GRINDING

Quoc Cuong Nguyen^a, Viet Hung Vu^b and Marc Thomas^c,

^{a,b,c} Department of Mechanical Engineering, École de Technologie Supérieure,
1100 Notre-Dame West, Montreal, Quebec, H3C 1K3

Paper published in *the Surveillance, Vishno and AVE conferences, INSA-Lyon, Université de Lyon*, July 2019

AI-1 Résumé

L'utilisation d'un manipulateur flexible pour les processus de broyage in situ est devenue un service d'ingénierie rentable ces dernières années, en particulier pour la réparation et la remise à neuf de systèmes et de composants mécaniques. En comparaison avec les robots manipulateurs rigides traditionnels, le manipulateur flexible a prouvé son efficacité en termes de précision et de facilité. Cependant, en raison de sa structure compacte et flexible, des inquiétudes se posent quant à son comportement dynamique pendant le processus de broyage. Cet article propose une méthode utilisant un modèle ARX (autorégressif avec excitation exogène) pour analyser expérimentalement les vibrations d'un robot flexible lors d'une opération de meulage dans différents cas Single Input–Single Output (SISO) et Multi-Input–Multi-Output (MIMO). Simultanément, un dynamomètre permet la mesure de la force d'entrée triaxiale tandis que trois accéléromètres montés sur l'effecteur terminal enregistrent les sorties de vibration. Grâce à l'analyse modale opérationnelle (OMA), les propriétés dynamiques du robot peuvent être identifiées directement en fonctionnement. Les résultats ont montré que le modèle ARX est efficace pour analyser la vibration opérationnelle dans des systèmes complexes avec plusieurs degrés de liberté et plusieurs directions. La détermination des paramètres modaux et des fonctions de réponse en fréquence (FRF) identifiées permet de prédire le comportement dynamique du système et de simuler les vibrations dans des

conditions de travail réelles. D'autres études sur le problème inverse sont prometteuses pour estimer les forces d'excitation alors que celles-ci ne sont pas disponibles et ne sont pas mesurées en pratique dans les applications industrielles.

Mots-clés : Analyse modale opérationnelle, manipulateur flexible, procédé de broyage, modèle ARX, fonctions de transfert, identification de force.

AI-2 Abstract

Using a flexible manipulator for the grinding processes in situ has become a cost-effective engineering service in recent years, especially for the repair and refurbishment of mechanical systems and components. In comparison with traditional rigid robot manipulators, the flexible manipulator has proved its efficiency in terms of accuracy and facility. However, because of its compact and flexible structure, concerns arise regarding its dynamic behavior during the grinding process. This paper proposes a method using an ARX (autoregressive with exogenous excitation) model for experimentally analyzing the vibrations of a flexible robot during grinding operation in different cases Single Input–Single Output (SISO) and Multi-Input–Multi-Output (MIMO). Simultaneously, a dynamometer allows for triaxial input force measurement while three accelerometers mounted at the end effector record the vibration outputs. Due to the Operational Modal Analysis (OMA), the dynamical properties of the robot can be identified directly in operation. The results have shown that the ARX model is efficient for analyzing the operational vibration in complex systems with multi degrees of freedom and multi directions. The determination of modal parameters and identified Frequency Response Functions (FRFs) enable the prediction of the dynamic behavior of the system and simulate the vibration in real working conditions. Further studies on the inverse problem are promising for estimating the excitation forces while these later are not available and not practically measured in industrial applications.

Keywords: Operational modal analysis, flexible manipulator, grinding process, ARX model, transfer functions, force identification.

AI-3 Introduction

Nowadays robots sufficiently conduct manifold manipulation works with a high degree of autonomy and rigorousness. Portable manipulator systems are regarded as an effective and profitable solution for the automation maintenance tasks on large hydroelectric equipment. The SCOMPI (Super COMPact robot Ireq) was developed at IREQ (Hydro Quebec's research institute) and is particularly designed with flexible links and flexible joints for working in hard-to-reach areas or confined spaces of hydraulic turbines in a hostile environment (Hazel, Côté, Laroche, & Mongenot, 2012). Because of its flexible structure, vibration problems of Scompi become crucial since producing chatter and a bad surface finish. A numerical simulation (Santos, Liu, & Hazel, 2015) has been constructed in MSC/Adams in different configurations including impact force, sinusoidal and operational forces. There is a great number of researches that focus on identifying the modal parameters of the system in order to understand the dynamical behavior of the robot (Li, Vu, Liu, Thomas, & Hazel, 2017b; Mokdad *et al.*, 2011; Rafieian, Liu, & Hazel, 2009; V.-H. Vu, Liu, Thomas, & Hazel, 2015; V.-H. Vu, Liu, Thomas, Li, & Hazel, 2016), and estimate the operational forces from the actual accelerations measured on the robot (V. H. Vu, Liu, Thomas, Tahvilian, & Hazel, 2015). Knowing a system's frequency response function is key to many system analysis and control synthesis methods (V. H. Vu, Zhaoheng, Thomas, Tahvilian, & Hazel, 2016). The main problem comes from that these modal parameters are changing with the robot motion and position and thus a time-varying method is proposed for studying this kind of non-stationary structure (Li, Vu, Liu, Thomas, & Hazel, 2015, 2017a). Researchers are particularly interested in the identification of continuous-time systems by using discrete data (Soderstrom, Fan, Carlsson, & Bigi, 1997).

This paper presents a technique to identify the modal parameters as well as the transfer function of Scompi robot by applying the Autoregressive with eXogenous input (ARX) model (Chiuso, 2007; da Silva, Dias Junior, & Lopes Junior, 2007; Soderstrom *et al.*, 1997). This method reveals a convenient and advantageous for Operational Modal Analysis of structures (OMA), which allows for determining the operational modal model excited by ambient noise and vibration. The modal parameters are estimated and identified by applying straightforward

methods such as Ordinary Least Squares (OLS) (Lennart, 1999; Soderstrom et al., 1997). The results are validated by another approach based on the updated Auto-Regressive (AR) model in (V.-H. Vu *et al.*, 2016) and show a great accuracy of identified modal parameters. This study enables us to predict the dynamical behavior of SCOMPI for identifying excitation forces during operations of grinding and consequently improving the quality of the surface finish.

AI-4 Auto Regressive Exogenous excitation model (ARX)

The ARX model (Chiuso, 2007; da Silva *et al.*, 2007; Lennart, 1999; Soderstrom *et al.*, 1997) is a primary choice because of its simplicity. It has been applied to numerous practical applications, especially in control systems. However, the critical motivation for choosing the ARX model is its correlation to the state-space model (Jer-Nan, 1997; Raath & Waveren, 1998; Strejc & Dolezal, 1982; Wang, Wan, & Zheng, 2017) which can be implemented for inverse problems with the aim of reconstructing the excitation forces acting on vibrating structures (V. H. Vu *et al.*, 2015), which is impossible to obtain from direct measurement in the real systems. The ARX model is a convenient model to obtain the general relation between input and output signals for different cases, such as Single Input – Single Output (SISO) or Multiple Input – Multiple Output (MIMO), which can reliably represent the dynamic properties of the system. Figure A I-1 illustrates the block diagram of the ARX model.

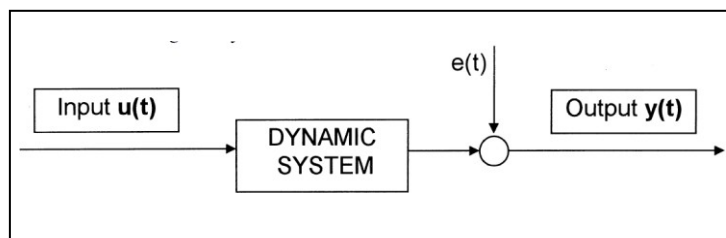


Figure A I-1 Block diagram of ARX model

This model has a simple structure and strong robustness. It is very efficient when the noise is low. However, when the noise is large, the order of the model must increase to compensate for the impact of system identification precision from noise (Wang *et al.*, 2017).

Examine a c dimensional vector input $\mathbf{u}(t)$ and a d dimensional vector output $\mathbf{y}(t)$ of a Multiple Input and Multiple Output (MIMO) system.

The ARX model can be described as a linear difference equation:

$$\mathbf{y}(t) + \mathbf{A}_1 \mathbf{y}(t-1) + \dots + \mathbf{A}_{n_a} \mathbf{y}(t-n_a) = \mathbf{B}_0 \mathbf{u}(t) + \mathbf{B}_1 \mathbf{u}(t-1) + \dots + \mathbf{B}_{n_b} \mathbf{u}(t-n_b) + \mathbf{e}(t) \quad (\text{A I.1})$$

where:

\mathbf{A}_i – are $d \times d$ matrices and

\mathbf{B}_i – are $d \times c$ matrices.

The general ARX model can be rewritten in the polynomial form:

$$\mathbf{A}(q) \mathbf{y}(t) = \mathbf{B}(q) \mathbf{u}(t) + \mathbf{e}(t) \quad (\text{A I.2})$$

where:

$$\mathbf{A}(q) = \mathbf{I} + \mathbf{A}_1 q^{-1} + \mathbf{A}_2 q^{-2} + \dots + \mathbf{A}_{n_a} q^{-n_a} \quad (\text{A I.3})$$

$$\mathbf{B}(q) = \mathbf{B}_0 + \mathbf{B}_1 q^{-1} + \mathbf{B}_2 q^{-2} + \dots + \mathbf{B}_{n_b} q^{-n_b} \quad (\text{A I.4})$$

Model (A I.2) is an ARX model where AR refers to the Autoregressive part $\mathbf{A}(q)\mathbf{y}(t)$ and X refers to the extra input $\mathbf{B}(q)\mathbf{u}(t)$ called the exogenous input. $\mathbf{y}(t)$ is considered as the output of the model while $\mathbf{u}(t)$ is the input to the model and $\mathbf{e}(t)$ is the innovation term at the time t . $\mathbf{A}(q)$ and $\mathbf{B}(q)$ are polynomials in the delay operator $q-1$ and n_a, n_b are the model order of $\mathbf{A}(q)$ and $\mathbf{B}(q)$ respectively. $\mathbf{A}(q)$ is a matrix whose elements are polynomials in $q-1$. This results in Matrix Fraction Description (MFD).

Defining the parameter matrix:

$$\boldsymbol{\theta} = [\mathbf{A}_1 \ \mathbf{A}_2 \ \dots \ \mathbf{A}_{n_a} \ \mathbf{B}_0 \ \mathbf{B}_1 \ \dots \ \mathbf{B}_{n_b}]^T \quad (\text{A I.5})$$

We may rewrite (A I.2) as a linear regression:

$$\mathbf{y}(t) = \boldsymbol{\theta}^T \boldsymbol{\phi}(t) + \mathbf{e}(t) \quad (\text{A I.6})$$

If we consider N consecutive values of the responses from $\mathbf{y}(k)$ to $\mathbf{y}(k+N-1)$, the model parameters can be obviously estimated by least square method (Lennart, 1999) by minimizing the norm of $\mathbf{e}(t)$:

$$\Phi = \arg \min \left(\frac{1}{N} \sum_{t=k}^{k+N-1} \|\mathbf{e}(t)\|^2 \right) = \arg \min \left(\frac{1}{N} \sum_{t=k}^{k+N-1} \|\mathbf{y}(t) - \mathbf{\Theta}^T \phi(t)\|^2 \right) \quad (\text{A I.7})$$

After obtaining the measured force and acceleration signals on all channels, the model ARX can be used to fit the data. The ARX model creates a regressive connection between the input vector $\mathbf{u}(t)$ and the output vector $\mathbf{y}(t)$ through a residual vector $\mathbf{e}(t)$. By applying the least square method, the modal parameters matrices \mathbf{A} and \mathbf{B} can be estimated. In vibration measurement application, it can be seen that force (input) and acceleration (output) are normally synchronized, thus the two parts may be modeled with the same order $n_a = n_b$.

Once the model parameters of the system are identified, the state matrix can be determined as in the form of autoregressive parameters:

$$\mathbf{A}|_{(n_a \times n_b)} = \begin{bmatrix} -\mathbf{A}_1 & -\mathbf{A}_2 & -\mathbf{A}_3 & \dots & -\mathbf{A}_p \\ I & 0 & 0 & \dots & 0 \\ 0 & I & 0 & \dots & 0 \\ \dots & \dots & \dots & \dots & \dots \\ 0 & 0 & 0 & I & 0 \end{bmatrix} \quad (\text{A I.8})$$

There is a remarkable coincidence that the poles of the model are also the roots of the characteristic polynomial of the state matrix. Consequently, the continuous eigenvalues, system natural frequencies, and damping rates of the structure can be calculated for each pole by using the subsequent standard equations:

$$\text{Eigenvalues:} \quad [V, \lambda] = \text{eig}(\mathbf{A}) \quad (\text{A I.9})$$

$$\text{Frequencies:} \quad f_i = \frac{\sqrt{\text{Re}^2(\lambda_i) + \text{Im}^2(\lambda_i)}}{2\pi} \quad (\text{A I.10})$$

$$\text{Damping rates:} \quad \xi_i = -\frac{\text{Re}(\lambda_i)}{2\pi f_i} \quad (\text{A I.11})$$

When the modal parameters are estimated, we can construct the transfer function which is regarded as the frequency response function of the system. All the systems can be described by linear constant coefficients and represented by transfer functions that are “rational polynomial in q ”.

$$\mathbf{G}(q) = \frac{\mathbf{B}(q)}{\mathbf{A}(q)} = q^{-n_k} \frac{\mathbf{B}_1 q^{-1} + \mathbf{B}_2 q^{-2} + \dots + \mathbf{B}_{n_b} q^{-n_b}}{\mathbf{I} + \mathbf{A}_1 q^{-1} + \mathbf{A}_2 q^{-2} + \dots + \mathbf{A}_{n_a} q^{-n_a}} \quad (\text{A I.12})$$

with n_k is the transport delay.

AI-5 Application to a flexible manipulator during grinding process

AI-5.1 Brief introduction of the SCOMPI robot

The proposed approach is now implemented to the portable robot SCOMPI. Figure 2 presents the structure of SCOMPI, which is used for repair tasks in Hydro Québec power plants, particularly for grinding or welding jobs (Hazel *et al.*, 2012). Because of its compact and flexible structure, the question is raised up from its dynamical behavior under operating conditions. Hence, the flexibility of the joints and links needs to be taken into consideration, which might affect the stabilization of the robot at the end effector during the operational process (V.-H. Vu *et al.*, 2016). The aim of SCOMPI is to achieve both a high Material Removal Rate (MMR) and a polished surface finish with great precision. However, because of the portable and lightweight design, undesired chatter vibrations can appear during the machining process which produces an undesirable waviness surface. Therefore, the monitoring of its modal parameters as well as the transfer functions of the structure in the grinding operation is necessary for minimizing vibration at the end effector while controlling the chatter phenomenon and improving the quality of the grinding surface.

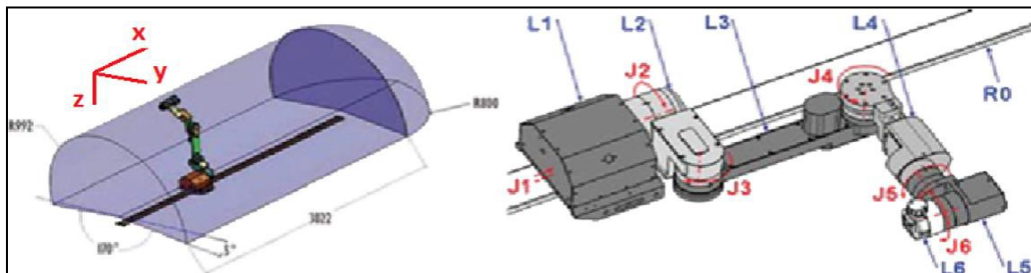


Figure A I-2 SCOMPI robot

AI-5.2 Presentation of the experimental setup

As can be seen from Figure A I-3, a SCOMPI robot is tested under a real grinding operation. Due to the interest in the typical dynamic behavior of the robot at the end effector, the SCOMPI is set to its home configuration. Three accelerometers are mounted at the end effector in triaxial directions X, Y, and Z. Meanwhile, a Kistler table dynamometer CH8408 is placed under the workpiece for measuring the forces. The power is set up at 1500 W and the grinding motor is rotated at a constant speed of 3225 (rpm) for conducting each single grinding pass within 12 seconds. A multi-component dynamometer is used for measuring the grinding forces in three directions at the tool piece contact point. After obtaining the measured signals from the dynamometer and accelerometers, we acquired them at the frequency rate of 512 (Hz) (Figure A I-4,5).

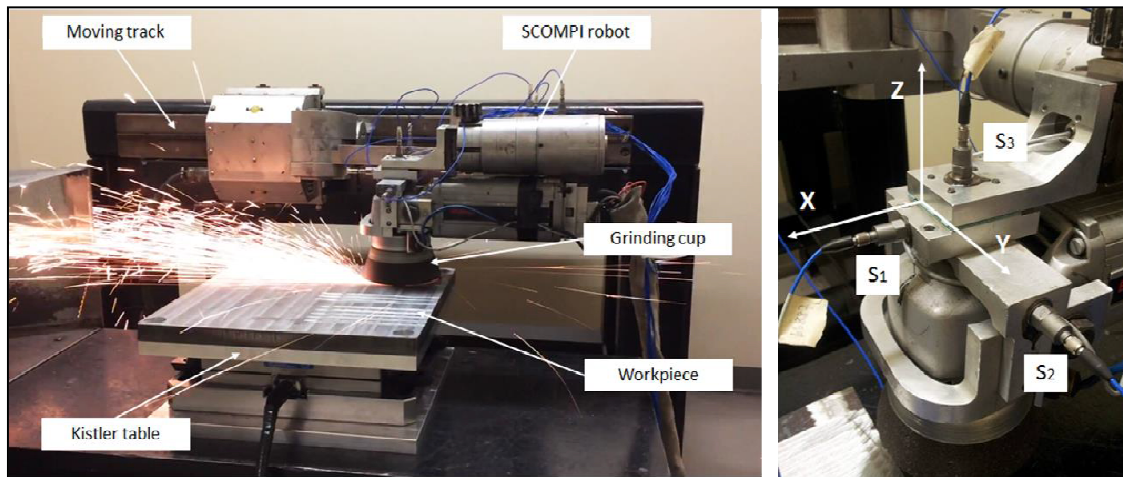


Figure A I-3 Overall configuration of the experimental setup

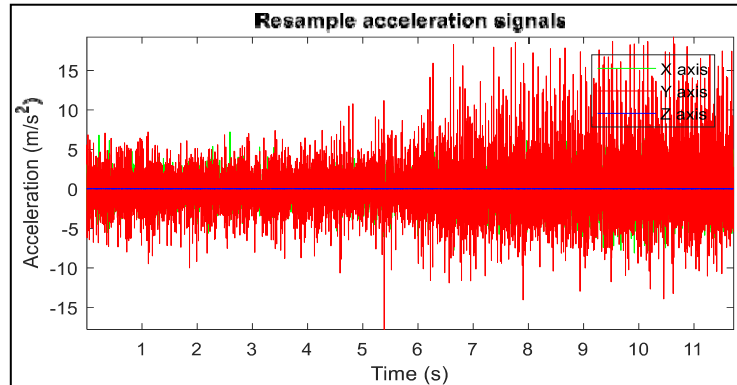


Figure A I-4 Measured acceleration signals during grinding process

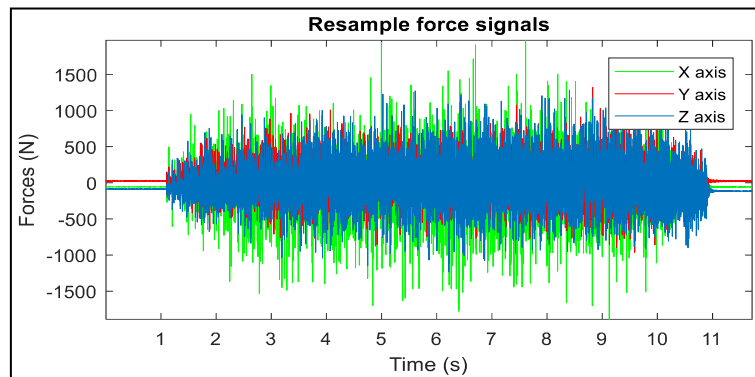


Figure A I-5 Measured force signals during grinding process

Taking three measured acceleration signals in X, Y, and Z directions, by applying Fast Fourier Transform (FFT) analysis, we can easily see the measured signals in both time and frequency domain as shown in Figure A I-6. As indicated, there are some significant frequencies in the frequency domain such as 53.9 (Hz) - the first harmonic; 93.7 (Hz); 106.2 (Hz) - the second harmonic; 146.8 (Hz) and 200.8 (Hz).

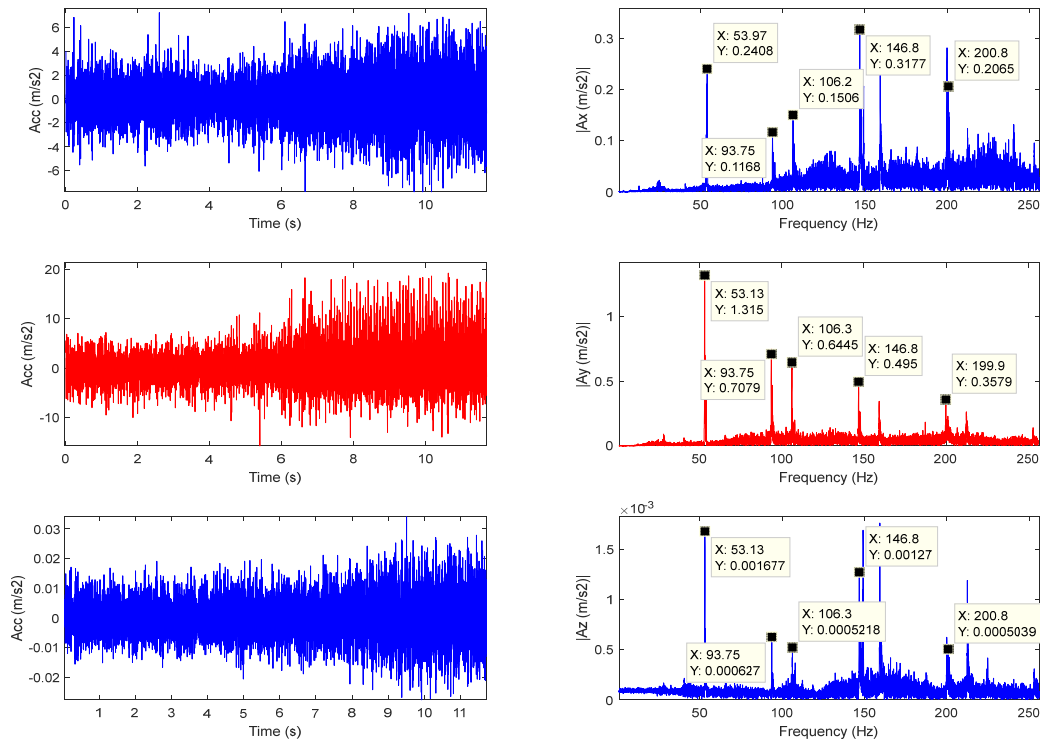


Figure A I-6 Time domain and frequency domain of the acceleration signals in three directions

AI-6 Results and discussion

Operating in tridimensional space, the ARX model is applied on Scmpi structure to fit the measured signals on each direction ($S_1 - F_x$); ($S_2 - F_y$); ($S_3 - F_z$) for constructing frequency stabilization in different cases Single Input – Single Output (SISO) and Multi-Input – Multi-Output (MIMO). Figures A I-7–10 demonstrated the frequency stabilization diagrams up to 250 (Hz) with a model order up to 100 where all the interesting frequencies may be observed. The model order is chosen at 100 for the computation of the modal parameters with low uncertainties. In addition, another stabilization given in Figure A I-11 is computed by MODALAR based on the updated AR model (V.-H. Vu *et al.*, 2016) with an aim of validation between two approaches. The 53.75 (Hz) electric frequency of grinding and its harmonics are clearly revealed in the stabilization diagrams.

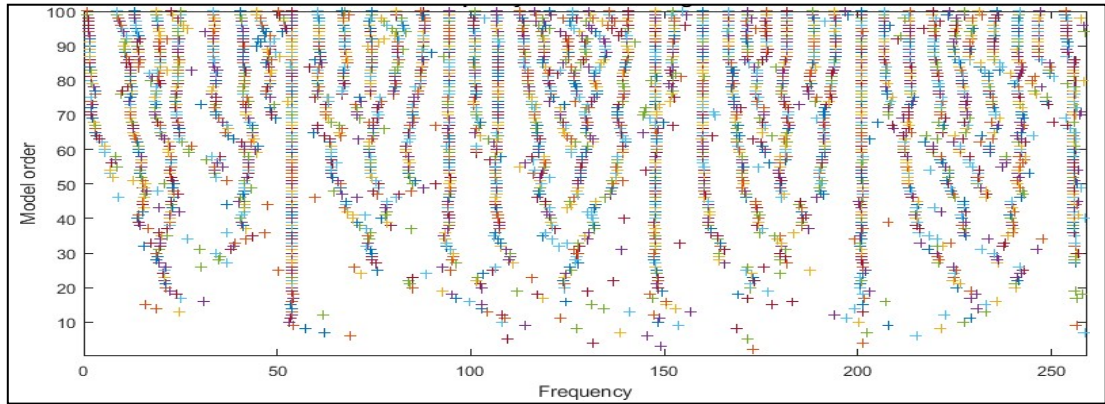


Figure A I-7 Frequency stabilization diagram on X direction

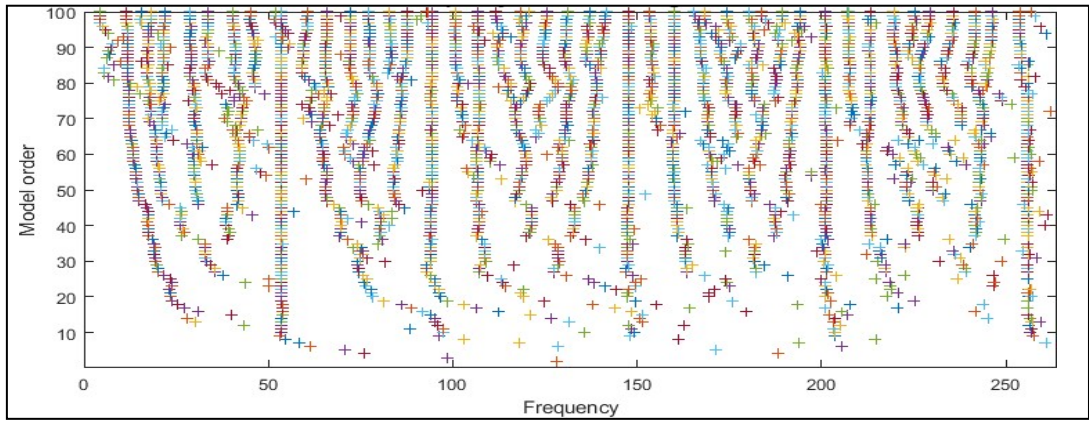


Figure A I-8 Frequency stabilization diagram on Y direction

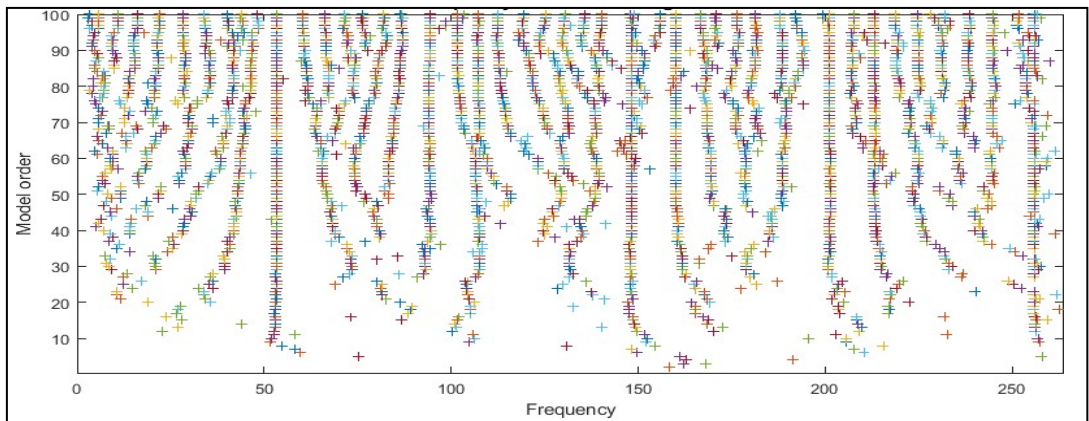


Figure A I-9 Frequency stabilization diagram on Z direction

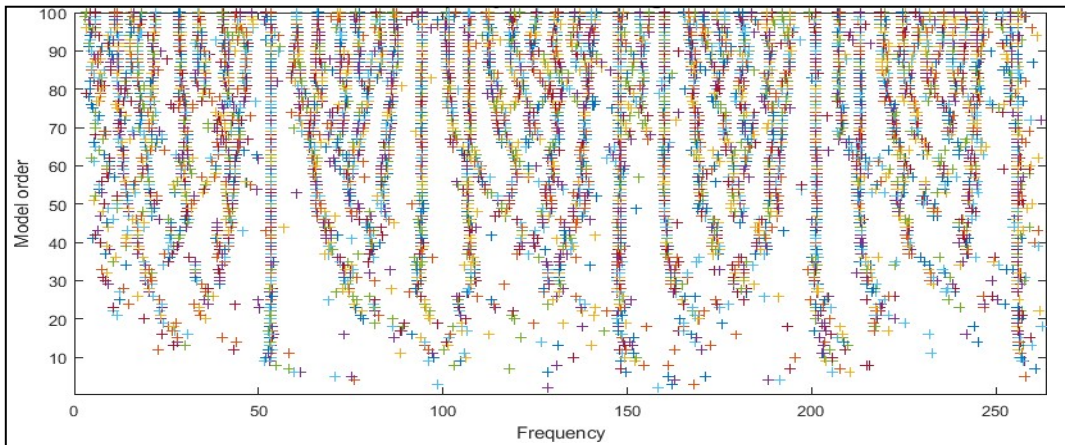


Figure A I-10 Frequency stabilization diagram in MIMO case (three inputs and three outputs)

Synthetically, the natural frequencies and damping ratios are estimated directly from the frequency stabilization diagram of the MIMO case, where all the exciting modes can observe clearly in multi directions. Figure A I-12 illustrated the stabilization diagrams of the damping ratio with 95% uncertainties. The natural and harmonic frequencies identified by two methods with their damping ratio are given in Table A I-1. The harmonic frequencies are identified with their damping rates close to zero.

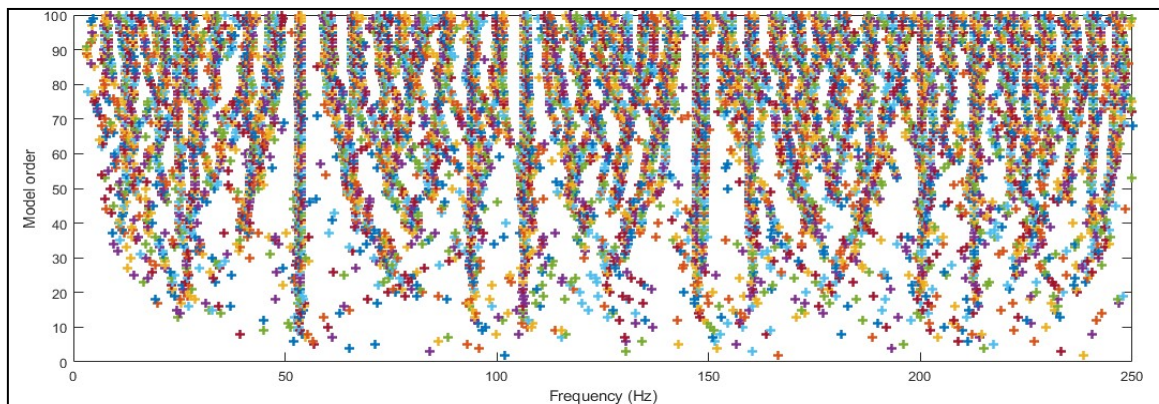


Figure A I-11 Frequency stabilization diagram by MODALAR

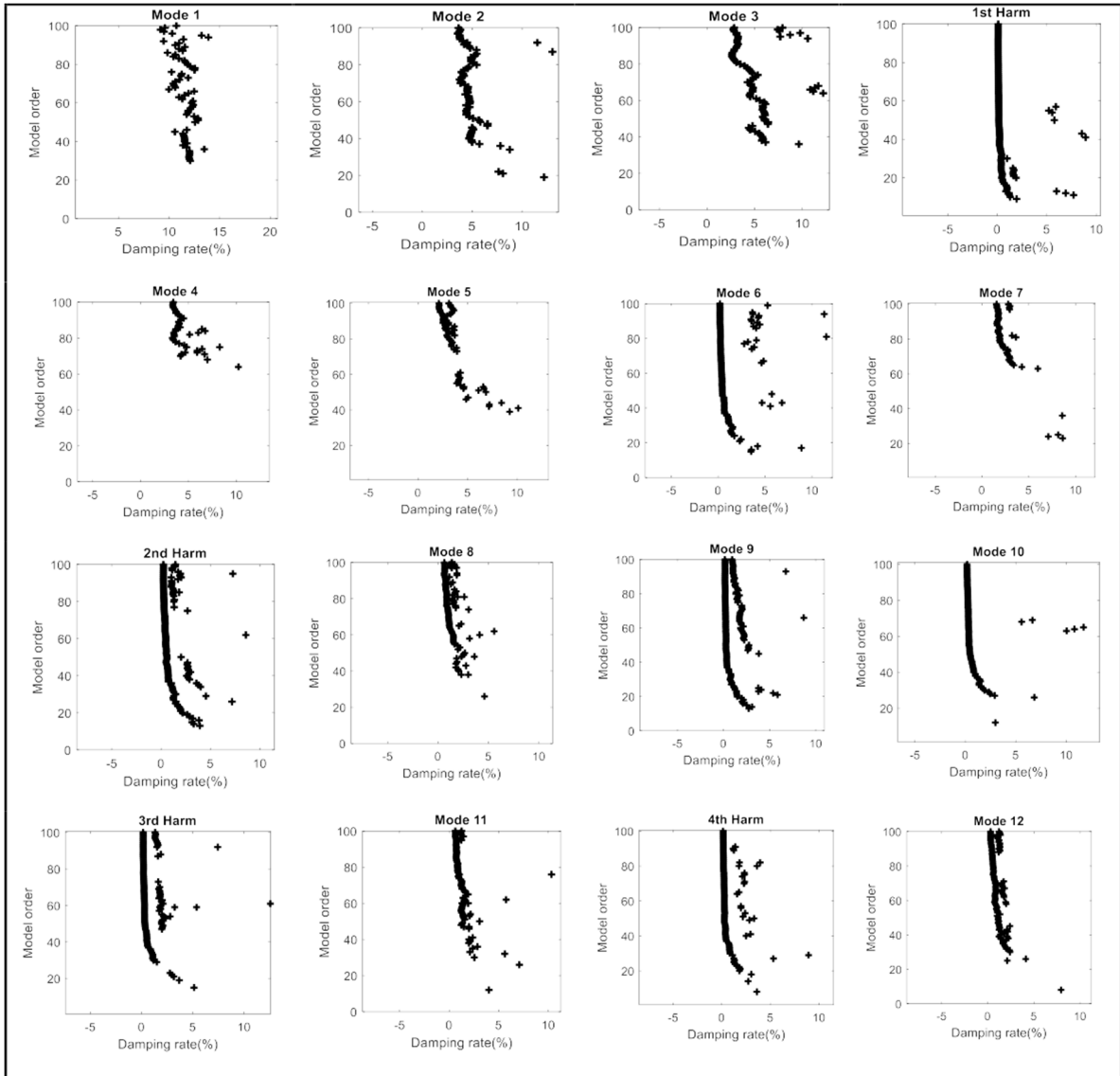


Figure A I-12 Damping ratio stabilization diagrams

Figures A I-13-21 present the transfer functions identified by the ARX model at order 100. The identified transfer function from the working condition is crucial for the assessment of the robot dynamics and for further simulations under different loadings.

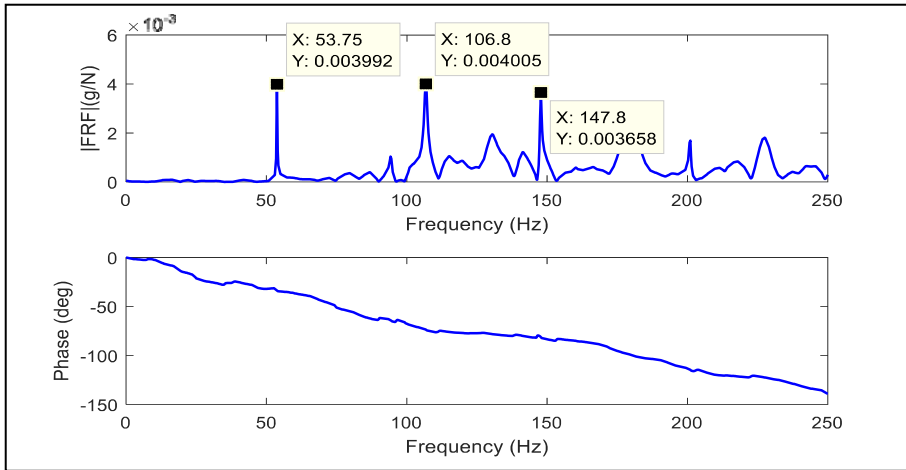


Figure A I-13 Identified Transfer Function FRF_{xx}

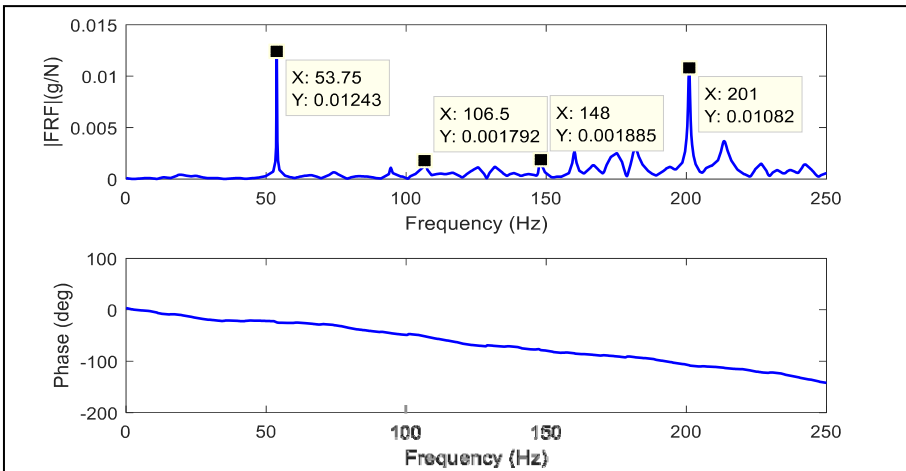


Figure A I-14 Identified Transfer Function FRF_{xy}

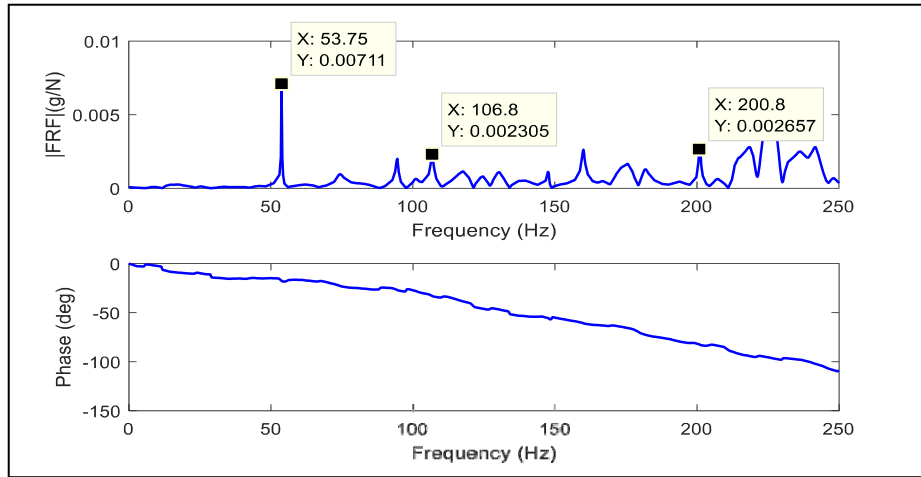


Figure A I-15 Identified Transfer Function FRF_{xz}

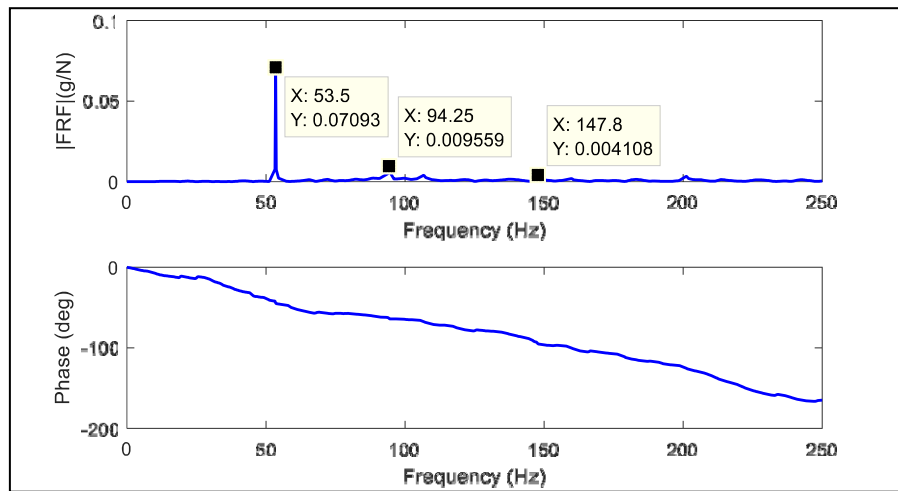


Figure A I-16 Identified Transfer Function FRF_{yx}

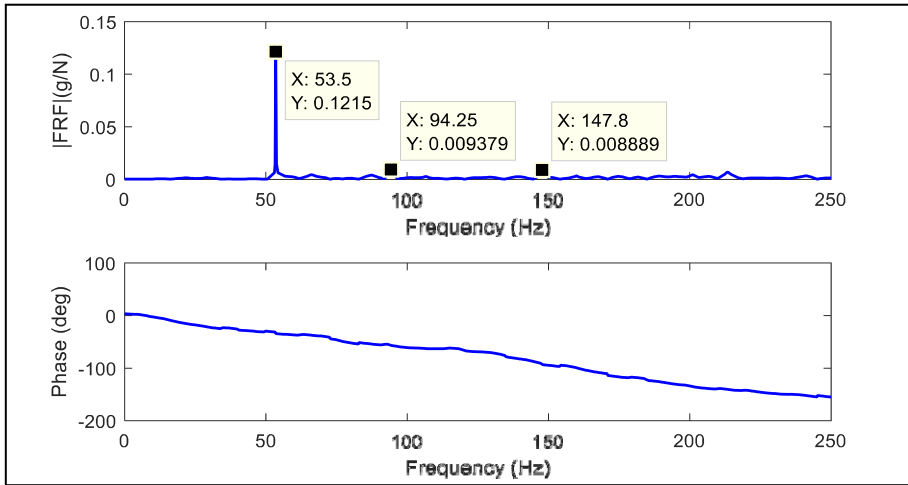


Figure A I-17 Identified Transfer Function FRF_{yy}

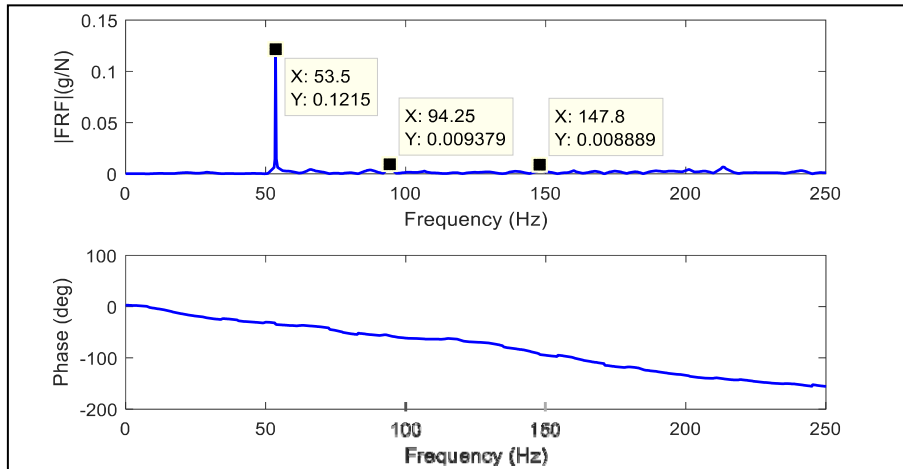
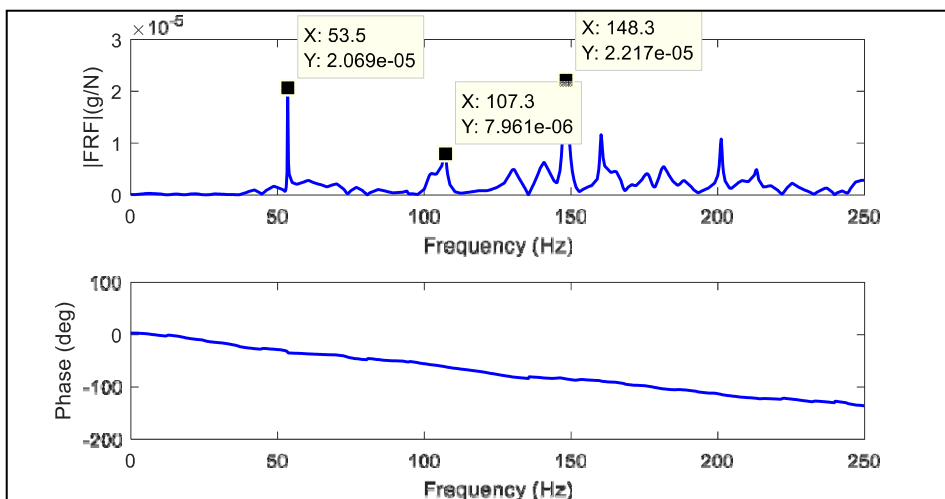
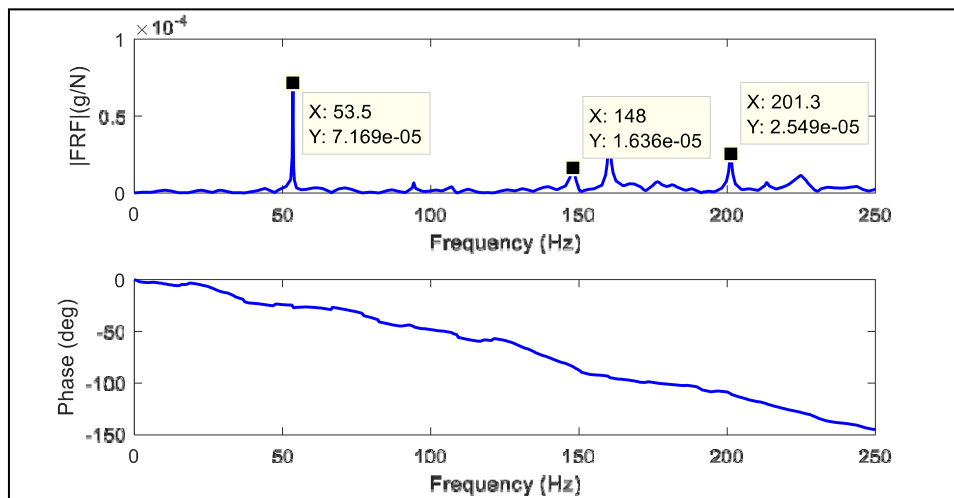


Figure A I-18 Identified Transfer Function FRF_{yz}

Figure A I-19 Identified Transfer Function FRF_{zx} Figure A I-20 Identified Transfer Function FRF_{zy}

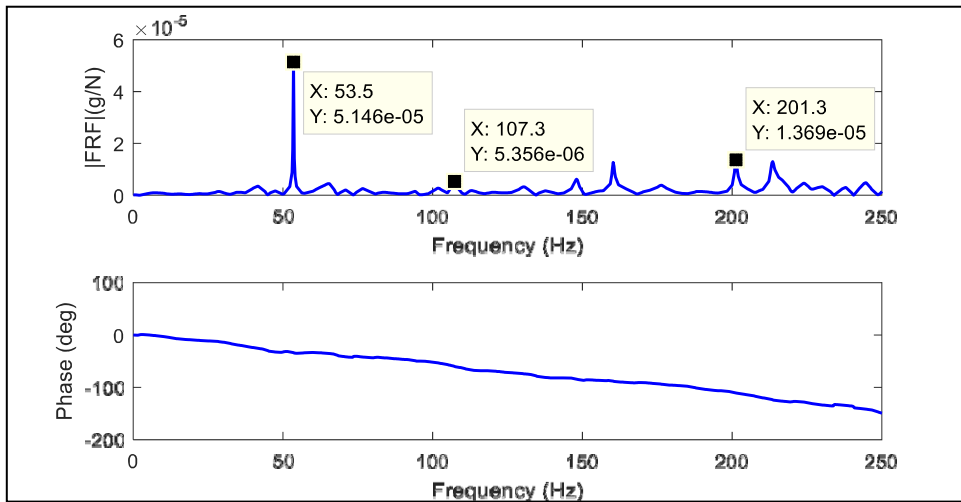


Figure A I-21 Identified Transfer Function FRF_{zz}

By comparison to the identified frequencies by MODALAR based on the updated AR model (V.-H. Vu *et al.*, 2016) shown in table A I-1, the approach reveals high accuracy in identified natural and harmonic frequencies with their damping ratios. Moreover, the frequency response function is directly identified from the grinding operation based on the ARX model. The results are better observed in the X and Y directions, this can be explained by the configuration of SCOMPI when working on a horizontal surface to perform the grinding task.

Table AI-1 Identified frequencies and damping ratios

Mode	M 1	M 2	M 3	1st harm	M 4	M 5	M 6	M 7
Frequencies (Hz) - ARX	14.2	24.4	28.2	53.3	61.2	66.2	94	101.5
Frequencies (Hz) - AR	12.7	24.6	28.2	54.2	60.1	66.2	93.9	101.3
Damping (%) - ARX	11.5	3.7	3.3	0	3.4	2.7	0.2	1.5
Mode	2nd harm	M 8	M 9	M 10	3rd harm	M 11	4th harm	M 12
Frequencies (Hz) - ARX	106.3	111.7	147.5	149.2	159.5	200.4	212.6	224.6
Frequencies (Hz) - AR	106.3	113.5	147.3	149.1	159.5	201.3	213.8	225.1
Damping (%) - ARX	0	0.6	0.2	0.2	0	0.2	0	0.7

AI-7 Conclusion

This work is a part of an ongoing research program on investigating vibration problems of flexible manipulators. The frequencies, damping ratios, and operational FRFs can be constructed, and the most exciting modes are revealed during the grinding process. In this paper, operational FRFs of a structure are identified directly from measured signals via an ARX model. The results illustrated the sensibility of the acceleration in the X and Y directions while the contrary is proved in the Z direction with low magnitudes of the FRFs. Furthermore, as damping of the grinding process and equivalent stiffness are in command of cutting stability, their identification is crucial to predict and avoid detrimental chatter occurrence. In the ongoing research, the inverse of the ARX model will be applied in order to estimate the excitation force in the working conditions, with the integration of phase and coupling between directions. The interest lies in the reconstruction of excitation forces that gave rise to measured response signals based on the ARX model. This approach is expected to serve for monitoring and vibration control design of the robot during the machining operation.

AI-8 Acknowledgments

The authors would like to thank IREQ (Institute de recherche d'Hydro Québec) for technical support.

AI-9 References

- Chiuso, A. (2007). *The Role of Vector Autoregressive Modeling in Subspace Identification*.
- da Silva, S., Dias Junior, M., & Lopes Junior, V. (2007). Damage Detection in a Benchmark Structure Using AR-ARX Models and Statistical Pattern Recognition. *Journal of The Brazilian Society of Mechanical Sciences and Engineering - J BRAZ SOC MECH SCI ENG*, 29. doi:10.1590/S1678-58782007000200007
- Hazel, B., Côté, J., Laroche, Y., & Mongenot, P. (2012). A portable, multiprocess, track-based robot for in situ work on hydropower equipment. *Journal of Field Robotics*, 29(1), 69-101. doi:<https://doi.org/10.1002/rob.20425>
- Jer-Nan, J. (1997). *State-Space System Realization With Input- and Output-Data Correlation*. Retrieved from
- Lennart, L. (1999). *System identification: theory for the user*. PTR Prentice Hall, Upper Saddle River, NJ, 28.
- Li, W., Vu, V.-H., Liu, Z., Thomas, M., & Hazel, B. (2015). Automatic structural mode extraction for time-varying structures via vector time-dependent autoregressive model.
- Li, W., Vu, V.-H., Liu, Z., Thomas, M., & Hazel, B. (2017a). Application of adaptable functional series vector time-dependent autoregressive model for extraction of real modal parameters for identification of time-varying systems. *Measurement*, 103, 143-156. doi:<https://doi.org/10.1016/j.measurement.2017.02.027>
- Li, W., Vu, V.-H., Liu, Z., Thomas, M., & Hazel, B. (2017b). Extraction of modal parameters for identification of time-varying systems using data-driven stochastic subspace identification. *Journal of Vibration and Control*, 24(20), 4781-4796. doi:10.1177/1077546317734670

- Mokdad, F., Vu, V. H., Thomas, M., Rafieian, F., Liu, Z., & Hazel, B. (2011). *Online Modal Analysis of a Flexible Robot During Grinding*.
- Raath, A. D., & Waveren, C. C. V. (1998). A time domain approach to load reconstruction for durability testing. *Engineering Failure Analysis*, 5, 113-119.
- Rafieian, F., Liu, Z., & Hazel, B. (2009). *Dynamic Model and Modal Testing for Vibration Analysis of Robotic Grinding Process with a 6DOF Flexible-joint Manipulator*.
- Santos, T., Liu, Z., & Hazel, B. (2015). Study and validation testing of the dynamics of a robotic system with flexible links and joints. *2015 IEEE International Conference on Mechatronics and Automation (ICMA)*, 1891-1897.
- Soderstrom, T., Fan, H., Carlsson, B., & Bigi, S. (1997). Least squares parameter estimation of continuous-time ARX models from discrete-time data. *IEEE Transactions on Automatic Control*, 42(5), 659-673. doi:10.1109/9.580871
- Strejcek, V., & Dolezal, J. (1982). State Space Theory of Discrete Linear Control. *IEEE Transactions on Systems, Man, and Cybernetics*, 12(5), 684-684. doi:10.1109/TSMC.1982.4308892
- Vu, V.-H., Liu, Z., Thomas, M., & Hazel, B. (2015). Modal analysis of a light-weight robot with a rotating tool installed at the end effector. *Proceedings of the Institution of Mechanical Engineers, Part C: Journal of Mechanical Engineering Science*, 231(9), 1664-1676. doi:10.1177/0954406215619451
- Vu, V.-H., Liu, Z., Thomas, M., Li, W., & Hazel, B. (2016). Output-only identification of modal shape coupling in a flexible robot by vector autoregressive modeling. *Mechanism and Machine Theory*, 97, 141-154. doi:<https://doi.org/10.1016/j.mechmachtheory.2015.11.005>
- Vu, V. H., Liu, Z., Thomas, M., Tahvilian, A. M., & Hazel, B. (2015). *Dynamic forces identification and modeling of a robotic grinding process*.
- Vu, V. H., Zhaoheng, L., Thomas, M., Tahvilian, A. M., & Hazel, B. (2016). *Identification of frequency response functions of a flexible robot as tool-holder for robotic grinding process*.

Wang, T., Wan, Z., & Zheng, W. (2017). An improved state space method for force identification based on function interpolation in the presence of large noise. *Journal of Vibroengineering*, 19, 751-768. doi:10.21595/jve.2017.16917

LIST OF BIBLIOGRAPHICAL REFERENCES

- Auger, F., Hilairet, M., Guerrero, J. M., Monmasson, E., Orłowska-Kowalska, T., & Katsura, S. (2013). Industrial Applications of the Kalman Filter: A Review. *IEEE Transactions on Industrial Electronics*, 60(12), 5458-5471. doi:10.1109/TIE.2012.2236994
- Arevalo Reggeti, Juan Carlos (2017). Parameter identification and modeling of contact properties for robotic applications. *Thesis (Doctoral), E.T.S.I. Industriales (UPM)* <<https://oa.upm.es/view/institution/Industriales/>>.
- Beri, B., & Stepan, G. (2018). Stability of turning process with tool subjected to compression. *Procedia CIRP*, 77, 179-182. doi:<https://doi.org/10.1016/j.procir.2018.08.275>
- Book, W. J., & Majette, M. (1983). Controller design for flexible, distributed parameter mechanical arms via combined state space and frequency domain techniques.
- Box, G. E., Jenkins, G. M., & MacGregor, J. F. (1974). Some recent advances in forecasting and control. *Journal of the Royal Statistical Society: Series C (Applied Statistics)*, 23(2), 158-179.
- Box, G. E., Jenkins, G. M., Reinsel, G. C., & Ljung, G. M. (2015). *Time series analysis: forecasting and control*: John Wiley & Sons.
- Box, G. E., & Pierce, D. A. (1970). Distribution of residual autocorrelations in autoregressive-integrated moving average time series models. *Journal of the American Statistical Association*, 65(332), 1509-1526.
- Brincker, R., & Andersen, P. (2006). *Understanding stochastic subspace identification*. Paper presented at the Conference Proceedings: IMAC-XXIV: A Conference & Exposition on Structural Dynamics.
- Brockwell, P. J., & Davis, R. A. (2002). *Introduction to time series and forecasting*: Springer.
- Brown, D. L., Allemang, R. J., & Zimmerman, R. (1979). *Parameter Estimation Techniques for Modal Analysis*. <https://doi.org/10.4271/790221>
- Bruyninckx, H., Demey, S., Dutré, S., & De Schutter, J. (1995). Kinematic Models for Model-Based Compliant Motion in the Presence of Uncertainty. *The International Journal of Robotics Research*, 14(5), 465-482. doi:10.1177/027836499501400505

- Choi, B. O., & Krishnamurthy, K. (1994). Unconstrained and constrained motion control of a planar two-link structurally flexible robotic manipulator. *Journal of Robotic Systems*, *11*(6), 557-571. doi:<https://doi.org/10.1002/rob.4620110609>
- DeLio, T., Tlustý, J., & Smith, S. (1992). Use of Audio Signals for Chatter Detection and Control. *Journal of Engineering for Industry*, *114*, 146-157.
- Di Renzo, A., & Di Maio, F. P. (2004). Comparison of contact-force models for the simulation of collisions in DEM-based granular flow codes. *Chemical Engineering Science*, *59*(3), 525-541. doi:<https://doi.org/10.1016/j.ces.2003.09.037>
- Dwivedy, S. K., & Eberhard, P. (2006). Dynamic analysis of flexible manipulators, a literature review. *Mechanism and Machine Theory*, *41*(7), 749-777. doi:<https://doi.org/10.1016/j.mechmachtheory.2006.01.014>
- Eftekhar Azam, S., Chatzi, E., & Papadimitriou, C. (2015). A dual Kalman filter approach for state estimation via output-only acceleration measurements. *Mechanical Systems and Signal Processing*, *60-61*, 866-886. doi:<https://doi.org/10.1016/j.ymsp.2015.02.001>
- Erickson, D., Weber, M., & Sharf, I. (2003). Contact Stiffness and Damping Estimation for Robotic Systems. *The International Journal of Robotics Research*, *22*(1), 41-57. doi:10.1177/0278364903022001004
- Erickson, J. S., Sundaram, S., & Stebe, K. J. (2000). Evidence that the Induction Time in the Surface Pressure Evolution of Lysozyme Solutions Is Caused by a Surface Phase Transition. *Langmuir*, *16*(11), 5072-5078. doi:10.1021/la991179y
- Faassen, R. P. H., Doppenberg, e., N, W., Oosterling, H., & Nijmeijer, H. (2006). Online detection of the onset and occurrence of machine tool chatter in the milling process. *Brain Research - BRAIN RES.*
- Fassois, S. D. (2001). MIMO LMS-ARMAX IDENTIFICATION OF VIBRATING STRUCTURES—PART I: THE METHOD. *Mechanical Systems and Signal Processing*, *15*(4), 723-735. doi:<https://doi.org/10.1006/mssp.2000.1382>
- Feldman, M. (1994). Non-linear system vibration analysis using Hilbert transform--I. Free vibration analysis method'Freevib'. *Mechanical Systems and Signal Processing*, *8*(2), 119-127.

- Flores, P., & Ambrósio, J. (2010). On the contact detection for contact-impact analysis in multibody systems. *Multibody System Dynamics*, 24(1), 103-122. doi:10.1007/s11044-010-9209-8
- Gagnon, M., Tahan, S.-A., Coutu, A., & Thomas, M. (2006). *Analyse modale opérationnelle en présence d'excitations harmoniques: étude de cas sur des composantes de turbine hydroélectrique*. Paper presented at the Proceedings of the 24th Seminar on machinery vibration, Montréal.
- Ghayesh, M. H., Amabili, M., & Farokhi, H. (2013). Nonlinear forced vibrations of a microbeam based on the strain gradient elasticity theory. *International Journal of Engineering Science*, 63, 52-60.
- Grabbe, M. T., Carroll, J. J., Dawson, D. M., & Qu, Z. (1992, 12-14 May 1992). *Robust control of robot manipulators during constrained and unconstrained motion*. Paper presented at the Proceedings 1992 IEEE International Conference on Robotics and Automation.
- Gul, M., & Catbas, N. (2011). Structural health monitoring and damage assessment using a novel time series analysis methodology with sensor clustering. *Journal of Sound and Vibration*, 330, 1196-1210. doi:10.1016/j.jsv.2010.09.024
- Harvey, A. C. (1990). *The econometric analysis of time series*: Mit Press.
- Hazel, B., Côté, J., Laroche, Y., & Mongenot, P. (2012a). Field repair and construction of large hydropower equipment with a portable robot. *Journal of Field Robotics*, 29(1), 102-122. doi:<https://doi.org/10.1002/rob.20427>
- Hazel, B., Côté, J., Laroche, Y., & Mongenot, P. (2012b). A portable, multiprocess, track-based robot for in situ work on hydropower equipment. *Journal of Field Robotics*, 29(1), 69-101. doi:<https://doi.org/10.1002/rob.20425>
- Hermans, L., & Van Der Auweraer, H. (1999). MODAL TESTING AND ANALYSIS OF STRUCTURES UNDER OPERATIONAL CONDITIONS: INDUSTRIAL APPLICATIONS. *Mechanical Systems and Signal Processing*, 13(2), 193-216. doi:<https://doi.org/10.1006/mssp.1998.1211>
- Hillary, B., and D. J. Ewins. (1984). The use of strain gauges in force determination and frequency response function measurements. *Proceedings of IMAC. , Vol. 2*.

- Hollandsworth, P. E., & Busby, H. R. (1989). Impact force identification using the general inverse technique. *International Journal of Impact Engineering*, 8(4), 315-322. doi:[https://doi.org/10.1016/0734-743X\(89\)90020-1](https://doi.org/10.1016/0734-743X(89)90020-1)
- Huang, B. C., Leung, A. Y. T., Lam, K. M., & Cheung, Y. K. (1996). Analytical determination of equivalent modal damping ratios of a composite tower in wind-induced vibrations. *Computers & Structures*, 59(2), 311-316. doi:[https://doi.org/10.1016/0045-7949\(95\)00258-8](https://doi.org/10.1016/0045-7949(95)00258-8)
- Ibrahim, S. R., & Mikulcik, E. C. (1977). *A method for the direct identification of vibration parameters from the free response*.
- Iqbal, A. (2019). *Application of an Extended Kalman Filter in nonlinear mechanics*.
- Julier, S. J., & Uhlmann, J. K. (1997). *New extension of the Kalman filter to nonlinear systems*. Paper presented at the Defense, Security, and Sensing.
- Kalman, R. E. (1960). A New Approach to Linear Filtering and Prediction Problems. *Journal of Basic Engineering*, 82(1), 35-45. doi:10.1115/1.3662552
- Katayama, T. (2005). *Subspace methods for system identification* (Vol. 1): Springer.
- Khachan, S., & Ismail, F. (2009). Machining chatter simulation in multi-axis milling using graphical method. *International Journal of Machine Tools and Manufacture*, 49(2), 163-170. doi:<https://doi.org/10.1016/j.ijmachtools.2008.09.002>
- Khatib, E. I. A., Jaradat, M. A., Abdel-Hafez, M., & Roigari, M. (2015, 8-10 Dec. 2015). *Multiple sensor fusion for mobile robot localization and navigation using the Extended Kalman Filter*. Paper presented at the 2015 10th International Symposium on Mechatronics and its Applications (ISMA).
- Khoo, S. Y., Ismail, Z., Kong, K. K., Ong, Z. C., Noroozi, S., Chong, W. T., & Rahman, A. G. A. (2014). Impact force identification with pseudo-inverse method on a lightweight structure for under-determined, even-determined and over-determined cases. *International Journal of Impact Engineering*, 63, 52-62. doi:<https://doi.org/10.1016/j.ijimpeng.2013.08.005>
- Lefebvre, T., Bruyninckx, H., & Schutter, J. D. (2003). Polyhedral contact formation modeling and identification for autonomous compliant motion. *IEEE Transactions on Robotics and Automation*, 19(1), 26-41. doi:10.1109/TRA.2002.805677

- Leonard, M., & Wolfe, B. (2005). Mining transactional and time series data. *abstract, presentation and paper, SUGI*, 10-13.
- Li, W., Vu, V.-H., Liu, Z., Thomas, M., & Hazel, B. (2017). Extraction of modal parameters for identification of time-varying systems using data-driven stochastic subspace identification. *Journal of Vibration and Control*, 24(20), 4781-4796. doi:10.1177/1077546317734670
- Liu, H., He, J., & Chen, S. (2012). Parameter Identification Research Based on ARX Model. *Applied Mechanics and Materials*, 190-191, 292-296. doi:10.4028/www.scientific.net/AMM.190-191.292
- Lourens, E., Reynders, E., De Roeck, G., Degrande, G., & Lombaert, G. (2012). An augmented Kalman filter for force identification in structural dynamics. *Mechanical Systems and Signal Processing*, 27, 446-460. doi:<https://doi.org/10.1016/j.ymsp.2011.09.025>
- Lu, Y., & Gao, F. (2004). A novel time-domain auto-regressive model for structural damage diagnosis. *Journal of Sound and Vibration*, 1031–1049
- Ma, C.-K., Tuan, P.-C., Lin, D.-C., & Liu, C.-S. (1998). A study of an inverse method for the estimation of impulsive loads. *International journal of systems science*, 29(6), 663-672.
- Ma, C. K., Chang, J. M., & Lin, D. C. (2003). INPUT FORCES ESTIMATION OF BEAM STRUCTURES BY AN INVERSE METHOD. *Journal of Sound and Vibration*, 259(2), 387-407. doi:<https://doi.org/10.1006/jsvi.2002.5334>
- Magalhães, F., Cunha, Á., Caetano, E., & Brincker, R. (2010). Damping estimation using free decays and ambient vibration tests. *Mechanical Systems and Signal Processing*, 24(5), 1274-1290. doi:<https://doi.org/10.1016/j.ymsp.2009.02.011>
- Masjedian, M. H., & Keshmiri, M. (2009). A review on operational modal analysis researches: Classification of methods and applications. *IOMAC 2009 - 3rd International Operational Modal Analysis Conference*, 707-716.
- Merritt, H. (1965). Theory of self-excited machine-tool chatter: contribution to machine-tool chatter research—1.

- Minchul, S., & Dongsoo, K. (2015, 28-30 Oct. 2015). *Implementation of extended Kalman filter with PI control and modeling effect reduction for precise motor speed estimation in disturbance*. Paper presented at the 2015 12th International Conference on Ubiquitous Robots and Ambient Intelligence (URAI).
- Mohanty, P., & Rixen, D. (2004). A modified Ibrahim time domain algorithm for operational modal analysis including harmonic excitation. *Journal of Sound and Vibration*, 275, 375-390. doi:10.1016/j.jsv.2003.06.030
- Moore, S. M., Lai, J. C. S., & Shankar, K. (2007a). ARMAX modal parameter identification in the presence of unmeasured excitation—I: Theoretical background. *Mechanical Systems and Signal Processing*, 21(4), 1601-1615. doi:<https://doi.org/10.1016/j.ymsp.2006.07.003>
- Moore, S. M., Lai, J. C. S., & Shankar, K. (2007b). ARMAX modal parameter identification in the presence of unmeasured excitation—II: Numerical and experimental verification. *Mechanical Systems and Signal Processing*, 21(4), 1616-1641. doi:<https://doi.org/10.1016/j.ymsp.2006.07.004>
- Motte, K., Weijtjens, W., Devriendt, C., & Guillaume, P. (2015). Operational Modal Analysis in the Presence of Harmonic Excitations: A Review. In (pp. 379-395).
- Movahhedy, M. R., & Mosaddegh, P. (2006). Prediction of chatter in high speed milling including gyroscopic effects. *International Journal of Machine Tools and Manufacture*, 46(9), 996-1001. doi:<https://doi.org/10.1016/j.ijmachtools.2005.07.043>
- Mu, X., & Sharf, I. (2007). *Nonlinear Contact Parameter Estimation for Robotic Systems With Payload*. <https://doi.org/10.1115/DETC2007-35391>
- Muthukumar, S., & DesRoches, R. (2006). A Hertz contact model with non-linear damping for pounding simulation. *Earthquake Engineering & Structural Dynamics*, 35(7), 811-828. doi:<https://doi.org/10.1002/eqe.557>
- Nardini, D., & Brebbia, C. (1983). A new approach to free vibration analysis using boundary elements. *Applied mathematical modelling*, 7(3), 157-162.
- Nguyen, Q.-C., Vu, V.-H., & Thomas, M. (2022). A Kalman filter based ARX time series modeling for force identification on flexible manipulators. *Mechanical Systems and Signal Processing*, 169, 108743. doi:<https://doi.org/10.1016/j.ymsp.2021.108743>

- Nguyen, Q.-C., Vu, V.-H., & Thomas, M. (2022). Optimal ARMAX Model Order Identification of Dynamic Systems. *London Journal of Engineering Research*, Volume 22, Issue 01, Compilation 1.0.
- Ödeen, S., & Lundberg, B. (1991). Prediction of impact force by impulse response method. *International Journal of Impact Engineering*, 11(2), 149-158. doi:[https://doi.org/10.1016/0734-743X\(91\)90002-W](https://doi.org/10.1016/0734-743X(91)90002-W)
- Odry, Á., Fuller, R., Rudas, I., & Odry, P. (2018). Kalman filter for mobile-robot attitude estimation: Novel optimized and adaptive solutions. *Mechanical Systems and Signal Processing*, 110. doi:10.1016/j.ymsp.2018.03.053
- Papageorgiou, A. V., & Gantes, C. J. (2010). Equivalent modal damping ratios for concrete/steel mixed structures. *Computers & Structures*, 88(19), 1124-1136. doi:<https://doi.org/10.1016/j.compstruc.2010.06.014>
- Peeters, B. (2000). System Identification and Damage Detection in Civil Engineering.
- Peeters, B., & De Roeck, G. (2001). Stochastic System Identification for Operational Modal Analysis: A Review. *Journal of Dynamic Systems, Measurement, and Control*, 123(4), 659-667. doi:10.1115/1.1410370
- Peng, C., Wang, L., & Liao, T. W. (2015). A new method for the prediction of chatter stability lobes based on dynamic cutting force simulation model and support vector machine. *Journal of Sound and Vibration*, 354, 118-131.
- Quintana, G., & Ciurana, J. (2011). Chatter in machining processes: A review. *International Journal of Machine Tools and Manufacture*, 51(5), 363-376. doi:<https://doi.org/10.1016/j.ijmachtools.2011.01.001>
- Quintana, G., Ciurana, J., Ferrer, I., & Rodriguez, C. (2009). Sound mapping for identification of stability lobe diagrams in milling processes. *International Journal of Machine Tools and Manufacture*, 49, 203-211. doi:10.1016/j.ijmachtools.2008.11.008
- Rafieian, F., Hazel, B., & Liu, Z. (2014). Vibro-impact dynamics of material removal in a robotic grinding process. *International Journal of Advanced Manufacturing Technology*, 72, 1-24. doi:10.1007/s00170-014-5838-z

- Rafieian, F., Hazel, B., & Liu, Z. (2014). Regenerative Instability of Impact-cutting Material Removal in the Grinding Process Performed by a Flexible Robot Arm. *Procedia CIRP*, 14, 406-411. doi:<https://doi.org/10.1016/j.procir.2014.03.099>
- Rainieri, C., & Fabbrocino, G. (2014). Operational modal analysis of civil engineering structures. *Springer, New York, 142*, 143.
- Rajkumar, S., Alok Dewanand Bhagat, C. Sujatha, and S. Narayanan. (2015). Comparison of various techniques used for estimation of input force and computation of frequency response function (FRF) from measured response data. *In The 22nd International Congress on Sound and Vibration, Glorence, Italy*.
- Reynders, E., Maes, K., Lombaert, G., & De Roeck, G. (2016). Uncertainty quantification in operational modal analysis with stochastic subspace identification: Validation and applications. *Mechanical Systems and Signal Processing*, 66-67, 13-30. doi:<https://doi.org/10.1016/j.ymsp.2015.04.018>
- Sabourin, M., Paquet, F., Hazel, B., Côté, J., & Mongenot, P. (2010, 5-7 Oct. 2010). *Robotic approach to improve turbine surface finish*. Paper presented at the 2010 1st International Conference on Applied Robotics for the Power Industry.
- Sánchez, L. A., Le, M. Q., Liu, C., Zemiti, N., & Poignet, P. (2012, 14-18 May 2012). *The impact of interaction model on stability and transparency in bilateral teleoperation for medical applications*. Paper presented at the 2012 IEEE International Conference on Robotics and Automation.
- Sciavicco, L., & Siciliano, B. (2001). *Modelling and control of robot manipulators*: Springer Science & Business Media.
- Shaw, S. (1985). Forced vibrations of a beam with one-sided amplitude constraint: theory and experiment. *Journal of Sound and Vibration*, 99(2), 199-212.
- Skrinjar, L., Slavič, J., & Boltežar, M. (2018). A review of continuous contact-force models in multibody dynamics. *International Journal of Mechanical Sciences*, 145, 171-187. doi:<https://doi.org/10.1016/j.ijmecsci.2018.07.010>
- Smail, M., Thomas, M., & Lakis, A. (1999). ARMA models for modal analysis: effect of model orders and sampling frequency. *Mechanical Systems and Signal Processing*, 13(6), 925-941.

- Soderstrom, T., Fan, H., Carlsson, B., & Bigi, S. (1997). Least squares parameter estimation of continuous-time ARX models from discrete-time data. *IEEE Transactions on Automatic Control*, 42(5), 659-673. doi:10.1109/9.580871
- Sorenson, H. W. (1966). Kalman filtering techniques. In *Advances in control systems* (Vol. 3, pp. 219-292): Elsevier.
- Stevens, K. K. (1987). *Force identification problems an overview*. Paper presented at the Proceedings of the 1987 SEM Spring Conference on Experimental Mechanics, Houston, TX, USA.
- S.Rajkumar, Bhagat, A. D., C.Sujatha, & S.Narayanan. (2015). Comparison of various techniques used for estimation of input force and computation of frequency response function form measured data. *International Congress on Sound and Vibration*.
- Tokhi, M., Azad, A., Morris, A., & Hossain, M. (1994). *Modelling and simulation of a flexible manipulator system*. Paper presented at the 1994 International Conference on Control-Control'94.
- Van Vliet, J., Sharf, I., & Ma, O. (2000). Experimental Validation of Contact Dynamics Simulation of Constrained Robotic Tasks. *The International Journal of Robotics Research*, 19(12), 1203-1217. doi:10.1177/02783640022068039
- Vela-Martínez, L., Jáuregui-Correa, J. C., Rubio-Cerda, E., Herrera-Ruiz, G., & Lozano-Guzmán, A. (2008). Analysis of compliance between the cutting tool and the workpiece on the stability of a turning process. *International Journal of Machine Tools and Manufacture*, 48(9), 1054-1062. doi:<https://doi.org/10.1016/j.ijmachtools.2007.10.016>
- Vu, V.-H., Liu, Z., Thomas, M., & Hazel, B. (2015). Modal analysis of a light-weight robot with a rotating tool installed at the end effector. *Proceedings of the Institution of Mechanical Engineers, Part C: Journal of Mechanical Engineering Science*, 231(9), 1664-1676. doi:10.1177/0954406215619451
- Vu, V. H., Liu, Z., Thomas, M., Tahvilian, A. M., & Hazel, B. (2015). *Dynamic forces identification and modeling of a robotic grinding process*.
- Vu, V. H., Thomas, M., Lakis, A. A., & Marcouiller, L. (2011). Operational modal analysis by updating autoregressive model. *Mechanical Systems and Signal Processing*, 25(3), 1028-1044. doi:<https://doi.org/10.1016/j.ymsp.2010.08.014>

- Vukobratović, M. K., & Potkonjak, V. (1999). Dynamics of contact tasks in robotics. Part I: general model of robot interacting with environment. *Mechanism and Machine Theory*, 34(6), 923-942. doi:[https://doi.org/10.1016/S0094-114X\(97\)00091-8](https://doi.org/10.1016/S0094-114X(97)00091-8)
- Waki, Y., Mace, B., & Brennan, M. (2009). Free and forced vibrations of a tyre using a wave/finite element approach. *Journal of Sound and Vibration*, 323(3-5), 737-756.
- Wan, E. A., & Merwe, R. V. D. (2000, 4-4 Oct. 2000). *The unscented Kalman filter for nonlinear estimation*. Paper presented at the Proceedings of the IEEE 2000 Adaptive Systems for Signal Processing, Communications, and Control Symposium (Cat. No.00EX373).
- Wang, M. L., & Kreitinger, T. J. (1994). Identification of force from response data of a nonlinear system. *Soil Dynamics and Earthquake Engineering*, 13(4), 267-280. doi:[https://doi.org/10.1016/0267-7261\(94\)90031-0](https://doi.org/10.1016/0267-7261(94)90031-0)
- Weber, M., Patel, K., Ma, O., & Sharf, I. (2005). Identification of Contact Dynamics Model Parameters From Constrained Robotic Operations. *Journal of Dynamic Systems, Measurement, and Control*, 128(2), 307-318. doi:10.1115/1.2192839
- Wei, W. W. (2006). Time series analysis. In *The Oxford Handbook of Quantitative Methods in Psychology: Vol. 2*.
- Wiercigroch, M., Wiercigroch, M., & Budak, E. (2001). Sources of nonlinearities, chatter generation and suppression in metal cutting. *Philosophical Transactions of the Royal Society of London. Series A: Mathematical, Physical and Engineering Sciences*, 359(1781), 663-693. doi:10.1098/rsta.2000.0750
- Yao, Z., Mei, D., & Chen, Z. (2010). On-line chatter detection and identification based on wavelet and support vector machine. *Journal of Materials Processing Technology*, 210(5), 713-719. doi:<https://doi.org/10.1016/j.jmatprotec.2009.11.007>
- Zengxi, P., Hui, Z., Zhenq, Z., & Jianjun, W. (2006). Chatter analysis of robotic machining process. *Journal of Materials Processing Technology*, Volume 173, Issue 3, 301-309.